

# **Modern Photocatalytic Approaches to Carbon-centered Radical Generation for Sustainable Synthesis of Pharmaceutically Relevant Scaffolds**

Vor der Fakultät für Mathematik, Informatik und Naturwissenschaften der RWTH Aachen  
University zur Erlangung des akademischen Grades eines Doktors der Naturwissenschaften  
genehmigte Dissertation

vorgelegt von

**Dan Liu, M.Sc.**

aus

Anhui, China

Berichter: Universitätsprofessor Dr. rer. nat. Frederic W. Patureau  
Universitätsprofessor Dr. rer. nat. Markus Albrecht

Tag der mündlichen Prüfung: 21.05.2025

Diese Dissertation ist auf den Internetseiten der Universitätsbibliothek online verfügbar



Eidesstattliche Erklärung

Declaration of Authorship

I, Dan Liu, declare that this thesis and the presented work are my original research.

Hiermit erkläre ich an Eides statt / I do solemnly swear that:

1. This work was conducted entirely or primarily during my candidacy for the doctoral degree at this faculty and university.
2. Any portion of this thesis that has been previously submitted for a degree or other academic qualification-whether at this or another institution-has been explicitly indicated.
3. Whenever I have referenced the published work of others or my own prior research, proper attribution has been provided.
4. Any direct quotations from other sources, including my own publications, are duly cited. Except for these quoted materials, the entirety of this thesis represents my original work.
5. All significant sources of support and contributions have been duly acknowledged
6. In cases where this thesis includes collaborative work, I have clearly specified my contributions as well as those of my co-researchers.
7. Parts of this work have been published previously. A full list of references is provided below.
8. ChatGPT were used for the language corrections of this thesis.



The doctoral work in this thesis was performed from October 2021 until February 2025 at the Institute of Organic Chemistry, RWTH Aachen University, under the supervision of Professor Dr. Frederic W. Patureau.

The doctoral work has led to the following publications:

1. **D. Liu**, F. Xiao, B. Ebel, I. M. Oppel and F. W. Patureau, Visible-light-mediated radical  $\alpha$ -C(sp<sup>3</sup>)-H *gem*-difluoroallylation of amides with trifluoromethyl alkenes via halogen atom transfer and 1,5-hydrogen atom transfer. *Org. Lett.* **2025**, 27, 2377.
2. **D. Liu**, and F. W. Patureau, Visible-light-induced photocatalytic deoxygenative benzylation of quinoxalin-2-(1*H*)-ones with carboxylic acid anhydrides. *Org. Lett.* **2024**, 26, 6841.
3. **D. Liu**, Y. Zhao and F. W. Patureau, NaI/PPh<sub>3</sub>-catalyzed visible-light-mediated decarboxylative radical cascade cyclization of *N*-arylacrylamides for the efficient synthesis of quaternary oxindoles. *Beilstein J. Org. Chem.* **2023**, 19, 57.



## Table of contents

1 Introduction.....	1
1.1 Photocatalysis.....	1
1.2 Photocatalyzed radical generation from carboxylic acids and their derivatives.....	3
1.2.1 Alkyl radical generation via decarboxylation.....	3
1.2.2 Aryl radical generation via P <sup>III</sup> -assisted deoxygenation .....	15
1.3 Photocatalyzed radical generation via 1,5-HAT.....	20
1.3.1 Aryl radical-mediated 1,5-HAT.....	20
1.3.2 Vinyl radical-mediated 1,5-HAT .....	21
1.3.3 Alkyl radical-mediated 1,5-HAT .....	24
1.4 Conclusion .....	25
2 Results and discussion .....	26
2.1 NaI/PPh <sub>3</sub> -catalyzed visible-light-mediated decarboxylative radical cascade cyclization of <i>N</i> -arylacrylamides for the efficient synthesis of quaternary oxindoles .....	26
2.1.1 Introduction .....	26
2.1.2 Condition optimizations .....	27
2.1.3 Substrate scope studies.....	29
2.1.4 Mechanistic investigation.....	31
2.1.5 Conclusion .....	33
2.2 Visible-light-induced photocatalytic deoxygenative benzylation of quinoxalin-2-(1 <i>H</i> )-ones with carboxylic acid anhydrides.....	34
2.2.1 Introduction.....	34
2.2.2 Condition optimizations .....	36
2.2.3 Substrate scope studies.....	37
2.2.4 Synthetic applications .....	39
2.2.5 Mechanistic studies .....	39
2.2.6 Conclusion .....	41
2.3 Visible-light-mediated radical $\alpha$ -C(sp <sup>3</sup> )-H <i>gem</i> -difluoroallylation of amides with trifluoromethyl alkenes via halogen atom transfer and 1,5-hydrogen atom transfer.....	42
2.3.1 Introduction.....	42
2.3.2 Condition optimizations .....	43
2.3.3 Substrate scope studies.....	44
2.3.4 Mechanistic studies .....	46
2.3.5 Conclusion .....	47
3 Summary and outlook .....	48
4 Experiment and data.....	50
4.1 General information .....	50
4.2 Experimental methods and data .....	52
4.2.1 NaI/PPh <sub>3</sub> -catalyzed visible-light-mediated decarboxylative radical cascade cyclization of <i>N</i> -arylacrylamides for the efficient synthesis of quaternary oxindoles ....	52
4.2.2 Visible-light-induced photocatalytic deoxygenative benzylation of quinoxalin-2-(1 <i>H</i> )-ones with carboxylic acid anhydrides .....	65
4.2.3 Visible-light-mediated radical $\alpha$ -C(sp <sup>3</sup> )-H <i>gem</i> -difluoroallylation of amides with	

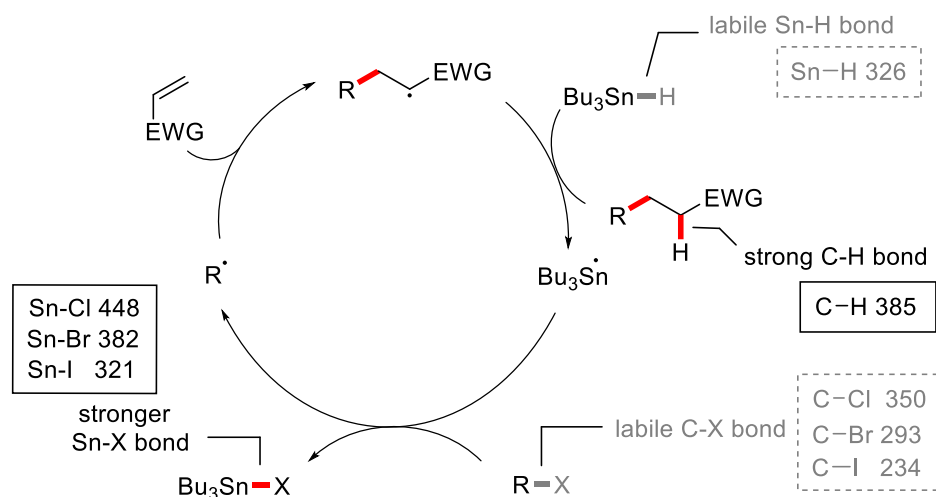
trifluoromethyl alkenes via halogen atom transfer and 1,5-hydrogen atom transfer.....	84
5 List of abbreviation .....	105
6 References.....	107
7 Acknowledgements .....	116
8 Curriculum vitae .....	117



# 1 Introduction

## 1.1 Photocatalysis

As a significant class of open-shell species, carbon-centered radicals are intriguing neutral intermediates that have gained broad utility in the fields of modern organic synthesis, material science and biological chemistry, despite the early doubt regarding their potential application.<sup>1-5</sup> Particularly, alkyl and benzoyl radical generation under mild conditions, along with their controlled and selective transformations, have become research topics of increasing interest. An early example of generating alkyl radicals from organic halides is illustrated in **Scheme 1**. Organotin compounds were identified as essential for promoting radical chain reactions, as reported nearly 60 years ago.<sup>6</sup> The discovery of  $\text{Bu}_3\text{SnH}$  represented a major advancement in radical chemistry, as it enabled the production of  $\text{Bu}_3\text{Sn}\cdot$  as the radical chain carrier and served as a hydrogen atom donor to complete the catalytic cycle. Subsequently, the alkyl or benzoyl radicals<sup>7-8</sup> formed via tin-mediated processes were effectively trapped by various radical acceptors, facilitating the construction of novel functional molecules. Analysis of bond dissociation energies (BDE) of the reactants revealed that the key of this method lies in the formation of stronger  $\text{Sn-X}$  and  $\text{C-H}$  bonds, driven by the homolytic cleavage of the weaker  $\text{Sn-H}$  and  $\text{C-X}$  bonds (**Scheme 1**).<sup>9-10</sup>



Bond energies are reported in kJ/mol from Ref. 9 and Ref. 10

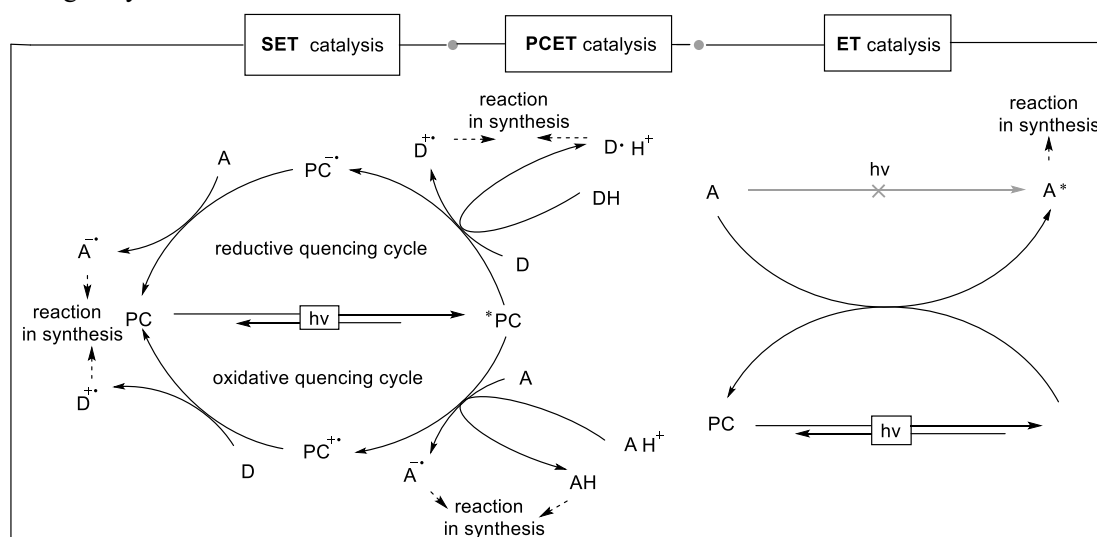
**Scheme 1** Thermal radical initiation from alkyl halides using organotin compounds

Although organotin molecules performed competitively in the radical-generating processes,<sup>11-14</sup> the use of these highly versatile species raised significant concerns regarding environmental and health safety,<sup>15</sup> due to the substantial toxicity and high biological activity of triorganotin molecules. Studies disclosed an  $\text{LD}_{50}$  of approximately 0.7 mmol/kg in murine species and prolonged persistence of these organotins in aquatic environment,<sup>16</sup> these inherent issues necessitate the exploration of viable alternatives.

Efforts have been made to replace toxic tin derivatives with reagents such as  $(\text{TMS})_3\text{SiH}$ ,<sup>17</sup> peroxides,<sup>18-22</sup> xanthates,<sup>23</sup> organoboranes,<sup>24</sup> thiols,<sup>25</sup> P-H based reagents,<sup>25</sup> various metal oxidants<sup>26</sup> or reductants<sup>27-28</sup> or others.<sup>29</sup> However, these traditional methods generating alkyl or benzoyl radicals typically require harsh reaction conditions such as harmful UV irradiation or high temperatures, stoichiometric amounts of hazardous reagents, or strong oxidants and reductants,

which limit their practical utility in synthetic chemistry. Herein, more sustainable and attractive synthetic strategies based on radical chemistry is desirable.

In recent years, visible-light-mediated photocatalysis has emerged as a powerful tool for the generation of a wide range of radical species, opening up new opportunities in synthesizing diverse organic scaffolds.<sup>30-37</sup> Upon the irradiation of light, photocatalysts (PCs) or photoactive molecules absorb the energy of photons and are promoted to excited state  $^*PC$ , enabling various chemical processes such as single electron transfer (SET), proton-coupled electron transfer (PCET) or energy transfer (ET).<sup>38-44</sup> These processes have expanded the range of accessible radical precursors, even revolutionized the way to carry out radical chemistry (**Scheme 2**). A key factor in this transformation is the photon itself, which serves as an ideal component for chemical reactions, acting as a traceless reagent, catalyst, or promoter that leaves no toxic residues in the final mixture.<sup>45-46</sup> All these unique features of photocatalysis make it an ideal and elegant strategy for achieving alkylation and benzoylation reactions, which are key steps in the synthesis of versatile natural products and biologically active molecules.<sup>47-48</sup>



**Scheme 2** Mechanistic pathways of photoredox catalysis. D: donor, A: acceptor, PC: photocatalyst

## 1.2 Photocatalyzed radical generation from carboxylic acids and their derivatives

The transformations of functional groups serve as a fundamental pillar of modern organic synthesis. Notably, the efficient interconversion of existing functional groups in widely accessible chemical feedstocks into other valuable functionalities has attracted significant attention in recent studies. Toward this goal, using carboxylic acids and their derivatives as starting materials is synthetically appealing, these privileged chemical entities are advantageous due to their abundant chemical sources, commercial availabilities and chemical versatility, which collectively enhance synthetic efficiency.

### 1.2.1 Alkyl radical generation via decarboxylation

Compared to transition-metal catalyzed reactions that typically rely on organohalides or pseudohalides as electrophiles coupled with organometallic intermediates,<sup>49-52</sup> which are mostly moisture-sensitive and require fresh preparation, photocatalyzed decarboxylative reactions have provided a powerful platform to construct diverse carbon-carbon and carbon-heteroatom bonds.<sup>53-54</sup> Among them, using readily accessible alkyl carboxylic acids and their derivatives to generate versatile alkyl radicals are appealing. Those alkyl radicals from photochemical decarboxylation are synthetically equivalent to nucleophilic organometallic species in coupling reactions, this eliminates the need for expensive and labile carbon nucleophilic reagents. Furthermore, under oxidative conditions, alkyl species with electrophilic reactivity are possibly generated via decarboxylation and serve as a substitute of alkylhalides, which are more challenging in transition-metal catalyzed coupling reaction due to the risk of  $\beta$ -hydride elimination of alkyl metal components formed in situ during catalytic cycle. Therefore, many efforts have been devoted to developing photocatalyzed decarboxylative reactions employing aliphatic carboxylic acids and their derivatives as C(sp<sup>3</sup>) source, with the purpose of complex and functional molecules synthesis.<sup>55-57</sup>

#### 1.2.1.1 Reactions involving carboxylic acids

The nature of organic fragments attached to the carboxylic acid (COOH) group can have a significant impact on radical generation, radical stability and subsequent coupling reactions. For instance, the bond dissociation energy (BDE) of the alkyl-COOH bond (~380 kJ/mol) is lower than that of the vinyl-COOH (435 kJ/mol) and arene-COOH (426 kJ/mol) bonds. This difference arises from the stronger C(sp<sup>2</sup>)-COOH bond, making it easier to generate alkyl radicals from alkyl carboxylic acids via decarboxylation under relatively mild conditions.<sup>58-60</sup> Additionally, carboxylic acids with benzylic, allylic,  $\alpha$ -carbonyl, or  $\alpha$ -heteroatom substituents exhibit higher reactivity compared to other less reactive carboxylic acids.<sup>61-64</sup> Regardless of the cleavage efficiency of diverse carboxylic acid bonds, decarboxylative reactions involving carboxylic acids can be broadly categorized into three types from a photocatalytic perspective:

##### I redox-neutral photocatalysis

In a redox-neutral photocatalysis, decarboxylation proceeds through the action of the light and photocatalysts without requiring any external stoichiometric oxidants or reductants, this process features a photoredox catalyst-mediated electron shuttle cycle between two reactants, which is the key to decarboxylative coupling.

##### II dual catalysis.

Dual catalysis, also referred to as metallaphotocatalysis, combines redox-neutral photocatalysis with transition metal co-catalysis. In this pathway, a radical species, generated by the photocatalyst, reacts with an intermediate formed via the oxidative addition of a low-valent transition metal catalyst into an organic (pseudo) halide. This process is followed by reductive elimination, yielding targeted product.

### III with super-stoichiometric external oxidant

In a few examples, excess oxidants are required in oxidative decarboxylative reaction.

Some pioneered works belong to **type I** are presented here.

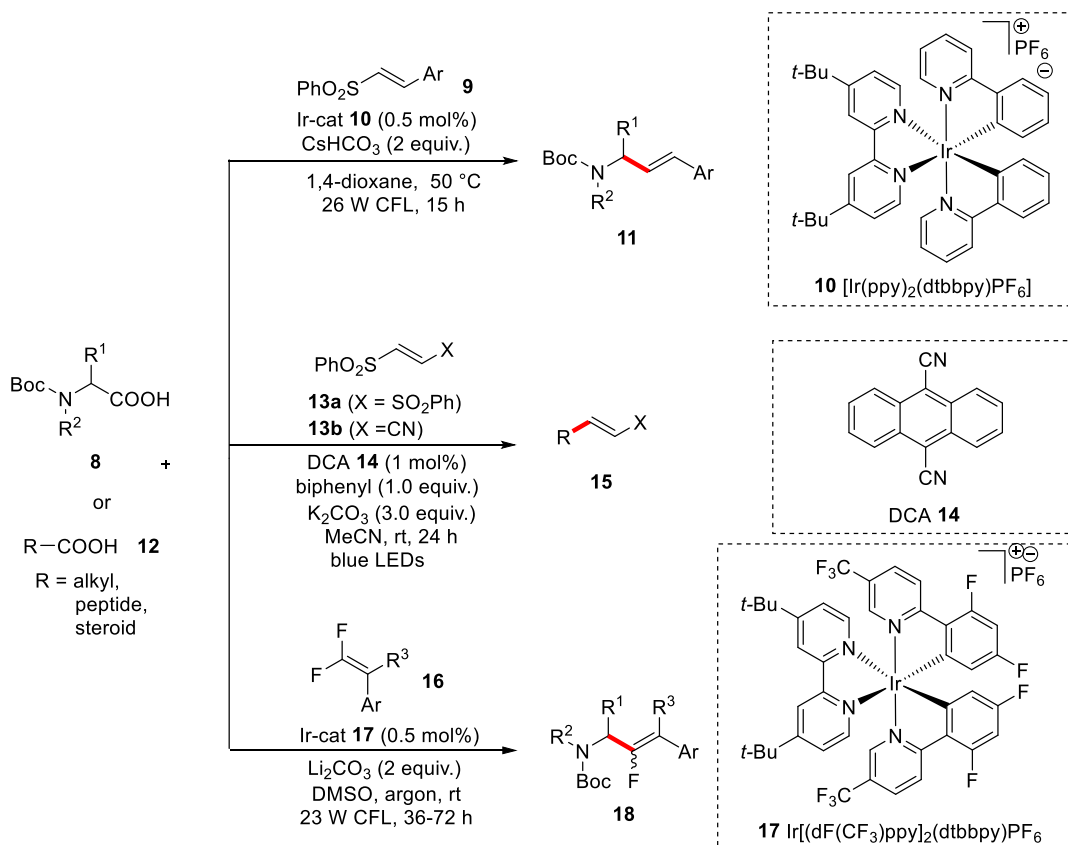
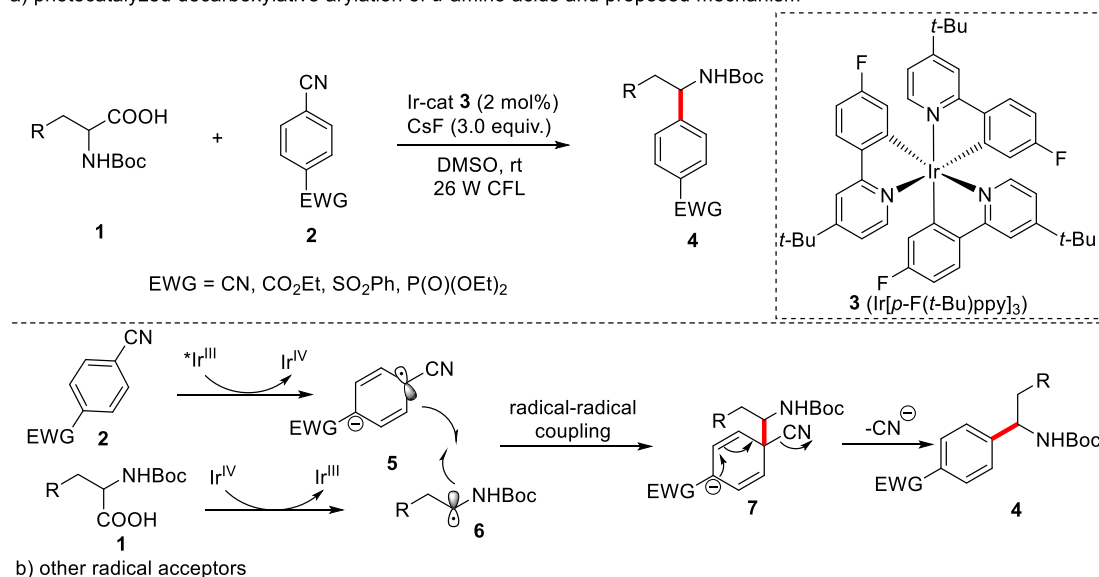
In 2007, Yoshimi and Hatanaka group reported decarboxylative reduction of free aliphatic carboxylic acids via a photogenerated radical cation of phenanthrene, with thiols serving as hydrogen atom donors.<sup>65</sup> During this process, C(sp<sup>3</sup>)-C(sp<sup>2</sup>) coupling side reactions were observed between alkyl radicals generated from carboxylic acids and 1,4-dicyanobenzene. Soon after, this side reaction was systematically explored, and revealed that a lot of aliphatic carboxylate ions could couple with dicyanobenzenes in the presence of phenanthrene under irradiation with a 500W high-pressure mercury lamp through a Pyrex filter, which restricts the light to > 300 nm wavelength.<sup>66</sup>

Recognizing the potential application of these C(sp<sup>3</sup>)-C(sp<sup>2</sup>) coupling products, in 2014 MacMillan group disclosed a redox-neutral decarboxylative coupling of  $\alpha$ -amino acids and electron-deficient cyanoaromatics (**Scheme 3a**).<sup>67</sup> Inspired by their earlier work involving Ir(ppy)<sub>3</sub>-mediated single electron reduction of 1,4-dicyanobenzene,<sup>68</sup> the more strongly oxidizing Ir[*p*-F(*t*-Bu)ppy]<sub>3</sub> **3** (E<sub>1/2red</sub> [Ir(IV)\*/Ir(III)] = -1.67 V vs SCE) was identified as a suitable photocatalyst to promote this decarboxylative arylation. In the optimized condition, the  $\alpha$ -amino acid **1** and cyanoarene **2** could smoothly react to afford desired product **4** utilizing iridium photocatalyst **3** and CsF as a base in DMSO under the irradiation of a compact fluorescent lamp (CFL). This method was proved efficiently for a number of  $\alpha$ -amino and  $\alpha$ -oxy acids, which underwent radical-radical coupling with cyanoarenes bearing electron-deficient substituents including nitrile, sulfonyl, carboxylic ester and phosphonate, offering rapid access to prevalent benzylic amine architectures. Compared to previous work of Yoshimi and Hatanaka,<sup>66</sup> this protocol is more operative due to a simple, energy-efficient CFL without the need of specialized glass apparatus connected with mercury lamp. In the proposed reaction pathway, cyanoarene **2** is converted to radical anion **5** through the photoexcited iridium photocatalyst **3**. Subsequently, single electron oxidation of protected  $\alpha$ -amino acid **1** generates relatively stable  $\alpha$ -aminoalkyl radical **6**. Finally, the coupling of radical **5** and radical **6** formed target product **4**, accompanied by the elimination of cyanide.

In 2016, Opatz reported transition-metal-free decarboxylative arylation of carboxylic acids with cyanobenzenes, a loading of 75 mol% of inexpensive organic photosensitizer phenanthrene was used under conditions similar to those reported by Yoshimi and Hatanaka.<sup>66</sup> This approach exhibited a broader substrate scope, encompassing  $\alpha$ -amino,  $\alpha$ -oxy,  $\alpha$ -benzyl and  $\alpha$ -tertiary carboxylic acids.<sup>69</sup> Three years later, Wang group developed an improved transition-metal-free protocol using 3-amino-9H-fluorene-2,4-dicarbonitrile as an organo-photocatalyst. Remarkably, only 2 mol% of the catalyst was required for effective decarboxylative cross-coupling with aromatic nitriles, significantly enhancing the reaction efficiency and practicality.<sup>70</sup>

In addition of C(sp<sup>3</sup>)-(hetero)aryl C(sp<sup>2</sup>) bond formation in decarboxylative reaction, in 2014, Noble and MacMillan disclosed a photocatalytic decarboxylative alkenylation.<sup>71</sup> With the treatment of *N*-Boc- $\alpha$ -amino acid **8** with vinyl sulfone **9** in the presence of photocatalyst [Ir(ppy)<sub>2</sub>(dtbbpy)]PF<sub>6</sub> **10** and CsHCO<sub>3</sub> as the base under the irradiation of 24 W CFL in 1,4-dioxane, various allylic amines

a) photocatalyzed decarboxylative arylation of  $\alpha$ -amino acids and proposed mechanism



**Scheme 3** Redox-neutral photocatalyzed decarboxylative reaction for constructing C(sp<sup>3</sup>)-C(sp<sup>2</sup>) bond

**11** could be obtained in good yields and with great *E/Z* selectivity (*E/Z* > 94:6) (**Scheme 3b**). A variety of  $\beta$ -(hetero)aryl vinyl sulfones bearing electron-rich and electron-deficient aromatic rings performed well with a range of  $\alpha$ -amino acids, providing a complementary method to allyl amines in comparison to stoichiometric metal-based methods.<sup>72</sup>

Moreover, Opatz and coworkers reported an efficient transition-metal free decarboxylative synthesis of  $\beta$ -alkylated vinyl sulfones or (acrylic) nitriles from structurally diverse carboxylic acids **12** including peptides and steroids, 1,2-bis(phenylsulfonyl)ethylenes **13a** or 1-cyano-2-phenylsulfonyl

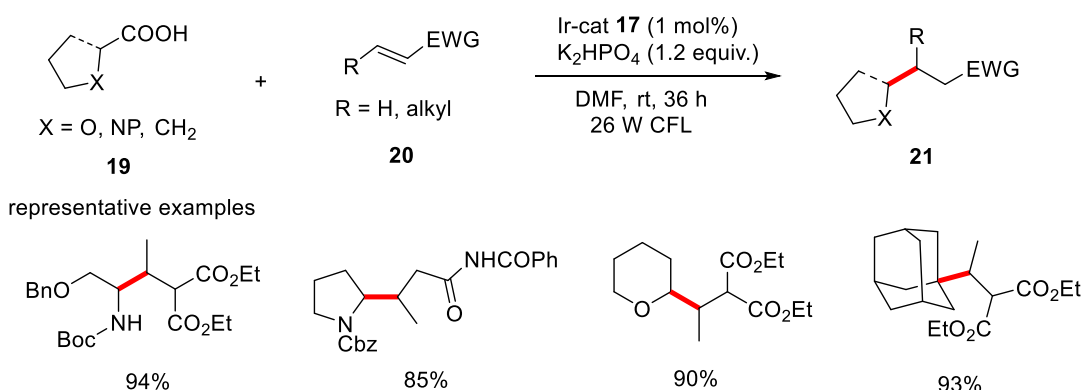
ethylenes **13b** was demonstrated as viable radical acceptors in the presence of 9,10-dicyanoanthracene (DCA **14**) and redox mediator biphenyl (**Scheme 3b**).<sup>73</sup>

Notably, *gem*-difluoroalkenes **16** were reported by Fu group to react with  $\alpha$ -amino acids **8** with Ir[dF(CF<sub>3</sub>)ppy]<sub>2</sub>(dtbbpy)PF<sub>6</sub> **17**, and Li<sub>2</sub>CO<sub>3</sub> in DMSO irradiated by 23 W CFL under argon atmosphere, a monofluoroallylamine mixture **18** of *Z*-isomer and *E*-isomer was obtained efficiently in this decarboxylative vinylation regardless of electronic properties of aryl rings attached to *gem*-difluoroalkenes (**Scheme 3b**).<sup>74</sup>

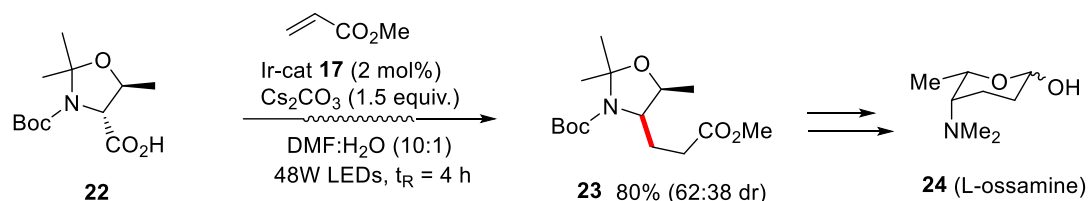
Among the earliest examples for forging C(sp<sup>3</sup>)-C(sp<sup>3</sup>) bonds via decarboxylative coupling, in 2014, the MacMillan group developed a radical-mediated decarboxylative coupling of carboxylic acids **19** with electron-deficient alkenes **20** using iridium photocatalyst **17** (1 mol%) (**Scheme 4a**).<sup>75</sup> The reaction has a broad substrate scope of carboxylic acids including  $\alpha$ -amino acids,  $\alpha$ -oxy acids, and secondary and tertiary alkyl carboxylic acids. Additionally, a diverse array of electron-deficient olefins, such as  $\alpha,\beta$ -unsaturated esters, sulfones, imides, malonates and maleates, were good Michael acceptors in this decarboxylative 1,4-conjugate addition reaction. Notably, unlike earlier methods reported by the Yoshimi and Hatanaka group,<sup>76</sup> this procedure operates under simple conditions using a household CFL without the need for specialized glass apparatus.

Subsequently this 1,4-conjugate radical addition strategy was extended to decarboxylative coupling of  $\alpha$ -heteroatom substituted carboxylic acids with a distinct class of styrene-based, electron-deficient alkenes.<sup>77</sup> The reaction was conducted under conditions similar to the MacMillan protocol.<sup>75</sup>

a) Ir-photocatalyzed decarboxylative 1,4-conjugate addition to alkenes



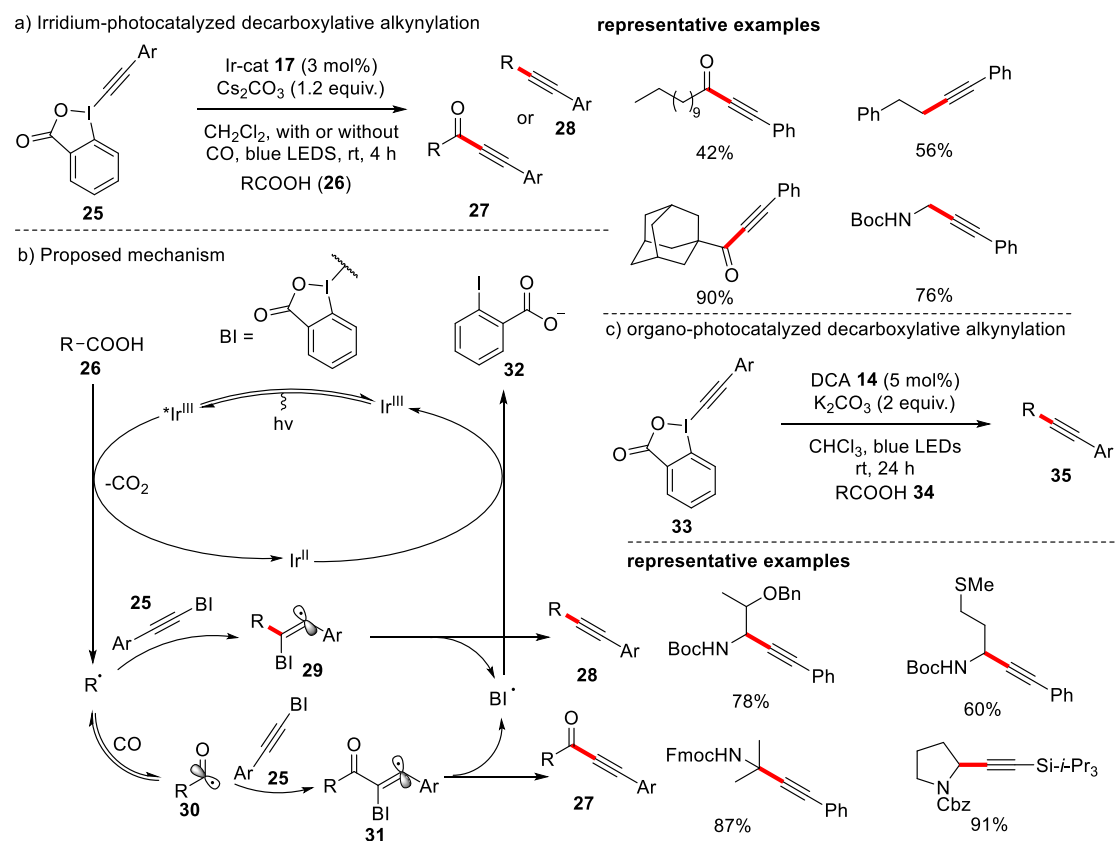
b) synthesis of L-ossamine



**Scheme 4** Redox-neutral photocatalysis for C(sp<sup>3</sup>)-C(sp<sup>2</sup>) coupling

In 2017, the Fujimoto group elegantly extended the application of 1,4-conjugate radical addition method to the formal preparation of L-ossamine (**24**) prevalent in natural product ossamycin.<sup>78</sup> The protected *D*-threonine **22** was subjected to react with methyl acrylate under the conditions of Ir-catalyst **17**, Cs<sub>2</sub>CO<sub>3</sub> as the base, and a DMF/H<sub>2</sub>O (10:1) solvent system. The reaction was performed in a flow reactor, irradiated with blue LEDs, and maintained at a residence time (*t<sub>R</sub>*) of 4 hours to afford the addition product **23**, which was subsequently converted into *L*-ossamine **24** (**Scheme 4b**).

To expand the range of Michael acceptors in this photocatalyzed decarboxylative radical addition process, Aggarwal<sup>79</sup> in 2018 described a procedure involving the addition of alkyl radicals to vinyl boronic esters, which are relatively weakly electron-deficient alkenes compared to acrylates. Recently, Shah developed a Giese-type radical addition protocol for synthesizing racemic unnatural  $\alpha$ -amino acids by using a variety of carboxylic acids with dehydroalanine esters.<sup>80</sup>



**Scheme 5** Redox-neutral photocatalysis for C(sp<sup>3</sup>)-C(sp) bond formation

Regarding C(sp<sup>3</sup>)-C(sp) bond formation in decarboxylative coupling reaction, the Xiao and Lu group in 2015 reported visible light-induced decarboxylative alkynylation and carbonylative alkynylation of readily available carboxylic acids **26** with ethynylbenziodoxolones **25** as the alkynyating agent in the presence of Ir-cat **17** and Cs<sub>2</sub>CO<sub>3</sub> as the base. A wide variety of alkyl carboxylic acids including  $\alpha$ -heteroatom substituted acids performed well in this coupling reaction.<sup>81</sup> Interestingly, the addition of carbon monoxide enabled the production of carbonylative products **27** with high efficiency. In contrast to Li's approach,<sup>82</sup> this reaction demonstrated a broader carboxylic acid substrate scope and good functional group tolerance, attributed to the absence of additional oxidants (**Scheme 5a**).

In the first proposed pathway, alkyl radical R<sup>•</sup>, generated through SET oxidation of carboxylic salt of **26** by photoexcited iridium catalyst, undergoes radical addition with reagent **25**, leading to alkenyl radical **29**. Then the elimination of benziodoxolonyl radical species (BI<sup>•</sup>) affords product alkyl-substituted alkyne **28**. In the second proposed pathway involving CO, the alkyl radical R<sup>•</sup> combines with CO to generate acyl radical **30**. This intermediate undergoes radical addition and elimination steps analogous to those in the first pathway, ultimately yielding the  $\alpha$ -carbonylated alkyne **27**. Within the photocatalytic cycle, the iridium catalyst in its Ir<sup>II</sup> state reduces the benziodoxolonyl radical BI<sup>•</sup>, producing byproduct **32** and regenerating the Ir<sup>III</sup> photocatalyst to

Soon after, DCA **14** as a more cost-effective alternative to expensive iridium photocatalyst was investigated to catalyzed this photoredox decarboxylative alkynylation by Li and co-workers (**Scheme 5c**).<sup>83</sup> Diverse  $\alpha$ -heteroatom substituted and tri-alkylsilyl substituted alkyne **35** were efficiently synthesized under the optimized conditions of DCA **14** (5 mol%), K<sub>2</sub>CO<sub>3</sub> (2.0 equiv.) in CHCl<sub>3</sub> irradiated with blue LEDs for 24 h.

**a) Ir-catalyzed asymmetric decarboxylative arylation**

Reaction scheme showing the Ir-catalyzed asymmetric decarboxylative arylation of **36** (R<sup>1</sup>-X-CH(R<sup>2</sup>)-COOH) with aryl bromide **37** (R-Br) to form product **39** (R<sup>1</sup>-X-CH(R<sup>2</sup>)-Ar). Conditions: Ir-cat **17** (1 mol%), NiCl<sub>2</sub>•DME (10 mol%), dtbbpy **38** (15 mol%), Cs<sub>2</sub>CO<sub>3</sub> (1.5 equiv.), DMF, 26 W CFL, rt, 72 h.

**Representative examples**

Y = I, 74%  
Y = Br, 82%  
Y = Cl, 65%  
X = Br, 83%

**proposed mechanism**

The mechanism involves Ir(III) species **40** reacting with **36** to form Ir(III) species **41** and **39**. Ir(III) species **41** is then reduced by Ar-Y **37** to Ir(II) species **42**, which is further reduced to Ir(I) species **43** by Ir(III) species **40**. Ir(I) species **43** reacts with **36** to form Ir(III) species **40** and **39**.

**b) photoredox/Ni-catalyzed asymmetric decarboxylative arylation**

Reaction scheme showing the photoredox/Ni-catalyzed asymmetric decarboxylative arylation of **43** (R-CH(R<sup>2</sup>)-COOH) with aryl bromide **44** (Ar-Br) to form product **46** (R-CH(R<sup>2</sup>)-Ar). Conditions: Ir-cat **17** (1 mol%), NiCl<sub>2</sub>•DME (2 mol%), ligand **45** (2.2 mol%), TBAI (10 mol%), Cs<sub>2</sub>CO<sub>3</sub> (1.8 equiv.), DME:toluene (1:20), blue LEDs, 18°C, 36 h.

**c) photoredox/Ni-catalyzed enantioselective decarboxylative arylation**

Reaction scheme showing the photoredox/Ni-catalyzed enantioselective decarboxylative arylation of **47** (R-CH(R<sup>2</sup>)-COOH) with aryl bromide **48** (Ar-Br) to form product **50** (R-CH(R<sup>2</sup>)-Ar). Conditions: 4CzIPN (4 mol%), NiCl<sub>2</sub>•DME (10 mol%), ligand **49** (15 mol%), Cs<sub>2</sub>CO<sub>3</sub> (1.5 equiv.), acetone, blue LEDs, rt, 15 h.

**Representative reactions demonstrating dual catalysis approach are summarized below.**

The pioneering work on metallaphotocatalysis was conducted by the MacMillan and Doyle groups,<sup>84</sup> who designed a dual catalyst system merging photocatalysis and nickel catalysis. This innovative approach enabled the decarboxylative coupling of a broad range of (hetero)aryl halides as sp<sup>2</sup>-hybridized carbon sources. Notably, this strategy provided a novel platform for C(sp<sup>3</sup>)-C(sp<sup>2</sup>) bond formation, which could not be achieved using either photoredox catalysis or transition metal catalysis alone. Under optimized conditions, the treatment of carboxylic acid **36** and aryl halide **37** with Ir-cat **17**, NiCl<sub>2</sub>·DME, the ligand 4,4'-di-*tert*-butyl-2,2'-bipyridine (dtbbpy, **38**) and base Cs<sub>2</sub>CO<sub>3</sub> in DMF under irradiation of 26 W CFL yielded desired product **39** in respectable yields. A variety of  $\alpha$ -amino acids and  $\alpha$ -oxy acids were proved to be highly efficient partners with aryl and



heteroaryl halides bearing diverse electron donating and electron-withdrawing substituents (**Scheme 6a**).

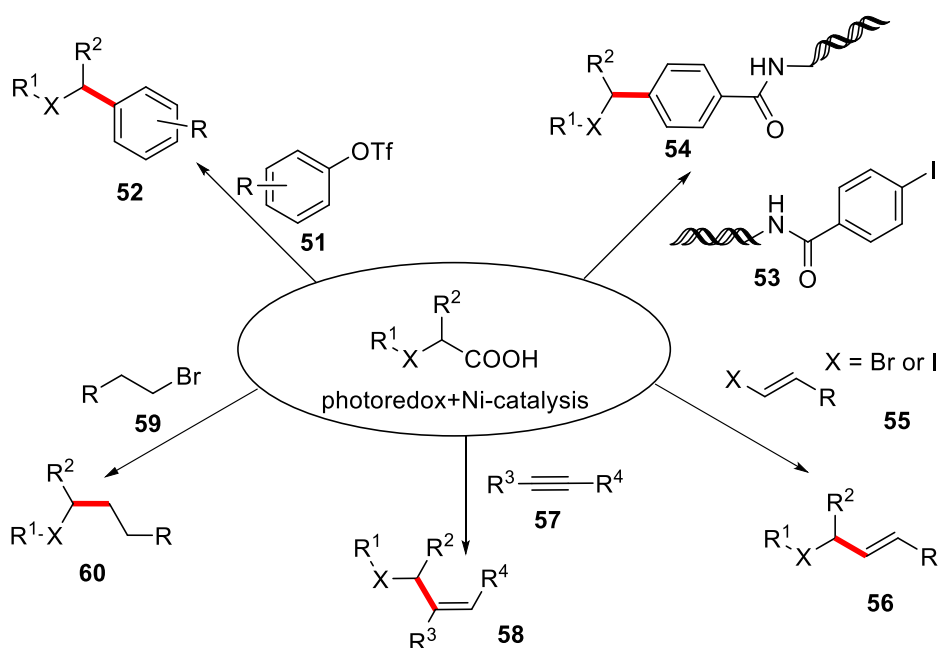
In the postulated mechanism, the SET oxidation of carboxylic salt of **36** by photoexcited  $^*\text{Ir}^{\text{III}}$  generates  $\alpha$ -amino/oxy alkyl radical **40** and  $\text{Ir}^{\text{III}}$  species. Then alkyl radical **40** is captured by intermediate **41** formed through oxidative addition of  $\text{Ni}^0$  catalyst to aryl halides **37**, leading to the formation of  $\text{Ni}^{\text{III}}$  complex **42**. Next the reductive elimination of **42** produces coupling product **39** and  $\text{Ni}^{\text{I}}$  species. Finally, the  $\text{Ni}^0$  catalyst and  $\text{Ir}^{\text{III}}$  photocatalyst are regenerated via SET process between  $\text{Ir}^{\text{III}}$  species and  $\text{Ni}^{\text{I}}$  species, thereby completing their respective catalytic cycle (**Scheme 6a**).

Furthermore, using cost-effective organophotocatalyst 4CzIPN (2,4,5,6-tetrakis(carbazol-9-yl)-1,3-dicyanobenzene) in place of more expensive iridium catalysts was demonstrating to be viable in these decarboxylative reactions, delivering diverse  $\text{C}(\text{sp}^3)\text{-C}(\text{sp}^2)$  cross-coupling arenes including bioactive aryl and heteroaryl-*C*-nucleoside.<sup>85</sup>

Later, this multi-catalyst system was extended to decarboxylative asymmetric synthesis of  $\text{C}(\text{sp}^3)\text{-C}(\text{sp}^2)$  bond by the Fu and MacMillan group in 2016.<sup>86</sup> While employing the same combination of an Ir-photocatalyst and a Ni-catalyst as used in their previous studies,<sup>84</sup> the chiral cyanobisoxazoline ligand **45** was introduced in place of the achiral bipyridine ligand for Ni. This modification enabled the enantioselective coupling process, facilitating the synthesis of chiral benzyl amine **46** with good to excellent enantiomeric excess (**Scheme 6b**). Unlike the racemic methods,<sup>84,87</sup> which allowed electronically unbiased aryl halides to serve as effective coupling partners, this enantioselective decarboxylative arylation was limited to electron-deficient aryl bromides as substrate.

Soon after, the Davidson and Bonifazi group expanded the substrate scope to  $\alpha$ -amino-*N*-heterocyclic carboxylic acid **47** for asymmetric decarboxylative  $\text{C}(\text{sp}^3)\text{-C}(\text{sp}^2)$  cross-coupling reaction with electron-withdrawing aryl bromides.<sup>88</sup> A synergistic merger of the organophotocatalyst 4CzIPN and a Ni-catalyst combined with a chiral pyridine-oxazoline **49** (PyOX) ligands was used to achieve an enantioselective synthesis of *N*-benzyl-substituted heterocycles **50** in good enantioselectivity and efficiency (**Scheme 6c**).

Building upon these foundational work, aryl triflates **51**<sup>89</sup> and DNA-tagged aryl iodide **53**<sup>90</sup> respectively were identified as competent substrates for visible-light mediated Ir/Ni-catalyzed decarboxylative arylation under conditions similar to those established by the MacMillan and Doyle protocol<sup>84</sup> (**Scheme 7**).



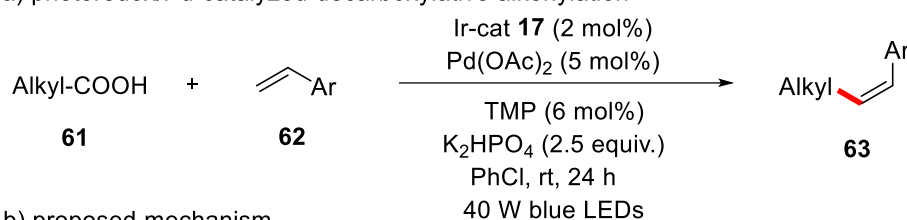
**Scheme 7** Photoredox/Ni-catalyzed decarboxylative reactions

As an extension of metallaphotoredox-catalyzed decarboxylative arylation,<sup>84</sup> MacMillan and co-workers reported radical decarboxylative alkenylation of alkyl carboxylic acid with vinyl halide **55** in 2015.<sup>91</sup> Diverse vinyl iodides and bromides give rise to vinylation products **56** in high efficiency and with good stereoselectivities (**Scheme 7**). Afterwards, they exploited a dual catalytic system for the decarboxylative hydroalkylation of unactivated terminal and internal alkynes **57**, delivering alkylated olefin **58** with excellent *Z/E* selectivity (**Scheme 7**).<sup>92</sup> Moreover, in 2016 the MacMillan group developed photoredox/Ni-catalyzed decarboxylative alkylation with alkyl bromides (**Scheme 7**).<sup>93</sup> A wide range of bromoalkanes bearing epoxide, alcohol, aldehyde, olefin ester and chloride functional groups were compatible partners to couple with  $\alpha$ -amino acids,  $\alpha$ -oxy acids, and primary and secondary alkyl carboxylic acids. This discovery represents a significant breakthrough in the realm of C-C bond formation since both coupling partners are bench-stable and commercially available.

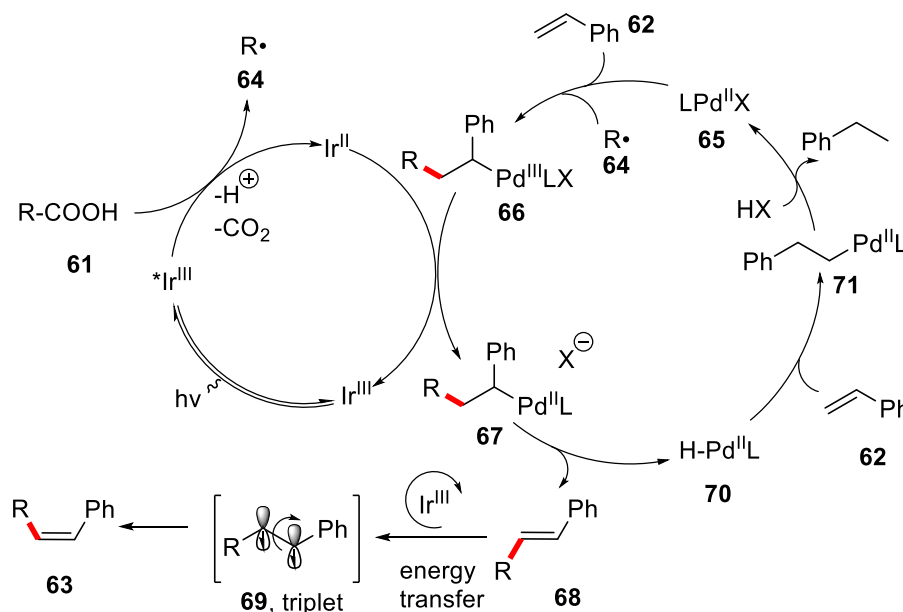
In an effort towards selectively synthesize thermodynamically disfavored (*Z*)-olefins, Na and Shang developed a decarboxylative cross-coupling reaction between carboxylic acids and styrenes by integrating photoredox catalysis with palladium catalysis.<sup>94</sup> Through extensive screening experiments, they identified a catalytic system comprising Ir-cat **17** and Pd(OAc)<sub>2</sub>/TMP (3,4,7,8-tetramethyl-1,10-phenanthroline) as highly effective in producing  $\beta$ -alkylated styrenes **63** with excellent (*Z*)-selectivity (**Scheme 8a**).

The proposed mechanism involves the alkyl radical **64** formed via SET oxidation of carboxylic salt of **61** by excited Ir photocatalyst, which is subsequently intercepted by styrene **62** and Pd<sup>II</sup> species **65** to form Pd<sup>III</sup> complex **66**. Then the SET reduction of **66** generates Pd<sup>II</sup> intermediate **67**, which undergoes a  $\beta$ -elimination to offer *E*-olefin **68** and Pd<sup>II</sup>-H species **70**. Next the Pd<sup>II</sup>-H species **70** inserts into styrene **62** to generate phenethyl Pd<sup>II</sup> **71** followed by protonation to give ethylbenzene and regenerated Pd<sup>II</sup> catalyst **65**. Simultaneously, the excited Ir photocatalyst in its triplet state facilitates the sensitization of *E*-olefin **68** to its triplet state **69** through energy transfer process. This energetically uphill step drives the conversion of the *E*-olefin **68** to its thermodynamically less stable (*Z*)-product **63**. (**Scheme 8b**).

a) photoredox/Pd-catalyzed decarboxylative alkenylation



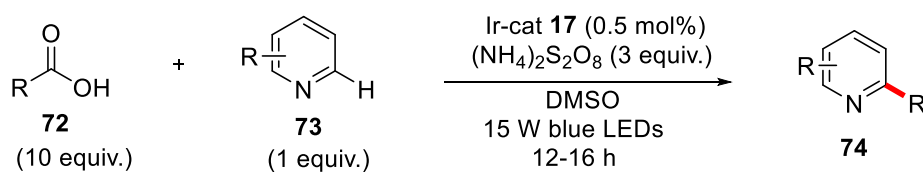
b) proposed mechanism



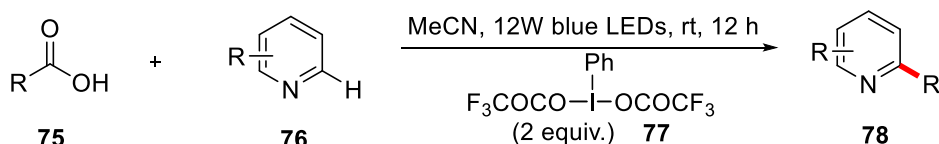
**Scheme 8** Photoredox/Pd-catalyzed decarboxylative alkenylation

In Minisci-type reaction research belong to **type III**, Glorius<sup>95</sup> employed excess carboxylic acid **72** to react with heterocycles **73** under irradiation of visible light in the presence of a combination of Ir-cat **17** and peroxydisulfate, generating alkylated heterocycles **74** (**Scheme 9a**). Afterward, a facile procedure for the expedient alkylation of electron-deficient *N*-heterocycles **76** with alkyl carboxylic acids **75** was developed. It proceeded under mild and metal-free conditions that relied upon visible light irradiation, albeit in the absence of a photocatalyst and acid additive (**scheme 9b**).<sup>96</sup>

a) photo-induced, Ir-catalyzed Minisci-type reaction



b) photocatalyst-free photo-induced Minisci-type reaction



**Scheme 9** Photoinduced external oxidants-required Minisci-type reaction

### 1.2.1.2 Reactions involving redox-active esters

Redox-active esters (RAEs) of carboxylic acids such as *N*-(acyloxy) phthalimides (NHPI esters) were first introduced to photochemistry by Okada<sup>97</sup> as a substitute for the Barton ester.<sup>98-101</sup> These

are readily prepared from a wide range of carboxylic acids and *N*-hydroxyphthalimide under standard coupling conditions. Visible-light-induced photocatalyzed decarboxylative coupling of redox-active esters provides a novel and versatile route to construct functionalized molecules<sup>56,102</sup> In this aspect, three distinct catalytic pathways are concluded based on the role of the radical formed and necessity for the inclusion of an additional reductant in the catalytic cycle:

**i. visible-light induced photocatalysis with additional reductants**

In this case, visible-light-activated photocatalyst facilitates a chemical transformation, with the help of an external reductant to drive the catalytic cycle forward. The reductant plays a crucial role in regenerating the photocatalyst and/or providing electrons for the reaction, enabling the overall process to proceed efficiently.

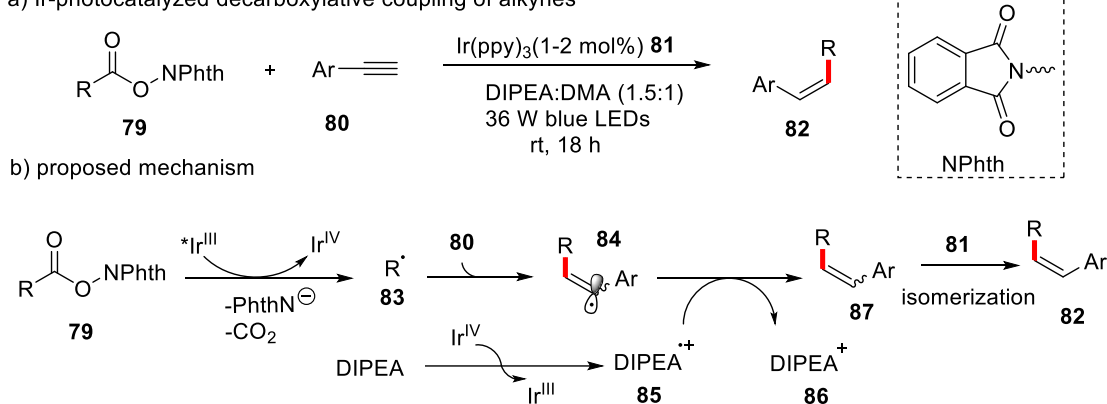
**ii. visible-light-induced dual catalysis**

By the merger of photocatalysis and another catalysis, this approach leverages the complementary reactivity of both catalytic systems, often resulting in chemical transformations that would be challenging or inefficient with a single catalyst.

**iii. visible-light-induced photocatalysis with radical intermediates as the reductant**

The key alkyl radical or derived radical, generated during the photocatalytic cycle, serves as the reductant to transfer electrons to the photocatalyst species or other intermediates. This results in their oxidation to carboncationic species, which are subsequently trapped by nucleophiles to form the final product. It is also a photo-mediated redox-neutral process and eliminates the need for external reductants by relying on in situ generated radicals, thereby making the process more self-sustaining and efficient.

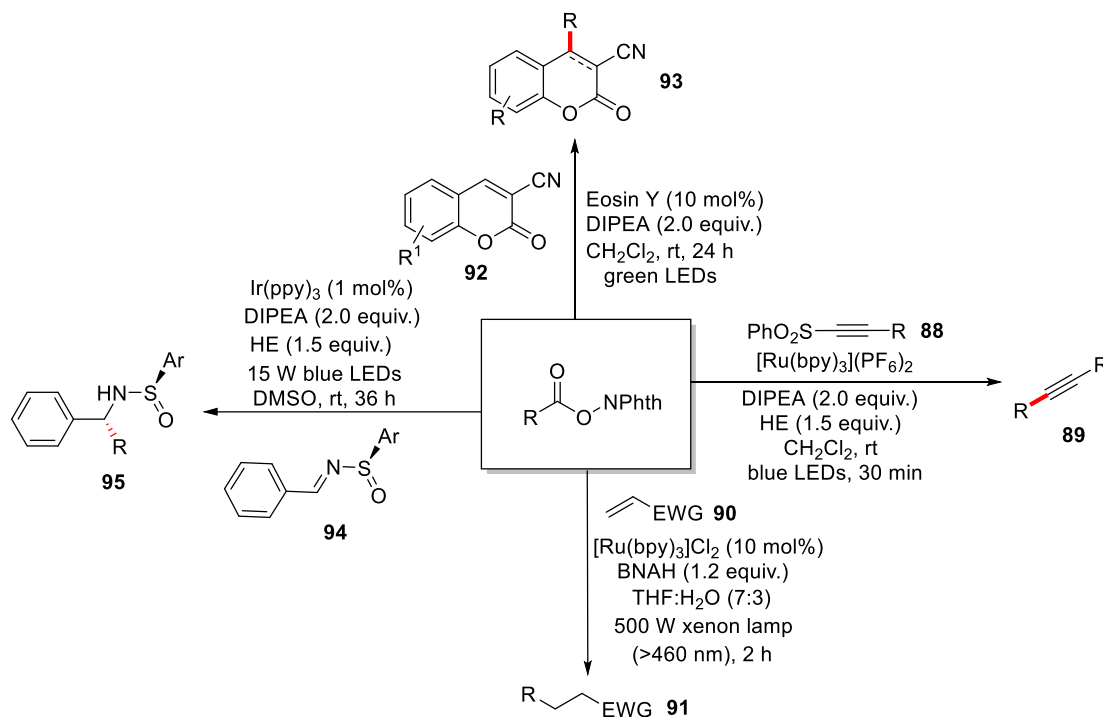
a) Ir-photocatalyzed decarboxylative coupling of alkynes



**Scheme 10** Ir-photoredox-catalyzed decarboxylative coupling with alkynes and its proposed mechanism

A representative example of **pathway i** is reported by Luo and co-workers.<sup>103</sup> They developed a visible-light-mediated Ir(ppy)<sub>3</sub>-catalyzed decarboxylative coupling of NHPI ester **79** with terminal aryl alkyne **80**, enabling the stereoselective synthesis of thermodynamically disfavored (*Z*)-alkene **82** (**Scheme 10a**). This approach features a broad substrate scope with no apparent sensitivity to the electronic properties and substitutional pattern of substrates. In the postulated mechanism, the SET reduction of NHPI ester **79** by photoexcited \*Ir<sup>III</sup> generates alkyl radical **83** and oxidized Ir<sup>IV</sup> species. Subsequently radical addition of **83** to alkyne **80** at the terminal position forms vinyl radical **84**. Concurrently, DIPEA reduces Ir<sup>IV</sup> species to regenerate Ir<sup>III</sup> photocatalyst while it is oxidized to DIPEA<sup>•+</sup> **85**. Then the hydrogen atom transfer from **85** to **84** affords alkylated alkenes **87**, which further isomerizes selectively to less stable (*Z*)-isomer **82** in the presence of photocatalyst Ir(ppy)<sub>3</sub> **81**. (**Scheme 10b**)

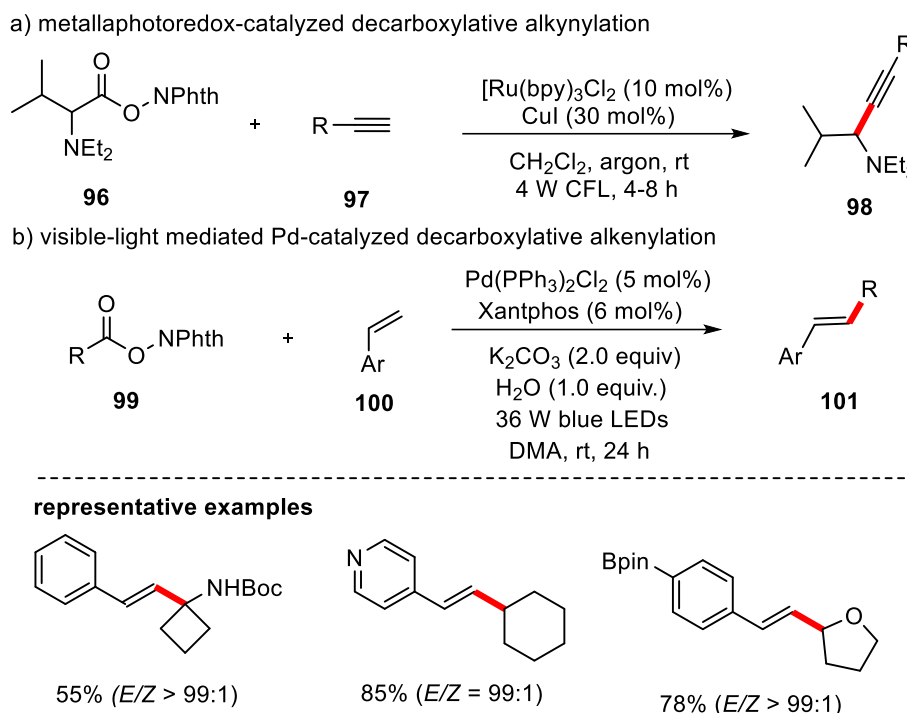
Some other decarboxylative reactions via **pathway i** are summarized in **Scheme 11**, different radical acceptors such as alkynyl phenyl sulfone **88**,<sup>104</sup> electron-withdraw alkene **90**,<sup>105</sup> 3-cyanocoumarin **92**,<sup>106</sup> *N*-sulfinaldimines **94**,<sup>107</sup> were demonstrated as competent substrates for coupling with NHPI esters under the combination action of the photocatalyst and the reductant (**Scheme 11**). These reactions yield C–C coupling products with high efficiency, highlighting the versatility and utility of this methodology.



**Scheme 11** Photoredox-catalyzed decarboxylative reactions with NHPI esters via pathway i

A representative example via **pathway ii** was reported in 2017 by Fu and co-workers,<sup>108</sup> they developed a metallaphotoredox-mediated protocol for the coupling of NHPI ester of *N,N*-dialkyl- $\alpha$ -amino acids **96** with terminal alkyne **97** bearing aliphatic or aromatic group, leading to synthetically useful propargylamines **98** (**Scheme 12a**).

One year later, the Fu and Shang group developed an irradiation-induced palladium-catalyzed decarboxylative Heck reaction between vinyl arenes and NHPI esters.<sup>109</sup> In this method, Pd catalyst Pd(PPh<sub>3</sub>)Cl<sub>2</sub> in combination with 4,5-bis(diphenylphosphino)-9,9-dimethylxanthene (Xantphos) under irradiation plays the role of traditional photocatalyst, inducing single-electron transfer to activate *N*-(acyloxy)phthalimides **99**. Accompanied Pd-catalyzed insertion and  $\beta$ -H elimination process, diverse secondary, tertiary, and quaternary carboxylates, including  $\alpha$ -amino acid derived esters were efficiently transformed to substituted styrene **101** with a high ratio of *Z/E* (**Scheme 12b**).



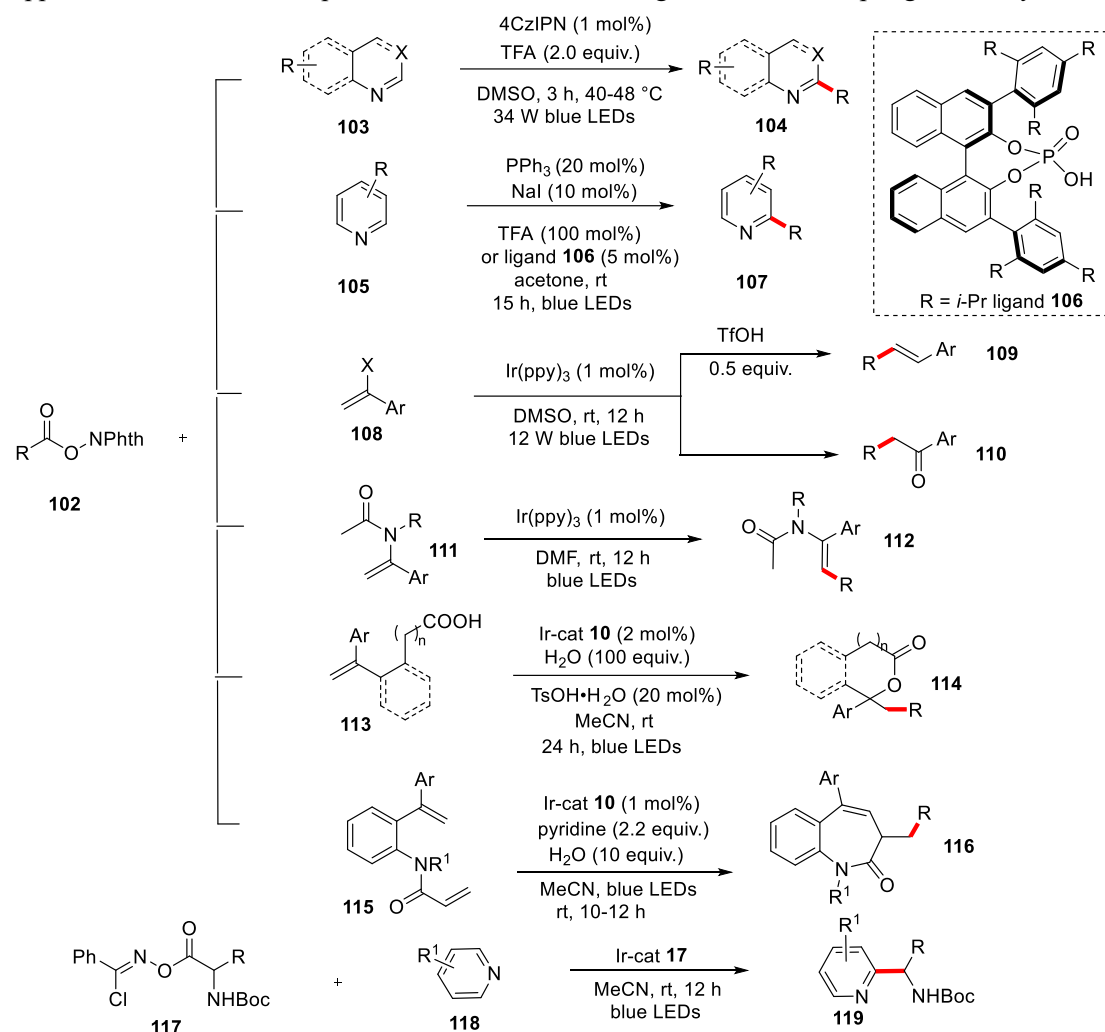
**Scheme 12** Photoredox-catalyzed decarboxylative reactions with NHPI esters via pathway ii

A classical reaction associated with **pathway iii** is decarboxylative Minisci-type reaction. In 2018, Sherwood and co-workers described a one-pot process for decarboxylative Minisci-type reaction using generated NHPI esters in situ with quinolines **103**.<sup>110</sup> The organic photocatalyst 4CzIPN was identified as highly suitable for this one-pot reaction and only near-stoichiometric levels of radical precursor was required, thereby enhancing the method's cost efficiency and practicality (**Scheme 13**). However, partly reactions proceeding at 48 °C resulted in varying amount of bis-alkylated heteroarenes including pyridine, quinoline and phthalazine.

Later, Shang and Fu discovered that a complex of PPh<sub>3</sub> and NaI under blue LEDs irradiation could efficiently catalyze the decarboxylative Minisci-type addition of NHPI esters to heteroarenes.<sup>111</sup> This phosphine-iodide-based photoredox system offers significant advantages for industrial applications and large-scale synthesis due to its low cost compared to traditional dye-based or metal-based photocatalysis. In their study, the NHPI esters **102** of various alkyl carboxylic acids were treated with heteroarene **105** in the presence of catalytic PPh<sub>3</sub> and NaI, along with TFA as an acid additive, in acetone under blue LED irradiation, yielding the alkylated *N*-heteroarene **107** with high efficiency (up to 97% yield). Notably, replacing TFA with chiral biphenyl-based phosphoric acid **106** enabled the enantioselective synthesis of heteroaryl-substituted amines, marking a significant advancement in asymmetric Minisci-type alkylation (**Scheme 13**). These findings highlight the potential of this EDA complex system in the development of cost-effective and sustainable methodologies for organic synthesis.

Through **pathway iii** certain alkenes were proved to be efficiently partners to couple with NHPI esters, providing a mild method to construct alkylated alkenes via radical addition or heterocycles via radical cascade cyclization. (**Scheme 13**)<sup>112-115</sup> Additionally, *N*-hydroxybenzimidoyl chloride (NHBC) esters **117** as an alternative of NHPI esters were applied to photoredox decarboxylative Minisci-type coupling with heteroarenes. (**Scheme 13**)<sup>116</sup> Interestingly, this method obviates the need for any acidic additives, distinguishing it from the majority of Minisci-type reactions that

typically proceed under redox-neutral conditions and necessitate the protonation of *N*-heteroarenes to facilitate radical addition. This result expanded the scope of Minisci-type reactions, offering new opportunities for the development of acid-free methodologies in radical coupling chemistry.



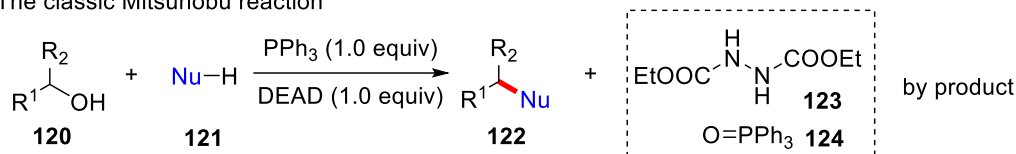
**Scheme 13** Photoredox-catalyzed decarboxylative reactions with NHPI esters via pathway iii

### 1.2.2 Aroyl radical generation via P<sup>III</sup>-assisted deoxygenation

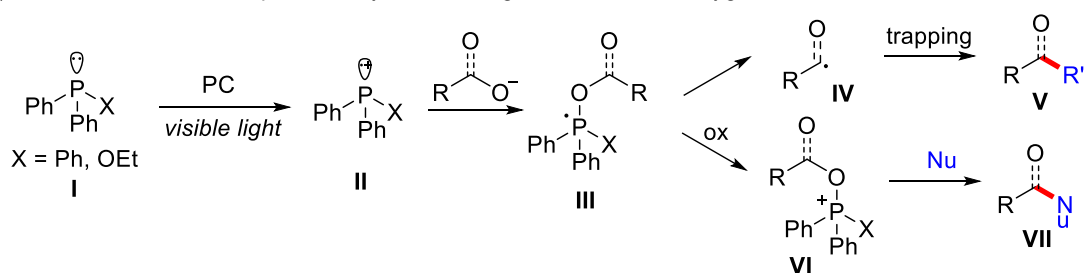
The Mitsunobu reaction<sup>117–119</sup> is a widely recognized method in modern organic synthesis for the substitution of hydroxyl groups in alcohols or carboxylic acids. This reaction utilizes the PPh<sub>3</sub>/diethyl azodicarboxylate (DEAD) system to overcome the inherent limitation of the hydroxyl group as a poor leaving group. Activation of the hydroxyl group is achieved through the formation of acyloxyphosphonium intermediates via phosphorus(III) reagents. (**Scheme 14a**) Despite its utility, the Mitsunobu reaction has significant drawbacks. It requires the use of stoichiometric amounts or slight excesses of DEAD, a toxic and potentially explosive oxidant, making it less suitable for large-scale synthesis. Furthermore, the process inevitably generates hydrazine derivatives as by-products, contributing to waste.<sup>120</sup> Therefore, the development of more atom-economic and practical methods for the efficient conversion of hydroxyl groups remains a highly desirable goal in organic synthesis. In recent years, photoredox and P<sup>III</sup>-mediated deoxygenative reactions provide a powerful platform to achieve hydroxyl-containing substrates conversion.<sup>121</sup> The general mechanism involves the SET oxidation of P<sup>III</sup> reagent **I** to phosphorous radical cation **II**. Subsequently this intermediate **II** combines with carboxylate salt to generate phosphoranyl radical **III**. Then two different processes

could occur. In the first pathway, the intermediate **III** experience  $\beta$ -selective C-O bond cleavage to product acyl or alkyl radical, followed by trapped by reaction partners to afford coupling products. In the second pathway, species **III** is oxidized to further phosphonium cations **VI**, then undergoes nucleophilic substitution to form target compounds **VII**. (Scheme 14b) Representative examples of these transformations are summarized here, highlighting the versatility and utility of this approach.

a) The classic Mitsunobu reaction



b) General mechanism of photocatalyzed P<sup>III</sup>-reagent-mediated deoxygenative reactions



**Scheme 14** P<sup>III</sup> reagent-mediated deoxygenative reactions

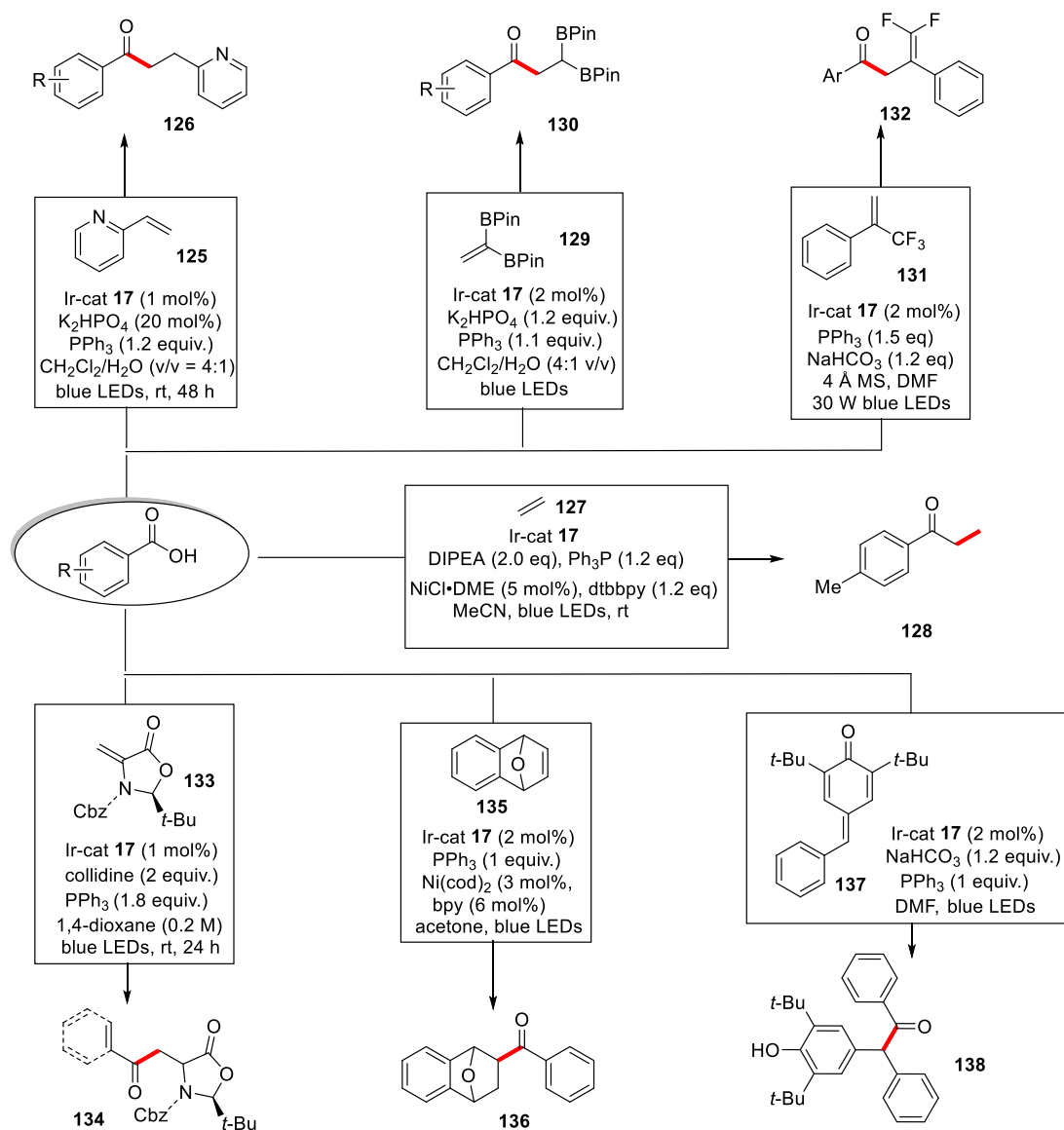
In order to synthesize a wide range of C(sp<sup>2</sup>)-C(sp<sup>3</sup>) coupling products, in 2018,<sup>122</sup> Zhu and Xie group made a great advancement for the streamlined synthesis of aromatic ketones from feedstock chemicals (Scheme 15a). In the optimized conditions, Ir-cat **17** as photocatalyst, K<sub>2</sub>HPO<sub>4</sub> as base, and PPh<sub>3</sub> as additive in CH<sub>2</sub>Cl<sub>2</sub>/H<sub>2</sub>O (v/v = 4:1) irradiated by blue LEDs were chosen. Commercially cheap aromatic carboxylic acids reacted smoothly with conjugate alkenes such as 2-vinyl pyridines **125**, styrenes and electron-deficient alkenes, affording structurally diverse ketones **126** in moderate to good yields. Notably, this synthetic robustness was supported by the late-stage modification of several pharmaceutical compounds and complex molecules. In the propose mechanism visible-light photoredox catalysis facilitates the direct deoxygenation of acids as acyl sources with PPh<sub>3</sub>, representing a distinct perspective on radical activation mode.

Afterwards, photoredox/nickel-catalyzed hydroacylation of ethylene **127** with aromatic acids was also reported by Xie and coworkers,<sup>123</sup> proving a general, practical and scalable method to prepare high-value-added aromatic ketone **128**. Beyond ethylene **127**, other alkenes like vinyl boronic esters **129**,<sup>124</sup>  $\alpha$ -trifluoromethyl alkene **131**,<sup>125</sup> Karady–Beckwith alkene **133**,<sup>126</sup> oxabenzonorbornadiene **135**,<sup>127</sup> and *p*-quinone methides **137**<sup>128</sup> featuring a merger of alkenyl and carbonyl moieties, were found to be suitable radical acceptors in deoxygenative coupling. These transformations offered wide acyl products with good yields under mild conditions (Scheme 15a).

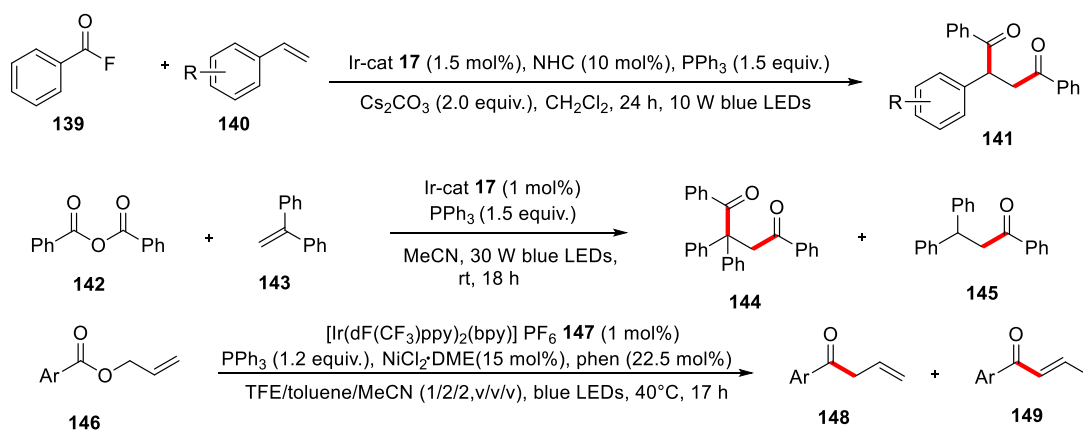
Moreover, several carboxylic acid derivatives including benzoyl fluorine **139**<sup>129</sup> and carboxylic acid anhydrides **142**<sup>130</sup> effectively engaged in PPh<sub>3</sub>-mediated deoxygenative reactions. These reactions facilitated the regioselective diacylation of alkenes, further broadening the scope of accessible acylated products. Additionally, the Tobisu<sup>131</sup> group demonstrated a synergistic photoredox and nickel-catalyzed method for converting allylic esters **146** into the corresponding ketones **148** or **149** through the formal deletion of an oxygen atom using PPh<sub>3</sub>. This innovative approach highlighted new opportunities for synthesizing acyl products, though challenges such as site-selectivities need further investigation (Scheme 15b).



a) photoredox PPh<sub>3</sub>-mediated deoxygenative coupling of aryl carboxylic acids for constructing C(sp<sup>2</sup>)-C(sp<sup>3</sup>) bond



b) photoredox PPh<sub>3</sub>-mediated deoxygenative coupling of aryl carboxylic acid derivatives for constructing C(sp<sup>2</sup>)-C(sp<sup>3</sup>) bond

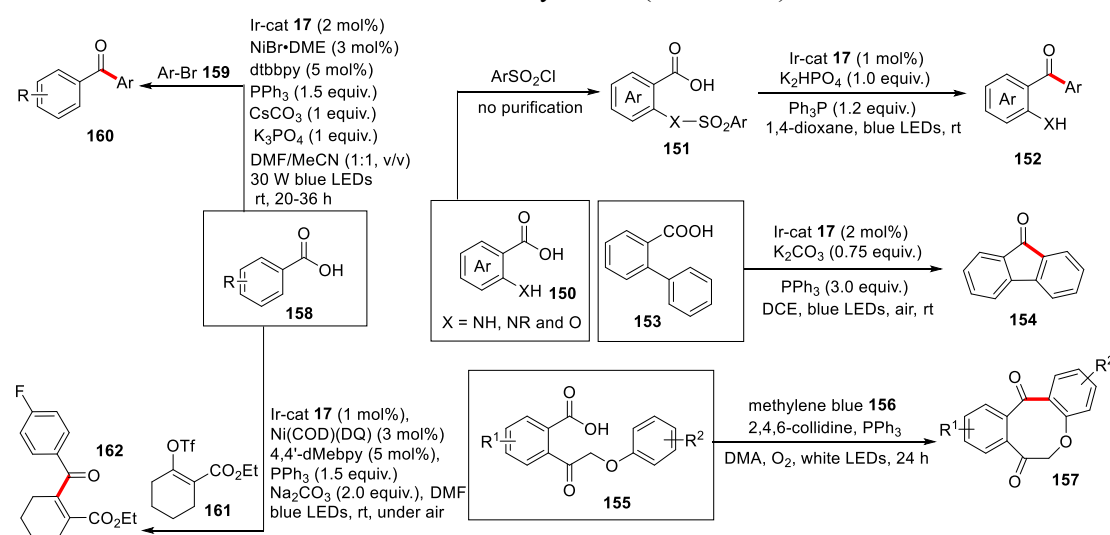


**Scheme 15** Photoredox-catalyzed deoxygenative reactions of carboxylic acids and derivatives for the construction of C(sp<sup>2</sup>)-C(sp<sup>3</sup>) bond

For the constructing of C(sp<sup>2</sup>)-C(sp<sup>3</sup>) coupling products, photocatalyzed P<sup>III</sup>-mediated

intramolecular deoxygenative reaction provide a viable approach. For examples, *ortho*-substituted benzoic acids **150**,<sup>132</sup> **153**,<sup>133</sup> and **155**<sup>134</sup> were discovered to prepare asymmetric diaryl ketones **152**, fluorenones **154**, eight-membered dibenzocycloketones **157** respectively. (Scheme 16) Although these diaryl ketone products were able to be gained efficiently, limited substrate scope restricts their broader applicability in synthetic chemistry.

With the continued advancement of metallaphotoredox system in modern organic synthesis, the Xie group in 2020 reported an upgrading protocol for ketone synthesis using commercially available carboxylic acids **158** and organohalides **159** (Scheme 16).<sup>135</sup> The combined action of Ir-cat **17** [Ir(dF(CF<sub>3</sub>)ppy)<sub>2</sub>(dtbbpy)]PF<sub>6</sub>, nickel catalyst NiBr·DME and phosphoranyl radical allows for concise synthesis of highly functionalize diaryl ketones or arylketones. Notably, this approach eliminates the need for pre-activation of carboxylic acids or the use of organometallic reagents, which are typically required in conventional protocols such as the Weinreb ketone synthesis, thereby representing this strategy practicality. Building on this work,<sup>135</sup> in 2022, they introduced vinyl triflates **161** to the PPh<sub>3</sub>-mediated deoxygenative coupling of carboxylic acids under similar Ir-photoredox/Ni-catalyzed conditions.<sup>136</sup> This approach enabled the highly selective synthesis of all-carbon tetrasubstituted olefins under mild conditions, even in the presence of significant steric hindrance and uncontrolled *Z/E* stereoselectivity issues. (Scheme 16)



**Scheme 16** Photoredox-catalyzed deoxygenative reactions of carboxylic acids for the construction of C(sp<sup>2</sup>)-C(sp<sup>2</sup>) bond

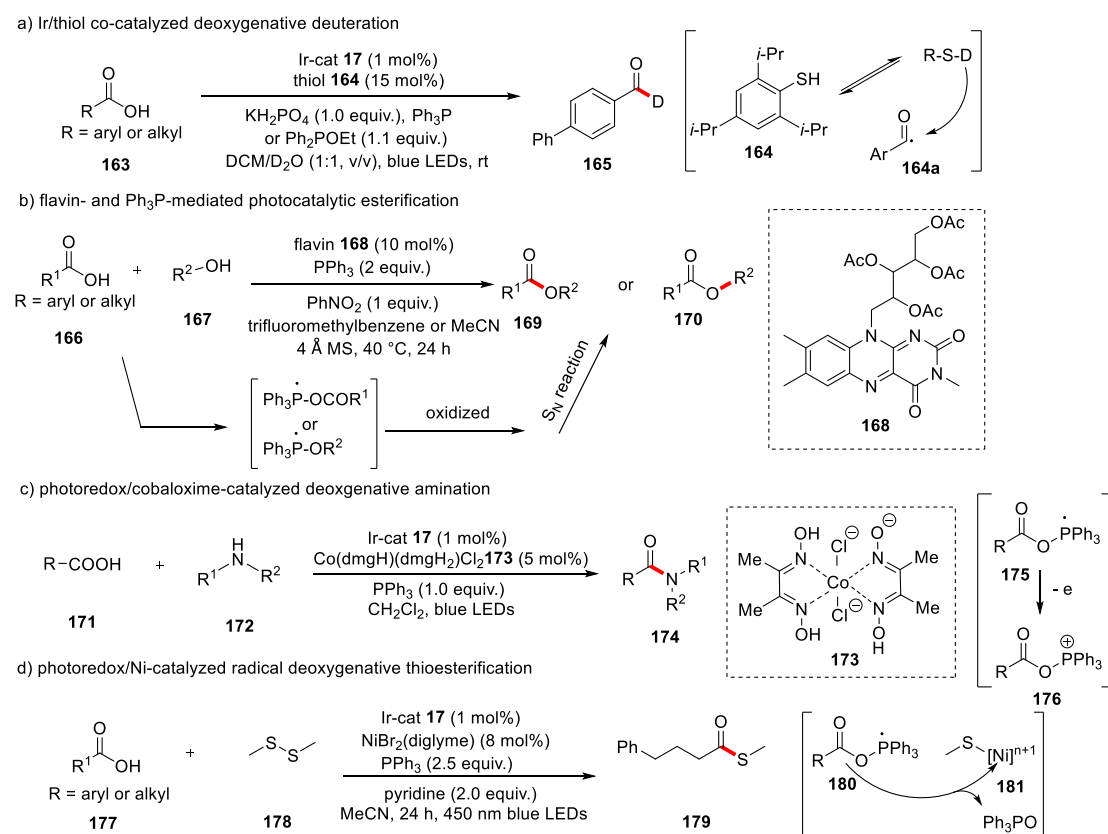
In 2018, Xie group developed a synergistic catalysis strategy for deoxygenative deuteration of carboxylic acids with D<sub>2</sub>O.<sup>137</sup> The optimized reaction conditions include [Ir(dF(CF<sub>3</sub>)ppy)<sub>2</sub>(dtbbpy)]PF<sub>6</sub> **17** as the photocatalyst, 2,4,6-trisopropylbenzenethiol **164** as the HAT catalyst, Ph<sub>3</sub>P or Ph<sub>2</sub>POEt as an oxygen-atom transfer reagent, and CH<sub>2</sub>Cl<sub>2</sub>/D<sub>2</sub>O (1:1, v/v) as the solvent. Under these conditions, the desired deuterated aldehydes **165** could be prepared in good yields with high levels of D incorporation (Scheme 17a). This precise and efficient deoxygenation strategy shows great promise for the late-stage deoxygenative deuteration of natural product derivatives and pharmaceutical compounds. The method's ability to achieve high deuterium incorporation under mild conditions makes it particularly valuable for applications in drug development and isotopic labeling studies.

As a complement to classic Mitsunobu reaction, in 2018 Cibulka and co-workers reported an organophotocatalyzed azodicarboxylate-free esterification of carboxylic acids.<sup>138</sup> This protocol

relied on flavin **168** (3-methyl riboflavin tetraacetate) as photocatalyst,  $\text{PPh}_3$  as deoxygenative reagent and  $\text{PhNO}_2$  as sacrificial oxidant under blue LEDs irradiation in the presence of 4Å molecular sieves (MS). The proposed mechanism involved alcohol nucleophilic substitution to crucial reactive phosphonium species. (**Scheme 17b**)

The utilization of secondary amines as nucleophiles in  $\text{PPh}_3$ -mediated photoredox-catalyzed deoxygenation coupling was developed by Zhao group in 2022 (**Scheme 17c**).<sup>139</sup> The combination of Ir-photocatalyst **17** and cobaloxime catalyst ( $\text{Co}(\text{dmgH})(\text{dmgH}_2)\text{Cl}_2$ ) **173** enables the catalytic generation of acyloxyphosphonium ions **176** for subsequent nucleophilic additions. This method provides a practical route to amines due to the avoidance of stoichiometric oxidants, making it possible for late-stage amidation of drug molecules.

Recently, Glorius, and Qi, and Temps group developed a radical thioesterification via nickel-catalyzed sensitized electron transfer.<sup>140</sup> Under the conditions of Ir-cat **17** as photocatalyst,  $\text{NiBr}_2(\text{diglyme})$  as metal catalyst,  $\text{PPh}_3$  as additives and pyridine as base in MeCN under irradiation of blue LEDs, diverse carboxylic acids could undergo deoxygenative coupling with dimethyl disulfide **178**, constructing C-S products with good efficiency (**Scheme 17d**). The mechanism involves the acyloxyphosphorous radical **180** trapped by Ni adduct **181**.



**Scheme 17** Photoredox-catalyzed deoxygenative reactions of carboxylic acids for the construction of C-D and C-heteroatom bond

### 1.3 Photocatalyzed radical generation via 1,5-HAT

The selective and efficient functionalization of specific C(sp<sup>3</sup>)-H bonds has long been a significant objective in synthetic chemistry, owing to their substantial synthetic utility.<sup>141-143</sup> However, achieving this remains challenging due to the intrinsically low reactivity of these bonds.<sup>144</sup> While transition-metal (TM)-catalyzed C-H activation is well-established,<sup>145-146</sup> radical-mediated hydrogen atom transfer (HAT) strategies have emerged as a compelling alternative.<sup>147-149</sup> These methods enable selective functionalization of remote C(sp<sup>3</sup>)-H bonds in complex molecules under relatively mild conditions. Early examples of 1,5-hydrogen atom transfer (1,5-HAT) include the Hofmann-Löffler-Freytag (HLF) and Barton reactions, both of which involve the generation of nitrogen- or oxygen-centered radicals.<sup>150-152</sup> These radicals undergo intramolecular 1,5-HAT to form carbon-centered radicals, which are subsequently functionalized, providing a regioselective approach to modify remote C(sp<sup>3</sup>)-H bonds. Despite being discovered in the late 19th century, the utility of 1,5-HAT with heteroatom-centered radicals for such transformations remained limited for decades due to the requirement for harsh reaction conditions. However, recent advancements in photochemistry have revitalized this field. By integrating visible-light photoredox catalysis with 1,5-HAT, diverse methods for the remote functionalization of C(sp<sup>3</sup>)-H bonds have been developed, greatly expanding the scope and applicability of this approach.<sup>153-154</sup> In this section, representative 1,5-HAT reactions triggered by carbon-centered radical are summarized

#### 1.3.1 Aryl radical-mediated 1,5-HAT

In 2016, Xu and co-workers reported an intramolecular radical cascade cyclization from 2-iodoacetanilides **182** under photocatalytic conditions.<sup>155</sup> The key step involved a 1,5-HAT process occurring at the transient aryl radical intermediate **182a**, which was generated through SET reduction by photoexcited \*Ir<sup>III</sup>. This step led to the formation of an alkyl radical **182b**, which subsequently underwent cyclization to afford the desired oxindole products **183** (Scheme 18a).

By utilizing this Ir-photocatalyzed system mediated by 1,5-HAT, the intermolecular coupling reactions involving 2-iodoarenes were also demonstrated to be feasible. These reactions enabled the construction of diverse coupling products, including C(sp<sup>3</sup>)-C(sp<sup>2</sup>),<sup>156-157</sup> C(sp<sup>3</sup>)-C(sp<sup>3</sup>),<sup>158</sup> C(sp<sup>2</sup>)-C(sp<sup>2</sup>),<sup>159</sup> and C(sp<sup>3</sup>)-P<sup>160</sup> bonds, thus showcasing the broad applicability of this methodology.

In 2020, Gevorgyan group introduced a visible-light-mediated Pd-catalyzed intramolecular C-H arylation of acetanilides **184** to synthesize oxindoles **185**.<sup>161</sup> The reaction features a key 1,5-HAT of hybrid aryl palladium intermediates **184a** to **184b**. Interestingly, aryl triflates **184** were utilized as precursors for the formation of the hybrid aryl palladium radical intermediates, although the precise mechanism governing this transformation has yet to be fully clarified (Scheme 18b).

Based on this pioneered work,<sup>161</sup> Chen, Yang et al devoted many efforts to this dual photoredox/palladium-catalyzed remote functionalization. In their research, this aryl-to-alkyl radical relay strategy was effectively applied to a variety of transformations, including desaturation of amides,<sup>162</sup> radical (cascade domino) Heck coupling,<sup>163-164</sup> desaturation/sulfonation cascade,<sup>165</sup> radical relay formal [5+2] reactions respectively<sup>166</sup>. These contributions have provided valuable insights into photoinduced palladium catalysis, significantly expanding the scope of this field.

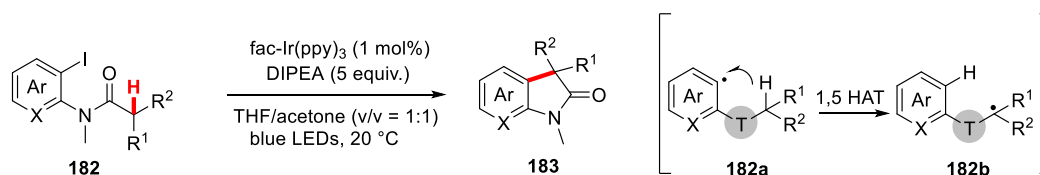
In 2022, Gevorgyan reported that cleavage of C-I bond of amines **186** could be induced by blue LEDs irradiation of EDA complex formed between amines **186** and B<sub>2</sub>cat<sub>2</sub> (2,2'-bis-1,3,2-benzodioxaborole). The following 1,5-HAT and coupling with another B<sub>2</sub>cat<sub>2</sub> lead to highly regio- and diastereo-selective synthesis of valuable  $\alpha$ -amino-boronates **187** (Scheme 18c). Remarkably,

this protocol provides a general, mild, transition-metal and strong-base-free method to achieve radical  $\alpha$ -C(sp<sup>3</sup>)-H borylation of aliphatic amines, enabling it employed in late-stage functionalization of structurally complex amines.<sup>167</sup>

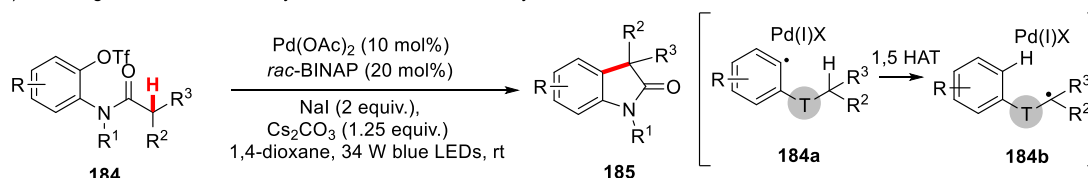
In 2023, Chen and co-workers reported an EDA complex strategy for the photoactivation of unprotected *o*-anilide aryl chlorides/iodides **188**.<sup>168</sup> In this method, toluene anion or *t*-BuOK forms an EDA complex with chloride, then blue light trigger of the EDA complex enabled the synthesis of heterocycles **189** (Scheme 18d).

Recently, Guo and Zhang group presented photoinduced EDA-enabled C(sp<sup>3</sup>)-H alkenylation of amines using *t*-BuOLi as electron donor under ambient air.<sup>169</sup> This strategy offered a general, operationally simple, and transition-metal free route to prepare prevalent and synthetically valuable allylic amines **192** in excellent *E/Z* and diastereoselectivities (Scheme 18e).

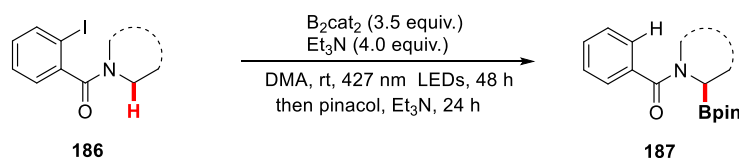
a) visible-light-mediated Ir-photocatalyzed 1,5-HAT reactions of aryl iodides



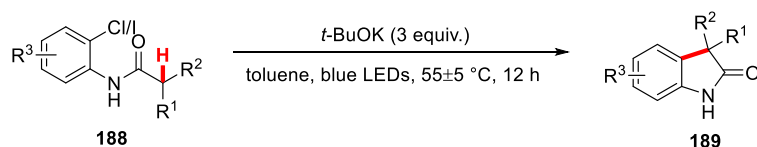
b) visible-light-mediated Pd-catalyzed 1,5-HAT reaction of aryl triflates



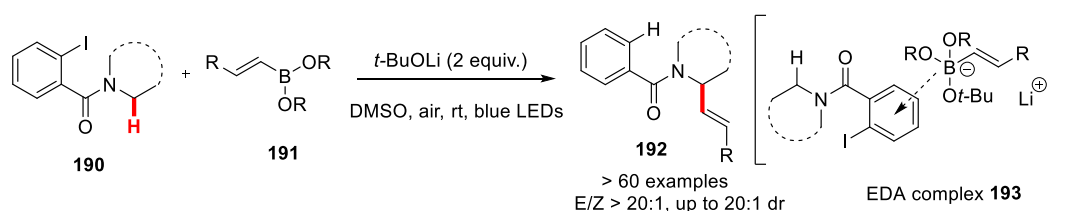
c) photoactivated metal-free radical  $\alpha$ -C-H borylation of aliphatic amines



d) visible-light-mediated 1,5-HAT of aryl chlorides and aryl iodides



e) photoinduced EDA-complex-enabled  $\alpha$ -C(sp<sup>3</sup>)-H alkynylation of amines



Scheme 18 1,5-HAT of aryl radicals

### 1.3.2 Vinyl radical-mediated 1,5-HAT

In 2019,<sup>170</sup> Zhu group reported a method for regioselectively incorporating alkenyl groups into aliphatic sites under Ir-photocatalyzed conditions. The pathway for this remote C(sp<sup>3</sup>)-H bond vinylation involves the CF<sub>3</sub>· generation by the SET reduction of Togni's reagent **195**. The following CF<sub>3</sub>· addition to propargyl alcohols **194** product vinyl radical **197**, Then 1,5-HAT of **197** form alkyl

radical species **198**, which undergoes intramolecular radical addition to C-C double bond to access five-membered ring intermediate **199**. Accompanied with ring-opening rearrangement and subsequent SET oxidation via photocatalyst, fluoroalkylated alkenes **196** could be obtained. The reaction demonstrates high product diversity and synthetic efficiency, enabling the synthesis of a wide range of synthetically valuable *E*-alkenes featuring tri-, di-, or mono-fluoromethyl as well as perfluoroalkyl groups. (Scheme 19a)

Subsequently, the same group demonstrated site-selective remote C(sp<sup>3</sup>)-H bond vinylation using sulfonyl chloride as radical precursors. A broad scope of  $\alpha,\beta$ -unsaturated sulfones were accessed under mild conditions.<sup>171</sup>

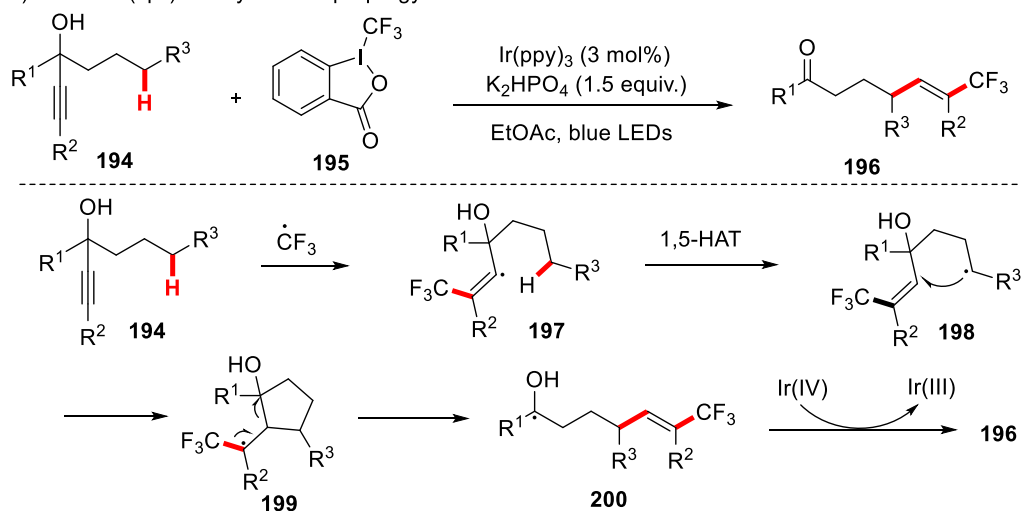
In 2019, Zhu and co-workers developed an efficient way to synthesize a variety of fluoroalkylated cyclic ketones **203** from alkynyl aldehydes **201** and bromofluoroalkanes **202**.<sup>172</sup> Two selective HAT processes under visible-light irradiation are the key of this transformation. On the one hand, the 1,5-HAT of alkenyl radical **204** provides formyl radical **205**, which then occurs a 5-exo-trig cyclization to afford alkyl radical **206**. On the other hand, a polarity-matched intermolecular HAT from nucleophilic 2-CH of THF to the electrophilic  $\alpha$ -perfluoroalkyl carbon radical **206** provides targeted compounds **203**. (Scheme 19b)

Later, Sun and co-workers reported similar HAT process presented at the coupling of 2-alkynylarylethers **207** and sodium sulfinate **208** under photocatalytic conditions. This domino approach enabled the synthesis of diverse sulfonyl substituted dihydrobenzofurans **209**. (Scheme 19c)<sup>173</sup>

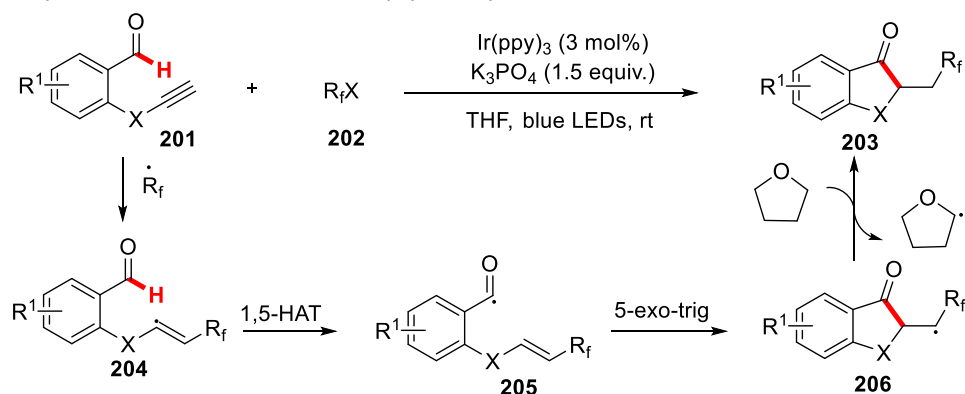
In 2020, Chu group reported a three-component decarboxylative coupling via Ir/Ni dual catalysis.<sup>174</sup> Treatment of cyclic oxalates **210**, aryl halide **211** and aliphatic alkyne **212** in the presence of photocatalyst Ir-cat **17**, nickel catalyst NiCl<sub>2</sub>(Py)<sub>4</sub>, ligand dtbbpy and additive bis(4-methoxyphenyl)methanone in DMSO irradiated by blue LEDs, providing a wide range of site-selective 1,3-difunctionalized cycloalkanes **213** in one single operation. The decarboxylative vinylation/C-H arylation relies on the formation of crucial alkyl radical **215** via 1,5-HAT of addition product **214**. And the subsequent Ni<sup>I</sup> complex **216** from **215** and Ni catalyst facilitates aryl coupling. (Scheme 19d)

In addition, Gevorgyan group focused on photocatalytic active palladium species and reported a novel and mild hydrogen atom translocation/atom-transfer radical cyclization cascade of vinyl iodide **217** via Pd(OAc)<sub>2</sub> and DPEphos (bis[(2-diphenylphosphino)phenyl] ether) system. This protocol involves a 1,5-HAT process mediated hybrid vinyl palladium radical intermediates, thus resulting in iodomethyl carbo- and heterocyclic structures **218**. (Scheme 19e)<sup>175</sup>

a) remote C(sp<sup>3</sup>)-H vinylation of propargyl alcohols



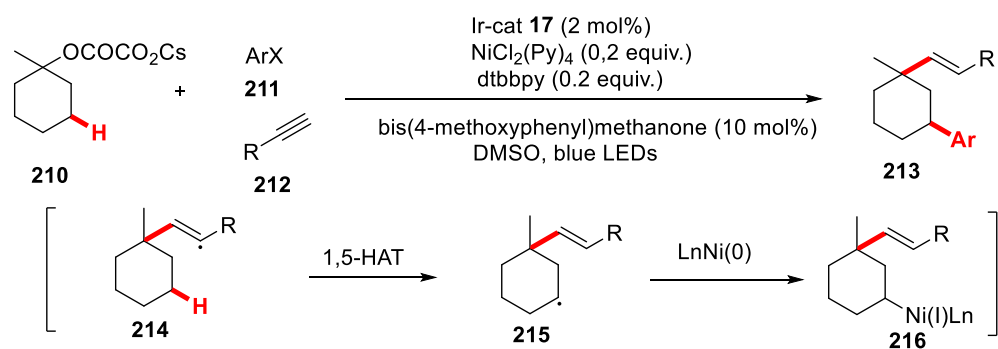
b) alkenyl radical-mediated 1,5-HAT of alkynyl aldehydes



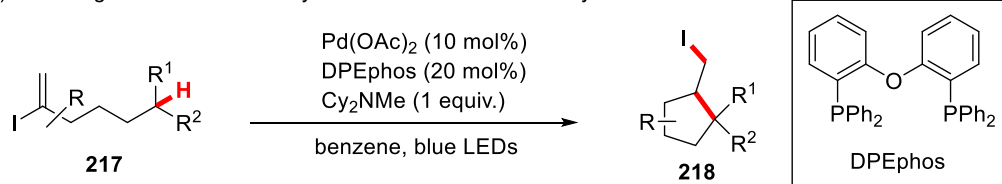
c) synthesis of sulfonfylated dihydrobenzofurans



d) photoredox/Ni-catalyzed decarboxylative vinylation/C-H arylation of cyclic oxalates



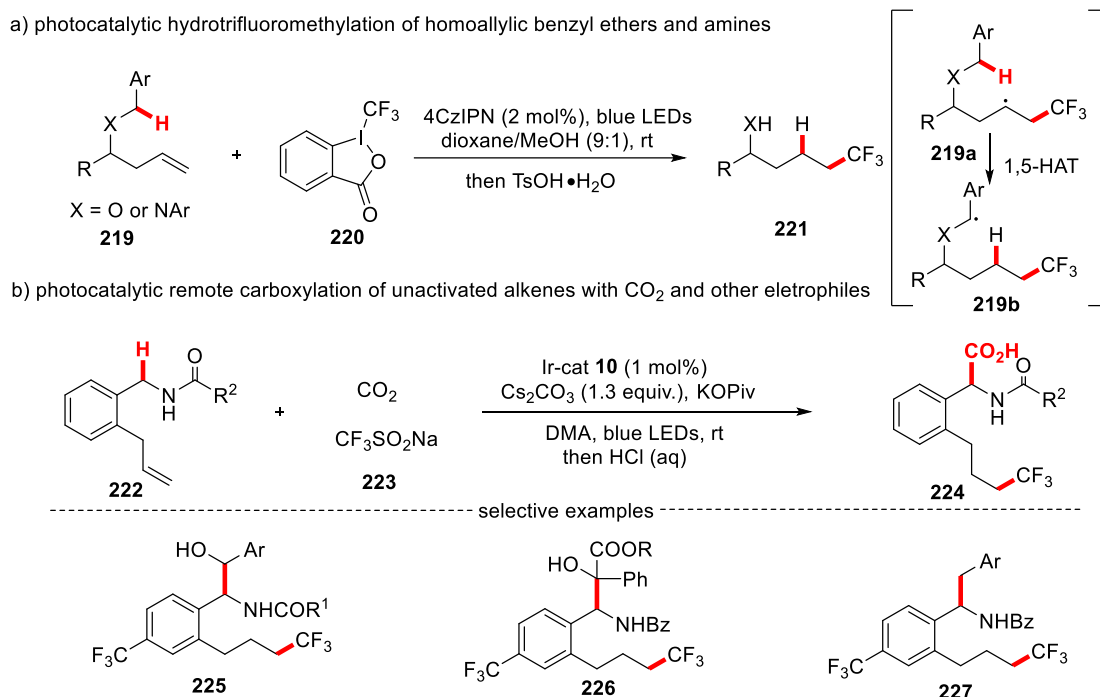
e) visible-light-induced Pd-catalyzed atom-transfer radical cyclization cascade



Scheme 19 1,5-HAT of alkenyl radicals

### 1.3.3 Alkyl radical-mediated 1,5-HAT

In 2019, Xu group described a competent metal-free photoredox-catalyzed hydrotrifluoromethylation of benzyl-protected homoallylic alcohols or amines **219**. Valuable  $\delta$ -fluoromethylated free alcohols and amines **221** were delivered with in situ deprotection of benzyl protecting group under mild conditions. The difference of BDE between the benzylic proton of benzyl ethers or benzyl amines ( $\sim 85$  kcal/mol) and the secondary aliphatic C(sp<sup>3</sup>)-H ( $\sim 98$  kcal/mol) rendered the 1,5-HAT of intermediate **219a** to **219b** thermodynamically favorable (Scheme 20a)<sup>176</sup>. Afterwards Yu<sup>177</sup> et al reported remote difunctionalizing carboxylation of unactivated alkenes **222** with CO<sub>2</sub> via photoinduced 1,5-HAT. Other electrophiles, such as aldehydes,  $\alpha$ -ketoesters and benzyl bromides, can be used to couple with unactivated alkenes **222** to afford corresponding products **225-227**. (Scheme 20b)



Scheme 20 1,5-HAT of alkyl radicals



## 1.4 Conclusion

(1) Carboxylic acids and their derivatives are abundant and cost-effective chemical feedstocks, which have been widely applied in versatile organic synthesis. Among these transformations, decarboxylative reactions triggered by the light and photocatalyst provide a powerful platform to construct diverse molecules under mild conditions. As discussed in the introduction part, redox-neutral photoinduced methods and dual catalysis methods have broadened extensively scope of substrates. Despite the successful development of various coupling products, most decarboxylative reactions relied on metal reagents and additives. The use of metals, particularly rare or expensive ones, along with additives, increases undoubtedly the reaction cost and poses challenges for large-scale production. Moreover, residual metal reagents in final products have raised environmental and safety concerns. Therefore, developing green decarboxylative methods remains a longstanding objective in sustainable chemistry. In this context, exploring transition-metal-free and additives-free catalytic systems in decarboxylative reactions is much more significant and requires further research. Especially, applying these practical methods to synthesize pharmaceutically relevant molecule scaffolds is in great demand, as they have great potential for drug design and development.

(2) Carboxylic acids and their derivatives are privileged chemical entities due to their wide availability, low cost, and structural diversity. Recently, they have been extensively applied in  $P^{III}$ -assisted deoxygenation under light irradiation. Satisfactorily, these well-developed methods provide a mild and efficient way to construct carbonyl-containing compounds. However, functional group transformations involving carboxylic acids remain relatively underexplored. Herein, the development of novel reactivity patterns and reaction modes in photocatalyzed deoxygenation is essential, providing more possibilities for using readily available carboxylic acids and their derivatives to the functionalization of molecules especially bioactive molecules.

(3) Direct and site-selective  $C(sp^3)$ -H activation has been a longstanding challenging subject due to its intrinsic inert nature. The merger of photoredox catalysis and 1,5-hydrogen atom transfer (1,5-HAT) strategies have emerged as a powerful tool to achieve selectively remote  $C(sp^3)$ -H functionalization under mild conditions. Although photoinduced HLF-type and Barton-type transformations have been extensively developed, most of these strategies focused on the generation of heteroatom-centered radicals. In contrast, reactions triggered by carbon-centered radicals remain underdeveloped and continued efforts are required in this regard to access more valuable drug-like frameworks.

## 2 Results and discussion

### 2.1 NaI/PPh<sub>3</sub>-catalyzed visible-light-mediated decarboxylative radical cascade cyclization of *N*-arylacrylamides for the efficient synthesis of quaternary oxindoles

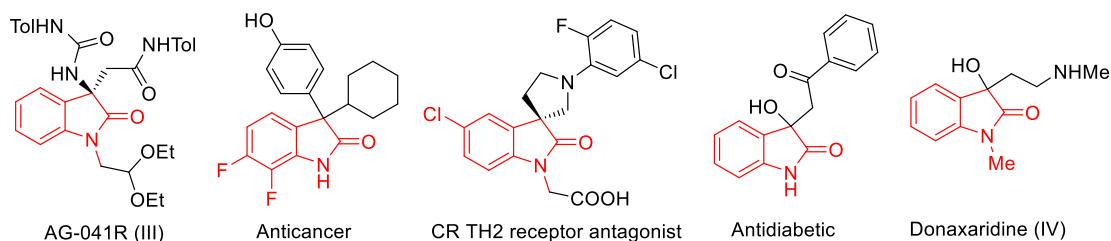
Author contributions: D. L. performed the corresponding experiments and drafted the manuscript. Y. Z. finished the preparation of some starting materials. Prof. Dr. Patureau supervised the project and revised the draft.

This work has been published: *Beilstein J. Org. Chem.* **2023**, *19*, 57.

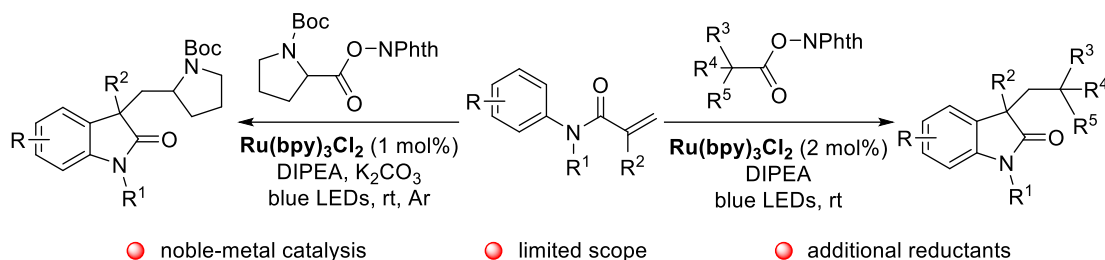
#### 2.1.1 Introduction

Radical-triggered cascade reactions have emerged as a powerful tool in organic synthesis, enabling the formation of multiple carbon-carbon and carbon-heteroatom bonds in one pot. This efficiency makes them particularly valuable for developing new synthetic methodologies, facilitating the construction of complex natural products and pharmaceuticals.<sup>178</sup> Recently, radical-initiated cascade cyclizations involving acrylamides have garnered increasing attention due to their potential for assembling functional oxindole scaffolds. These structures are widely present in functional molecules and bioactive compounds, which play crucial roles in drug discovery (**Scheme 1-1**)<sup>179-181</sup>. Despite the progress in this area,<sup>182-185</sup> existing methods often require stoichiometric reagents<sup>186-193</sup> or high reaction temperatures,<sup>194-203</sup> limiting their practicality and broader application.

In recent years, photocatalytic reactions have been demonstrated as one of the most powerful methods in developing radical-initiated addition/cyclization cascades from acrylamides.<sup>204-206</sup> Significant advancements have been made in generating diverse radicals from alkyl halides,<sup>207-209</sup> carboxylic acids,<sup>210-212</sup> simple alkanes,<sup>213</sup> alkylboronic acids,<sup>214</sup> and isocyanides,<sup>215</sup> or other.<sup>216-218</sup> In this context, the Fu group reported a Ru(bpy)<sub>3</sub>Cl<sub>2</sub>-catalyzed synthesis of *N*-Boc proline oxindole derivatives under visible-light irradiation, utilizing *N*-hydroxyphthalimide (NHPI) esters as efficient alkyl radical precursors.<sup>212</sup> Similarly, in 2015, Cheng and colleagues developed a visible-light-mediated tandem radical cyclization of *N*-arylacrylamides with *N*-(acyloxy)phthalimides, producing 3,3-dialkylated oxindoles in the presence of [Ru(bpy)<sub>3</sub>Cl<sub>2</sub>]·6H<sub>2</sub>O.<sup>211</sup> However, the reliance on noble-metal photocatalysts and the limited substrate scope have restricted the broader application of these approaches. (**Scheme 1-2**)



**Scheme 1-1** Representative examples containing oxindole moiety



**Scheme 1-2** Photocatalytic decarboxylative radical cascade cyclization via transition-metal catalysis

As the field of green chemistry continues to advance, there is a growing demand for cost-effective and transition-metal-free photocatalysis. In 2019,<sup>111</sup> Fu and Shang introduced a pioneering photocatalytic system based on a NaI/PPh<sub>3</sub> electron donor-acceptor (EDA) complex, enabling decarboxylative alkylation of silyl enol ethers and *N*-heteroarenes. Compared to conventional radical-based methods, this catalytic system offers several advantages: it eliminates the need for external redox additives and noble metals, relies on inexpensive and readily available and cost-effective reagents NaI/PPh<sub>3</sub>, and operates under mild conditions. Building on this foundation, NaI/PPh<sub>3</sub> catalysis has since been applied to various transformations, including alkene functionalization, decarboxylative C(sp<sup>3</sup>)–X bond formation, and cyclization of 1,7-enynes.<sup>219</sup> Despite its demonstrated potential, iodide/phosphine catalysis remains somewhat underutilized in organic synthesis, particularly in the preparation of biologically significant oxindole derivatives. Given the broad utility of these molecules in pharmaceuticals and bioactive compounds,<sup>179-181</sup> further exploration of iodide/phosphine-based radical methodologies could unlock new opportunities for their efficient and sustainable synthesis.

### 2.1.2 Condition optimizations

Initially, *N*-arylacrylamide **1-1a** and redox-active ester **1-2a** were chosen as model substrates to react for 36 h under 456 nm blue LEDs irradiation and N<sub>2</sub> atmosphere. Key results of screening iodides are summarized in **Table 1-1**. Surprisingly, NaI delivered desired oxindole derivative **1-3aa** with 72 % isolated yield (entry 1). When changing NaI to other iodides, LiI, KI, RbI, CsI and CaI<sub>2</sub> were all effective catalysts at providing **1-3aa**, albeit in slightly lower yields (entries 2-6). In addition, the oxindole product **1-3aa** could be afforded with moderate yield in the presence of *n*-Bu<sub>4</sub>NI (entry 7). It should be noted that all tested iodides were found to be soluble under those conditions.

**Table 1-1** Screening of iodide sources<sup>a</sup>

entry	iodide	<b>1-3aa</b> , yield (%) <sup>b</sup>
1	NaI	76 (72) <sup>c</sup>
2	LiI	70
3	KI	62
4	RbI	64
5	CsI	39

6	CaI <sub>2</sub>	56
7	<i>n</i> -Bu <sub>4</sub> Ni	57

<sup>a</sup>Unless otherwise noted, the reaction conditions were as follows: **1-1a** (0.3 mmol), **1-2a** (0.2 mmol), iodide (0.04 mmol), and PPh<sub>3</sub> (0.04 mmol) in MeCN (2 mL) irradiated by 456 nm blue LEDs for 36 h at room temperature. <sup>b</sup>The yield was determined by <sup>1</sup>H NMR analysis of the crude reaction mixture using 1,3,5-trimethoxybenzene as an internal standard. <sup>c</sup>isolated yield.

Then different phosphines were screened (**Table 1-2**). Aromatic phosphines including PPh<sub>3</sub>, tris(4-fluorophenyl)phosphine P(4-F-C<sub>6</sub>H<sub>4</sub>)<sub>3</sub>, tris(4-methoxyphenyl)phosphine P(4-OMe-C<sub>6</sub>H<sub>4</sub>)<sub>3</sub> performed well, the cheapest PPh<sub>3</sub> remaining however optimal (entries 1-3). In contrast, tricyclohexylphosphine PCy<sub>3</sub> was tested and performed poorly (entry 4), and bulky tri-*o*-tolylphosphine P(2-Me-C<sub>6</sub>H<sub>4</sub>)<sub>3</sub> almost shut down the reaction (entry 5). These results suggest that the accessibility of the phosphorus center plays a crucial role.

**Table 1-2** Screening of phosphine source<sup>a</sup>

entry	phosphine	<b>1-3aa</b> , yield (%) <sup>b</sup>
1	PPh <sub>3</sub>	76 (72) <sup>c</sup>
2	P(4-F-C <sub>6</sub> H <sub>4</sub> ) <sub>3</sub>	73
3	P(4-OMe-C <sub>6</sub> H <sub>4</sub> ) <sub>3</sub>	60
4	PCy <sub>3</sub>	23
5	P(2-Me-C <sub>6</sub> H <sub>4</sub> ) <sub>3</sub>	trace

<sup>a</sup>Unless otherwise noted, the reaction conditions were as follows: **1-1a** (0.3 mmol), **1-2a** (0.2 mmol), NaI (0.04 mmol), and phosphine (0.04 mmol) in MeCN (2 mL) irradiated by 456 nm blue LEDs for 36 h at room temperature.

<sup>b</sup>The yield was determined by <sup>1</sup>H NMR analysis of the crude reaction mixture using 1,3,5-trimethoxybenzene as an internal standard. <sup>c</sup>isolated yield.

In further condition optimization (**Table 1-3**), replacing acetonitrile (MeCN) with dimethyl sulfoxide (DMSO), or dimethylacetamide (DMA) or acetone, or ethyl acetate (EA), led to inferior yields (entries 1-5), and no product was detected using 1,4-dioxane and CH<sub>2</sub>Cl<sub>2</sub> as reaction solvents (entries 6-7). Control experiments indicate both PPh<sub>3</sub> and irradiation are essential for this decarboxylative tandem cyclization (entries 9-10). Although the reaction proceeded without NaI, it resulted in a low yield of **1-3aa** (entry 8).

**Table 1-3** Screening of solvents and control experiments<sup>a</sup>

entry	variation from standard conditions	<b>1-3aa</b> , yield (%) <sup>b</sup>
1	MeCN	76 (72) <sup>c</sup>
2	DMSO instead of MeCN	60
3	DMA instead of MeCN	44
4	acetone instead of MeCN	52

5	EA instead of MeCN	57
6	CH <sub>2</sub> Cl <sub>2</sub> instead of MeCN	N.D.
7	1,4-dioxane instead of MeCN	N.D.
8	without NaI	14
9	without PPh <sub>3</sub>	N.D.
10	without blue LEDs	N.D.

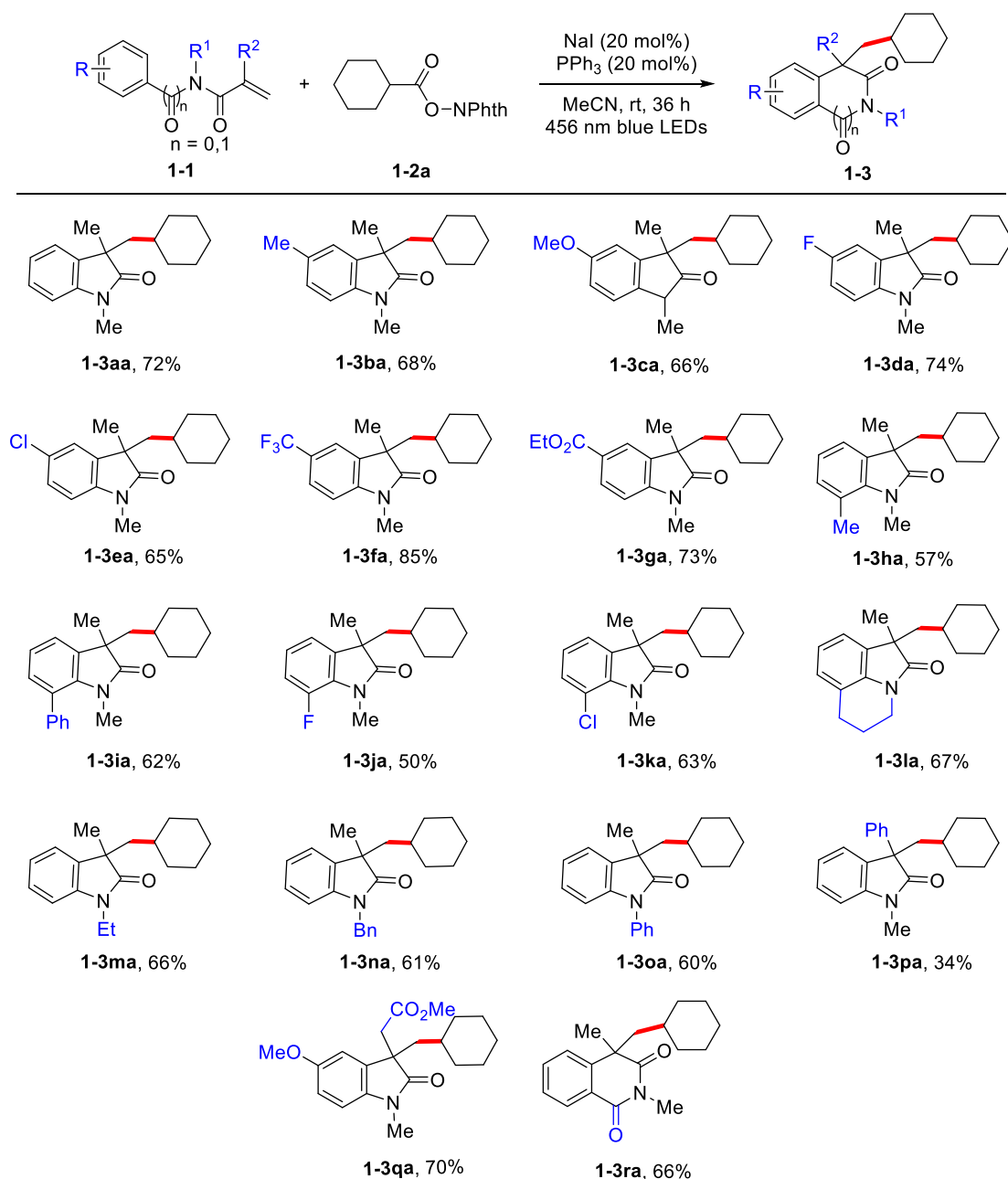
<sup>a</sup>Unless otherwise noted, the standard reaction conditions were as follows: **1-1a** (0.3 mmol), **1-2a** (0.2 mmol), NaI (0.04 mmol), and PPh<sub>3</sub> (0.04 mmol) in MeCN (2 mL) irradiated by 456 nm blue LEDs for 36 h at room temperature.

<sup>b</sup>The yield was determined by <sup>1</sup>H NMR analysis of the crude reaction mixture using 1,3,5-trimethoxybenzene as an internal standard. <sup>c</sup>isolated yield.

### 2.1.3 Substrate scope studies

With the optimized conditions established, a diverse range of acrylamides featuring various substituents was synthesized and evaluated. Under standard conditions, numerous acrylamides demonstrated excellent compatibility, yielding the desired oxindoles in moderate to good efficiencies (**Scheme 1-3**). Electron-donating groups, such as methyl and methoxy, positioned at the *para*-location of phenyl rings slightly reduced reaction activity, yet the corresponding products were still obtained in 68% and 66% yield, respectively (**1-3ba** and **1-3ca**). When these substituents were replaced with common halogens or electron-withdrawing groups, they all reacted smoothly with redox-active ester **1-2a** to afford the target oxindoles (**1-3da-1-3ga**) in good yields. Notably, the presence of a trifluoromethyl group enhanced performance, delivering **1-3fa** in very high 85% yield. Furthermore, *ortho*-substitution on the *N*-aryl moiety was well tolerated, though it led to a slight reduction in yield (**1-3ha-1-3ka**, 50%-63%).

Interestingly, a cyclic *N*-arylacrylamide derivative also proved to be a viable substrate, affording the corresponding polycyclic structure **1-3la** in a 67% yield. Variations in the *N*-substituent, including ethyl, benzyl, and phenyl, were well accommodated, providing the expected products (**1-3ma-1-3oa**) in good efficiency. A noteworthy observation was the significant impact of substituent modifications at the 2-position of the *N*-arylacrylamide core. Replacing a methyl group with a phenyl ring led to a substantial drop in yield from 72% to 34% (**1-3pa**), highlighting the steric and electronic influence of the substituent. Encouragingly, substrate **1-1q** successfully underwent decarboxylative cascade cyclization, furnishing **1-3qa** in 70% yield. This compound serves as a key intermediate in the synthesis of (±)-physovenine and (±)-physostigmine alkyl analogues, known for their inhibitory activity against acetylcholinesterase and butyrylcholinesterase.<sup>195,220,221</sup> To further broaden the scope of this methodology, a benzamide-derived acrylamide **1-1r** was subjected to the reaction, resulting in the formation of the anticipated six-membered annulated product **1-3ra** with a commendable yield of 66%.

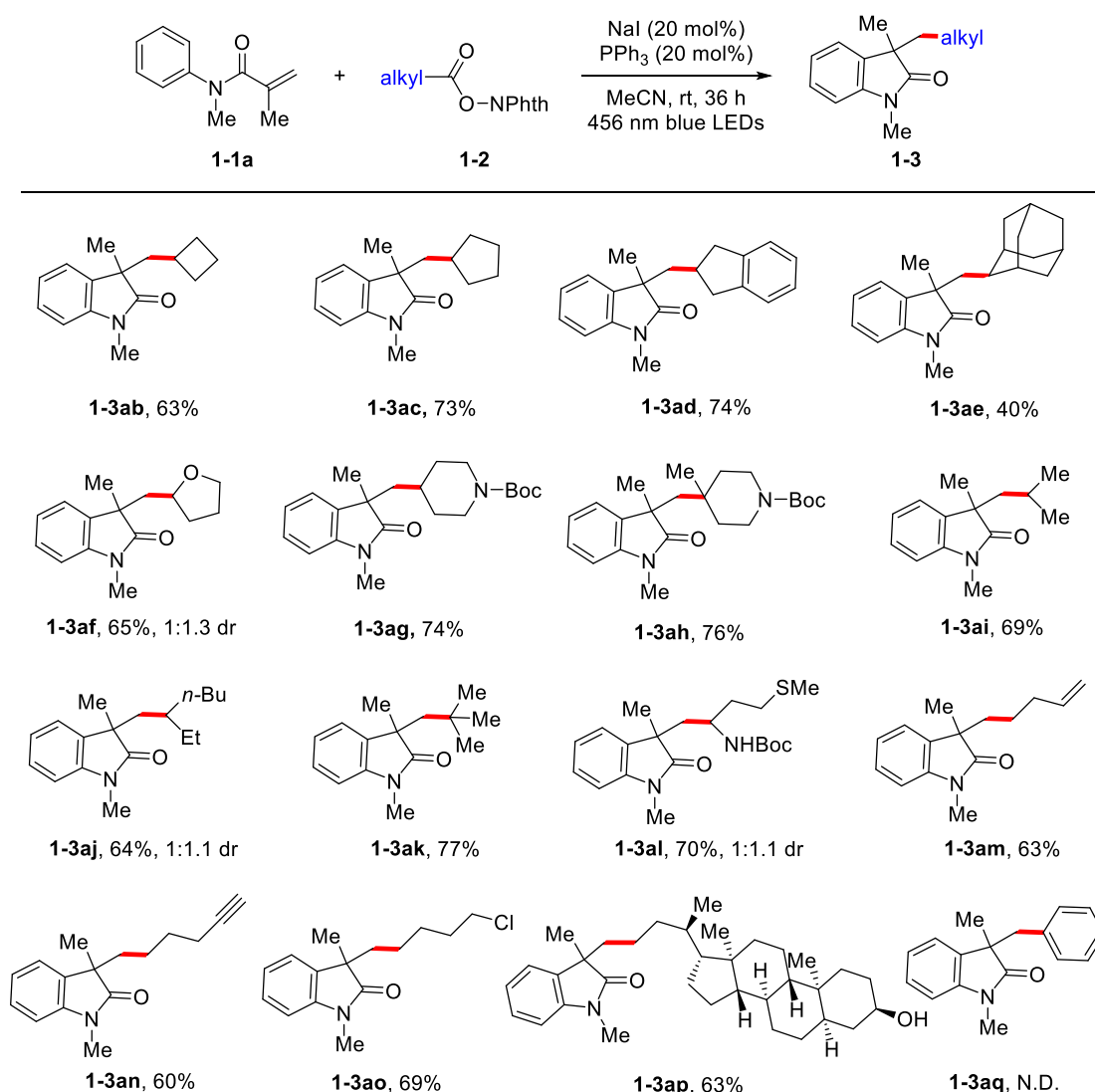


<sup>a</sup>Reaction conditions: **1-1** (0.3 mmol), **1-2** (0.2 mmol), NaI (0.04 mmol), and PPh<sub>3</sub> (0.04 mmol) in MeCN (2 mL) irradiated by 456 nm blue LEDs for 36 h at room temperature. Isolated yields are reported.

**Scheme 1-3** Scopes of acrylamides<sup>a</sup>

To further explore catalytic efficiency through the decarboxylative radical cascade cyclization, then the scope of redox-active esters was evaluated (**Scheme 1-4**). It was demonstrated that redox-active esters that derived from primary, secondary, and tertiary aliphatic carboxylic acids were all well-suited to this approach. Cyclic substrates containing cyclobutyl, cyclopentyl, and indenyl groups successfully yielded the corresponding products in good efficiency (**1-3ab-1-3ad**, 63–74%), whereas the incorporation of an adamantyl-derived substituent posed greater difficulty, affording **1-3ae** in a moderate 40% yield. Additionally, cyclic systems featuring oxygen- or nitrogen-containing rings proved effective, delivering the target oxindoles (**1-3af-1-3ah**) in yields ranging from 65% to 76%. Furthermore, a symmetrically  $\alpha$ -substituted redox-active ester led to the formation of quaternary oxindole **1-3ai** in 69% yield, while an asymmetrically  $\alpha$ -branched precursor underwent the reaction with comparable efficiency, generating oxindole **1-3aj** as a 1:1.1 mixture of

diastereomers. Notably, this strategy facilitated the synthesis of the sterically demanding oxindole **1-3ak** in good yield using a *tert*-butyl *N*-hydroxyphthalimide ester as the *tert*-butyl radical source. Significantly, a redox-active ester derived from methionine was efficiently transformed into the  $\alpha$ -aminoalkylation product **1-3al** in overall 70% yield, demonstrating the method's potential for modifying and derivatizing both natural and synthetic amino acids. Moreover, functional groups such as a terminal alkene **1-3am**, a terminal alkyne **1-3an**, and an alkyl chloride **1-3ao** were well-tolerated, yielding the corresponding products in encouraging efficiencies. To further highlight the versatility of this protocol, we applied it to a complex scaffold derived from lithocholic acid, which underwent smooth decarboxylative cyclization to furnish oxindole **1-3ap** in 63% yield. Finally, it should be noted that benzoyl ester substrate **1-2q** did not deliver the corresponding cyclized product **1-3aq**.



<sup>a</sup>Reaction conditions: **1-1** (0.3 mmol), **1-2** (0.2 mmol), NaI (0.04 mmol), and PPh<sub>3</sub> (0.04 mmol) in MeCN (2 mL) irradiated by 456 nm blue LEDs for 36 h at room temperature. Isolated yields are reported.

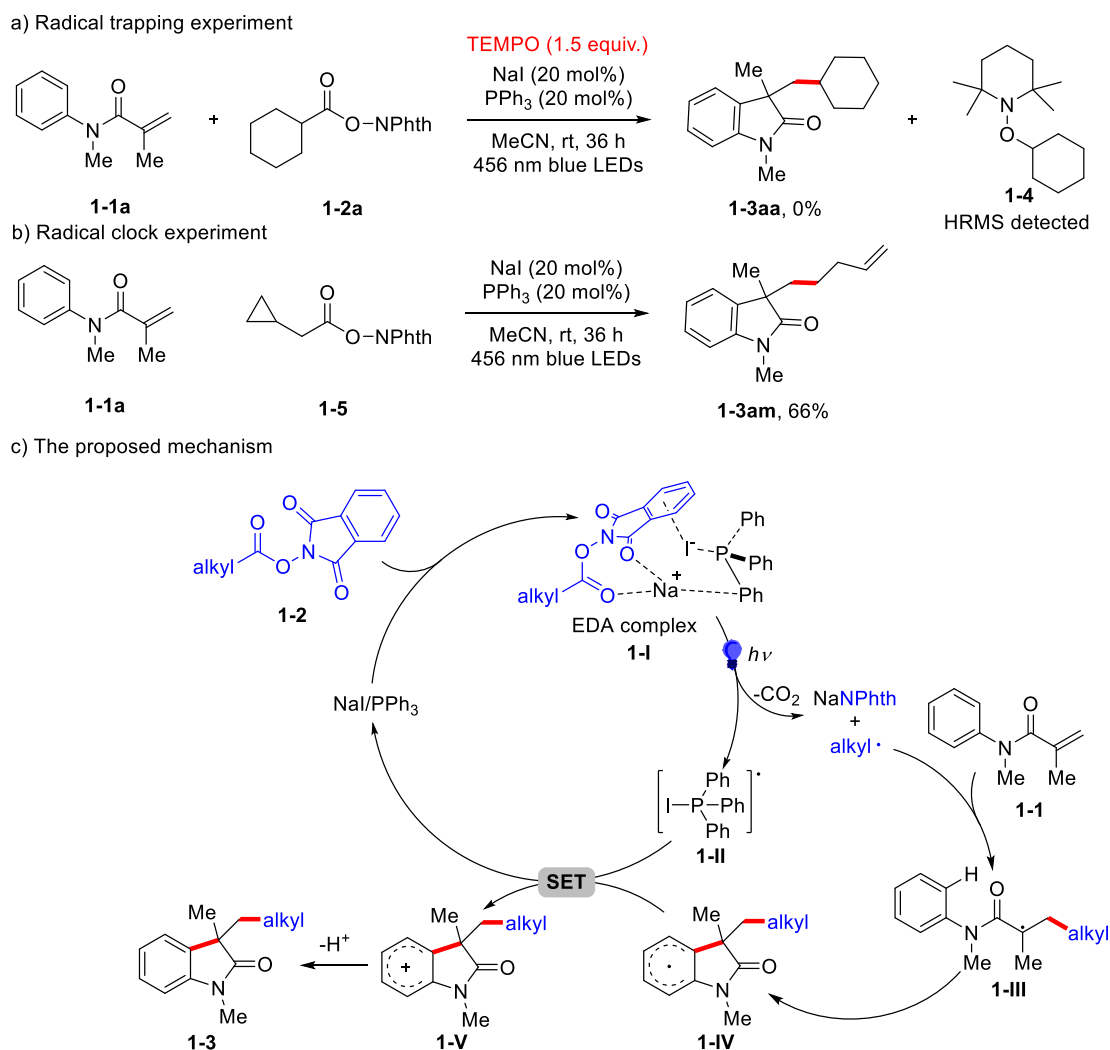
**Scheme 1-4** Scope of alkyl radical precursors<sup>a</sup>

## 2.1.4 Mechanistic investigation

To better understand the reaction mechanism, several control experiments were conducted. When a radical scavenger, such as 2,2,6,6-tetramethyl-1-piperidinyloxy (TEMPO), was introduced into the

catalytic system under standard conditions, the reaction was completely suppressed, and a TEMPO-trapped adduct **1-4** was detected by HRMS (**Scheme 1-5a**). Additionally, a radical clock experiment using redox-active ester **1-5** in a reaction with acrylamide **1-1a** yielded the radical-mediated ring-opening product **1-3am** in 66% yield (**Scheme 1-5b**). These findings strongly suggest that a radical species plays a key role in the NaI/PPh<sub>3</sub>-catalyzed decarboxylative cascade cyclization leading to oxindoles.

Based on these experimental results and previous reports,<sup>219</sup> a plausible catalytic cycle involving a radical pathway was proposed (**Scheme 1-5c**). The reaction is initiated by photoactivation of a transient electron donor-acceptor (EDA) complex (**1-I**), formed in situ from NaI, PPh<sub>3</sub>, and redox-active ester **1-2a** in MeCN. This activation leads to the generation of an alkyl radical and a PPh<sub>3</sub>-I radical species **1-II**, accompanied by the release of carbon dioxide and NaNPhth. The alkyl radical then undergoes addition to acrylamide **1-1**, forming radical intermediate **1-III**. This intermediate undergoes an intramolecular radical C-H functionalization, yielding cyclic intermediate **1-IV**. Subsequent oxidation of the delocalized radical species **1-IV** by **1-II** generates the cationic intermediate **1-V** while simultaneously regenerating the NaI/PPh<sub>3</sub> photocatalyst for the next cycle. Finally, deprotonation of **1-V** produces the desired oxindole product **1-3**.



**Scheme 1-5** Control experiments and proposed catalytic cycle of NaI/PPh<sub>3</sub> photoredox catalysis



### 2.1.5 Conclusion

In this study, we developed an efficient photocatalytic decarboxylative radical cascade cyclization of *N*-arylacrylamides using a range of redox-active esters derived from readily available carboxylic acids. Conducted under mild conditions, this approach offers a practical alternative to conventional transition-metal and organophotocatalysis<sup>222</sup>. Notably, the inexpensive and easily accessible NaI/PPh<sub>3</sub> system serves as an effective photoredox catalyst, providing a cost-efficient route to construct oxindole scaffolds featuring a quaternary carbon center.

This methodology is distinguished by its broad substrate scope, high functional group tolerance, and operational simplicity. Mechanistic studies suggested that the reaction proceeds via a radical cascade pathway, further supporting the role of NaI/PPh<sub>3</sub> in facilitating the transformation. We expect that these findings will inspire further exploration of NaI/PPh<sub>3</sub>-catalyzed reactions and related radical-based synthetic strategies for functional molecules.

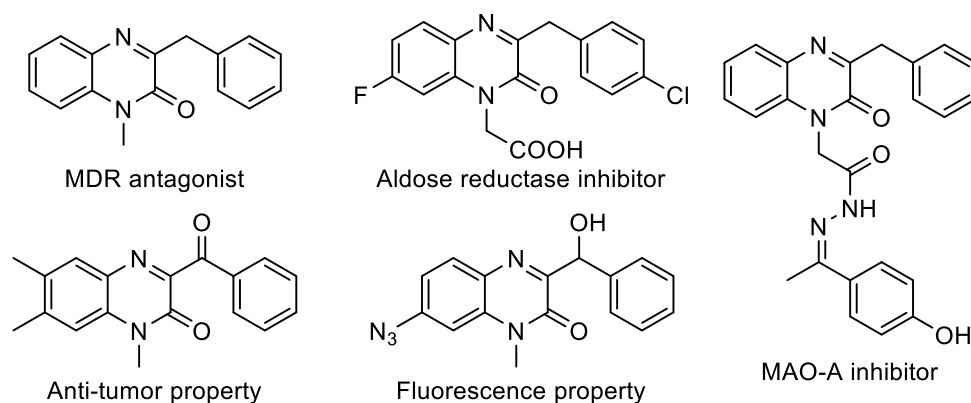
## 2.2 Visible-light-induced photocatalytic deoxygenative benzylation of quinoxalin-2-(1*H*)-ones with carboxylic acid anhydrides

Author contributions: D. L. performed the corresponding experiments and drafted the manuscript. Prof. Dr. Patureau supervised the project and revised the draft.

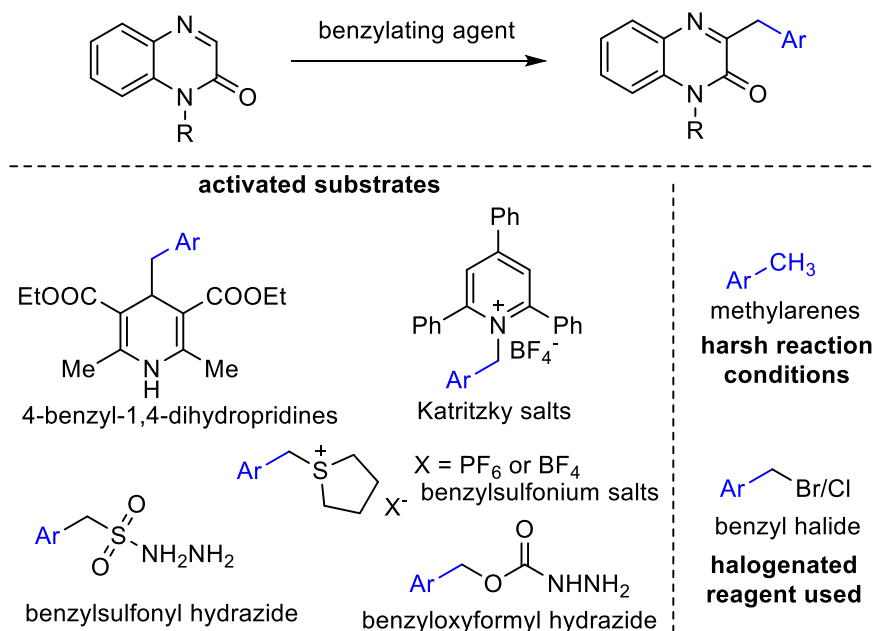
This work has been published: *Org. Lett.* **2024**, 26, 6841.

### 2.2.1 Introduction

Quinoxalin-2(1*H*)-ones are an important class of nitrogen-containing heterocycles with broad applications in pharmaceutical and synthetic chemistry.<sup>223-225</sup> In particular, 3-benzylquinoxalin-2(1*H*)-ones are commonly found in functional molecules and therapeutic agents, exhibiting diverse activities such as multidrug resistance (MDR) antagonism, aldose reductase inhibition, *N*-type calcium channel blockade, fluorescence property, and monoamine oxidase A (MAO-A) inhibition (**Scheme 2-1**).<sup>226-229</sup> Given their significance, the efficient synthesis of these compounds has attracted considerable attention in recent years, with substantial efforts focused on direct C3 benzylation via step- and atom-economical C–H bond activation/ functionalization strategies.<sup>230-233</sup> However, early methods often required excess peroxides as radical initiators at high temperatures,<sup>231-233</sup> resulting in harsh reaction conditions and poor tolerance for sensitive functional groups.

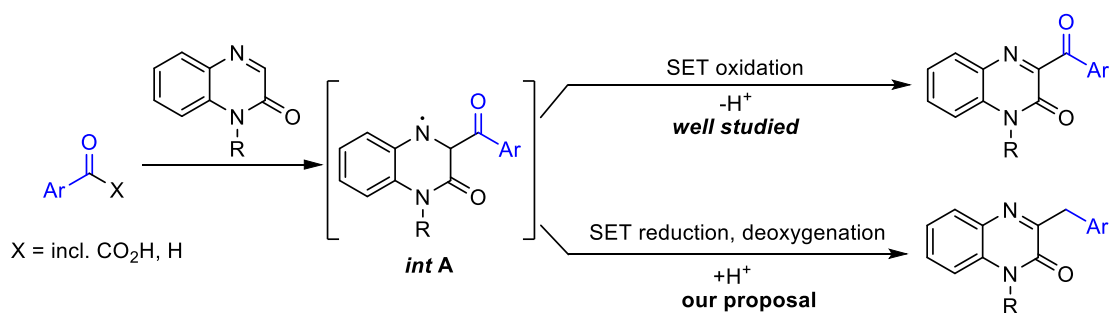


**Scheme 2-1** Representative compounds bearing the 3-benzylquinoxalin-2-(1*H*)-one scaffold



**Scheme 2-2** Reported benzylating reagents for C3 benzylation of quinoxaline-2(1*H*)-ones

In recent years, visible-light-induced photocatalysis has emerged as a powerful, mild, and practical approach for constructing C–C and C–heteroatom bonds through radical processes.<sup>30–44</sup> This has led to some progress in the direct C3 benzylation of quinoxalin-2(1*H*)-ones under visible-light irradiation (**Scheme 2-2**).<sup>234–238</sup> In 2020, the Xuan group developed an acetoxybenziodoxole-accelerated benzylation strategy using 4-benzyl-1,4-dihydropyridines as benzyl radical precursors.<sup>234</sup> Later, in 2022, Yang and Adiyala independently demonstrated the use of benzylsulfonium hydrazides and Katritzky salts for the photochemical benzylation of *N*-heteroarenes.<sup>235–236</sup> More recently, the Yang and Yu groups reported direct benzylation using benzyl halides under visible-light photocatalysis.<sup>237–238</sup> Despite these advancements, many of these methods suffer from limitations such as the need for complex benzylation reagents or the use of toxic components. Consequently, developing safer, more efficient strategies for synthesizing 3-benzylquinoxalin-2(1*H*)-ones remains an important goal.



**Scheme 2-3** Direct synthesis of C3-functional quinoxaline-2(1*H*)-ones via SET oxidation

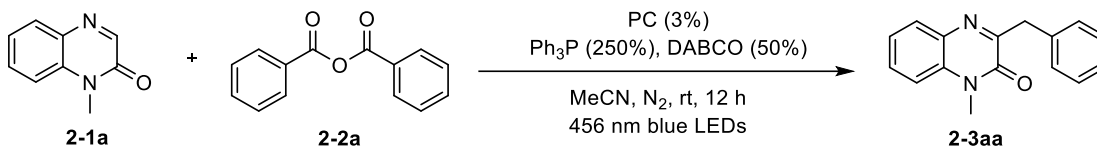
Carboxylic acids and their derivatives are highly valuable synthetic precursors due to their abundance, wide availability, and structural diversity. Recently, they have been extensively explored for the C3 functionalization of quinoxalin-2(1*H*)-ones under visible-light irradiation.<sup>239–248</sup> However, most reported methods focus on generating 3-acylquinoxalin-2(1*H*)-one derivatives via single electron transfer (SET) oxidation of acyl radical intermediates (**Scheme 2-3**). Inspired by recent phosphoranyl radical-mediated deoxygenative functionalizations of carboxylic acids,<sup>121–140</sup> we

envisioned a complementary approach: a photochemical SET reduction of intermediate A, followed by deoxygenative reduction, to efficiently access valuable 3-benzylquinoxalin-2(1*H*)-ones.

## 2.2.2 Condition optimizations

To evaluate the feasibility of our photochemical reaction design, we selected *N*-methylquinoxalin-2(1*H*)-one **2-1a** and benzoic anhydride **2-2a** as model substrates. Under blue LEDs irradiation in an anhydrous MeCN solvent and N<sub>2</sub> atmosphere, the desired 3-benzylquinoxalin-2(1*H*)-one **2-3aa** was successfully obtained in 77% isolated yield using Ir[dF(CF<sub>3</sub>)ppy]<sub>2</sub>(dtbbpy)PF<sub>6</sub> as the PC, with Ph<sub>3</sub>P and DABCO as additives (entry 1). In contrast, alternative photocatalysts such as Ir(ppy)<sub>3</sub>, Ru(bpy)<sub>3</sub>Cl<sub>2</sub>·6H<sub>2</sub>O, and 4CzIPN proved ineffective, failing to facilitate the reaction (Table 2-1 entries 2–4).

Table 2-1 PC screening<sup>a</sup>

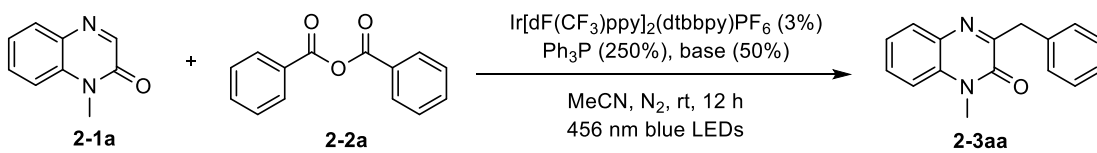
		
entry	PC	<b>2-3aa</b> , yield (%) <sup>b</sup>
1	Ir[dF(CF <sub>3</sub> )ppy] <sub>2</sub> (dtbbpy)PF <sub>6</sub>	81 (77) <sup>c</sup>
2	Ir(ppy) <sub>3</sub>	0
3	Ru(bpy) <sub>3</sub> Cl <sub>2</sub> ·6H <sub>2</sub> O	0
4	4CzIPN	0

<sup>a</sup>Unless otherwise noted, the reaction conditions were as follows: **2-1a** (0.15 mmol), **2-2a** (0.3 mmol), PC (3%), Ph<sub>3</sub>P (250%), DABCO (50%) in MeCN (1.5 mL), irradiation by 40W blue LEDs under N<sub>2</sub> at room temperature for 12 h.

<sup>b</sup>The yield was determined by <sup>1</sup>H NMR analysis of the crude reaction mixture using 1,3,5-trimethoxybenzene as an internal standard. <sup>c</sup>isolated yield.

Then, diverse organic base and inorganic base were investigated (Table 2-2). Among them, DABCO proved to be the most effective (entry 1). Substituting DABCO with other bases led to significantly lower yields, while no product formation was observed when TMEDA or DIPEA was used (entries 2–7).

Table 2-2 Base screening

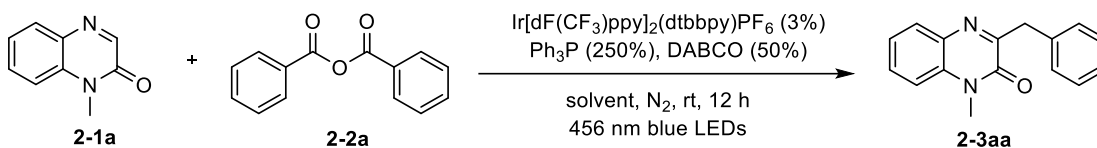
		
entry	base	<b>2-3aa</b> , yield (%) <sup>b</sup>
1	DABCO	81 (77) <sup>c</sup>
2	K <sub>2</sub> HPO <sub>4</sub>	70
3	K <sub>2</sub> CO <sub>3</sub>	68
4	K <sub>3</sub> PO <sub>4</sub>	58
5	DBU	22
6	TMEDA	0
7	DIPEA	0

<sup>a</sup>Unless otherwise noted, the reaction conditions were as follows: **2-1a** (0.15 mmol), **2-2a** (0.3 mmol), Ir[dF(CF<sub>3</sub>)ppy]<sub>2</sub>(dtbbpy)PF<sub>6</sub> (3%), Ph<sub>3</sub>P (250%), base (50%) in MeCN (1.5 mL), irradiation by 40W blue LEDs under N<sub>2</sub> at room temperature for 12 h. <sup>b</sup>The yield was determined by <sup>1</sup>H NMR analysis of the crude reaction mixture using 1,3,5-trimethoxybenzene as an internal standard. <sup>c</sup>isolated yield.

Next, various solvents to optimize the reaction conditions was evaluated (Table 2-3). Acetone provided a yield comparable to MeCN, whereas reactions conducted in DCE and DMF resulted in

significantly lower yields of 17% and 53%, respectively (entries 2-4). Control experiments confirmed that the photocatalyst, light, Ph<sub>3</sub>P, and DABCO were all essential for successful C3 benzylation with benzoic anhydride (entry 5). Additionally, altering the light source yielded suboptimal results. For instance, using a 370 nm wavelength led to diminished efficiency (entry 6), and simply heating the reaction to 60 °C failed to substitute for light irradiation (entry 7). Finally, replacing benzoic anhydride **2-2a** with benzoic acid severely reduced the yield, emphasizing the crucial role of the anhydride structure in substrate activation (entry 8).

**Table 2-3** Solvent screening and control experiments<sup>a</sup>

		
entry	variation from standard conditions	<b>2-3aa</b> , yield <sup>b</sup>
1	MeCN as the solvent	81 (77) <sup>c</sup>
2	DCE as the solvent	17
3	DMF as the solvent	53
4	acetone as the solvent	72
5	no light or no PC, or no PPh <sub>3</sub> or no DABCO	0
6	λ = 370 nm	62
7	no light @ 60 °C	0
8	benzoic acid (0.3 mmol) instead of <b>2-2a</b>	19

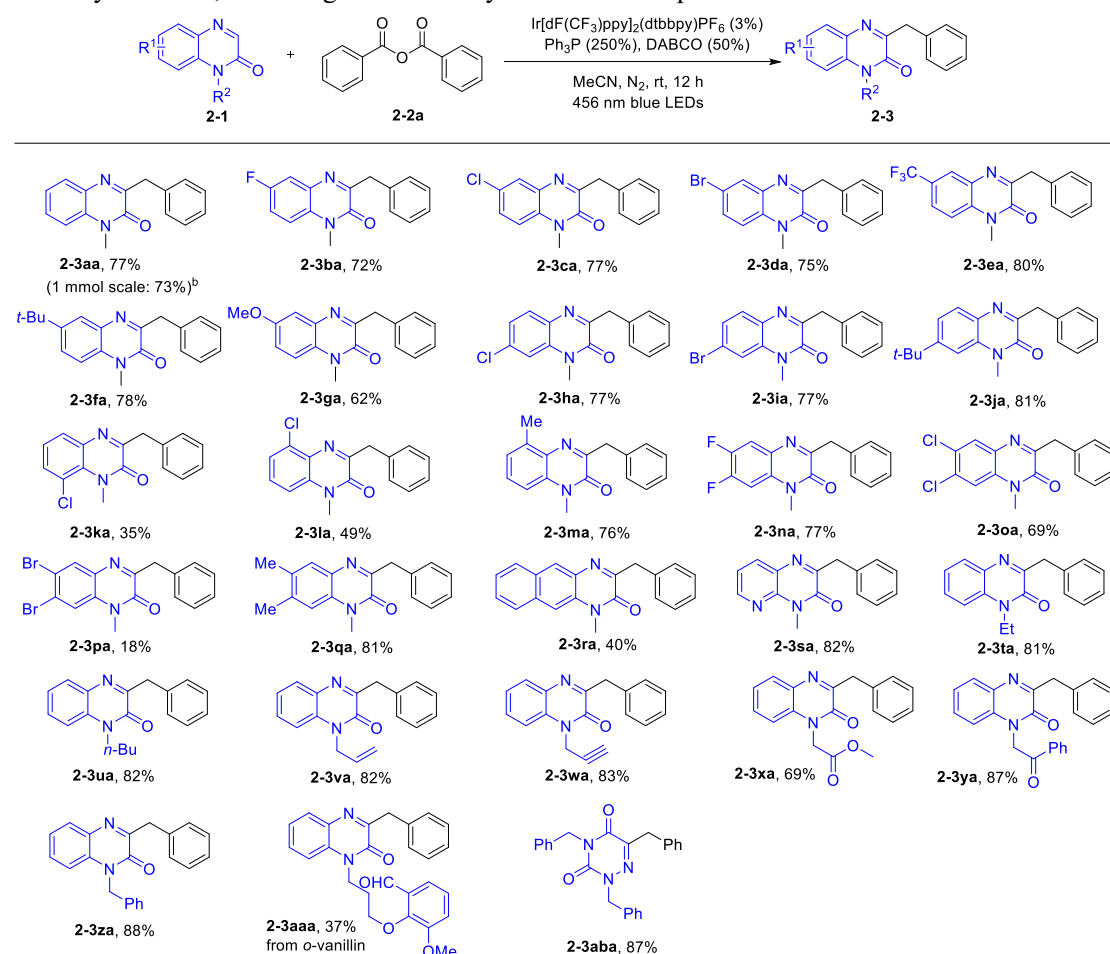
<sup>a</sup>Unless otherwise noted, the standard reaction conditions were as follows: **2-1a** (0.15 mmol), **2-2a** (0.3 mmol), Ir[dF(CF<sub>3</sub>)ppy]<sub>2</sub>(dtbbpy)PF<sub>6</sub> (3%), Ph<sub>3</sub>P (250%), DABCO (50%) in solvent (1.5 mL), irradiation by 40W blue LEDs under N<sub>2</sub> at room temperature for 12 h. <sup>b</sup>The yield was determined by <sup>1</sup>H NMR analysis of the crude reaction mixture using 1,3,5-trimethoxybenzene as an internal standard. <sup>c</sup>isolated yield.

### 2.2.3 Substrate scope studies

With the optimized conditions in hand, the substrate scope of quinoxalin-2(1*H*)-ones in this photocatalytic reductive benzylation reaction was explored (**Scheme 2-4**). A broad range of quinoxalin-2(1*H*)-ones with varying substituents on the aromatic ring proved to be compatible under standard conditions. Halogens such as fluoro, chloro, and bromo at the C6 or C7 positions were well tolerated, affording the corresponding 3-benzylquinoxalin-2(1*H*)-ones in good yields (**2-3ba**, **2-3ca**, **2-3da**, **2-3ha**, **2-3ia**, 72–77%). Likewise, substituents with electron-donating or electron-withdrawing groups yielded the desired products efficiently (**2-3ea**, **2-3fa**, **2-3ga**, **2-3ja**; 62–81%). The benzylation reaction also proceeded smoothly with 8-chloro- and 5-chloroquinoxalin-2(1*H*)-ones, albeit with slightly reduced yields (**2-3ka**, 35% and **2-3la**, 49%). Moreover, 5-methylquinoxalin-2(1*H*)-one demonstrated excellent reactivity, affording **2-3ma** in 76% yield. Additionally, difluoro-, dichloro-, and dimethyl-substituted derivatives underwent the reaction effectively, delivering the target products with high efficiency (**2-3na**, **2-3oa**, **2-3qa**). However, a dibromo-substituted quinoxalin-2(1*H*)-one yielded only 18% (**2-3pa**), likely due to its limited solubility.

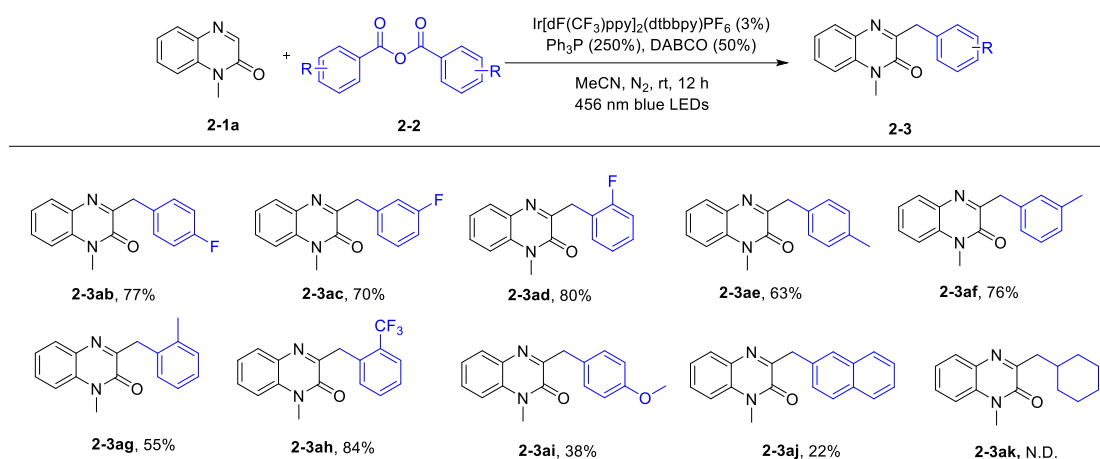
Quinoxalin-2(1*H*)-ones with extended aromatic or heteroaromatic ring produced **2-3ra** and **2-3sa** in 40% and 82% yield, respectively. Furthermore, various *N*-protecting groups, including ethyl, *n*-butyl, allyl, propargyl, ester, benzoyl, and benzyl, were well accommodated, yielding products **2-3ta**–**2-3za** in good to excellent yields (69–88%). Notably, this method tolerated an *o*-vanillin moiety, enabling the synthesis of product **2-3aaa**, which holds potential for pharmaceutical applications.

Finally, we successfully applied this strategy to the benzylation of the 6-azauracil-derived heterocycle **2-1ab**, achieving an excellent yield of 87% for product **2-3aba**.



**Scheme 2-4** Scope of quinoxaline-2-(1*H*)-ones<sup>a</sup>

To further assess the versatility of this benzylation reaction, the scope of benzoic anhydride derivatives was examined, as shown in **Scheme 2-5**. Fluorinated benzoic anhydrides, regardless of whether the fluoro substituent was positioned at the *para*, *meta*, or *ortho* site on the phenyl ring, exhibited good reactivity, yielding the corresponding products efficiently (**2-3ab-2-3ad**). Interestingly, the *meta*-methyl-substituted anhydride delivered a higher yield (76%) compared to its *para*- and *ortho*-methyl counterparts (**2-3ae-2-3ag**). Additionally, the reaction proceeded well with a trifluoromethyl-substituted anhydride (**2-3ah**), demonstrating compatibility with strongly electron-withdrawing groups. In contrast, electron-donating groups led to a significant decline in yields (**2-3ai**, **2-3aj**). Moreover, cyclohexanecarboxylic anhydride failed to produce the expected coupling product (**2-3ak**). Encouragingly, this protocol was successfully scaled up to a 1 mmol reaction, yielding 182 mg of product **2-3aa** (73%) after 24 hours of blue-light irradiation (**Scheme 2-4**; see **Part 4.2.2** for details).

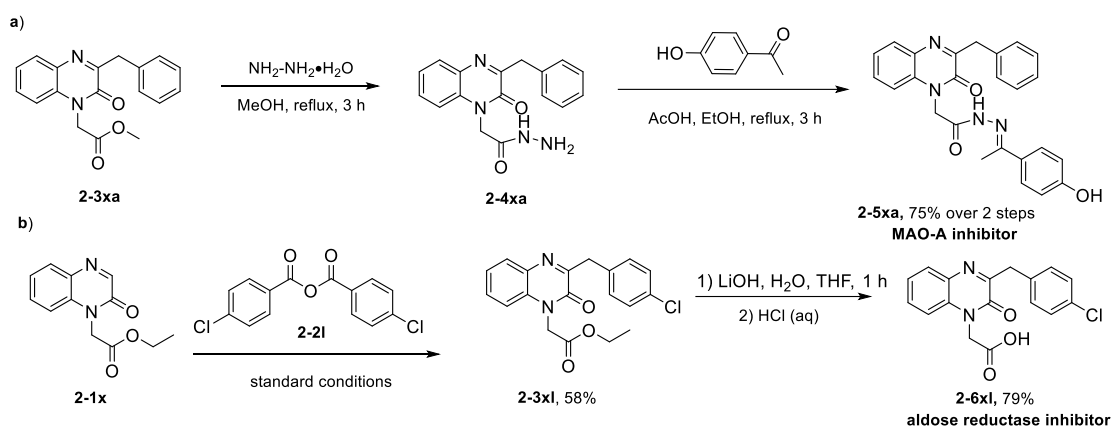


<sup>a</sup>Reaction conditions: same as **Scheme 2-4**. Isolated yields are reported.

**Scheme 2-5** Scope of carboxylic anhydrides<sup>a</sup>

## 2.2.4 Synthetic applications

To further highlight the utility and practicality of this reductive benzylation strategy, we applied it to the synthesis of bioactive molecules derived from simple 3-benzylquinoxalin-2(1*H*)-ones. For example, compound **2-3xa** was treated with hydrazine hydrate in methanol, yielding hydrazide derivative **2-4xa**. Subsequent condensation of **2-4xa** with 4-hydroxyacetophenone led to the formation of MAO-A inhibitor **2-5xa**<sup>229</sup>, achieving an overall 75% isolated yield (**Scheme 2-6a**). In another application, quinoxalin-2(1*H*)-one **2-1x** underwent benzylation with anhydride **2-2l** under standard conditions, affording product **2-3xl** in 58% yield. Further hydrolysis of **2-3xl** produced derivative **2-6xl** with 79% yield (**Scheme 2-6b**). Product **2-6xl** has previously been investigated for its potential as an aldose reductase inhibitor.<sup>249</sup>



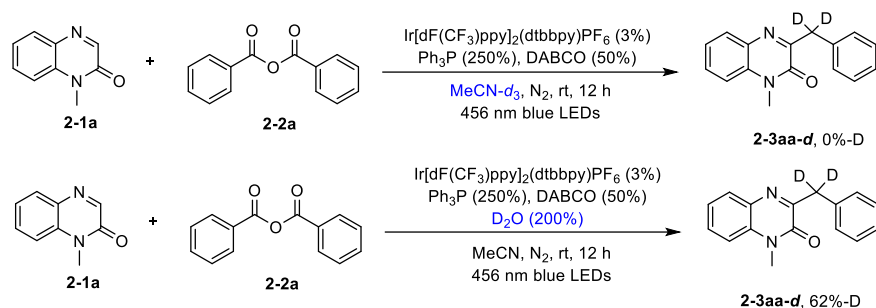
**Scheme 2-6** Synthetic applications

## 2.2.5 Mechanistic studies

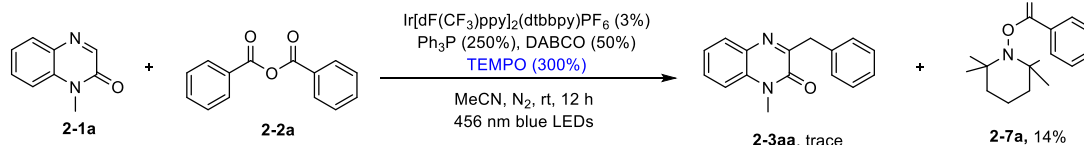
To gain deeper insight into the reaction mechanism, a series of control experiments were conducted. First, when the reaction was performed in deuterated acetonitrile (MeCN-*d*<sub>3</sub>) under standard conditions, no deuterium incorporation was detected in product **2-3aa-d** (**Scheme 2-7a**). However, upon adding 2 equivalents of D<sub>2</sub>O to anhydrous MeCN, 62% deuterium labeling was observed at the benzylic position. This finding suggests that trace amounts of water, potentially originating from the reagents or reactants, may serve as a hydrogen source in the reaction. Additionally, the introduction of the radical scavenger 2,2,6,6-tetramethylpiperidin-1-oxyl (TEMPO) significantly

suppressed the reaction, yielding only trace amounts of **2-3aa**, and the benzoyl-TEMPO adduct **2-7a** was successfully isolated and characterized, strongly indicating the involvement of an acyl radical pathway (**Scheme 2-7b**). Interestingly, no evidence of a TEMPO-trapped benzyl radical intermediate was found in the crude reaction mixture. Inspired by previous reports featuring C3 functionalization of quinoxalin-2(1*H*)-ones under visible-light irradiation,<sup>239-248</sup> we synthesized ketone **2-8** and benzyl alcohol **2-9** and subjected them to the standard reaction conditions (**Scheme 2-7c**). Notably, only benzyl alcohol **2-9** was efficiently converted to product **2-3aa**, achieving 86% isolated yield, whereas ketone **2-8** remained unreacted. These observations suggest that benzyl alcohol **2-9** is a plausible intermediate in the transformation. Next, Stern–Volmer fluorescence quenching experiments provided additional mechanistic insights. The iridium photocatalyst exhibited fluorescence quenching in the presence of Ph<sub>3</sub>P, quinoxalin-2(1*H*)-one **2-1a**, and DABCO, but not with anhydride **2-2a** (see **Part 4.2.2** for details).

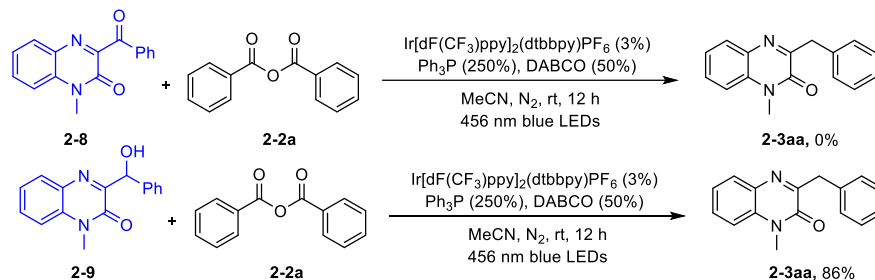
a) Deterium labeling experiments



b) Radical trapping experiment



c) Control experiments

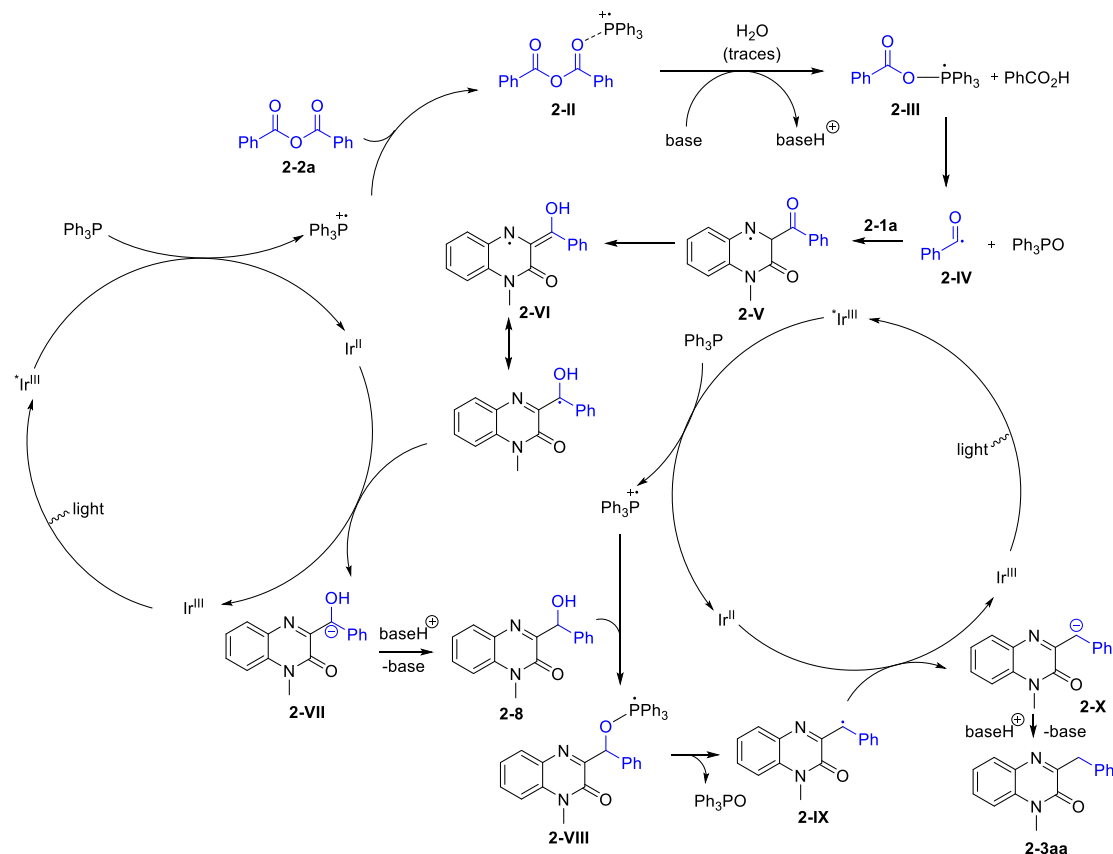


**Scheme 2-7** Mechanistic investigations

Building on the experimental results and previous studies,<sup>250-252</sup> we propose the reaction pathway illustrated in **Scheme 2-8**. Initially, the photoexcited <sup>\*</sup>Ir<sup>III</sup> catalyst abstracts an electron from Ph<sub>3</sub>P, generating a phosphine radical cation. Due to its strong affinity for oxygen, this phosphine radical cation facilitates the activation of anhydride intermediate **2-II**. The resulting intermediate undergoes hydrolysis to form intermediate **2-III**, followed by the elimination of phosphine oxide, which generates the corresponding benzoyl radical **2-IV**. This benzoyl radical is then captured by quinoxalin-2(1*H*)-one **2-1a**, leading to the formation of stabilized radical intermediates **2-V** and **2-VI**. Subsequent one-electron reduction of these intermediates yields anionic intermediate **2-VII** and protonated intermediate **2-8**, which we have previously identified as a viable intermediate (**Scheme 2-7c**). This species then reacts with another equivalent of the phosphine radical cation (intermediate **2-VIII**), triggering a second phosphine oxide elimination step to form intermediate **2-IX**. Another



round of one-electron reduction produces intermediate **2-X**, completing this portion of the catalytic cycle. The significant presence of triphenylphosphine oxide was confirmed through  $^{31}\text{P}$  NMR analysis of the crude reaction mixture, supporting the proposed mechanistic pathway. As for the role of DABCO, it may act as a proton shuttle, consistent with the observation that other bases also facilitate the reaction (**Table 2-2**, entries 2-4). However, its potential function as a redox relay cannot be entirely ruled out.



**Scheme 2-8** Proposed mechanism

## 2.2.6 Conclusion

In summary, we have developed a visible-light-driven photocatalytic deoxygenative benzylation method for the efficient synthesis of 3-benzylquinoxalin-2(1H)-ones. This reaction is characterized by mild, safe conditions and demonstrates excellent functional group compatibility, as well as the broad availability of starting materials. A variety of 3-benzylquinoxalin-2(1H)-ones were synthesized in a single step with generally high yields. Additionally, this approach was successfully applied to the rapid synthesis of two compounds with notable pharmacological potential.

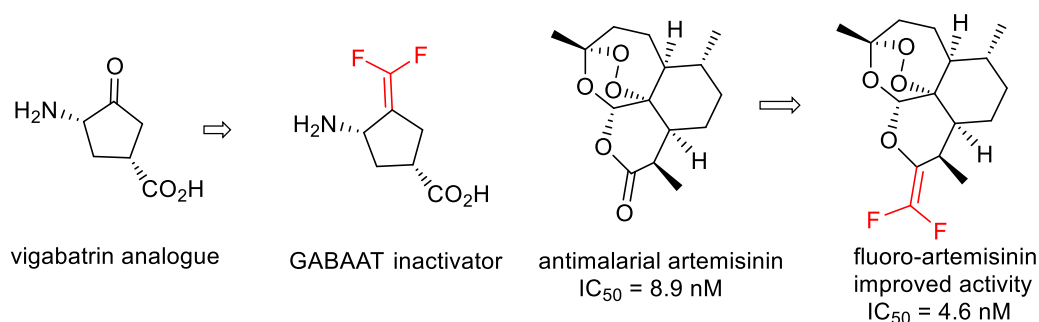
## 2.3 Visible-light-mediated radical $\alpha$ -C(sp<sup>3</sup>)-H *gem*-difluoroallylation of amides with trifluoromethyl alkenes via halogen atom transfer and 1,5-hydrogen atom transfer

Author contributions: D. L. performed the corresponding experiments and drafted the manuscript. F. X. finished some starting material preparation. Prof. Dr. Oppel and B. E. measured and analyzed crystal structure. Prof. Dr. Patureau supervised the project and revised the draft.

This work has been published: *Org. Lett.* **2025**, 27, 2377.

### 2.3.1 Introduction

*gem*-Difluoroalkenes have found widespread applications in synthetic chemistry, pharmaceutical development, and materials science.<sup>253-254</sup> These versatile fluorinated motifs serve as precursors for various organofluorine derivatives, including monofluoromethylenes, difluoromethylenes, and *gem*-difluorocyclopropanes.<sup>255-256</sup> Notably, their incorporation into biomolecules as carbonyl bioisosteres has been shown to enhance pharmaceutical efficacy, metabolic stability, and target specificity, offering new avenues for drug discovery (**Scheme 3-1**).<sup>257-258</sup> Conventional methods for synthesizing *gem*-difluoroalkenes often involve harsh reaction conditions, highly reactive intermediates, or well-defined organometallic reagents.<sup>259-264</sup> These approaches frequently suffer from limited substrate scope and poor functional group tolerance due to their strong basic or nucleophilic nature.

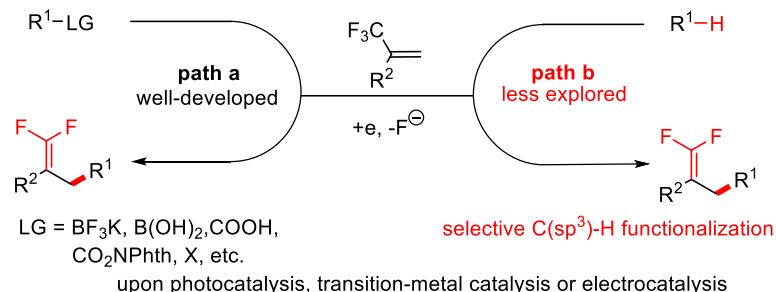


**Scheme 3-1** Representative biologically active *gem*-difluoroalkenes

In recent years, mild radical defluorinative strategies for constructing *gem*-difluoroalkenes have gained increasing interest, leveraging transition-metal catalysis,<sup>265-270</sup> photocatalysis,<sup>271-279</sup> and electrocatalysis.<sup>280-282</sup> These methodologies typically involve radical generation through the cleavage of C–halogen, C–B, C–Si, C–C, C–O, or C–S bonds in various substrates (**Scheme 3-2, path a**). Compared to these radical precursors-utilized approaches, radical C(sp<sup>3</sup>)-H functionalization<sup>153,283-286</sup> offers a practical and efficient route to access structurally diverse *gem*-difluoroalkenes (**Scheme 3-2, path b**). In this field, several pioneering studies have achieved site-selective defluorinative *gem*-difluoroallylation of C(sp<sup>3</sup>)-H bonds using photocatalysis or synergistic light/metal catalysis.<sup>287-293</sup> For instance, in 2020, the Zhou group employed a photoredox/organocatalytic system to achieve  $\beta$ -C-H *gem*-difluoroallylation of aliphatic aldehydes and cyclic ketones.<sup>287</sup> In the following year, the Martin group successfully introduced *gem*-difluoroalkenes at saturated hydrocarbon sites via selective defluorinative C(sp<sup>3</sup>)-H alkylation of amides.<sup>289</sup> More recently, the Guo group reported a metal-free, visible-light-induced *gem*-difluoroallylation of glycine derivatives.<sup>292</sup> However, these methods primarily target  $\alpha$ -heteroatom

C(sp<sup>3</sup>)-H sites<sup>289-293</sup> or remote C(sp<sup>3</sup>)-H positions.<sup>287-289</sup>

Despite these advances, the direct incorporation of *gem*-difluoroalkene units at  $\alpha$ -carbonyl C(sp<sup>3</sup>)-H bonds remains an unresolved challenge. Herein, developing novel approaches that enable direct access to carbon-centered radicals at  $\alpha$ -carbonyl positions remains a crucial goal for expanding the scope of functionalized  $\alpha$ -carbonyl derivatives.



**Scheme 3-2** Radical defluorinative routes to *gem*-difluoroalkenes

### 2.3.2 Condition optimizations

Inspired by recent progress in 1.5-HAT,<sup>153-177</sup> we selected iodoamide **3-1a** and trifluoromethyl alkene **3-2a** as model substrates. Encouragingly, when the reaction was conducted under N<sub>2</sub> using a catalytic amount of Ir(ppy)<sub>3</sub> and 1,3,5-trimethyl-1,3,5-triazinane as an additive in MeCN, irradiation with 456 nm blue LEDs for 12 hours yielded the desired *gem*-difluoroalkene **3-3aa** in 58% isolated yield (entry 1). Substituting Ir(ppy)<sub>3</sub> with alternative photocatalysts, such as Ru(bpy)<sub>3</sub>Cl<sub>2</sub>·6H<sub>2</sub>O, Ir[dF(CF<sub>3</sub>)ppy]<sub>2</sub>(dtbbpy)PF<sub>6</sub>, or 4CzIPN, led to a significant reduction in efficiency (entries 2-4). Various amines, including TMEDA, DIPEA, and Et<sub>3</sub>N, facilitated the reaction but proved less effective than triazinane (entries 5-7). Interestingly, DABCO was found inferior, (entry 8) presumably because it is less prone to  $\alpha$ -amino radical formation which is crucial in XAT. Notably, replacing triazinane with either K<sub>2</sub>HPO<sub>4</sub> or pyridine completely suppressed product formation (entries 9-10), suggesting that the amines function as electron transfer mediators in the photocatalytic *gem*-difluoroallylation of amides. Additionally, the reaction proceeded in other polar solvents such as acetone, DCE, and DMSO, though with reduced yields (entries 11-13). Control experiments showed that the presence of light, the photocatalyst, and triazinane were all indispensable for the successful  $\alpha$ -C(sp<sup>3</sup>)-H *gem*-difluoroallylation of **3-1a** with trifluoromethyl alkene **3-2a** (entry 14). Finally, adjusting the wavelength to 370 nm provided **3-3aa** in lower yield (entry 15). The reaction was not improved by replacing the iridium photocatalyst with 10-phenyl-phenothiazine (PHT, entry 16).

**Table 3-1** Condition optimizations<sup>a</sup>

entry	variations from standard conditions	<b>3-3aa</b> , yield (%) <sup>b</sup>
1	none	65 (58) <sup>c</sup>
2	Ru(bpy) <sub>3</sub> Cl <sub>2</sub> ·6H <sub>2</sub> O instead of Ir(ppy) <sub>3</sub>	8

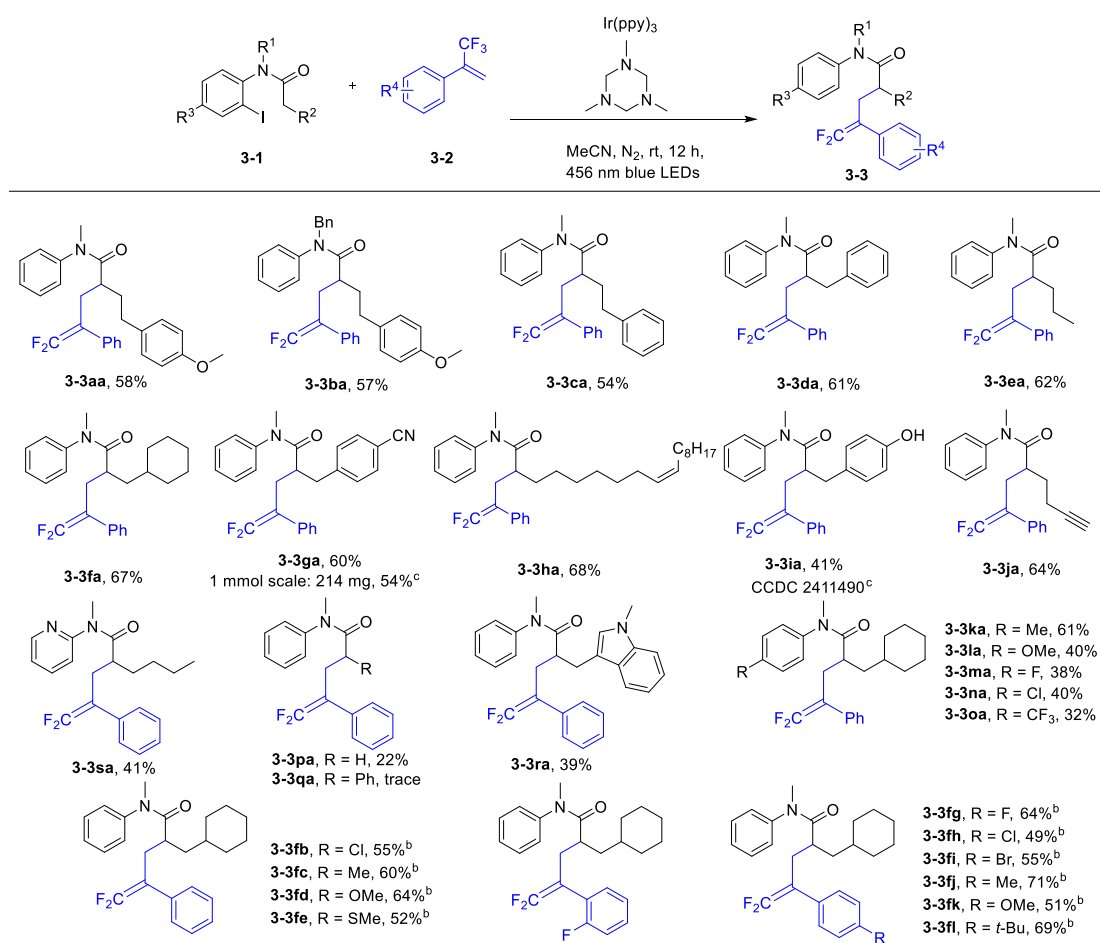
3	Ir[dF(CF <sub>3</sub> )ppy] <sub>2</sub> (dtbbpy)PF <sub>6</sub> instead of Ir(ppy) <sub>3</sub>	18
4	4CzIPN instead of Ir(ppy) <sub>3</sub>	21
5	TMEDA instead of triazinane	34
6	DIPEA instead of triazinane	51
7	Et <sub>3</sub> N instead of triazinane	52
8	DABCO instead of triazinane	17
9	K <sub>2</sub> HPO <sub>4</sub> instead of triazinane	0
10	Pyridine instead of triazinane	0
11	Acetone instead of MeCN	48
12	DCE instead of MeCN	53
13	DMSO instead of MeCN	42
14	no light, or photocatalyst, or no triazinane	0
15	λ = 370 nm (40 W) instead of 456 nm	52
16	λ = 370 nm (40 W) with PHT as PC	trace

<sup>a</sup>Unless otherwise noted, the standard reaction conditions were as follows: **3-1a** (0.15 mmol, 1 equiv.), **3-2a** (0.3 mmol, 2 equiv.), photocatalyst (0.003 mmol, 2 mol %), and base (0.3 mmol, 2 equiv.) in solvent (1.5 mL) with irradiation by 40W LEDs (λ = 456 nm) under N<sub>2</sub> at room temperature for 12 h. <sup>b</sup>The yields were determined by <sup>19</sup>F NMR analysis of the crude reaction mixture using benzotrifluoride as an internal standard. <sup>c</sup>isolated yield.

### 2.3.3 Substrate scope studies

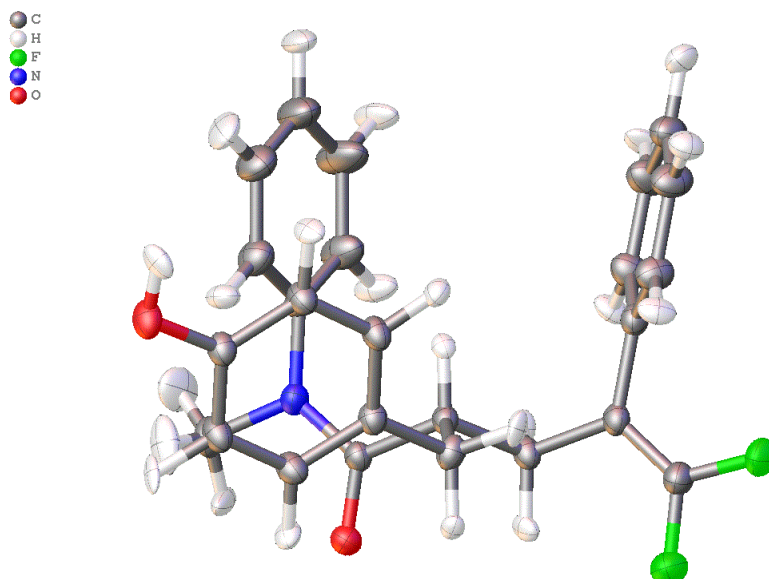
With the optimized conditions established, the substrate scope of this  $\alpha$ -C(sp<sup>3</sup>)-H *gem*-difluoroallylation reaction was explored (**Scheme 3-3**). Notably, altering the *N*-protecting group from methyl to benzyl had little impact on efficiency, yielding **3-3ba** in 57%. Several commonly used amides (**3-1c–3-1f**) were successfully transformed into their corresponding *gem*-difluoroallylated products (**3-3ca–3-3fa**) in 54%–67% yields. Delightedly, amides featuring diverse functional groups at the carbonyl fragment—including nitrile, alkene, phenol, and alkyne—were well tolerated under the optimized conditions, affording products **3-3ga–3-3ja** in moderate to good yields (41%–68%). The structure of **3-3ia** was definitively confirmed by X-ray single-crystal analysis (**Scheme 3-4**). Furthermore, iodoarene substrates bearing electron-donating groups, such as methyl or methoxy (**3-1k–3-1l**), provided the target compounds in 61% and 40% yield, respectively. Likewise, amides containing *para*-substituted fluoro, chloro, or trifluoromethyl groups delivered the desired products in yields of 32%–40% (**3-3ma–3-3oa**). Importantly, a primary  $\alpha$ -carbon iodoamide substrate (**3-1p**) could also be converted to the expected *gem*-difluoroalkene **3-3pa**, however in degraded yield (22%). Unfortunately, a benzylic  $\alpha$ -carbon iodoamide substrate **3-1q** led only to traces amount of the corresponding coupling product **3-3qa**. These results illustrate some of the limits of the method. We also investigated whether the method would tolerate some heterocycles. Fortunately, incorporate both a pyridine unit and an indole core was achieved with encouraging yields (**3-3ra–3-3sa**, 39–41%).

Next the scope of trifluoromethyl alkenes in the  $\alpha$ -C(sp<sup>3</sup>)-H *gem*-difluoroallylation of amide **3-1f** was examined. *meta*-Substituted trifluoromethyl styrenes with chloro, methyl, methoxy, or methylthio functionalities yielded the corresponding products in 52%–64% (**3-3fb–3-3fe**). Similarly, Trifluoromethyl styrenes bearing halogens (fluoro, chloro, bromo) or electron-rich groups (methyl, methoxy, *tert*-butyl) exhibited good reactivity, producing the target compounds in satisfactory yields (**3-3fg–3-3fl**, 49%–71%). However, *ortho*-fluoro substitution led to a significant drop in efficiency, affording only 30% yield (**3-3ff**).



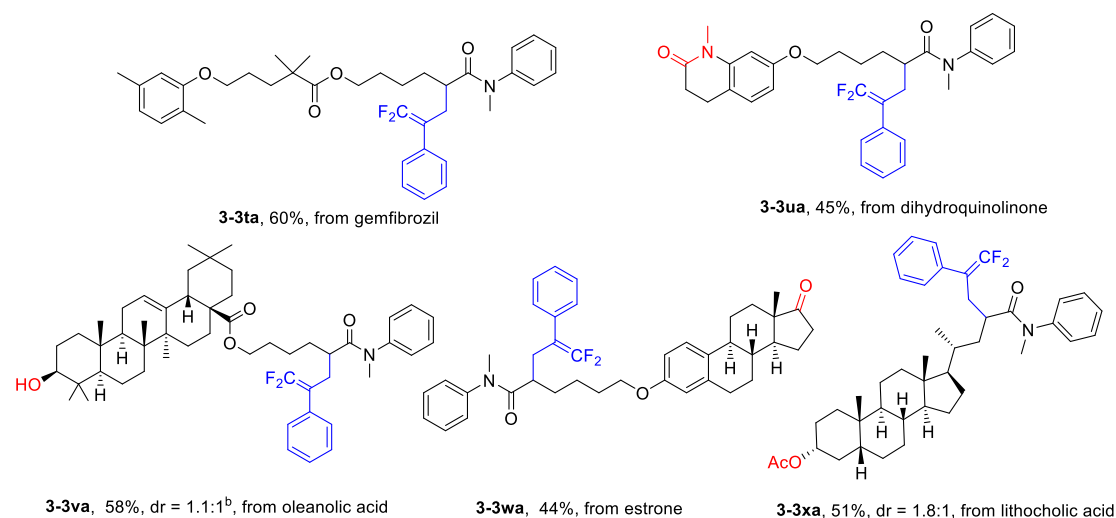
<sup>a</sup>Reaction conditions: **3-1** (0.15 mmol, 1 equiv.), **3-2** (0.3 mmol, 2 equiv.),  $\text{Ir(ppy)}_3$  (0.003 mmol, 2 mol%), and triazinane (0.3 mmol, 2 equiv.) in anhydrous MeCN (1.5 mL) with irradiation by 40W LEDs ( $\lambda = 456 \text{ nm}$ ) under  $\text{N}_2$  at room temperature for 12 h. <sup>b</sup>0.45 mmol **3-2** (3 equiv.) and 2.0 mL MeCN was used. <sup>c</sup>1 mmol scale: anhydrous MeCN (10 mL), react for 24 h. <sup>c</sup>see scheme **3-4** for detail.

**Scheme 3-3** Scope of amides and trifluoromethyl alkenes<sup>a</sup>



**Scheme 3-4** X-ray image of **3-3ia**. Suitable single crystal for X-ray diffraction were grown by liquid-liquid diffusion from a concentrated solution of compound **3-3ia** in  $\text{CH}_2\text{Cl}_2$  and *n*-hexane. And B.E. and Prof. Oppel measured and analyzed crystal structure. CCDC: 2411490

Moreover, the *gem*-difluoroallylation strategy was successfully applied to the late-stage modification of complex bioactive molecules (**Scheme 3-5**). Amides derived from gemfibrozil, dihydroquinolinone, and lithocholic acid were smoothly converted into their respective *gem*-difluoroalkene products in 60%, 45%, and 51% yield (**3-3ta**, **3-3ua**, **3-3xa**). Remarkably, amide **3-1v**, synthesized from oleanolic acid, underwent selective  $\alpha$ -carbonyl functionalization, affording **3-3va** in good yield while preserving its free hydroxyl group. Additionally, an estrone amide derivative **3-1w** was efficiently transformed under the mild conditions, providing **3-3wa** in 44% yield. Importantly, no *gem*-difluoroallylation occurred at the ketone moiety of **3-1w**, the lactam core of **3-1u**, or the ester functionality of **3-1x**, highlighting the high 1,5-regiospecificity of this transformation.



<sup>a</sup>Reaction conditions: **3-1** (0.15 mmol, 1 equiv.), **3-2** (0.3 mmol, 2 equiv.), Ir(ppy)<sub>3</sub> (0.003 mmol, 2 mol%), and triazinane (0.3 mmol, 2 equiv.) in anhydrous MeCN (1.5 mL) with irradiation by 40W LEDs ( $\lambda = 456$  nm) under N<sub>2</sub> at room temperature for 12 h. <sup>b</sup>dr ratios were determined by <sup>19</sup>F NMR analysis of purified product.

**Scheme 3-5** Late-stage *gem*-difluoroallylation of complex molecules<sup>a</sup>

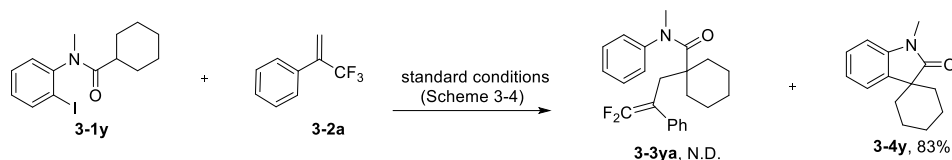
### 2.3.4 Mechanistic studies

Next, a tertiary  $\alpha$ -carbon iodoamide substrate **3-1y** was considered (**Scheme 3-6a**). However, only the known intramolecular spiro cyclization product **3-4y** could be found, and in good yield (83%).<sup>294</sup> The *gem*-difluoroallylation coupling product **3-3ya** could not be detected. In order to gain more insight into the reaction mechanism, we first performed a radical trapping experiment. The addition of 2,2,6,6-tetramethyl-1-piperidinyloxy (TEMPO) as a radical scavenger significantly suppressed the reaction, and the TEMPO-adduct **3-5a** was isolated in 38% yield (**Scheme 3-6b**). This finding suggests that the  $\alpha$ -C(sp<sup>3</sup>)-H *gem*-difluoroallylation of amides proceeds via a radical pathway. Next, fluorescence quenching experiments were conducted to assess interactions between the photocatalyst Ir(ppy)<sub>3</sub> and key reaction components, including the triazinane, iodoarene **3-1f**, and trifluoromethyl styrene **3-2a** (see Part 4.2.3 for details). Stern-Volmer analysis revealed pronounced quenching by the triazinane and minor quenching by iodoarene **3-1f**, supporting the hypothesis that the reaction is initiated by a photoredox cycle in which the triazinane participates in a reductive quenching process.

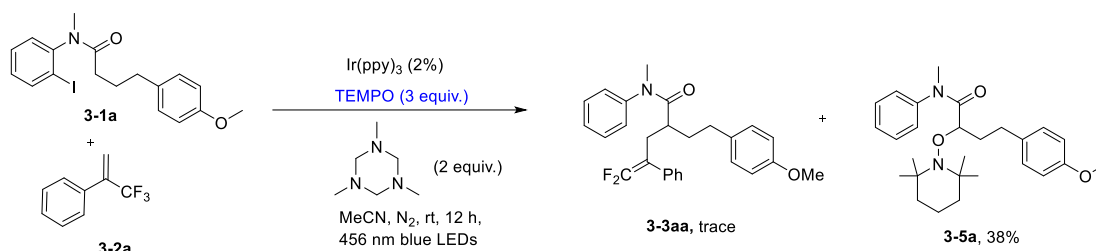
Based on these mechanistic studies, including the Stern-Volmer analysis and TEMPO inhibition experiment, and drawing from previous reports identifying the triazinane as a halogen atom transfer (XAT) agent,<sup>295-296</sup> a plausible reaction mechanism involving XAT and 1,5-hydrogen atom transfer (1,5-HAT) was proposed (**Scheme 3-6c**). Upon visible-light irradiation, the photocatalyst Ir(ppy)<sub>3</sub>

undergoes photoexcitation and engages in a single-electron transfer (SET) event, oxidizing the triazinane to its radical cation form. Deprotonation then generates a diamino-substituted radical **3-I**, which facilitates halogen atom transfer (XAT) to activate substrate **3-1**, yielding the aryl radical intermediate **3-III**. Subsequently, an intramolecular 1,5-HAT process converts intermediate **3-III** into  $\alpha$ -carbonyl radical **3-IV**, which is then intercepted by trifluoromethyl styrene **3-2**, forming intermediate **3-V**. Finally, single-electron reduction of intermediate **3-V** promotes C-F bond cleavage, leading to the formation of the target *gem*-difluoroalkene **3-3** while simultaneously regenerating the photocatalyst to complete the catalytic cycle.

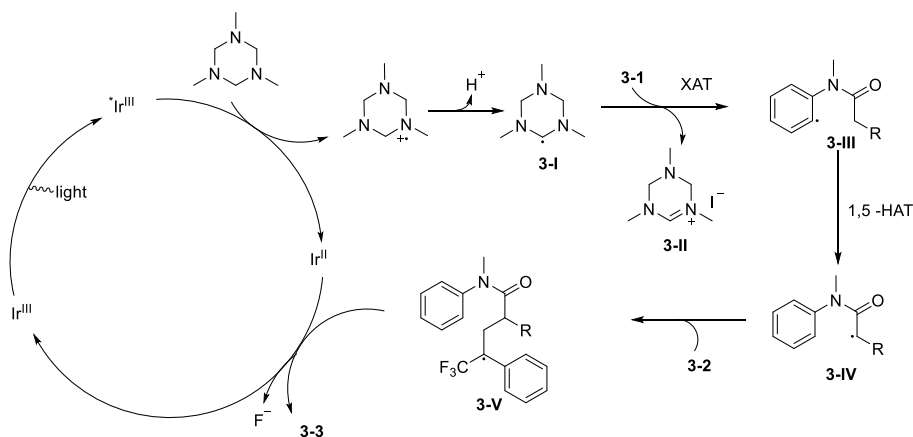
a) Tertiary  $\alpha$ -carbon substrate



b) Radical trapping experiment



c) Proposed mechanism



Scheme 3-6 Mechanistic study and proposed catalytic cycle

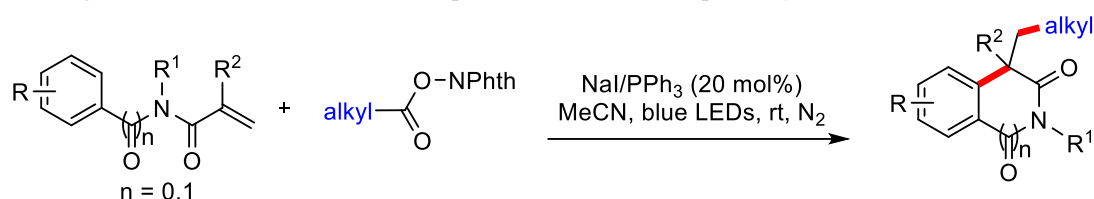
### 2.3.5 Conclusion

In summary, a visible-light-driven aryl-to-alkyl radical relay strategy for the *gem*-difluoroallylation of amides using trifluoromethyl alkenes was developed. This approach leverages a mild and selective iodoarene-mediated photoredox process, integrating halogen atom transfer (XAT) and hydrogen atom transfer (HAT) to enable  $\alpha$ -C(sp<sup>3</sup>)-H functionalization. The method exhibits broad functional group tolerance and efficiently delivers a variety of carbonyl-containing *gem*-difluoroalkenes. Furthermore, its applicability to the late-stage modification of bioactive molecules underscores its potential significance in drug discovery and development.

### 3 Summary and outlook

Oxindoles, quinoxalinones, and *gem*-difluoroalkenes are important motifs ubiquitous in nature products, drugs and bioactive molecules. Here we employed visible-light-mediated photochemical protocol to access these valuable compounds under mild conditions and with good efficiency.

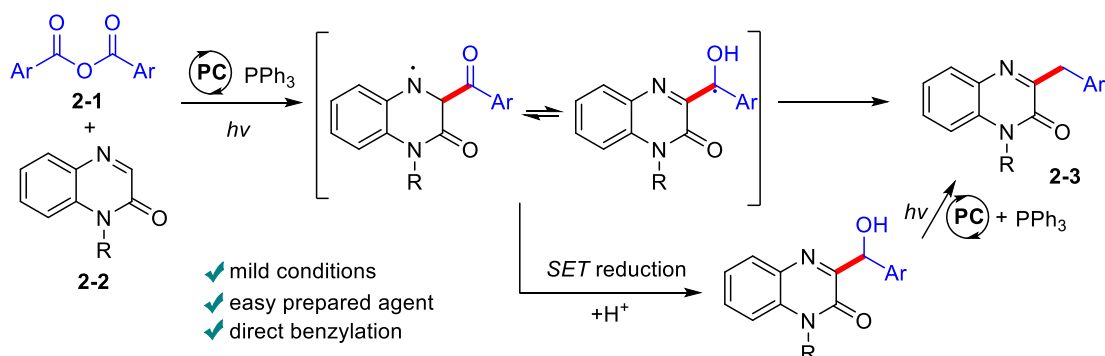
First, a practical NaI/PPh<sub>3</sub>-catalyzed decarboxylative radical cascade cyclization of *N*-arylacrylamides with redox-active esters was developed, utilizing visible light irradiation as a key driving force. This transition-metal-free strategy offers a mild, cost-effective, and highly efficient approach for constructing diverse oxindoles with a C3 quaternary stereogenic center. A broad scope of substrates, including  $\alpha$ -amino acid-derived compounds and various carboxylic acid derivatives, were demonstrated under this optimal, simple and cheap catalytic system. Mechanistic investigations indicate that the reaction proceeds via a radical pathway (**Scheme 4-1**).



✓ transition-metal-free catalysis    ✓ optimal, simple and cheap catalytic system    ✓ broad scope

**Scheme 4-1** Photocatalytic decarboxylative cyclization via NaI/PPh<sub>3</sub> catalysis

Next, a visible-light-driven photocatalytic strategy for the deoxygenative benzylation of quinoxalin-2(1*H*)-ones was reported. This innovative method offers a straightforward, mild, and practical approach to synthesizing 3-benzylquinoxalin-2(1*H*)-ones using readily available and non-hazardous carboxylic acid anhydrides. A diverse array of substrates bearing various functional groups exhibited excellent compatibility, leading to the efficient formation of functionalized 3-benzylquinoxalin-2(1*H*)-ones with significant potential for pharmaceutical applications. Mechanistic studies indicate that H<sub>2</sub>O serves as the proton donor, while hydroxylated quinoxalin-2(1*H*)-ones may act as crucial intermediates in the deoxygenative photocatalytic transformation (**Scheme 4-2**).

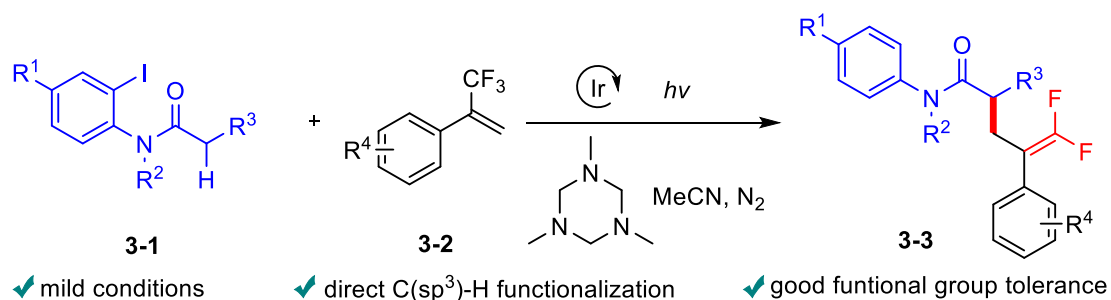


**Scheme 4-2** Photocatalyzed deoxygenative benzylation of quinoxalinones via SET reduction

Finally, we introduce a photocatalytic radical strategy for  $\alpha$ -C(sp<sup>3</sup>)-H *gem*-difluoroallylation of amides with trifluoromethyl alkenes, enabling the synthesis of target compounds in good yields with broad functional group compatibility. The mild and efficient reaction conditions facilitate the concise incorporation of *gem*-difluoroalkene motifs as carbonyl bioisosteres into structurally complex molecules, including derivatives of *gem*fibrozil and estrone, highlighting their potential for late-stage modifications of pharmaceuticals, natural products, and biologically relevant



intermediates. Mechanistic insights reveal a radical-driven process involving XAT and 1,5-HAT (Scheme 4-3).



**Scheme 4-3** Visible-light driven aryl-to-alkyl radical relay *gem*-difluoroallylation of amides

In the future, developing green and sustainable photochemistry for the synthesis of pharmaceutically relevant molecule scaffolds is the key in organic synthesis. Especially exploring non-metal photocatalyst like EDA complex and improving their reactivities are challenging and significant, and will open up new opportunities in radical generating. And researching these radical as versatile synthetic intermediates will play an important role in efficiently constructing structurally diverse functional molecules.

## 4 Experiment and data

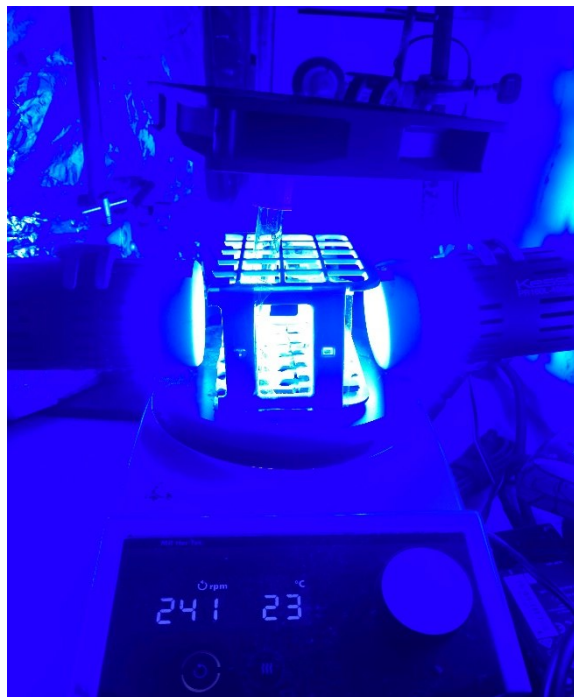
### 4.1 General information

#### Reagents

Unless otherwise noted, all commercially available compounds were used as provided without further purification and chemicals used for synthesis were purchased from Sigma Aldrich, Abcr, TCI, Fisher, Chempur and BLDPharm. Anhydrous solvents were obtained by using an Innovative Technology PS-MD-5 solvent purification system.

#### Photoreactor

All reactions with LEDs irradiation were carried out using a photo-reactor equipped with LED PhotoReaction Lighting (Model: PR160L,  $\lambda = 456$  nm or 370 nm, max 40W), which is bought from Kessil company. The glass vials were placed at approximately 4 cm away from the light source. In order to avoid overheating of the reaction system, the vials were cooled with a fan on top of the vials.



#### NMR spectroscopy

NMR spectra were recorded on an Agilent VNMRs 400 or a Bruker Av 600 using  $\text{CDCl}_3$  or  $\text{DMSO}-d_6$  as solvents. Chemical shifts  $\delta$  are given in ppm relative to TMS as reference. The following abbreviations were used for  $^1\text{H}$ ,  $^{13}\text{C}$  and  $^{19}\text{F}$  NMR spectra to indicate the signal multiplicity: s (singlet), d (doublet), t (triplet), q (quartet) and m (multiplet) as well as combinations of them.

#### IR spectra

IR spectra were measured on a PerkinElmer 100 FT-IR spectrometer with an UATR Diamond KRS-5 unit.

#### Mass spectra

High-resolution mass spectra (HRMS) were obtained on a Thermo Scientific LTQ Orbitrap XL spectrometer.

#### X-ray measurement

Crystallographic data were collected on a Bruker Kappa APEX II CCD-diffractometer with monochromatic Mo-K $\alpha$  radiation ( $\lambda=0.71073$  Å) and a CCD detector.

#### Stern–Volmer experiments

The Agilent Cary Eclipse Fluorescence Spectrometer is used to conduct Stern-Volmer fluorescence quenching analysis. We thank Steffen Schauerte and Prof. Dr. Markus Albrecht (Institute of Organic Chemistry, RWTH Aachen University) for access to the equipment.

#### Others

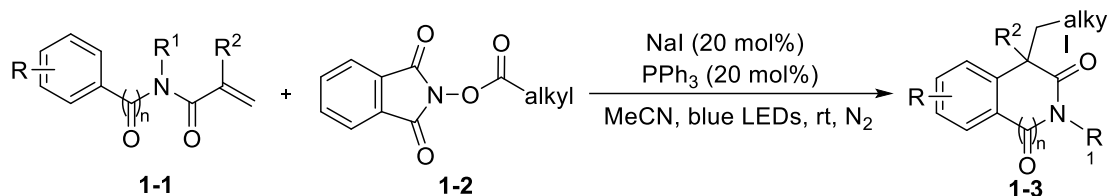
Aluminium blocks equipped with slots that accommodate the glass vial reactors were utilized for all experiments requiring heating. Thin-layer chromatography (TLC) was performed on VWR silica gel aluminium plates with F-254 indicator, visualized by UV light irradiation.

## 4.2 Experimental methods and data

### 4.2.1 NaI/PPh<sub>3</sub>-catalyzed visible-light-mediated decarboxylative radical cascade cyclization of

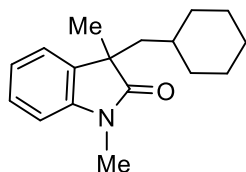
#### *N*-arylacrylamides for the efficient synthesis of quaternary oxindoles

##### General procedure for the synthesis of quaternary oxindoles



To an oven-dried vial equipped with a stirring bar, acrylamide **1-1** (0.3 mmol), redox-active ester **1-2** (0.2 mmol), NaI (6 mg, 0.04 mmol) and Ph<sub>3</sub>P (10.5 mg, 0.04 mmol) were added, then the tube was evacuated and filled with N<sub>2</sub> (three times) before anhydrous acetonitrile (MeCN, 2.0 mL) was added. The reaction was performed under blue LEDs irradiation (456 nm, 40 W) at room temperature. After 36 h, the solvent was removed in vacuo, and the residue was purified by column chromatography to give the corresponding quaternary oxindole products.

##### Product characterization



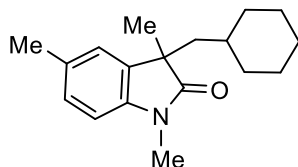
##### 3-(Cyclohexylmethyl)-1,3-dimethylindolin-2-one (**1-3aa**)

The crude mixture was purified by silica gel column chromatography with pentane/EA (10:1). 37 mg product was obtained by 72% isolated yield as colorless liquid.

<sup>1</sup>H NMR (600 MHz, Chloroform-*d*)  $\delta$  7.18 (t,  $J$  = 7.8 Hz, 1H), 7.08 (d,  $J$  = 7.2 Hz, 1H), 6.98 (t,  $J$  = 7.2 Hz, 1H), 6.76 (d,  $J$  = 7.8 Hz, 1H), 3.14 (s, 3H), 1.85 (dd,  $J$  = 14.4, 6.6 Hz, 1H), 1.65 (dd,  $J$  = 14.4, 5.4 Hz, 1H), 1.47 – 1.34 (m, 3H), 1.27 (d,  $J$  = 11.4 Hz, 1H), 1.24 (s, 3H), 1.14 (d,  $J$  = 12.0 Hz, 1H), 0.98 – 0.82 (m, 4H), 0.78 – 0.64 (m, 2H).

<sup>13</sup>C NMR (151 MHz, Chloroform-*d*)  $\delta$  181.1, 143.1, 134.4, 127.5, 122.7, 122.3, 107.9, 47.8, 45.4, 34.7, 34.5, 33.5, 26.2, 26.15, 26.10, 26.0.

Data is consistent with the literature.<sup>197</sup>



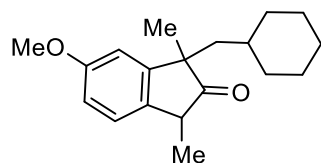
##### 3-(Cyclohexylmethyl)-1,3,5-trimethylindolin-2-one (**1-3ba**)

The crude mixture was purified by silica gel column chromatography with pentane/EA (10:1). 37 mg product was obtained by 68% isolated yield as colorless liquid.

<sup>1</sup>H NMR (600 MHz, Chloroform-*d*)  $\delta$  6.98 (d,  $J$  = 7.8 Hz, 1H), 6.89 (s, 1H), 6.65 (d,  $J$  = 7.8 Hz, 1H), 3.12 (s, 3H), 2.28 (s, 3H), 1.84 (dd,  $J$  = 14.4, 7.2 Hz, 1H), 1.63 (dd,  $J$  = 14.4, 5.4 Hz, 1H), 1.48 – 1.36 (m, 3H), 1.30 – 1.12 (m, 5H), 0.94 – 0.86 (m, 4H), 0.78 – 0.64 (m, 2H).

$^{13}\text{C}$  NMR (151 MHz, Chloroform-*d*)  $\delta$  181.1, 140.8, 134.5, 131.8, 127.7, 123.6, 107.6, 47.9, 45.4, 34.7, 34.5, 33.5, 26.3, 26.2, 26.1, 26.0, 21.2.

Data is consistent with the literature.<sup>197</sup>



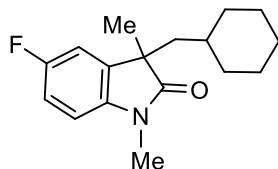
### 1-(Cyclohexylmethyl)-6-methoxy-1,3-dimethyl-1,3-dihydro-2H-inden-2-one (1-3ca)

The crude mixture was purified by silica gel column chromatography with pentane/EA (8:1). 38 mg product was obtained by 66% isolated yield as colorless liquid.

$^1\text{H}$  NMR (600 MHz, Chloroform-*d*)  $\delta$  6.73 – 6.69 (m, 2H), 6.68 – 6.65 (m, 1H), 3.74 (s, 3H), 3.12 (s, 3H), 1.85 (dd,  $J$  = 14.4, 7.2 Hz, 1H), 1.62 (dd,  $J$  = 14.4, 5.4 Hz, 1H), 1.47 – 1.36 (m, 3H), 1.38 – 1.12 (m, 5H), 0.94 – 0.82 (m, 4H), 0.82 – 0.63 (m, 2H).

$^{13}\text{C}$  NMR (151 MHz, Chloroform-*d*)  $\delta$  180.8, 155.9, 136.7, 135.9, 111.4, 110.5, 108.1, 55.8, 48.3, 45.4, 34.7, 34.4, 33.5, 26.6, 26.3, 26.1, 26.0.

Data is consistent with the literature.<sup>197</sup>



### 3-(Cyclohexylmethyl)-5-fluoro-1,3-dimethylindolin-2-one (1-3da)

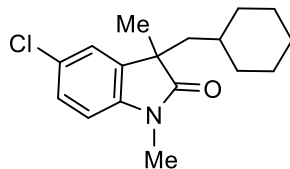
The crude mixture was purified by silica gel column chromatography with pentane/EA (20:1). 41 mg product was obtained by 74% isolated yield as colorless liquid.

$^1\text{H}$  NMR (400 MHz, Chloroform-*d*)  $\delta$  7.01 – 6.85 (m, 2H), 6.74 (dd,  $J$  = 8.4, 4.0 Hz, 1H), 3.19 (s, 3H), 1.92 (dd,  $J$  = 14.2, 6.8 Hz, 1H), 1.68 (dd,  $J$  = 14.2, 5.2 Hz, 1H), 1.55 – 1.42 (m, 3H), 1.34 – 1.18 (m, 5H), 1.02 – 0.88 (m, 4H), 0.85 – 0.71 (m, 2H).

$^{13}\text{C}$  NMR (101 MHz, Chloroform-*d*)  $\delta$  180.7, 159.3 (d,  $J$  = 242.4 Hz), 139.0 (d,  $J$  = 1.6 Hz), 136.2 (d,  $J$  = 8.1 Hz), 113.6 (d,  $J$  = 23.2 Hz), 111.8 (d,  $J$  = 25.2 Hz), 108.3 (d,  $J$  = 8.1 Hz), 48.3 (d,  $J$  = 1.6 Hz), 45.3, 34.7, 34.4, 33.4, 26.3, 26.1, 26.04, 26.01, 25.98.

$^{19}\text{F}$  NMR (376 MHz, Chloroform-*d*)  $\delta$  -121.02 (td,  $J$  = 8.7, 3.9 Hz).

Data is consistent with the literature.<sup>209</sup>



### 5-Chloro-3-(cyclohexylmethyl)-1,3-dimethylindolin-2-one (1-3ea)

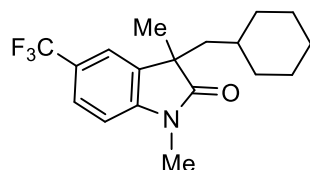
The crude mixture was purified by silica gel column chromatography with pentane/EA (10:1). 38 mg product was obtained by 65% isolated yield as colorless liquid.

$^1\text{H}$  NMR (600 MHz, Chloroform-*d*)  $\delta$  7.16 (dd,  $J$  = 8.4, 1.2 Hz, 1H), 7.06 (d,  $J$  = 2.4 Hz, 1H), 6.69 (d,  $J$  = 8.4 Hz, 1H), 3.13 (s, 3H), 1.86 (dd,  $J$  = 14.4, 7.2 Hz, 1H), 1.63 (dd,  $J$  = 14.4, 5.4 Hz, 1H), 1.49 – 1.34 (m, 3H), 1.26 – 1.12 (m, 5H), 0.98 – 0.83 (m, 4H), 0.79 – 0.63 (m, 2H).

$^{13}\text{C}$  NMR (151 MHz, Chloroform-*d*)  $\delta$  180.6, 141.7, 136.2, 127.8, 127.5, 123.2, 108.9, 48.1, 45.3,

34.7, 34.4, 33.4, 26.3, 26.2, 26.1, 26.03, 25.98.

Data is consistent with the literature.<sup>209</sup>



### 3-(Cyclohexylmethyl)-1,3-dimethyl-5-(trifluoromethyl)indolin-2-one (1-3fa)

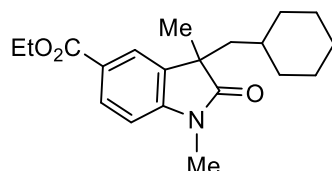
The crude mixture was purified by silica gel column chromatography with pentane/EA (10:1). 55 mg product was obtained by 85% isolated yield as colorless liquid.

<sup>1</sup>H NMR (600 MHz, Chloroform-*d*)  $\delta$  7.48 (d, *J* = 7.8 Hz, 1H), 7.31 (s, 1H), 6.84 (d, *J* = 7.8 Hz, 1H), 3.18 (s, 3H), 1.88 (dd, *J* = 14.4, 7.2 Hz, 1H), 1.68 (dd, *J* = 14.4, 5.4 Hz, 1H), 1.48 – 1.36 (m, 3H), 1.28 – 1.09 (m, 5H), 0.96 – 0.82 (m, 4H), 0.80 – 0.64 (m, 2H).

<sup>13</sup>C NMR (151 MHz, Chloroform-*d*)  $\delta$  181.0, 146.1, 135.0, 125.4 (q, *J* = 4.7 Hz), 124.6 (q, *J* = 33.5 Hz), 119.7 (q, *J* = 4.4 Hz, 1H), 107.7, 47.9, 45.3, 34.7, 34.4, 33.5, 26.4, 26.0, 25.98, 25.94.

<sup>19</sup>F NMR (282 MHz, Chloroform-*d*)  $\delta$  -61.32.

Data is consistent with the literature.<sup>197</sup>



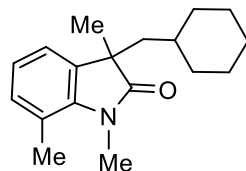
### Ethyl 3-(cyclohexylmethyl)-1,3-dimethyl-2-oxoindoline-5-carboxylate (1-3ga)

The crude mixture was purified by silica gel column chromatography with pentane/EA (10:1). 48 mg product was obtained by 73% isolated yield as colorless liquid.

<sup>1</sup>H NMR (600 MHz, Chloroform-*d*)  $\delta$  7.96 (d, *J* = 8.4 Hz, 1H), 7.76 (s, 1H), 6.80 (d, *J* = 8.4 Hz, 1H), 4.31 (q, *J* = 7.2 Hz, 2H), 3.18 (s, 3H), 1.87 (dd, *J* = 14.4, 7.2 Hz, 1H), 1.75 – 1.68 (dd, *J* = 14.4, 7.2 Hz, 1H), 1.48 – 1.37 (m, 3H), 1.34 (t, *J* = 7.2 Hz, 3H), 1.29 – 1.11 (m, 5H), 0.97 – 0.79 (m, 4H), 0.79 – 0.63 (m, 2H).

<sup>13</sup>C NMR (151 MHz, Chloroform-*d*)  $\delta$  181.4, 166.6, 147.2, 134.3, 130.3, 124.7, 123.9, 107.4, 60.9, 47.7, 45.3, 34.7, 34.4, 33.4, 26.4, 26.1, 26.0, 25.98, 14.4.

Data is consistent with the literature.<sup>197</sup>



### 3-(Cyclohexylmethyl)-1,3,7-trimethylindolin-2-one (1-3ha)

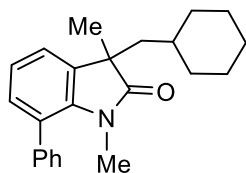
The crude mixture was purified by silica gel column chromatography with pentane/EA (10:1). 31 mg product was obtained by 57% isolated yield as colorless liquid.

<sup>1</sup>H NMR (600 MHz, Chloroform-*d*)  $\delta$  6.99 – 6.64 (m, 3H), 3.42 (s, 3H), 2.52 (s, 3H), 1.84 (dd, *J* = 14.4, 7.2 Hz, 1H), 1.61 (dd, *J* = 14.4, 5.4 Hz, 1H), 1.48 – 1.37 (m, 3H), 1.29 (d, *J* = 13.2 Hz, 1H), 1.21 (s, 3H), 1.15 (d, *J* = 13.2 Hz, 1H), 0.96 – 0.83 (m, 4H), 0.79 – 0.62 (m, 2H).

<sup>13</sup>C NMR (151 MHz, Chloroform-*d*)  $\delta$  181.9, 140.9, 135.1, 131.2, 122.2, 120.7, 119.5, 47.2, 45.7,

34.6, 34.5, 33.5, 29.5, 26.6, 26.1, 26.1, 26.0, 19.1.

Data is consistent with the literature.<sup>197</sup>



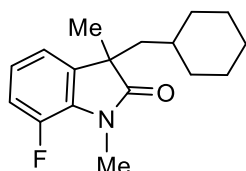
### 3-(Cyclohexylmethyl)-1,3-dimethyl-7-phenylindolin-2-one (1-3ia)

The crude mixture was purified by silica gel column chromatography with pentane/EA (10:1). 41 mg product was obtained by 62% isolated yield as colorless liquid.

<sup>1</sup>H NMR (600 MHz, Chloroform-*d*)  $\delta$  7.41 – 7.20 (m, 5H), 7.07 (d, *J* = 7.2 Hz, 1H), 7.04 – 6.91 (m, 2H), 2.65 (s, 3H), 1.88 (dd, *J* = 13.8, 7.2 Hz, 1H), 1.67 (dd, *J* = 13.8, 5.4 Hz, 1H), 1.56 – 1.37 (m, 3H), 1.33 (d, *J* = 12.0 Hz, 1H), 1.29 (s, 3H), 1.17 (d, *J* = 14.2 Hz, 1H), 0.98 – 0.89 (m, 4H), 0.80 – 0.67 (m, 2H).

<sup>13</sup>C NMR (151 MHz, Chloroform-*d*)  $\delta$  182.2, 140.1, 139.2, 135.5, 130.5, 130.0, 129.8, 127.9, 127.8, 127.6, 125.4, 121.7, 121.6, 47.2, 46.0, 34.8, 34.5, 33.6, 30.2, 26.3, 26.2, 26.14, 26.1.

Data is consistent with the literature.<sup>197</sup>



### 3-(Cyclohexylmethyl)-7-fluoro-1,3-dimethylindolin-2-one (1-3ja)

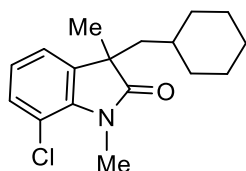
The crude mixture was purified by silica gel column chromatography with pentane/EA (10:1). 28 mg product was obtained by 50% isolated yield as colorless liquid.

<sup>1</sup>H NMR (600 MHz, Chloroform-*d*)  $\delta$  6.94 – 6.82 (m, 3H), 3.36 (s, 3H), 1.86 (dd, *J* = 14.4, 7.2 Hz, 1H), 1.64 (dd, *J* = 14.4, 5.4 Hz, 1H), 1.49 – 1.36 (m, 3H), 1.28 (d, *J* = 12.0 Hz, 1H), 1.24 (s, 3H), 1.14 (d, *J* = 12.0 Hz, 1H), 0.95 – 0.83 (m, 4H), 0.81 – 0.65 (m, 2H).

<sup>13</sup>C NMR (151 MHz, Chloroform-*d*)  $\delta$  180.7, 147.8 (d, *J* = 243.4 Hz), 137.5 (d, *J* = 3.0 Hz), 129.7 (d, *J* = 8.0 Hz), 122.9 (d, *J* = 6.3 Hz), 118.6 (d, *J* = 3.2 Hz), 115.6 (d, *J* = 19.3 Hz), 48.2 (d, *J* = 2.0 Hz), 45.6, 34.7, 34.4, 33.5, 28.7, 28.6, 26.4, 26.08, 26.06, 26.0.

<sup>19</sup>F NMR (565 MHz, Chloroform-*d*)  $\delta$  -136.73.

Data is consistent with the literature.<sup>197</sup>



### 7-Chloro-3-(cyclohexylmethyl)-1,3-dimethylindolin-2-one (1-3ka)

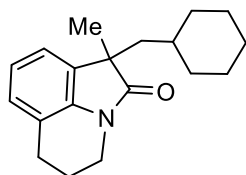
The crude mixture was purified by silica gel column chromatography with pentane/EA (10:1). 37 mg product was obtained by 63% isolated yield as colorless liquid.

<sup>1</sup>H NMR (600 MHz, Chloroform-*d*)  $\delta$  7.10 (d, *J* = 8.4 Hz, 1H), 6.96 (d, *J* = 7.2 Hz, 1H), 6.89 (t, *J* = 7.8 Hz, 1H), 3.51 (s, 3H), 1.86 (dd, *J* = 14.4, 7.2 Hz, 1H), 1.62 (dd, *J* = 14.4, 5.4 Hz, 1H), 1.49 – 1.37 (m, 3H), 1.27 (d, *J* = 13.8 Hz, 1H), 1.23 (s, 3H), 1.14 (d, *J* = 12.6 Hz, 1H), 0.95 – 0.82 (m, 4H),

0.78 – 0.65 (m, 2H).

$^{13}\text{C}$  NMR (151 MHz, Chloroform-*d*)  $\delta$  181.3, 139.0, 137.3, 129.9, 123.1, 121.2, 115.4, 47.7, 45.6, 34.6, 34.5, 33.5, 29.5, 26.6, 26.1, 26.0.

Data is consistent with the literature.<sup>209</sup>



### 1-(Cyclohexylmethyl)-1-methyl-5,6-dihydro-4H-pyrrolo[3,2,1-ij]quinolin-2(1H)-one (1-3la)

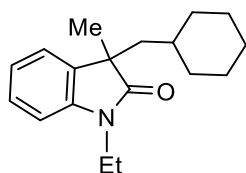
The crude mixture was purified by silica gel column chromatography with pentane/EA (10:1). 38 mg product was obtained by 67% isolated yield as colorless liquid.

$^1\text{H}$  NMR (600 MHz, Chloroform-*d*)  $\delta$  6.98 – 6.83 (m, 3H), 3.64 (t,  $J$  = 4.8 Hz, 2H), 2.76 – 2.68 (m, 2H), 1.96 – 1.86 (m, 2H), 1.83 (dd,  $J$  = 14.4, 7.2 Hz, 1H), 1.64 (dd,  $J$  = 14.4, 4.2 Hz, 1H), 1.47 – 1.37 (m, 3H), 1.32 (d,  $J$  = 13.2 Hz, 1H), 1.18 (d,  $J$  = 14.4 Hz, 1H), 1.25 (s, 3H), 0.96 – 0.88 (m, 4H), 0.80 – 0.67 (m, 2H).

$^{13}\text{C}$  NMR (151 MHz, Chloroform-*d*)  $\delta$  180.0, 138.9, 133.0, 126.3, 121.8, 120.6, 120.0, 49.2, 45.3, 38.8, 34.8, 34.5, 33.6, 26.15, 26.13, 26.0, 25.8, 24.7, 21.4.

HRMS (ESI-MS) Calcd. For  $\text{C}_{19}\text{H}_{25}\text{NONa}$   $[\text{M}+\text{Na}]^+$  306.18284, found: 306.18234.

IR (neat,  $\text{cm}^{-1}$ ):  $\tilde{\nu}$ : 3413, 2921, 1706, 1626, 1482, 1347, 1238, 1164, 1065, 956, 871, 749.



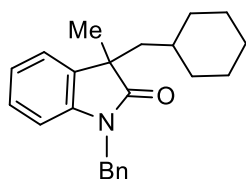
### 3-(Cyclohexylmethyl)-1-ethyl-3-methylindolin-2-one (1-3ma)

The crude mixture was purified by silica gel column chromatography with pentane/EA (10:1). 36 mg product was obtained by 66% isolated yield as colorless liquid.

$^1\text{H}$  NMR (600 MHz, Chloroform-*d*)  $\delta$  7.17 (td,  $J$  = 7.2, 1.2 Hz, 1H), 7.09 (dd,  $J$  = 7.8, 1.2 Hz, 1H), 6.97 (td,  $J$  = 7.2, 1.2 Hz, 1H), 6.78 (d,  $J$  = 7.8 Hz, 1H), 3.81 (dq,  $J$  = 14.4, 7.3 Hz, 1H), 3.83-3.78 (dq,  $J$  = 14.4, 7.2 Hz, 1H), 1.85 (dd,  $J$  = 14.4, 6.6 Hz, 1H), 1.64 (dd,  $J$  = 14.4, 6.6 Hz, 1H), 1.47 – 1.31 (m, 4H), 1.23 (s, 3H), 1.17 (t,  $J$  = 7.2 Hz, 3H), 1.12 – 1.07 (m, 1H), 0.95 – 0.82 (m, 4H), 0.79 – 0.61 (m, 2H).

$^{13}\text{C}$  NMR (151 MHz, Chloroform-*d*)  $\delta$  180.6, 142.2, 134.8, 127.4, 122.9, 122.1, 108.1, 47.7, 45.5, 34.8, 34.4, 34.38, 33.7, 26.1, 26.08, 26.0, 12.5.

Data is consistent with the literature.<sup>197</sup>



### 1-Benzyl-3-(cyclohexylmethyl)-3-methylindolin-2-one (1-3na)

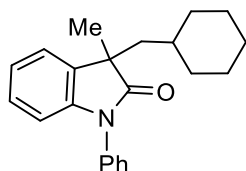
The crude mixture was purified by silica gel column chromatography with pentane/EA (10:1). 41 mg product was obtained by 61% isolated yield as colorless liquid.



$^1\text{H}$  NMR (600 MHz, Chloroform-*d*)  $\delta$  7.23 – 7.13 (m, 5H), 7.10 – 7.04 (m, 2H), 6.93 (t,  $J$  = 7.2 Hz, 1H), 6.66 (d,  $J$  = 7.8 Hz, 1H), 4.97 (d,  $J$  = 15.6 Hz, 1H), 4.72 (d,  $J$  = 15.6 Hz, 1H), 1.91 (dd,  $J$  = 13.8, 6.6 Hz, 1H), 1.68 (dd,  $J$  = 13.8, 6.0 Hz, 1H), 1.45 – 1.34 (m, 4H), 1.29 (s, 3H), 1.07 (d,  $J$  = 12.6 Hz, 1H), 0.96 – 0.74 (m, 5H), 0.67 – 0.59 (m, 1H).

$^{13}\text{C}$  NMR (151 MHz, Chloroform-*d*)  $\delta$  181.0, 142.3, 136.2, 134.6, 128.7, 127.5, 127.4, 122.8, 122.3, 109.0, 47.9, 45.5, 43.7, 34.8, 34.4, 34.0, 26.6, 26.12, 26.10, 26.06.

Data is consistent with the literature.<sup>197</sup>



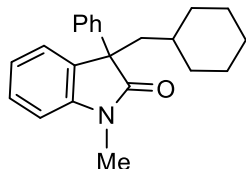
### 3-(Cyclohexylmethyl)-3-methyl-1-phenylindolin-2-one (1-3oa)

The crude mixture was purified by silica gel column chromatography with pentane/EA (10:1). 38 mg product was obtained by 60% isolated yield as colorless liquid.

$^1\text{H}$  NMR (600 MHz, Chloroform-*d*)  $\delta$  7.49 – 7.41 (m, 2H), 7.35 – 7.28 (m, 3H), 7.16 – 7.09 (m, 2H), 7.02 (t,  $J$  = 7.2 Hz, 1H), 6.76 (d,  $J$  = 7.8 Hz, 1H), 1.96 (dd,  $J$  = 13.8, 7.2 Hz, 1H), 1.73 (dd,  $J$  = 13.8, 5.4 Hz, 1H), 1.50 – 1.39 (m, 4H), 1.37 (s, 3H), 1.23 – 1.19 (m, 1H), 1.05 – 0.89 (m, 4H), 0.84 – 0.71 (m, 2H).

$^{13}\text{C}$  NMR (151 MHz, Chloroform-*d*)  $\delta$  180.5, 143.0, 134.8, 134.2, 129.6, 127.8, 127.4, 126.5, 123.0, 122.8, 109.3, 47.9, 45.9, 35.0, 34.4, 33.6, 26.5, 26.2, 26.1, 26.08.

Data is consistent with the literature.<sup>197</sup>



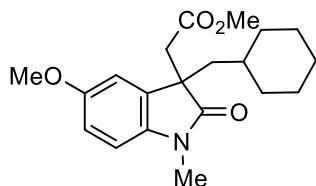
### 3-(Cyclohexylmethyl)-1-methyl-3-phenylindolin-2-one (1-3pa)

The crude mixture was purified by silica gel column chromatography with pentane/EA (10:1). 22 mg product was obtained by 34% isolated yield as colorless liquid.

$^1\text{H}$  NMR (600 MHz, Chloroform-*d*)  $\delta$  7.32 – 7.24 (m, 3H), 7.21 – 7.15 (m, 4H), 7.15 – 7.11 (m, 1H), 7.05 (t,  $J$  = 7.8 Hz, 1H), 6.83 (d,  $J$  = 7.8 Hz, 1H), 3.13 (s, 3H), 2.33 (dd,  $J$  = 13.8, 6.6 Hz, 1H), 2.07 (dd,  $J$  = 13.8, 5.4 Hz, 1H), 1.49 – 1.31 (m, 4H), 0.98 – 0.73 (m, 7H).

$^{13}\text{C}$  NMR (151 MHz, Chloroform-*d*)  $\delta$  179.0, 143.9, 141.6, 132.1, 128.4, 128.1, 127.1, 126.7, 125.3, 122.4, 108.3, 56.1, 45.3, 34.9, 34.6, 33.6, 29.7, 26.5, 26.2, 26.1

Data is consistent with the literature.<sup>197</sup>



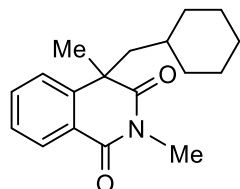
### Methyl 2-(3-(cyclohexylmethyl)-5-methoxy-1-methyl-2-oxoindolin-3-yl)acetate (1-3qa)

The crude mixture was purified by silica gel column chromatography with pentane/EA (10:1). 48 mg product was obtained by 70% isolated yield as colorless liquid.

$^1\text{H}$  NMR (600 MHz, Chloroform-*d*)  $\delta$  6.75 – 6.63 (m, 3H), 3.72 (s, 3H), 3.36 (s, 3H), 3.15 (s, 3H), 2.87 (d,  $J$  = 16.2 Hz, 1H), 2.70 (d,  $J$  = 16.2 Hz, 1H), 1.76 (dd,  $J$  = 13.8, 6.0 Hz, 1H), 1.63 (dd,  $J$  = 13.8, 5.4 Hz, 1H), 1.48 – 1.33 (m, 4H), 1.09 (d,  $J$  = 11.4 Hz, 1H), 0.96 – 0.85 (m, 4H), 0.82 – 0.74 (m, 1H), 0.69 – 0.63 (m, 1H).

$^{13}\text{C}$  NMR (151 MHz, Chloroform-*d*)  $\delta$  179.2, 170.1, 155.7, 138.0, 132.8, 112.0, 110.7, 108.1, 55.8, 51.5, 49.7, 45.2, 42.6, 34.6, 34.0, 33.9, 26.4, 26.1, 26.04, 26.02.

Data is consistent with the literature.<sup>209</sup>



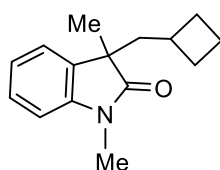
#### 4-(Cyclohexylmethyl)-2,4-dimethylisoquinoline-1,3(2H,4H)-dione (1-3ra)

The crude mixture was purified by silica gel column chromatography with pentane/EA (10:1). 38 mg product was obtained by 66% isolated yield as colorless liquid.

$^1\text{H}$  NMR (600 MHz, Chloroform-*d*)  $\delta$  8.19 (d,  $J$  = 7.8 Hz, 1H), 7.56 (t,  $J$  = 7.8 Hz, 1H), 7.40 – 7.29 (m, 2H), 3.32 (s, 3H), 2.26 (dd,  $J$  = 14.4, 7.8 Hz, 1H), 1.83 (dd,  $J$  = 14.4, 4.8 Hz, 1H), 1.49 (s, 3H), 1.46 – 1.35 (m, 3H), 1.18 (d,  $J$  = 8.4 Hz, 1H), 1.08 (d,  $J$  = 12.6 Hz, 1H), 0.94 – 0.63 (m, 6H).

$^{13}\text{C}$  NMR (151 MHz, Chloroform-*d*)  $\delta$  176.9, 164.5, 143.9, 133.7, 128.9, 127.2, 125.7, 124.6, 49.6, 46.7, 34.9, 34.3, 33.0, 31.7, 27.2, 26.03, 26.0, 26.96.

Data is consistent with the literature.<sup>209</sup>



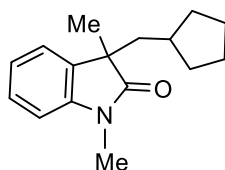
#### 3-(Cyclobutylmethyl)-1,3-dimethylindolin-2-one (1-3ab)

The crude mixture was purified by silica gel column chromatography with pentane/EA (10:1). 29 mg product was obtained by 63% isolated yield as colorless liquid.

$^1\text{H}$  NMR (600 MHz, Chloroform-*d*)  $\delta$  7.18 (t,  $J$  = 7.8 Hz, 1H), 7.09 (d,  $J$  = 7.8 Hz, 1H), 6.97 (t,  $J$  = 7.8 Hz, 1H), 6.75 (d,  $J$  = 7.8 Hz, 1H), 3.12 (s, 3H), 1.97 (dd,  $J$  = 12.6, 6.6 Hz, 1H), 1.87 – 1.76 (m, 2H), 1.66 – 1.59 (m, 1H), 1.57 – 1.47 (m, 3H), 1.43 – 1.37 (m, 1H), 1.36 – 1.28 (m, 1H), 1.25 (s, 3H).

$^{13}\text{C}$  NMR (151 MHz, Chloroform-*d*)  $\delta$  180.8, 143.3, 134.2, 127.6, 122.8, 122.2, 107.7, 47.9, 45.6, 32.9, 29.5, 28.9, 26.1, 23.9, 18.9.

Data is consistent with the literature.<sup>208</sup>



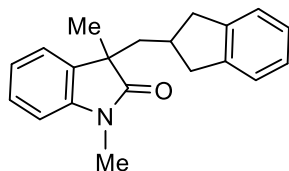
#### 3-(Cyclopentylmethyl)-1,3-dimethylindolin-2-one (1-3ac)

The crude mixture was purified by silica gel column chromatography with pentane/EA (10:1). 36 mg product was obtained by 73% isolated yield as colorless liquid.

$^1\text{H}$  NMR (600 MHz, Chloroform-*d*)  $\delta$  7.19 (t,  $J = 7.8$  Hz, 1H), 7.09 (d,  $J = 6.0$  Hz, 1H), 6.98 (t,  $J = 7.8$  Hz, 1H), 6.76 (d,  $J = 7.8$  Hz, 1H), 3.15 (s, 3H), 1.99 (dd,  $J = 13.8, 7.2$  Hz, 1H), 1.82 (dd,  $J = 13.8, 6.0$  Hz, 1H), 1.43 – 1.31 (m, 3H), 1.27 (s, 3H), 1.25 – 1.11 (m, 4H), 0.97 – 0.90 (m, 1H), 0.80 – 0.70 (m, 1H).

$^{13}\text{C}$  NMR (151 MHz, Chloroform-*d*)  $\delta$  181.2, 143.3, 134.4, 127.6, 122.9, 122.3, 107.9, 48.5, 44.5, 37.2, 33.8, 32.8, 26.2, 25.3, 24.9, 24.86.

Data is consistent with the literature.<sup>208</sup>



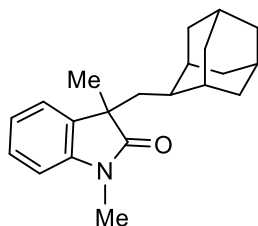
### 3-((2,3-Dihydro-1H-inden-2-yl)methyl)-1,3-dimethylindolin-2-one (1-3ad)

The crude mixture was purified by silica gel column chromatography with pentane/EA (10:1). 43 mg product was obtained by 74% isolated yield as colorless liquid.

$^1\text{H}$  NMR (600 MHz, Chloroform-*d*)  $\delta$  7.20 (t,  $J = 7.8$  Hz, 1H), 7.13 (d,  $J = 7.8$  Hz, 1H), 7.03 – 6.88 (m, 5H), 6.78 (d,  $J = 7.8$  Hz, 1H), 3.17 (s, 3H), 2.59 (dd,  $J = 15.6, 7.6$  Hz, 1H), 2.47 (dd,  $J = 15.6, 9.6$  Hz, 1H), 2.34 (dd,  $J = 15.6, 7.8$  Hz, 1H), 2.29 – 2.19 (m, 2H), 2.03 (dd,  $J = 13.8, 6.0$  Hz, 1H), 1.98 – 1.92 (m, 1H), 1.32 (s, 3H).

$^{13}\text{C}$  NMR (151 MHz, Chloroform-*d*)  $\delta$  180.8, 143.3, 143.2, 143.1, 134.0, 127.9, 126.1, 126.0, 124.1, 124.0, 122.9, 122.5, 108.0, 48.5, 43.9, 40.2, 39.5, 37.8, 26.3, 25.1.

Data is consistent with the literature.<sup>208</sup>



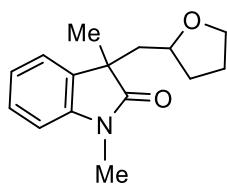
### 3-(((1r,3s,5r,7r)-Adamantan-2-yl)methyl)-1,3-dimethylindolin-2-one (1-3ae)

The crude mixture was purified by silica gel column chromatography with pentane/EA (10:1). 25 mg product was obtained by 40% isolated yield as colorless liquid.

$^1\text{H}$  NMR (600 MHz, Chloroform-*d*)  $\delta$  7.17 (t,  $J = 7.8$  Hz, 1H), 7.09 (d,  $J = 7.2$  Hz, 1H), 6.96 (t,  $J = 7.8$  Hz, 1H), 6.75 (d,  $J = 7.8$  Hz, 1H), 3.13 (s, 3H), 2.05 (dd,  $J = 13.8, 6.0$  Hz, 1H), 1.82 – 1.70 (m, 3H), 1.66 – 1.49 (m, 6H), 1.42 – 1.29 (m, 5H), 1.28 (s, 3H), 1.21 – 1.17 (m, 1H), 1.08 – 1.05 (m, 1H).

$^{13}\text{C}$  NMR (151 MHz, Chloroform-*d*)  $\delta$  180.9, 143.3, 134.3, 127.6, 122.6, 122.3, 107.8, 48.4, 41.7, 41.0, 39.0, 39.0, 38.1, 33.2, 32.6, 31.8, 31.7, 27.7, 27.6, 26.1, 25.1.

Data is consistent with the literature.<sup>208</sup>



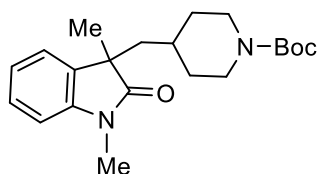
### 1,3-Dimethyl-3-((tetrahydrofuran-2-yl)methyl)indolin-2-one (1-3af)

The crude mixture was purified by silica gel column chromatography with pentane/EA (10:1). 32 mg (dr = 1:1.3) product was obtained by 65% isolated yield as colorless liquid.

$^1\text{H}$  NMR (600 MHz, Chloroform-*d*) mixture of diastereomers  $\delta$  7.24 – 7.09 (m, 4H), 7.00 – 6.95 (m, 2H), 6.78 – 6.76 (m, 2H), 3.64 – 3.59 (m, 2H), 3.46 – 3.41 (m, 3H), 3.37 – 3.32 (m, 1H), 3.14 (s, 6H), 2.18 – 2.13 (m, 2H), 1.97 (dd,  $J$  = 13.8, 7.8 Hz, 1H), 1.78 – 1.49 (m, 7H), 1.36 – 1.21 (m, 8H).  $^{13}\text{C}$  NMR (151 MHz, Chloroform-*d*) mixture of diastereomers  $\delta$  180.9, 180.6, 143.7, 142.9, 133.7, 133.6, 127.8, 127.7, 123.1, 122.8, 122.5, 121.9, 108.0, 107.9, 76.1, 75.6, 67.1, 67.09, 47.0, 46.8, 43.7, 43.2, 31.7, 31.4, 26.3, 26.2, 25.8, 25.3, 25.0, 24.8.

HRMS (ESI-MS) Calcd. For  $\text{C}_{15}\text{H}_{19}\text{NO}_2\text{Na}$   $[\text{M}+\text{Na}]^+$  268.13080, found: 268.13044.

IR (neat,  $\text{cm}^{-1}$ ):  $\tilde{\nu}$ : 3493, 2931, 1708, 1611, 1468, 1347, 1249, 1122, 1055, 930, 750, 699.



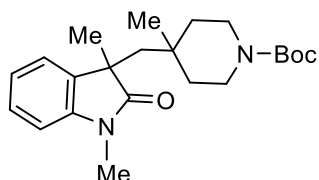
***tert*-Butyl 4-((1,3-dimethyl-2-oxoindolin-3-yl)methyl)piperidine-1-carboxylate (1-3ag)**

The crude mixture was purified by silica gel column chromatography with pentane/EA (10:1). 53 mg product was obtained by 74% isolated yield as colorless liquid.

$^1\text{H}$  NMR (600 MHz, Chloroform-*d*)  $\delta$  7.21 (t,  $J$  = 6.8 Hz, 1H), 7.09 (d,  $J$  = 7.2 Hz, 1H), 7.00 (t,  $J$  = 7.2 Hz, 1H), 6.79 (d,  $J$  = 7.8 Hz, 1H), 3.79 (s, 2H), 3.16 (s, 3H), 2.46 – 2.27 (m, 2H), 1.91 (dd,  $J$  = 14.4, 6.0 Hz, 1H), 1.69 (dd,  $J$  = 14.4, 5.4 Hz, 1H), 1.33 (s, 9H), 1.26 (s, 3H), 1.08 – 0.91 (m, 3H), 0.90 – 0.70 (m, 2H).

$^{13}\text{C}$  NMR (151 MHz, Chloroform-*d*)  $\delta$  180.7, 154.7, 143.0, 134.0, 127.8, 122.7, 122.6, 108.1, 79.1, 47.7, 44.4, 33.2, 33.0, 32.5, 28.4, 26.3, 26.2.

Data is consistent with the literature.<sup>208</sup>



***tert*-Butyl 4-((1,3-dimethyl-2-oxoindolin-3-yl)methyl)-4-methylpiperidine-1-carboxylate (1-3ah)**

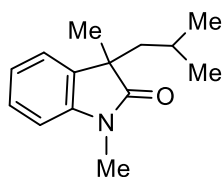
The crude mixture was purified by silica gel column chromatography with pentane/EA (10:1). 57 mg product was obtained by 76% isolated yield as colorless liquid.

$^1\text{H}$  NMR (600 MHz, Chloroform-*d*)  $\delta$  7.22 – 7.18 (m, 1H), 7.13 (d,  $J$  = 7.2 Hz, 1H), 6.97 (t,  $J$  = 7.8 Hz, 1H), 6.79 (d,  $J$  = 7.8 Hz, 1H), 3.51 – 3.43 (m, 2H), 3.16 (s, 3H), 2.88 – 2.84 (m, 1H), 2.78 – 2.73 (m, 1H), 2.08 (d,  $J$  = 14.4 Hz, 1H), 1.83 (d,  $J$  = 14.4 Hz, 1H), 1.34 (s, 9H), 1.26 – 1.21 (m, 4H), 1.06 – 0.91 (m, 2H), 0.77 – 0.75 (m, 1H), 0.50 (s, 3H).

$^{13}\text{C}$  NMR (151 MHz, Chloroform-*d*)  $\delta$  180.9, 154.8, 142.6, 134.0, 127.8, 123.7, 122.2, 108.2, 79.1, 50.1, 46.9, 38.2, 37.9, 32.8, 30.9, 28.5, 28.4, 26.3, 22.5.

HRMS (ESI-MS) Calcd. For  $\text{C}_{22}\text{H}_{32}\text{N}_2\text{O}_3\text{Na}$   $[\text{M}+\text{Na}]^+$  395.23051, found: 395.23091.

IR (neat,  $\text{cm}^{-1}$ ):  $\tilde{\nu}$ : 3395, 2923, 1683, 1609, 1418, 1367, 1248, 1159, 1090, 1023, 961, 862, 760, 699.



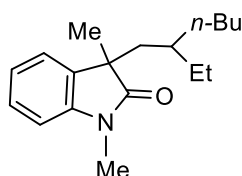
### 3-Isobutyl-1,3-dimethylindolin-2-one (1-3ai)

The crude mixture was purified by silica gel column chromatography with pentane/EA (10:1). 30 mg product was obtained by 69% isolated yield as colorless liquid.

$^1\text{H}$  NMR (600 MHz, Chloroform-*d*)  $\delta$  7.18 (t,  $J = 7.8$  Hz, 1H), 7.08 (d,  $J = 7.2$  Hz, 1H), 6.98 (t,  $J = 7.2$  Hz, 1H), 6.77 (d,  $J = 7.8$  Hz, 1H), 3.14 (s, 3H), 1.86 (dd,  $J = 13.8, 7.8$  Hz, 1H), 1.68 (dd,  $J = 13.8, 5.4$  Hz, 1H), 1.25 (s, 3H), 1.22 – 1.12 (m, 1H), 0.58 (d,  $J = 6.6$  Hz, 3H), 0.53 (d,  $J = 6.6$  Hz, 3H).

$^{13}\text{C}$  NMR (151 MHz, Chloroform-*d*)  $\delta$  181.1, 143.2, 134.2, 127.6, 122.8, 122.3, 107.9, 48.1, 46.8, 26.2, 26.1, 25.5, 24.1, 22.8.

Data is consistent with the literature.<sup>208</sup>



### 3-(2-Ethylhexyl)-1,3-dimethylindolin-2-one (1-3aj)

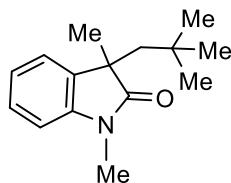
The crude mixture was purified by silica gel column chromatography with pentane/EA (10:1). 35 mg (dr = 1:1.1) product was obtained by 64% isolated yield as colorless liquid.

$^1\text{H}$  NMR (600 MHz, Chloroform-*d*) mixture of diastereomers  $\delta$  7.24 (t,  $J = 7.8$  Hz, 2H), 7.15 (dd,  $J = 7.2, 3.0$  Hz, 2H), 7.04 (t,  $J = 7.8$  Hz, 2H), 6.82 (d,  $J = 7.8$  Hz, 2H), 3.20 (d,  $J = 3.0$  Hz, 6H), 1.95 – 1.89 (m, 2H), 1.78 – 1.72 (m, 2H), 1.33 (s, 6H), 1.22 – 0.85 (m, 18H), 0.78 (t,  $J = 7.2$  Hz, 3H), 0.75 (t,  $J = 7.2$  Hz, 3H), 0.69 (t,  $J = 7.2$  Hz, 3H), 0.64 (t,  $J = 7.2$  Hz, 3H).

$^{13}\text{C}$  NMR (151 MHz, Chloroform-*d*) mixture of diastereomers  $\delta$  181.0, 180.98, 143.3, 143.27, 134.3, 134.25, 127.5, 122.9, 122.8, 122.22, 122.2, 107.82, 107.8, 48.09, 48.0, 42.02, 42.0, 35.72, 35.7, 33.2, 32.8, 28.3, 28.2, 26.5, 26.2, 26.1, 25.6, 25.5, 22.8, 22.7, 14.0, 14.99, 10.3, 10.29.

HRMS (ESI-MS) Calcd. For  $\text{C}_{18}\text{H}_{27}\text{NONa}$   $[\text{M}+\text{Na}]^+$  296.19849, found: 296.19804.

IR (neat,  $\text{cm}^{-1}$ ):  $\tilde{\nu}$ : 3418, 2925, 1712, 1611, 1465, 1375, 1247, 1123, 1025, 929, 749, 699.



### 1,3-Dimethyl-3-neopentylindolin-2-one (1-3ak)

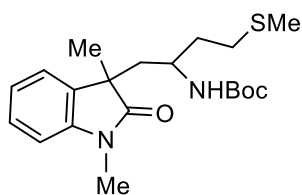
The crude mixture was purified by silica gel column chromatography with pentane/EA (10:1). 36 mg product was obtained by 77% isolated yield as colorless liquid.

$^1\text{H}$  NMR (600 MHz, Chloroform-*d*)  $\delta$  7.18 (d,  $J = 7.8$  Hz, 1H), 7.13 (d,  $J = 7.2$  Hz, 1H), 6.96 (t,  $J = 7.2$  Hz, 1H), 6.78 (d,  $J = 7.8$  Hz, 1H), 3.15 (s, 3H), 2.09 (d,  $J = 14.4$  Hz, 1H), 1.79 (d,  $J = 14.4$  Hz, 1H), 1.22 (s, 3H), 0.54 (s, 9H).

$^{13}\text{C}$  NMR (151 MHz, Chloroform-*d*)  $\delta$  181.0, 142.9, 134.2, 127.5, 123.9, 122.0, 108.0, 50.8, 47.4,

31.8, 30.8, 28.3, 26.2.

Data is consistent with the literature.<sup>208</sup>



**tert-Butyl (1-(1,3-dimethyl-2-oxoindolin-3-yl)-4-(methylthio)butan-2-yl)carbamate (1-3al)**

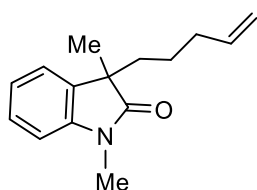
The crude mixture was purified by silica gel column chromatography with pentane/EA (10:1). 53 mg (dr = 1:1.1) product was obtained by 70% isolated yield as colorless liquid.

<sup>1</sup>H NMR (600 MHz, Chloroform-*d*) mixture of diastereomers  $\delta$  7.12 – 7.17 (m, 3H), 7.09 (d, *J* = 7.2 Hz, 1H), 7.03 – 6.99 (m, 2H), 6.79 – 6.74 (m, 2H), 4.13 (d, *J* = 9.6 Hz, 1H), 3.92 (d, *J* = 9.0 Hz, 1H), 3.45 (dt, *J* = 10.2, 4.8 Hz, 1H), 3.20 (dt, *J* = 10.2, 4.8 Hz, 1H), 3.20 (s, 3H), 3.14 (s, 3H), 2.36 – 2.20 (m, 4H), 2.10 – 1.89 (m, 10H), 1.56 – 1.38 (m, 4H), 1.28 – 1.18 (m, 24H).

<sup>13</sup>C NMR (151 MHz, Chloroform-*d*) mixture of diastereomers  $\delta$  181.4, 180.1, 154.7, 154.5, 143.1, 142.9, 133.9, 132.5, 128.1, 127.7, 122.75, 122.70, 122.57, 122.53, 108.4, 108.3, 78.80, 78.76, 47.9, 47.5, 47.2, 46.9, 42.5, 42.0, 36.8, 36.2, 30.3, 30.2, 28.4, 28.3, 26.35, 26.27, 25.6, 25.1, 15.47, 15.46.

HRMS (ESI-MS) Calcd. For C<sub>20</sub>H<sub>30</sub>N<sub>2</sub>O<sub>3</sub>SNa [M+Na]<sup>+</sup> 401.18693 found: 401.18666.

IR (neat, cm<sup>-1</sup>):  $\tilde{\nu}$ : 3339, 2970, 1697, 1612, 1496, 1364, 1244, 1167, 1124, 1046, 856, 750, 699.



**1,3-Dimethyl-3-(pent-4-en-1-yl)indolin-2-one (1-3am)**

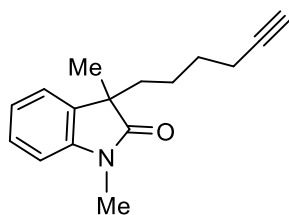
The crude mixture was purified by silica gel column chromatography with pentane/EA (10:1). 29 mg product was obtained by 63% isolated yield as colorless liquid.

<sup>1</sup>H NMR (600 MHz, Chloroform-*d*)  $\delta$  7.22 – 7.16 (m, 1H), 7.09 (d, *J* = 7.2 Hz, 1H), 6.99 (t, *J* = 7.8 Hz, 1H), 6.76 (d, *J* = 7.8 Hz, 1H), 5.58 (m, 1H), 4.87 – 4.75 (m, 2H), 3.13 (s, 3H), 1.92 – 1.77 (m, 3H), 1.65 (t, *J* = 13.2 Hz, 1H), 1.28 (s, 3H), 1.06 – 0.98 (m, 1H), 0.89 – 0.81 (m, 1H).

<sup>13</sup>C NMR (151 MHz, Chloroform-*d*)  $\delta$  180.7, 143.3, 138.2, 134.2, 127.7, 122.5, 122.46, 114.7, 107.9, 48.4, 38.0, 33.7, 26.1, 23.8.

HRMS (ESI-MS) Calcd. For C<sub>15</sub>H<sub>20</sub>NO [M+H]<sup>+</sup> 230.15394, found: 230.15397.

IR (neat, cm<sup>-1</sup>):  $\tilde{\nu}$ : 3416, 2927, 2324, 2087, 1912, 1710, 1611, 1467, 1346, 1248, 1124, 1019, 911, 749, 699.



**3-(Hex-5-yn-1-yl)-1,3-dimethylindolin-2-one (1-3an)**

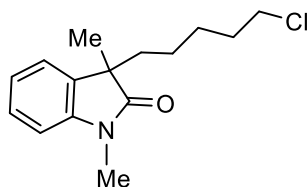
The crude mixture was purified by silica gel column chromatography with pentane/EA (10:1). 29 mg product was obtained by 60% isolated yield as colorless liquid.

$^1\text{H}$  NMR (600 MHz, Chloroform-*d*)  $\delta$  7.25 – 7.16 (m, 1H), 7.10 (d,  $J$  = 7.2 Hz, 1H), 6.99 (t,  $J$  = 7.8 Hz, 1H), 6.77 (d,  $J$  = 7.8 Hz, 1H), 3.14 (s, 3H), 1.99 (t,  $J$  = 7.2 Hz, 2H), 1.87 – 1.76 (m, 2H), 1.67 (td,  $J$  = 12.6, 4.2 Hz, 1H), 1.40 – 1.25 (m, 5H), 1.06 – 0.98 (m, 1H), 0.96 – 0.85 (m, 1H).

$^{13}\text{C}$  NMR (151 MHz, Chloroform-*d*)  $\delta$  180.7, 143.3, 134.1, 127.7, 122.5, 122.5, 107.9, 84.2, 68.3, 48.3, 37.9, 28.6, 26.1, 23.8, 23.7, 18.1.

HRMS (ESI-MS) Calcd. For  $\text{C}_{16}\text{H}_{19}\text{NONa}$   $[\text{M}+\text{Na}]^+$  264.13589, found: 264.13565.

IR (neat,  $\text{cm}^{-1}$ ):  $\tilde{\nu}$ : 4294, 2930, 1706, 1611, 1466, 1346, 1250, 1123, 750, 697.



### 3-(5-Chloropentyl)-1,3-dimethylindolin-2-one (1-3ao)

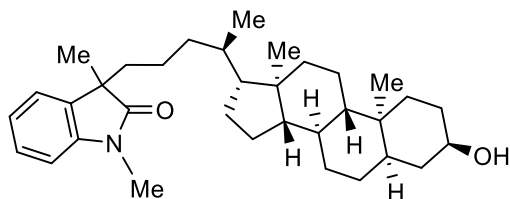
The crude mixture was purified by silica gel column chromatography with pentane/EA (10:1). 37 mg product was obtained by 69% isolated yield as colorless liquid.

$^1\text{H}$  NMR (600 MHz, Chloroform-*d*)  $\delta$  7.20 (t,  $J$  = 7.8 Hz, 1H), 7.09 (d,  $J$  = 7.2 Hz, 1H), 7.00 (t,  $J$  = 7.8 Hz, 1H), 6.77 (d,  $J$  = 7.8 Hz, 1H), 3.34 (t,  $J$  = 6.6 Hz, 2H), 3.14 (s, 3H), 1.89 – 1.79 (m, 1H), 1.68 – 1.63 (m, 1H), 1.59 – 1.54 (m, 2H), 1.30 – 1.17 (m, 5H), 0.97 – 0.89 (m, 1H), 0.85 – 0.71 (m, 1H).

$^{13}\text{C}$  NMR (151 MHz, Chloroform-*d*)  $\delta$  180.7, 143.3, 134.1, 127.7, 122.5, 122.4, 107.9, 48.4, 44.9, 38.2, 32.2, 26.9, 26.1, 23.9, 23.8.

HRMS (ESI-MS) Calcd. For  $\text{C}_{15}\text{H}_{20}\text{ClNONa}$   $[\text{M}+\text{Na}]^+$  288.11256, found: 288.11238.

IR (neat,  $\text{cm}^{-1}$ ):  $\tilde{\nu}$ : 2932, 1707, 1611, 1466, 1346, 1250, 1124, 1018, 931, 749, 700.



### 3-((*R*)-4-((3*R*,5*R*,8*R*,9*S*,10*S*,13*R*,14*S*,17*R*)-3-Hydroxy-10,13-dimethylhexadecahydro-1*H*-cyclopenta[*a*]phenanthren-17-yl)pentyl)-1,3-dimethylindolin-2-one (1-3ap)

The crude mixture was purified by silica gel column chromatography with pentane/EA (10:1). 64 mg product was obtained by 63% isolated yield as colorless liquid.

$^1\text{H}$  NMR (600 MHz, Chloroform-*d*)  $\delta$  7.22 – 7.17 (m, 1H), 7.10 (d,  $J$  = 7.2 Hz, 1H), 7.00 (t,  $J$  = 7.2 Hz, 1H), 6.77 (d,  $J$  = 7.8 Hz, 1H), 3.57 – 3.52 (m, 1H), 3.15 (s, 3H), 1.84 – 0.71 (m, 37H), 0.66 (d,  $J$  = 6.6 Hz, 3H), 0.51 (s, 3H).

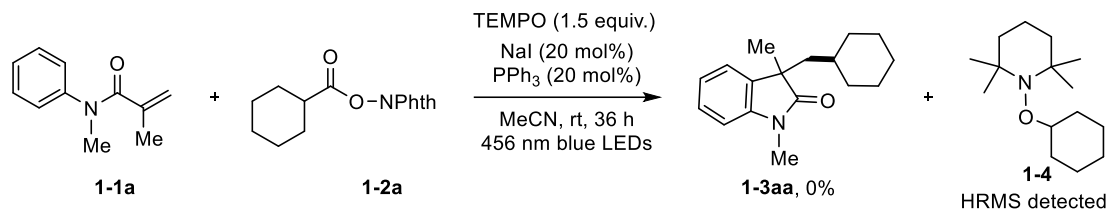
$^{13}\text{C}$  NMR (151 MHz, Chloroform-*d*)  $\delta$  180.9, 143.3, 134.4, 127.6, 122.5, 122.4, 107.86, 71.9, 56.5, 56.4, 48.5, 42.7, 42.1, 40.4, 40.2, 38.8, 36.5, 36.0, 35.8, 35.5, 35.4, 34.6, 30.6, 28.3, 27.2, 26.4, 26.1, 24.2, 23.8, 23.4, 21.2, 20.8, 18.5, 12.0.

HRMS (ESI-MS) Calcd. For  $\text{C}_{34}\text{H}_{51}\text{NO}_2\text{Na}$   $[\text{M}+\text{Na}]^+$  528.38120, found: 528.37952.

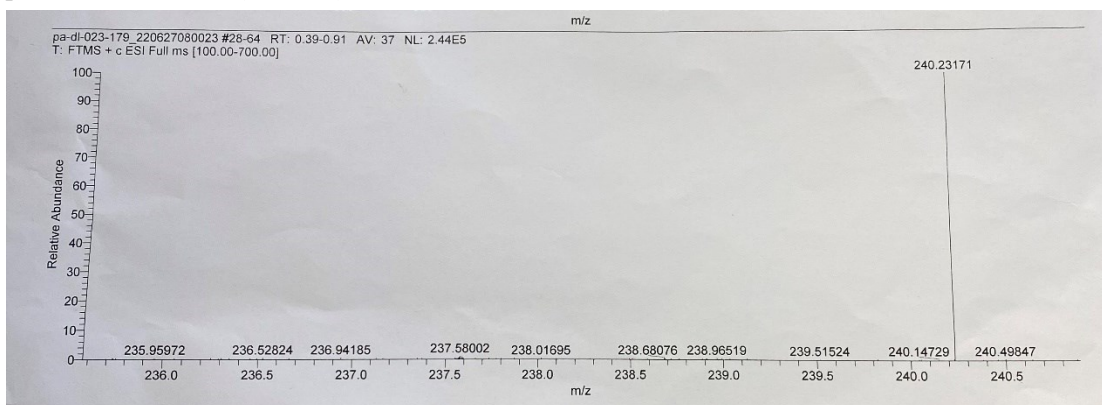
IR (neat,  $\text{cm}^{-1}$ ):  $\tilde{\nu}$ : 3414, 2928, 2245, 1701, 1612, 1464, 1375, 1251, 1123, 1037, 912, 852.

## Mechanism studies

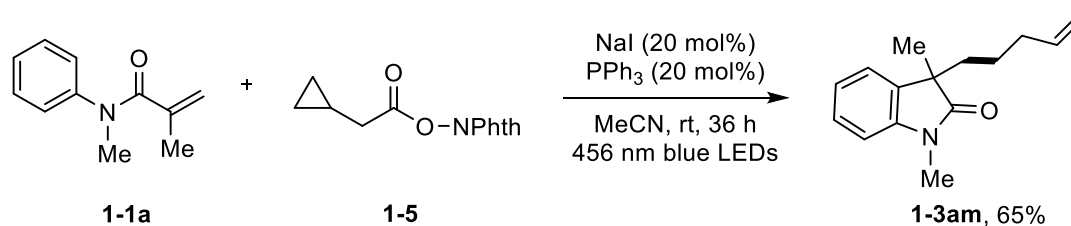
### (1) The radical trapping experiment



A clean oven-dried tube equipped with a PTFE-coated stir bar was charged with arylamide **1-1a** (53 mg, 0.3 mmol), cyclohexyl redox-active ester **1-2a** (55 mg, 0.2 mmol), Ph<sub>3</sub>P (10.5 mg, 0.04 mmol), NaI (6 mg, 0.04 mmol) and TEMPO (46.8 mg, 0.3 mmol), then the system was degassed and filled with nitrogen gas three times before the solvent anhydrous MeCN (2 mL) was added. The reaction was carried out irradiated using 40 W 456 nm blue LEDs at room temperature under fan cooling. After 36 h, the solvent was removed in vacuo, the desired product **1-3aa** was not detected by NMR analysis of the crude reaction mixture. HRMS of the crude reaction mixture shows the existence of product **1-4**. HRMS (ESI-MS) Calcd. For C<sub>15</sub>H<sub>30</sub>NO [M+H]<sup>+</sup> 240.23219, found: 240.23171.



## (2) The radical clock experiment

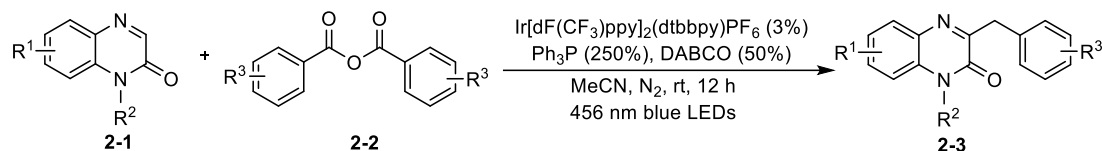


To a reaction tube with a stir bar, arylamide **1-1a** (53 mg, 0.3 mmol), redox-active ester **1-5** (49 mg, 0.2 mmol), PPh<sub>3</sub> (10.5 mg, 0.04 mmol), NaI (6 mg, 0.04 mmol) was added. After degassed and filled with nitrogen gas three times, the anhydrous solvent MeCN was added. The reaction was performed under blue LEDs irradiation (40 W, 456 nm) at room temperature under fan cooling. After 36 h, the crude reaction mixture was concentrated in vacuo and purified by silica gel column chromatography (Pentane/EA = 10:1) to obtain corresponding product. Colorless liquid: 30 mg, 65% yield. The compound data was in agreement with the compound **1-3am**.



## 4.2.2 Visible-light-induced photocatalytic deoxygenative benzylation of quinoxalin-2-(1*H*)-ones with carboxylic acid anhydrides

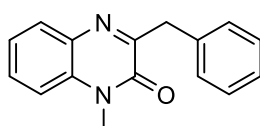
### General procedure for synthesis of 3-benzylquinoxalin-2-(1*H*)-ones



To a glass vial equipped with a stirring bar, quinoxalin-2(1*H*)-one **2-1** (0.15 mmol, 1 equiv.), carboxylic acid anhydride **2-2** (0.3 mmol, 2 equiv.), Ir[dF(CF<sub>3</sub>)ppy]<sub>2</sub>(dtbbpy)PF<sub>6</sub> (0.0045 mmol, 3 mol%), Ph<sub>3</sub>P (0.375 mmol, 2.5 equiv.) and DABCO (0.075 mmol, 50 mol%) were added. Then the vial with a screw cap and a silicone seal was evacuated and backfilled with N<sub>2</sub> (three times). After anhydrous acetonitrile (MeCN, 1.5 mL) was added, the reaction was performed under blue LEDs irradiation (40 W, 456 nm) at room temperature. After 12 h, saturated aqueous NaHCO<sub>3</sub> solution (15 mL) was added to the reaction. The mixture was stirred for another 1 h and then extracted with EA (3 × 5 mL). After being dried over anhydrous Na<sub>2</sub>SO<sub>4</sub> and concentrated in vacuo, the crude product was purified by column chromatography using pentane/EA as eluent to give the 3-benzylquinoxalin-2(1*H*)-one **2-3**.

Larger (1 mmol) scale: To a 50 mL vial equipped with a stirring bar, quinoxalin-2(1*H*)-one **2-1** (1 mmol, 1 equiv.), carboxylic acid anhydride **2-2** (2 mmol, 2 equiv.), Ir[dF(CF<sub>3</sub>)ppy]<sub>2</sub>(dtbbpy)PF<sub>6</sub> (0.03 mmol, 3 mol%), Ph<sub>3</sub>P (2.5 mmol, 2.5 equiv.) and DABCO (0.5 mmol, 50 mol%) were added. Then, the vial with sealed aluminous headspace cap was evacuated and backfilled with N<sub>2</sub> (three times). After anhydrous acetonitrile (MeCN, 10 mL) was added, the reaction was performed under blue LEDs irradiation (40 W, 456 nm) at room temperature for 24 h.

### Product characterization



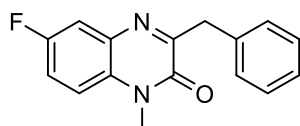
### 3-Benzyl-1-methylquinoxalin-2(1*H*)-one (**2-3aa**)

The crude mixture was purified by silica gel column chromatography with pentane/EA (8:1). 29 mg product was obtained by 77% isolated yield as yellow solid. Larger (1mmol) scale experiment: 182 mg, yellow solid (73%). Melting point: 87.3 – 88.5 °C.

<sup>1</sup>H NMR (400 MHz, Chloroform-*d*) δ 7.76 (d, *J* = 8.0 Hz, 1H), 7.48 – 7.31 (m, 3H), 7.28 – 7.07 (m, 5H), 4.18 (s, 2H), 3.56 (s, 3H).

<sup>13</sup>C NMR (101 MHz, Chloroform-*d*) δ 159.3, 154.7, 137.1, 133.4, 132.8, 129.9, 129.9, 129.6, 128.4, 126.6, 123.6, 113.6, 40.8, 29.1.

Data is in line with the literature.<sup>238</sup>



### 3-Benzyl-6-fluoro-1-methylquinoxalin-2(1H)-one (2-3ba)

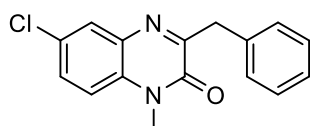
The crude mixture was purified by silica gel column chromatography with pentane/EA (10:1). 29 mg product was obtained by 72% isolated yield as yellow solid. Melting point: 95.0 – 97.9 °C.

<sup>1</sup>H NMR (400 MHz, Chloroform-*d*)  $\delta$  7.53 (dd, *J* = 8.8, 2.8 Hz, 1H), 7.44 (d, *J* = 7.2 Hz, 2H), 7.31 – 7.16 (m, 5H), 4.24 (s, 2H), 3.64 (s, 3H).

<sup>13</sup>C NMR (151 MHz, Chloroform-*d*)  $\delta$  160.9, 158.7 (d, *J* = 241.6 Hz), 154.4, 136.7, 133.3 (d, *J* = 11.3 Hz), 130.0 (d, *J* = 2.3 Hz), 129.6, 128.4, 126.7, 117.5 (d, *J* = 24.0 Hz), 115.4 (d, *J* = 22.5 Hz), 114.6 (d, *J* = 8.9 Hz), 40.7, 29.4.

<sup>19</sup>F NMR (376 MHz, Chloroform-*d*)  $\delta$  -119.06 to -119.16 (m).

Data is in line with the literature.<sup>236</sup>



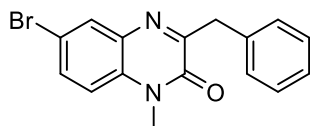
### 3-Benzyl-6-chloro-1-methylquinoxalin-2(1H)-one (2-3ca)

The crude mixture was purified by silica gel column chromatography with pentane/EA (8:1). 33 mg product was obtained by 77% isolated yield as yellow solid. Melting point: 105.6 – 107.7 °C.

<sup>1</sup>H NMR (600 MHz, Chloroform-*d*)  $\delta$  7.76 (d, *J* = 2.4 Hz, 1H), 7.42 – 7.32 (m, 3H), 7.22 (t, *J* = 7.8 Hz, 2H), 7.14 (t, *J* = 7.2 Hz, 1H), 7.11 (d, *J* = 8.4 Hz, 1H), 4.17 (s, 2H), 3.56 (s, 3H).

<sup>13</sup>C NMR (151 MHz, Chloroform-*d*)  $\delta$  160.7, 154.4, 136.7, 133.3, 132.0, 129.8, 129.6, 129.3, 128.9, 128.5, 126.7, 114.7, 40.7, 29.3.

Data is in line with the literature.<sup>234,297</sup>



### 3-Benzyl-6-bromo-1-methylquinoxalin-2(1H)-one (2-3da)

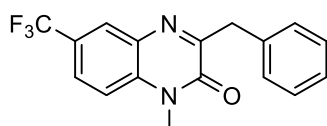
The crude mixture was purified by silica gel column chromatography with pentane/EA (10:1). 37 mg product was obtained by 75% isolated yield as yellow solid. Melting point: 116.4 – 118.1 °C.

<sup>1</sup>H NMR (600 MHz, Chloroform-*d*)  $\delta$  7.92 (s, 1H), 7.51 (d, *J* = 9.0 Hz, 1H), 7.37 (d, *J* = 7.8 Hz, 2H), 7.22 (t, *J* = 7.2 Hz, 2H), 7.14 (t, *J* = 7.2 Hz, 1H), 7.04 (d, *J* = 9.0 Hz, 1H), 4.17 (s, 2H), 3.55 (s, 3H).

<sup>13</sup>C NMR (151 MHz, Chloroform-*d*)  $\delta$  160.7, 154.4, 136.7, 133.6, 132.6, 132.5, 132.4, 129.6, 128.5, 126.7, 116.1, 115.0, 40.7, 29.3.

HRMS (ESI-MS) Calcd. For C<sub>16</sub>H<sub>13</sub>ON<sub>2</sub>BrNa [M+Na]<sup>+</sup> 351.0104, found: 351.0094.

IR (neat, cm<sup>-1</sup>):  $\tilde{\nu}$ : 3289, 3059, 2928, 2645, 2326, 2110, 1884, 1754, 1645, 1586, 1455, 1289, 1200, 1097, 948, 866, 806, 761, 731, 700.



### 3-Benzyl-1-methyl-6-(trifluoromethyl)quinoxalin-2(1H)-one (2-3ea)

The crude mixture was purified by silica gel column chromatography with pentane/EA (10:1). 38 mg product was obtained by 80% isolated yield as yellow solid. Melting point: 102.2 – 102.6 °C.

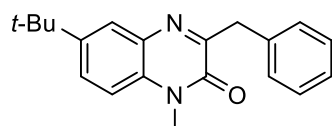
$^1\text{H}$  NMR (600 MHz, Chloroform-*d*)  $\delta$  8.06 (s, 1H), 7.65 (d,  $J$  = 8.4 Hz, 1H), 7.38 (d,  $J$  = 7.8 Hz, 2H), 7.28 (d,  $J$  = 9.0 Hz, 1H), 7.23 (t,  $J$  = 7.8 Hz, 2H), 7.15 (t,  $J$  = 7.2 Hz, 1H), 4.20 (s, 2H), 3.60 (s, 3H).

$^{13}\text{C}$  NMR (151 MHz, Chloroform-*d*)  $\delta$  161.1, 154.6, 136.4, 135.7, 132.1, 129.6, 128.5, 127.4 (q,  $J$  = 3.9 Hz), 126.8, 126.2 (q,  $J$  = 3.6 Hz), 125.9 (q,  $J$  = 33.6 Hz), 123.7 (q,  $J$  = 272.1 Hz), 114.2, 40.7, 29.4.

$^{19}\text{F}$  NMR (565 MHz, Chloroform-*d*)  $\delta$  -61.96.

HRMS (ESI-MS) Calcd. For  $\text{C}_{17}\text{H}_{13}\text{F}_3\text{N}_2\text{ONa}$   $[\text{M}+\text{Na}]^+$  341.0872, found: 341.0866.

IR (neat,  $\text{cm}^{-1}$ ):  $\tilde{\nu}$ : 3066, 2930, 2649, 2320, 2027, 1946, 1826, 1735, 1657, 1492, 1360, 1236, 1118, 1029, 913, 821, 700, 658.



### 3-Benzyl-6-(tert-butyl)-1-methylquinoxalin-2(1H)-one (2-3fa)

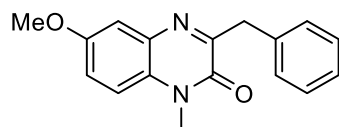
The crude mixture was purified by silica gel column chromatography with pentane/EA (10:1). 36 mg product was obtained by 78% isolated yield as yellow solid. Melting point: 126.6 – 127.2 °C.

$^1\text{H}$  NMR (600 MHz, Chloroform-*d*)  $\delta$  7.78 (d,  $J$  = 2.4 Hz, 1H), 7.49 (dd,  $J$  = 8.4, 2.4 Hz, 1H), 7.39 (d,  $J$  = 6.6 Hz, 2H), 7.21 (t,  $J$  = 7.8 Hz, 2H), 7.13 (d,  $J$  = 8.4 Hz, 2H), 4.19 (s, 2H), 3.57 (s, 3H), 1.30 (s, 9H).

$^{13}\text{C}$  NMR (151 MHz, Chloroform-*d*)  $\delta$  159.2, 154.8, 147.0, 137.2, 132.5, 131.1, 129.5, 128.4, 127.6, 126.6, 126.4, 113.2, 40.9, 34.5, 31.3, 29.1.

HRMS (ESI-MS) Calcd. For  $\text{C}_{20}\text{H}_{22}\text{N}_2\text{ONa}$   $[\text{M}+\text{Na}]^+$  329.1624, found: 329.1616.

IR (neat,  $\text{cm}^{-1}$ ):  $\tilde{\nu}$ : 2958, 2870, 2322, 2083, 1895, 1659, 1494, 1292, 1086, 966, 893, 735, 698.



### 3-Benzyl-6-methoxy-1-methylquinoxalin-2(1H)-one (2-3ga)

The crude mixture was purified by silica gel column chromatography with pentane/EA (8:1). 26 mg product was obtained by 62% isolated yield as yellow solid. Melting point: 127.2 – 129.3 °C.

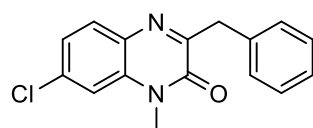
$^1\text{H}$  NMR (400 MHz, Chloroform-*d*)  $\delta$  7.39 (d,  $J$  = 7.3 Hz, 2H), 7.27 – 7.17 (m, 3H), 7.16 – 7.02 (m, 3H), 4.19 (s, 2H), 3.80 (s, 3H), 3.57 (s, 3H).

$^{13}\text{C}$  NMR (151 MHz, Chloroform-*d*)  $\delta$  159.9, 156.0, 154.4, 137.1, 133.5, 129.6, 128.4, 127.6, 126.6, 119.1, 114.5, 111.4, 55.8, 40.8, 29.3.

HRMS (EI-MS) Calcd. For  $\text{C}_{17}\text{H}_{16}\text{N}_2\text{O}_2$  280.1212, found: 280.1200.

IR (neat,  $\text{cm}^{-1}$ ):  $\tilde{\nu}$ : 3067, 2927, 2845, 2653, 2287, 2185, 2096, 1940, 1817, 1731, 1650, 1686, 1496, 1453, 1341, 1282, 1219, 1151, 1028, 963, 889, 744, 697.

Data is in line with the literature.<sup>235</sup>



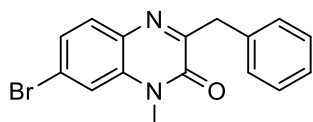
### 3-Benzyl-7-chloro-1-methylquinoxalin-2(1H)-one (2-3ha)

The crude mixture was purified by silica gel column chromatography with pentane/EA (8:1). 33 mg product was obtained by 77% isolated yield as yellow solid. Melting point: 161.1 – 164.1 °C.

<sup>1</sup>H NMR (600 MHz, Chloroform-*d*) δ 7.68 (d, *J* = 8.4 Hz, 1H), 7.37 (d, *J* = 6.6 Hz, 2H), 7.24 – 7.18 (m, 3H), 7.18 – 7.11 (m, 2H), 4.16 (s, 2H), 3.54 (s, 3H).

<sup>13</sup>C NMR (151 MHz, Chloroform-*d*) δ 159.4, 154.4, 136.8, 135.8, 134.2, 131.3, 131.0, 129.6, 128.4, 126.7, 123.9, 113.6, 40.7, 29.2.

Data is in line with the literature.<sup>298</sup>



### 3-Benzyl-7-bromo-1-methylquinoxalin-2(1H)-one (2-3ia)

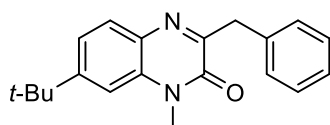
The crude mixture was purified by silica gel column chromatography with pentane/EA (8:1). 38 mg product was obtained by 77% isolated yield as yellow solid. Melting point: 177.6 – 179.2 °C.

<sup>1</sup>H NMR (600 MHz, Chloroform-*d*) δ 7.60 (d, *J* = 8.4 Hz, 1H), 7.39 – 7.30 (m, 4H), 7.21 (t, *J* = 7.8 Hz, 2H), 7.13 (t, *J* = 7.4 Hz, 1H), 4.15 (s, 2H), 3.53 (s, 3H).

<sup>13</sup>C NMR (151 MHz, Chloroform-*d*) δ 159.7, 154.4, 136.7, 134.4, 131.6, 131.2, 129.6, 128.5, 126.8, 126.7, 123.9, 116.6, 40.7, 29.2.

HRMS (ESI-MS) Calcd. For C<sub>16</sub>H<sub>13</sub>ON<sub>2</sub>BrNa [M+Na]<sup>+</sup> 351.0104, found: 351.0098.

IR (neat, cm<sup>-1</sup>):  $\tilde{\nu}$ : 3294, 3077, 2926, 2327, 2107, 1991, 1914, 1652, 1589, 1553, 1451, 1297, 1213, 1100, 1074, 1007, 935, 830, 733, 696, 667.



### 3-Benzyl-7-(tert-butyl)-1-methylquinoxalin-2(1H)-one (2-3ja)

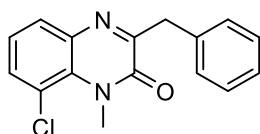
The crude mixture was purified by silica gel column chromatography with pentane/EA (10:1). 37 mg product was obtained by 81% isolated yield as yellow solid. Melting point: 78.4 – 78.9 °C.

<sup>1</sup>H NMR (600 MHz, Chloroform-*d*) δ 7.71 (d, *J* = 8.4 Hz, 1H), 7.37 (d, *J* = 7.2 Hz, 2H), 7.31 (dd, *J* = 8.4, 1.8 Hz, 1H), 7.19 (t, *J* = 7.8 Hz, 2H), 7.14 (d, *J* = 1.8 Hz, 1H), 7.11 (t, *J* = 7.8 Hz, 1H), 4.17 (s, 2H), 3.60 (s, 3H), 1.31 (s, 9H).

<sup>13</sup>C NMR (151 MHz, Chloroform-*d*) δ 158.4, 155.0, 153.8, 137.3, 133.0, 130.9, 129.5, 129.4, 128.4, 126.5, 121.4, 110.0, 40.8, 35.4, 31.3, 29.0.

HRMS (ESI-MS) Calcd. For C<sub>20</sub>H<sub>22</sub>N<sub>2</sub>ONa [M+Na]<sup>+</sup> 329.1624, found: 329.1615.

IR (neat, cm<sup>-1</sup>):  $\tilde{\nu}$ : 3030, 2960, 2870, 2290, 2075, 1906, 1652, 1455, 1308, 1257, 1094, 1009, 949, 829, 738, 698, 657.



### 3-Benzyl-8-chloro-1-methylquinoxalin-2(1H)-one (2-3ka)

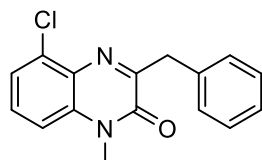
The crude mixture was purified by silica gel column chromatography with pentane/EA (10:1). 15 mg product was obtained by 35% isolated yield as yellow solid. Melting point: 98.6 – 99.7 °C.

<sup>1</sup>H NMR (600 MHz, Chloroform-*d*) δ 7.74 (dd, *J* = 7.8, 1.6 Hz, 1H), 7.51 (dd, *J* = 7.8, 1.6 Hz, 1H),

7.44 (d,  $J = 7.8$  Hz, 2H), 7.29 (t,  $J = 7.8$  Hz, 2H), 7.21 (t,  $J = 7.8$  Hz, 2H), 4.24 (s, 2H), 3.99 (s, 3H).  
 $^{13}\text{C}$  NMR (151 MHz, Chloroform- $d$ )  $\delta$  159.5, 155.8, 136.6, 135.2, 133.1, 131.6, 129.6, 129.5, 128.4, 126.7, 123.9, 119.5, 40.6, 35.6.

HRMS (ESI-MS) Calcd. For  $\text{C}_{16}\text{H}_{13}\text{ClN}_2\text{ONa}$   $[\text{M}+\text{Na}]^+$  307.0609, found: 307.0610.

IR (neat,  $\text{cm}^{-1}$ ):  $\tilde{\nu}$ : 3296, 2927, 2584, 2324, 2098, 1936, 1788, 1723, 1650, 1598, 1551, 1454, 1337, 1263, 1186, 1098, 999, 898, 730.



### 3-Benzyl-5-chloro-1-methylquinoxalin-2(1H)-one (2-3la)

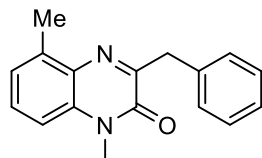
The crude mixture was purified by silica gel column chromatography with pentane/EA (10:1). 21 mg product was obtained by 49% isolated yield as yellow solid. Melting point: 139.8 – 141.5 °C.

$^1\text{H}$  NMR (600 MHz, Chloroform- $d$ )  $\delta$  7.43 (d,  $J = 7.8$  Hz, 2H), 7.33 – 7.31 (m, 2H), 7.22 (t,  $J = 7.8$  Hz, 2H), 7.13 (t,  $J = 7.2$  Hz, 1H), 7.09 – 7.07 (m, 1H), 4.24 (s, 2H), 3.57 (s, 3H).

$^{13}\text{C}$  NMR (151 MHz, Chloroform- $d$ )  $\delta$  159.8, 154.3, 136.7, 134.8, 134.8, 129.8, 129.7, 129.5, 128.4, 126.7, 124.5, 112.4, 40.8, 29.5.

HRMS (ESI-MS) Calcd. For  $\text{C}_{16}\text{H}_{13}\text{ClN}_2\text{ONa}$   $[\text{M}+\text{Na}]^+$  307.0609, found: 307.0602.

IR (neat,  $\text{cm}^{-1}$ ):  $\tilde{\nu}$ : 3298, 3081, 2926, 2855, 2323, 2066, 1912, 1744, 1654, 1586, 1461, 1292, 1109, 1074, 922, 839, 697.



### 3-Benzyl-1,5-dimethylquinoxalin-2(1H)-one (2-3ma)

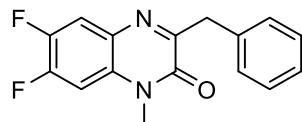
The crude mixture was purified by silica gel column chromatography with pentane/EA (10:1). 30 mg product was obtained by 76% isolated yield as yellow solid. Melting point: 112.4 – 113.1 °C.

$^1\text{H}$  NMR (600 MHz, Chloroform- $d$ )  $\delta$  7.39 (d,  $J = 7.2$  Hz, 2H), 7.29 (t,  $J = 7.8$  Hz, 1H), 7.21 (t,  $J = 7.8$  Hz, 2H), 7.12 (t,  $J = 7.2$  Hz, 1H), 7.09 (d,  $J = 7.8$  Hz, 1H), 7.00 (d,  $J = 8.4$  Hz, 1H), 4.19 (s, 2H), 3.56 (s, 3H), 2.58 (s, 3H).

$^{13}\text{C}$  NMR (151 MHz, Chloroform- $d$ )  $\delta$  157.3, 154.7, 138.7, 137.4, 133.4, 131.3, 129.6, 129.5, 128.3, 126.4, 124.8, 111.4, 40.6, 29.2, 17.5.

HRMS (ESI-MS) Calcd. For  $\text{C}_{17}\text{H}_{16}\text{N}_2\text{ONa}$   $[\text{M}+\text{Na}]^+$  287.1155, found: 287.1150.

IR (neat,  $\text{cm}^{-1}$ ):  $\tilde{\nu}$ : 3274, 3028, 2925, 2652, 2323, 2027, 1948, 1748, 1640, 1480, 1374, 1210, 1151, 1037, 939, 835, 781, 698.



### 3-Benzyl-6,7-difluoro-1-methylquinoxalin-2(1H)-one (2-3na)

The crude mixture was purified by silica gel column chromatography with pentane/EA (10:1). 33 mg product was obtained by 77% isolated yield as yellow solid. Melting point: 96.7 – 97.9 °C.

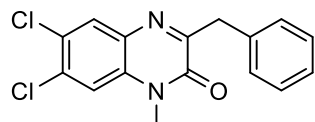
$^1\text{H}$  NMR (600 MHz, Chloroform- $d$ )  $\delta$  7.58 (dd,  $J = 10.2, 8.4$  Hz, 1H), 7.36 (d,  $J = 7.2$  Hz, 2H), 7.22

(t,  $J = 7.8$  Hz, 2H), 7.14 (t,  $J = 7.2$  Hz, 1H), 6.98 (dd,  $J = 11.4, 7.2$  Hz, 1H), 4.15 (s, 2H), 3.53 (s, 3H).

$^{13}\text{C}$  NMR (151 MHz, Chloroform- $d$ )  $\delta$  159.9 (d,  $J = 3.5$  Hz), 154.3, 151.2 (dd,  $J = 253.1, 14.2$  Hz), 146.7 (dd,  $J = 247.0, 13.9$  Hz), 136.6, 130.5 (dd,  $J = 8.6, 2.0$  Hz), 129.6, 129.0 (dd,  $J = 9.4, 3.2$  Hz), 128.5, 126.8, 117.6 (dd,  $J = 17.8, 2.1$  Hz), 102.2 (d,  $J = 23.0$  Hz), 40.6, 29.6.

$^{19}\text{F}$  NMR (376 MHz, Chloroform- $d$ )  $\delta$  -131.17 to -131.38 (m), -142.09 to -142.33 (m).

Data is in line with the literature.<sup>238</sup>



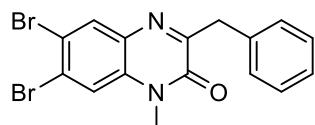
### 3-Benzyl-6,7-dichloro-1-methylquinoxalin-2(1H)-one (2-3oa)

The crude mixture was purified by silica gel column chromatography with pentane/EA (10:1). 33 mg product was obtained by 69% isolated yield as yellow solid. Melting point: 181.9 – 184.0 °C.

$^1\text{H}$  NMR (600 MHz, Chloroform- $d$ )  $\delta$  7.86 (s, 1H), 7.36 (d,  $J = 7.8$  Hz, 2H), 7.23 (t,  $J = 7.8$  Hz, 2H), 7.19 (s, 1H), 7.15 (t,  $J = 7.2$  Hz, 1H), 4.16 (s, 2H), 3.54 (s, 3H).

$^{13}\text{C}$  NMR (151 MHz, Chloroform- $d$ )  $\delta$  160.8, 154.1, 136.4, 133.9, 132.7, 131.8, 130.8, 129.6, 128.5, 127.4, 126.8, 115.1, 40.6, 29.4.

Data is in line with the literature.<sup>231</sup>



### 3-Benzyl-6,7-dibromo-1-methylquinoxalin-2(1H)-one (2-3pa)

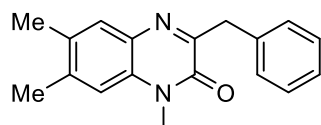
The crude mixture was purified by silica gel column chromatography with pentane/EA (10:1). 11 mg product was obtained by 18% isolated yield as yellow solid. Melting point: 205.5 – 207.3 °C.

$^1\text{H}$  NMR (600 MHz, Chloroform- $d$ )  $\delta$  8.07 (s, 1H), 7.52 (s, 1H), 7.42 (d,  $J = 7.8$  Hz, 2H), 7.29 (t,  $J = 7.8$  Hz, 2H), 7.22 (t,  $J = 7.8$  Hz, 1H), 4.22 (s, 2H), 3.60 (s, 3H).

$^{13}\text{C}$  NMR (151 MHz, Chloroform- $d$ )  $\delta$  161.0, 154.1, 136.3, 133.9, 133.2, 132.5, 129.6, 128.5, 126.8, 126.1, 118.7, 118.2, 40.7, 29.3.

HRMS (EI-MS) Calcd. For  $\text{C}_{16}\text{H}_{12}\text{Br}_2\text{N}_2\text{O}$  405.9311, found: 405.9311.

IR (neat,  $\text{cm}^{-1}$ ):  $\tilde{\nu}$ : 3312, 3088, 2923, 2854, 2325, 2091, 1900, 1740, 1661, 1548, 1454, 1388, 1289, 1198, 1004, 906, 884, 747, 700.



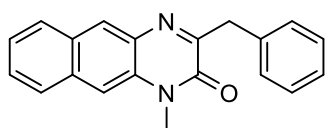
### 3-Benzyl-1,6,7-trimethylquinoxalin-2(1H)-one (2-3qa)

The crude mixture was purified by silica gel column chromatography with pentane/EA (10:1). 34 mg product was obtained by 81% isolated yield as yellow solid. Melting point: 171.0 – 171.8 °C.

$^1\text{H}$  NMR (600 MHz, Chloroform- $d$ )  $\delta$  7.60 (s, 1H), 7.45 (d,  $J = 7.2$  Hz, 2H), 7.28 (t,  $J = 7.8$  Hz, 2H), 7.19 (tt,  $J = 7.2, 1.2$  Hz, 1H), 7.02 (s, 1H), 4.24 (s, 2H), 3.63 (s, 3H), 2.39 (s, 3H), 2.34 (s, 3H).

$^{13}\text{C}$  NMR (151 MHz, Chloroform- $d$ )  $\delta$  158.0, 154.8, 139.6, 137.4, 132.4, 131.3, 131.2, 130.0, 129.5, 128.3, 126.5, 114.1, 40.7, 29.0, 20.5, 19.1.

Data is in line with the literature.<sup>238</sup>



### 3-Benzyl-1-methylbenzo[g]quinoxalin-2(1H)-one (2-3ra)

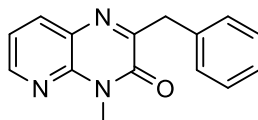
The crude mixture was purified by silica gel column chromatography with pentane/EA (8:1). 18 mg product was obtained by 40% isolated yield as yellow solid. Melting point: 196.4 – 198.0 °C.

<sup>1</sup>H NMR (600 MHz, Chloroform-*d*)  $\delta$  8.35 (s, 1H), 7.96 (d, *J* = 8.4 Hz, 1H), 7.88 (d, *J* = 8.4 Hz, 1H), 7.58 – 7.53 (m, 2H), 7.52 – 7.45 (m, 3H), 7.31 (t, *J* = 7.8 Hz, 2H), 7.22 (tt, *J* = 7.2, 1.2 Hz, 1H), 4.31 (s, 2H), 3.72 (s, 3H).

<sup>13</sup>C NMR (151 MHz, Chloroform-*d*)  $\delta$  159.8, 154.6, 136.9, 133.5, 132.1, 131.9, 129.7, 129.6, 129.0, 128.4, 128.4, 127.7, 127.1, 126.6, 125.2, 109.9, 40.8, 29.1.

HRMS (ESI-MS) Calcd. For C<sub>20</sub>H<sub>16</sub>N<sub>2</sub>ONa [M+Na]<sup>+</sup> 323.1155, found: 323.1150.

IR (neat, cm<sup>-1</sup>):  $\tilde{\nu}$ : 3283, 3057, 2925, 2855, 2651, 2321, 2078, 1816, 1594, 1493, 1359, 1279, 1162, 1036, 996, 865, 746, 668.



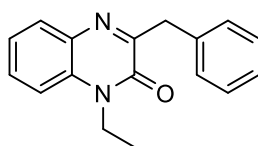
### 2-Benzyl-4-methylpyrido[2,3-b]pyrazin-3(4H)-one (2-3sa)

The crude mixture was purified by silica gel column chromatography with pentane/EA (6:1). 31 mg product was obtained by 82% isolated yield as yellow solid. Melting point: 112.5 – 114.0 °C.

<sup>1</sup>H NMR (600 MHz, Chloroform-*d*)  $\delta$  8.46 (dd, *J* = 4.8, 1.8 Hz, 1H), 8.05 (dd, *J* = 7.8, 1.8 Hz, 1H), 7.38 (d, *J* = 7.2 Hz, 2H), 7.25 – 7.18 (m, 3H), 7.14 (t, *J* = 7.2 Hz, 1H), 4.20 (s, 2H), 3.71 (s, 3H).

<sup>13</sup>C NMR (151 MHz, Chloroform-*d*)  $\delta$  160.7, 156.0, 149.0, 144.2, 137.2, 136.6, 129.6, 128.5, 128.1, 126.8, 119.5, 40.6, 27.8.

Data is in line with the literature.<sup>233</sup>



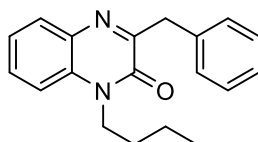
### 3-Benzyl-1-ethylquinoxalin-2(1H)-one (2-3ta)

The crude mixture was purified by silica gel column chromatography with pentane/EA (10:1). 32 mg product was obtained by 81% isolated yield as yellow solid. Melting point: 67.4 – 68.2 °C.

<sup>1</sup>H NMR (600 MHz, Chloroform-*d*)  $\delta$  7.78 (dd, *J* = 7.8, 1.6 Hz, 1H), 7.45 – 7.37 (m, 3H), 7.26 – 7.18 (m, 4H), 7.13 (t, *J* = 7.2 Hz, 1H), 4.20 (q, *J* = 7.2 Hz, 2H), 4.19 (s, 2H), 1.26 (t, *J* = 7.2 Hz, 3H).

<sup>13</sup>C NMR (151 MHz, Chloroform-*d*)  $\delta$  159.4, 154.2, 137.2, 133.1, 132.3, 130.2, 129.8, 129.6, 128.4, 126.5, 123.4, 113.4, 40.6, 37.4, 12.4.

Data is in line with the literature.<sup>238</sup>



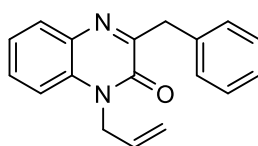
### 3-Benzyl-1-butylquinoxalin-2(1H)-one (2-3ua)

The crude mixture was purified by silica gel column chromatography with pentane/EA (10:1). 36 mg product was obtained by 82% isolated yield as yellow solid. Melting point: 77.1 – 78.3 °C.

<sup>1</sup>H NMR (600 MHz, Chloroform-*d*)  $\delta$  7.77 (dd,  $J$  = 7.8, 1.6 Hz, 1H), 7.45 – 7.35 (m, 3H), 7.25 – 7.16 (m, 4H), 7.12 (tt,  $J$  = 7.2, 1.2 Hz, 1H), 4.19 (s, 2H), 4.11 (t,  $J$  = 7.8 Hz, 2H), 1.66 – 1.59 (m, 2H), 1.42 – 1.33 (m, 2H), 0.90 (t,  $J$  = 7.2 Hz, 3H).

<sup>13</sup>C NMR (151 MHz, Chloroform-*d*)  $\delta$  159.3, 154.5, 137.2, 133.1, 132.5, 130.2, 129.8, 129.5, 128.4, 126.5, 123.3, 113.6, 42.2, 40.7, 29.3, 20.3, 13.8.

Data is in line with the literature.<sup>238</sup>



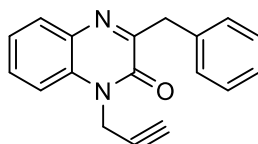
### 1-Allyl-3-benzylquinoxalin-2(1H)-one (2-3va)

The crude mixture was purified by silica gel column chromatography with pentane/EA (10:1). 34 mg product was obtained by 82% isolated yield as yellow solid. Melting point: 79.0 – 81.9 °C.

<sup>1</sup>H NMR (600 MHz, Chloroform-*d*)  $\delta$  7.78 (dd,  $J$  = 7.8, 1.8 Hz, 1H), 7.42 – 7.36 (m, 3H), 7.26 – 7.19 (m, 3H), 7.16 (dd,  $J$  = 8.4, 1.2 Hz, 1H), 7.13 (tt,  $J$  = 7.2, 1.2 Hz, 1H), 5.86 – 5.78 (m, 1H), 5.16 (broad d,  $J$  = 10.2 Hz, 1H), 5.06 (broad d,  $J$  = 10.2 Hz, 1H), 4.78 (dt,  $J$  = 5.4, 1.8 Hz, 2H), 4.20 (s, 2H).

<sup>13</sup>C NMR (151 MHz, Chloroform-*d*)  $\delta$  159.4, 154.3, 137.1, 133.0, 132.6, 130.7, 130.1, 129.8, 129.5, 128.4, 126.6, 123.6, 118.1, 114.1, 44.6, 40.7.

Data is in line with the literature.<sup>238</sup>



### 3-Benzyl-1-(prop-2-yn-1-yl)quinoxalin-2(1H)-one (2-3wa)

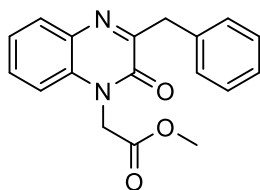
The crude mixture was purified by silica gel column chromatography with pentane/EA (10:1). 34 mg product was obtained by 83% isolated yield as yellow solid. Melting point: 153.0 – 155.7 °C.

<sup>1</sup>H NMR (600 MHz, Chloroform-*d*)  $\delta$  7.78 (dd,  $J$  = 7.8, 1.8 Hz, 1H), 7.47 ( $\approx$ t,  $J$  = 7.8 Hz, 1H), 7.39 (d,  $J$  = 7.8 Hz, 2H), 7.34 (d,  $J$  = 8.4 Hz, 1H), 7.27 ( $\approx$ t,  $J$  = 7.2 Hz, 1H), 7.22 (t,  $J$  = 7.8 Hz, 2H), 7.14 (t,  $J$  = 7.4 Hz, 1H), 4.93 (d,  $J$  = 2.4 Hz, 2H), 4.19 (s, 2H), 2.19 (t,  $J$  = 2.4 Hz, 1H).

<sup>13</sup>C NMR (151 MHz, Chloroform-*d*)  $\delta$  159.2, 153.7, 136.8, 133.0, 131.8, 130.1, 130.0, 129.6, 128.4, 126.7, 124.0, 114.1, 76.8, 73.3, 40.7, 31.5.

Data is in line with the literature.<sup>238</sup>





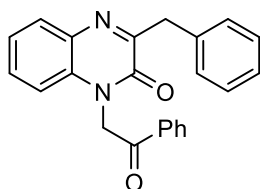
### Methyl 2-(3-benzyl-2-oxoquinoxalin-1(2H)-yl)acetate (2-3xa)

The crude mixture was purified by silica gel column chromatography with pentane/EA (8:1). 32 mg product was obtained by 69% isolated yield as yellow solid. Melting point: 104.5 – 105.7 °C.

<sup>1</sup>H NMR (600 MHz, Chloroform-*d*)  $\delta$  7.79 (d,  $J$  = 7.8 Hz, 1H), 7.44 – 7.34 (m, 3H), 7.26 (t,  $J$  = 7.8 Hz, 1H), 7.21 (t,  $J$  = 7.2 Hz, 2H), 7.13 (t,  $J$  = 7.2 Hz, 1H), 6.95 (d,  $J$  = 8.4 Hz, 1H), 4.92 (s, 2H), 4.20 (s, 2H), 3.67 (s, 3H).

<sup>13</sup>C NMR (151 MHz, Chloroform-*d*)  $\delta$  167.6, 159.1, 154.3, 136.8, 132.9, 132.4, 130.4, 130.1, 129.5, 128.4, 126.6, 123.9, 113.0, 52.8, 43.5, 40.6.

Data is in line with the literature.<sup>238</sup>



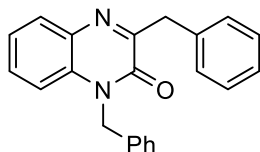
### 3-Benzyl-1-(2-oxo-2-phenylethyl)quinoxalin-2(1H)-one (2-3ya)

The crude mixture was purified by silica gel column chromatography with 14 pentane/EA (8:1). 46 mg product was obtained by 87% isolated yield as yellow solid. Melting point: 140.9 – 141.2 °C.

<sup>1</sup>H NMR (600 MHz, Chloroform-*d*)  $\delta$  8.06 – 8.00 (m, 2H), 7.88 (dd,  $J$  = 7.8, 1.8 Hz, 1H), 7.65 (tt,  $J$  = 7.8, 1.2 Hz, 1H), 7.52 (t,  $J$  = 7.8 Hz, 2H), 7.46 (d,  $J$  = 7.8 Hz, 2H), 7.40 (ddd,  $J$  = 8.4, 7.2, 1.6 Hz, 1H), 7.32 – 7.28 (m, 3H), 7.21 (tt,  $J$  = 7.8, 1.2 Hz, 1H), 6.91 (dd,  $J$  = 8.4, 1.2 Hz, 1H), 5.68 (s, 2H), 4.29 (s, 2H).

<sup>13</sup>C NMR (151 MHz, Chloroform-*d*)  $\delta$  191.1, 159.0, 154.5, 136.9, 134.5, 134.3, 132.9, 132.7, 130.2, 129.9, 129.5, 129.0, 128.4, 128.1, 126.6, 123.7, 113.5, 48.5, 40.7.

Data is in line with the literature.<sup>231</sup>



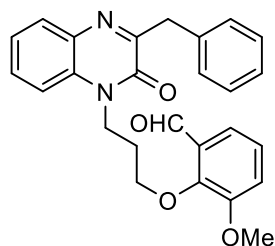
### 1,3-Dibenzylquinoxalin-2(1H)-one (2-3za)

The crude mixture was purified by silica gel column chromatography with pentane/EA (8:1). 43 mg product was obtained by 88% isolated yield as yellow solid. Melting point: 136.5 – 138.2 °C.

<sup>1</sup>H NMR (600 MHz, Chloroform-*d*)  $\delta$  7.77 (dd,  $J$  = 7.8, 1.5 Hz, 1H), 7.41 (d,  $J$  = 7.8 Hz, 2H), 7.30 (≈t,  $J$  = 7.8 Hz, 1H), 7.25 – 7.17 (m, 5H), 7.17 – 7.08 (m, 5H), 5.37 (s, 2H), 4.25 (s, 2H).

<sup>13</sup>C NMR (151 MHz, Chloroform-*d*)  $\delta$  159.5, 154.9, 137.1, 135.2, 133.1, 132.7, 130.1, 129.9, 129.6, 128.9, 128.5, 127.7, 126.8, 126.6, 123.6, 114.4, 46.0, 40.8.

Data is in line with the literature.<sup>238</sup>



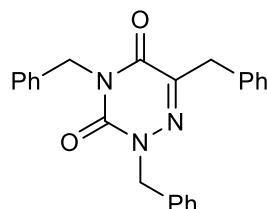
### 2-(3-(3-Benzyl-2-oxoquinoxalin-1(2H)-yl)propoxy)-3-methoxybenzaldehyde (2-3aaa)

The crude mixture was purified by silica gel column chromatography with pentane/EA (6:1). 24 mg product was obtained by 37% isolated yield as viscous yellow oil.

$^1\text{H}$  NMR (600 MHz, Chloroform-*d*)  $\delta$  10.35 (s, 1H), 7.93 (d,  $J$  = 8.4 Hz, 1H), 7.73 (d,  $J$  = 8.4 Hz, 1H), 7.54 (t,  $J$  = 7.8 Hz, 1H), 7.47 (t,  $J$  = 7.8 Hz, 1H), 7.35 (dd,  $J$  = 7.2, 2.4 Hz, 1H), 7.21 (d,  $J$  = 7.8 Hz, 2H), 7.11 – 7.97 (m, 5H), 4.61 (t,  $J$  = 6.0 Hz, 2H), 4.23 (s, 2H), 4.07 (t,  $J$  = 6.6 Hz, 2H), 3.69 (s, 3H), 2.21 (p,  $J$  = 6.6 Hz, 2H).

$^{13}\text{C}$  NMR (151 MHz, Chloroform-*d*)  $\delta$  190.1, 155.9, 153.0, 151.7, 149.3, 140.1, 138.6, 137.6, 130.0, 129.3, 129.0, 128.5, 128.3, 126.8, 126.5, 126.4, 124.2, 119.3, 118.0, 71.6, 63.2, 55.9, 40.4, 29.6.

Data is in line with the literature.<sup>238</sup>



### 2,4,6-Tribenzyl-1,2,4-triazine-3,5(2H,4H)-dione (2-3aba)

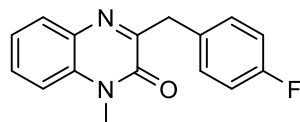
The crude mixture was purified by silica gel column chromatography with pentane/EA (6:1). 50 mg product was obtained by 87% isolated yield as yellow solid. Melting point: 99.8 – 100.7 °C.

$^1\text{H}$  NMR (600 MHz, Chloroform-*d*)  $\delta$  7.36 (d,  $J$  = 7.2 Hz, 2H), 7.28 (d,  $J$  = 6.6 Hz, 2H), 7.27 – 7.11 (m, 11H), 4.99 (s, 2H), 4.95 (s, 2H), 3.82 (s, 2H).

$^{13}\text{C}$  NMR (151 MHz, Chloroform-*d*)  $\delta$  155.8, 149.0, 144.5, 136.2, 135.8, 135.6, 129.5, 129.3, 128.8, 128.7, 128.6, 128.5, 128.2, 128.1, 126.9, 55.2, 44.3, 36.6.

HRMS (ESI-MS) Calcd. For  $\text{C}_{24}\text{H}_{21}\text{N}_3\text{O}_2\text{Na}$   $[\text{M}+\text{Na}]^+$  406.1526, found: 406.1522.

IR (neat,  $\text{cm}^{-1}$ ):  $\tilde{\nu}$ : 3031, 2853, 2323, 2048, 1954, 1891, 1709, 1654, 1597, 1493, 1349, 1263, 1143, 1073, 915, 822, 696.



### 3-(4-Fluorobenzyl)-1-methylquinoxalin-2(1H)-one (2-3ab)

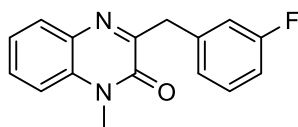
The crude mixture was purified by silica gel column chromatography with pentane/EA (10:1). 31 mg product was obtained by 77% isolated yield as yellow solid. Melting point: 112.8 – 113.3 °C.

$^1\text{H}$  NMR (600 MHz, Chloroform-*d*)  $\delta$  7.77 (dd,  $J$  = 7.8, 1.8 Hz, 1H), 7.45 (ddd,  $J$  = 8.4, 7.2, 1.6 Hz, 1H), 7.38 – 7.32 (m, 2H), 7.26 ( $\approx$ t,  $J$  = 8.4 Hz, 1H), 7.19 (d,  $J$  = 8.4 Hz, 1H), 6.93 – 6.84 (m, 2H), 4.15 (s, 2H), 3.59 (s, 3H).

$^{13}\text{C}$  NMR (151 MHz, Chloroform-*d*)  $\delta$  161.8 (d,  $J$  = 244.5 Hz), 159.1, 154.7, 133.3, 132.7, 132.6 (d,  $J$  = 3.3 Hz), 131.0 (d,  $J$  = 7.9 Hz), 130.0, 130.0, 123.7, 115.2 (d,  $J$  = 21.3 Hz), 113.6, 39.9, 29.1.

$^{19}\text{F}$  NMR (565 MHz, Chloroform-*d*)  $\delta$  -116.59 to -116.67 (m).

Data is in line with the literature.<sup>238</sup>



### 3-(3-Fluorobenzyl)-1-methylquinoxalin-2(1H)-one (2-3ac)

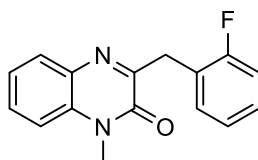
The crude mixture was purified by silica gel column chromatography with pentane/EA (8:1). 28 mg product was obtained by 70% isolated yield as yellow solid. Melting point: 77.7 – 78.8 °C.

$^1\text{H}$  NMR (600 MHz, Chloroform-*d*)  $\delta$  7.85 (dd,  $J$  = 7.8, 1.8 Hz, 1H), 7.53 (ddd,  $J$  = 8.4, 7.2, 1.8 Hz, 1H), 7.34 (ddd,  $J$  = 8.4, 7.2, 1.2 Hz, 1H), 7.29 – 7.22 (m, 3H), 7.18 – 7.14 (broad d,  $J$  = 10.2 Hz, 1H), 6.91 – 6.87 (m, 1H), 4.25 (s, 2H), 3.67 (s, 3H).

$^{13}\text{C}$  NMR (151 MHz, Chloroform-*d*)  $\delta$  162.8 (d,  $J$  = 245.7 Hz), 158.6, 154.7, 139.5 (d,  $J$  = 7.6 Hz), 133.3, 132.7, 130.1, 130.0, 129.7 (d,  $J$  = 8.2 Hz), 125.2 (d,  $J$  = 2.2 Hz), 123.7, 116.3 (d,  $J$  = 21.3 Hz), 113.6, 113.5 (d,  $J$  = 21.0 Hz), 40.4 (d,  $J$  = 1.8 Hz), 29.1.

$^{19}\text{F}$  NMR (565 MHz, Chloroform-*d*)  $\delta$  -113.52 (td,  $J$  = 9.1, 5.1 Hz).

Data is in line with the literature.<sup>233</sup>



### 3-(2-Fluorobenzyl)-1-methylquinoxalin-2(1H)-one (2-3ad)

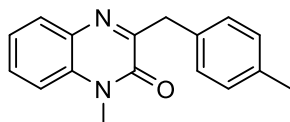
The crude mixture was purified by silica gel column chromatography with pentane/EA (10:1). 32 mg product was obtained by 80% isolated yield as yellow solid. Melting point: 133.7 – 134.8 °C.

$^1\text{H}$  NMR (600 MHz, Chloroform-*d*)  $\delta$  7.72 (d,  $J$  = 7.9 Hz, 1H), 7.44 (t,  $J$  = 7.4 Hz, 1H), 7.29 (t,  $J$  = 7.3 Hz, 1H), 7.25 – 7.19 (m, 2H), 7.17 – 7.11 (m, 1H), 7.02 – 6.93 (m, 2H), 4.24 (s, 2H), 3.61 (s, 3H).

$^{13}\text{C}$  NMR (151 MHz, Chloroform-*d*)  $\delta$  161.4 (d,  $J$  = 246.6 Hz), 158.1, 154.7, 133.3, 132.7, 131.6 (d,  $J$  = 4.2 Hz), 130.1, 130.0, 128.3 (d,  $J$  = 8.0 Hz), 124.2 (d,  $J$  = 15.7 Hz), 123.8 (d,  $J$  = 3.5 Hz), 123.6, 115.3 (d,  $J$  = 21.9 Hz), 113.5, 33.8 (d,  $J$  = 2.7 Hz), 29.1.

$^{19}\text{F}$  NMR (376 MHz, Chloroform-*d*)  $\delta$  -116.53 to -116.71 (m).

Data is in line with the literature.<sup>233</sup>



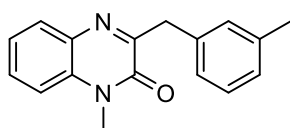
### 1-Methyl-3-(4-methylbenzyl)quinoxalin-2(1H)-one (2-3ae)

The crude mixture was purified by silica gel column chromatography with pentane/EA (10:1). 25 mg product was obtained by 63% isolated yield as yellow solid. Melting point: 112.6 – 113.2 °C.

$^1\text{H}$  NMR (400 MHz, Chloroform-*d*)  $\delta$  7.88 (dd,  $J$  = 7.8, 1.6 Hz, 1H), 7.53 (ddd,  $J$  = 8.4, 7.2, 1.6 Hz, 1H), 7.42 – 7.32 (m, 3H), 7.29 – 7.26 (m, 1H), 7.12 (d,  $J$  = 7.8 Hz, 2H), 4.25 (s, 2H), 3.67 (s, 3H), 2.32 (s, 3H).

$^{13}\text{C}$  NMR (151 MHz, Chloroform-*d*)  $\delta$  159.5, 154.7, 136.2, 133.9, 133.4, 132.7, 129.9, 129.8, 129.4, 129.1, 123.6, 113.5, 40.4, 29.1, 21.1.

Data is in line with the literature.<sup>238</sup>



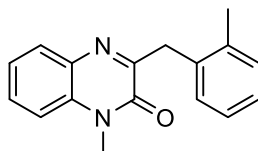
**1-Methyl-3-(3-methylbenzyl)quinoxalin-2(1H)-one (2-3af)**

The crude mixture was purified by silica gel column chromatography with pentane/EA (10:1). 30 mg product was obtained by 76% isolated yield as yellow solid. Melting point: 82.7 – 83.6 °C.

<sup>1</sup>H NMR (600 MHz, Chloroform-*d*)  $\delta$  7.86 (dd,  $J$  = 7.8, 1.8 Hz, 1H), 7.51 (ddd,  $J$  = 8.4, 7.2, 1.8 Hz, 1H), 7.33 (ddd,  $J$  = 8.4, 7.2, 1.2 Hz, 1H), 7.30 – 7.23 (m, 3H), 7.18 (t,  $J$  = 7.8 Hz, 1H), 7.02 (d,  $J$  = 7.5 Hz, 1H), 4.23 (s, 2H), 3.65 (s, 3H), 2.32 (s, 3H).

<sup>13</sup>C NMR (151 MHz, Chloroform-*d*)  $\delta$  159.4, 154.7, 138.0, 136.9, 133.4, 132.8, 130.2, 129.9, 129.8, 128.3, 127.4, 126.5, 123.5, 113.5, 40.7, 29.1, 21.4.

Data is in line with the literature.<sup>231</sup>



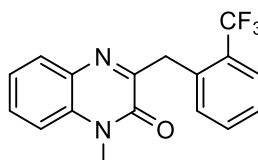
**1-Methyl-3-(2-methylbenzyl)quinoxalin-2(1H)-one (2-3ag)**

The crude mixture was purified by silica gel column chromatography with pentane/EA (8:1). 22 mg product was obtained by 55% isolated yield as yellow solid. Melting point: 92.9 – 93.7 °C.

<sup>1</sup>H NMR (600 MHz, Chloroform-*d*)  $\delta$  7.73 (dd,  $J$  = 7.8, 1.6 Hz, 1H), 7.44 (ddd,  $J$  = 8.4, 7.4, 1.6 Hz, 1H), 7.28 – 7.22 (m, 2H), 7.19 (d,  $J$  = 8.4 Hz, 1H), 7.12 – 7.00 (m, 3H), 4.21 (s, 2H), 3.60 (s, 3H), 2.38 (s, 3H).

<sup>13</sup>C NMR (151 MHz, Chloroform-*d*)  $\delta$  159.2, 154.8, 137.4, 135.5, 133.2, 132.7, 130.3, 130.1, 130.0, 129.8, 126.7, 125.8, 123.5, 113.5, 37.9, 29.1, 20.0.

Data is in line with the literature.<sup>231</sup>



**1-Methyl-3-(2-(trifluoromethyl)benzyl)quinoxalin-2(1H)-one (2-3ah)**

The crude mixture was purified by silica gel column chromatography with pentane/EA (8:1). 40 mg product was obtained by 84% isolated yield as yellow solid. Melting point: 149.8 – 151.7 °C.

<sup>1</sup>H NMR (600 MHz, Chloroform-*d*)  $\delta$  7.73 (broad d,  $J$  = 8.5 Hz, 1H), 7.69 (d,  $J$  = 7.8 Hz, 1H), 7.53 ( $\approx$ t,  $J$  = 7.8 Hz, 1H), 7.46 (t,  $J$  = 7.8 Hz, 1H), 7.35 (t,  $J$  = 7.8 Hz, 1H), 7.32 – 7.28 (m, 3H), 4.49 (s, 2H), 3.71 (s, 3H).

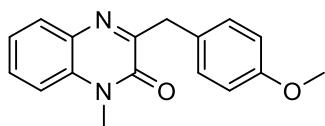
<sup>13</sup>C NMR (151 MHz, Chloroform-*d*)  $\delta$  158.4, 154.6, 135.8 (q,  $J$  = 1.5 Hz), 133.1, 132.6, 131.7, 131.5, 130.1, 130.0, 129.2 (q,  $J$  = 29.9 Hz), 126.6, 126.1 (q,  $J$  = 5.6 Hz), 124.5 (q,  $J$  = 274.2 Hz), 123.6, 113.6, 37.0 (q,  $J$  = 2.6 Hz), 29.1.

<sup>19</sup>F NMR (564 MHz, Chloroform-*d*)  $\delta$  -59.95.

HRMS (ESI-MS) Calcd. For C<sub>17</sub>H<sub>13</sub>F<sub>3</sub>N<sub>2</sub>ONa [M+Na]<sup>+</sup> 341.0872, found: 341.0870.

IR (neat, cm<sup>-1</sup>):  $\tilde{\nu}$ : 3036, 2923, 2855, 2262, 2063, 1942, 1736, 1637, 1465, 1371, 1315, 1176, 1099,

989, 952, 754, 674.



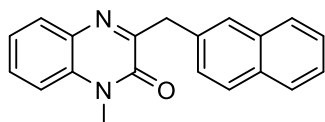
### 3-(4-Methoxybenzyl)-1-methylquinoxalin-2(1H)-one (2-3ai)

The crude mixture was purified by silica gel column chromatography with pentane/EA (6:1). 16 mg product was obtained by 38% isolated yield as yellow solid. Melting point: 129.8 – 131.7 °C.

<sup>1</sup>H NMR (600 MHz, Chloroform-*d*)  $\delta$  7.85 (dd,  $J$  = 7.8, 1.6 Hz, 1H), 7.50 (ddd,  $J$  = 8.4, 7.2, 1.6 Hz, 1H), 7.41 – 7.37 (m, 2H), 7.32 (ddd,  $J$  = 8.4, 7.2, 1.2 Hz, 1H), 7.25 (d,  $J$  = 8.0 Hz, 1H), 6.85 – 6.81 (m, 2H), 4.20 (s, 2H), 3.76 (s, 3H), 3.65 (s, 3H).

<sup>13</sup>C NMR (151 MHz, Chloroform-*d*)  $\delta$  159.5, 158.3, 154.7, 133.3, 132.8, 130.5, 129.9, 129.8, 129.0, 123.5, 113.8, 113.5, 55.2, 39.9, 29.1.

Data is in line with the literature.<sup>238</sup>



### 1-Methyl-3-(naphthalen-2-ylmethyl)quinoxalin-2(1H)-one (2-3aj)

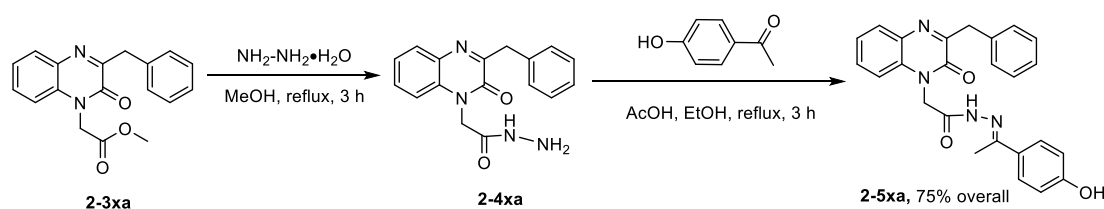
The crude mixture was purified by silica gel column chromatography with pentane/EA (6:1). 10 mg product was obtained by 22% isolated yield as yellow solid. Melting point: 131.0 – 132.7 °C.

<sup>1</sup>H NMR (600 MHz, Chloroform-*d*)  $\delta$  7.90 (s, 1H), 7.87 (dd,  $J$  = 7.8, 1.6 Hz, 1H), 7.80 – 7.75 (m, 3H), 7.62 (dd,  $J$  = 8.4, 1.8 Hz, 1H), 7.52 (ddd,  $J$  = 8.4, 7.2, 1.5 Hz, 1H), 7.44 – 7.37 (m, 2H), 7.34 (ddd,  $J$  = 8.4, 7.2, 1.2 Hz, 1H), 7.26 (dd,  $J$  = 8.4, 1.2 Hz, 1H), 4.43 (s, 2H), 3.65 (s, 3H).

<sup>13</sup>C NMR (151 MHz, Chloroform-*d*)  $\delta$  159.2, 154.7, 134.6, 133.5, 133.4, 132.8, 132.3, 130.0, 129.9, 128.0, 128.0, 127.9, 127.7, 127.6, 125.8, 125.4, 123.6, 113.6, 40.9, 29.1.

Data is in line with the literature.<sup>238</sup>

## Synthetic applications



A mixture of benzylation product **2-3xa** (30.9 mg, 0.1 mmol) and hydrazine hydrate  $\text{NH}_2\text{-NH}_2\cdot\text{H}_2\text{O}$  (0.02 mL, 0.4 mmol) in MeOH (2.5 mL) was heated at reflux for 3 h, then the reaction solution was concentrated in vacuo to give residue **2-4xa** (25 mg), which was used without further purification in the next step.

To a solution of residue **2-4xa**, 4-hydroxyacetophenone (21.8 mg, 0.16 mmol) in EtOH (1.5 mL) was added acetic acid (0.02 mL). The resulting mixture was stirred at reflux and monitored by thin layer chromatography (TLC). When the reaction was completed and cooled to room temperature, the final product **2-5xa** was obtained by direct filtration as white solid: 32 mg, 75% yield from **2-3xa**.

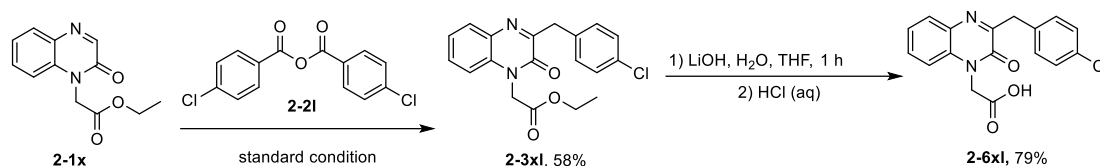
Compound **2-5xa** (8:2 mixture of isomers). Melting point: > 220 °C.

Major isomer (80%): <sup>1</sup>H NMR (600 MHz, DMSO-*d*<sub>6</sub>): δ 10.92 (s, 1H), 9.76 (s, 1H), 7.82 (d, *J* = 8.0 Hz, 1H), 7.73 (d, *J* = 8.3 Hz, 2H), 7.55 (t, *J* = 7.8 Hz, 1H), 7.38-7.33 (m, 4H), 7.30 (t, *J* = 7.5 Hz, 2H), 7.22 (t, *J* = 7.4 Hz, 1H), 6.80 (d, *J* = 8.4 Hz, 2H), 5.46 (s, 2H), 4.20 (s, 2H), 2.26 (s, 3H).

Minor isomer (20%): δ 10.76 (s, 1H), 9.76 (s, 1H), 7.63 (d, *J* = 8.3 Hz, 2H), 7.58 (t, *J* = 7.8 Hz, 1H), 7.46 (d, *J* = 8.4 Hz, 1H), 7.42-7.38 (m, 4H), 7.30 (t, *J* = 7.5 Hz, 2H), 7.22 (t, *J* = 7.4 Hz, 1H), 6.79 (d, *J* = 8.0 Hz, 2H), 5.15 (s, 2H), 4.18 (s, 2H), 2.29 (s, 3H).

<sup>13</sup>C NMR (151 MHz, DMSO-*d*<sub>6</sub>, major and minor together) δ 168.4, 163.3, 159.3, 159.2, 159.1, 159.0, 154.5, 154.5, 153.4, 149.5, 137.8, 137.7, 133.5, 132.4, 130.5, 129.6, 129.6, 129.3, 128.8, 128.4, 128.3, 126.9, 124.0, 123.9, 115.6, 115.5, 115.4, 44.6, 44.4, 14.6, 14.0 (some peaks overlapped with the solvent).

Data is in line with the literature.<sup>238</sup>



Under standard conditions, substrate **2-1x** could react with 4-chlorobenzoic anhydride **2-2l** to afford **2-3xl**.

**2-3xl**, white solid, 30 mg, 58% yield. Melting point: 181.6 – 182.0 °C.

<sup>1</sup>H NMR (400 MHz, Chloroform-*d*) δ 7.78 (dd, *J* = 8.0, 1.6 Hz, 1H), 7.41 (td, *J* = 8.0, 1.6 Hz, 1H), 7.28 (t, *J* = 8.8 Hz, 3H), 7.21 – 7.15 (m, 2H), 6.96 (d, *J* = 8.3 Hz, 1H), 4.91 (s, 2H), 4.15 (s, 2H), 3.68 (s, 3H).

<sup>13</sup>C NMR (101 MHz, Chloroform-*d*) δ 167.5, 158.6, 154.3, 135.3, 132.8, 132.5, 132.4, 130.9, 130.4, 130.3, 128.6, 124.0, 113.0, 52.9, 43.4, 40.0.

Compound **2-3xl** was dissolved in THF (2 mL) and H<sub>2</sub>O (2 mL), then LiOH (9.8 mg, 0.18 mmol) was added to reaction and stirred for 1 h. Then HCl (1 M) was added slowly until pH ≈ 3 and the solution was filtered to give desired product **2-6xl**.

Compound **2-6xl**, yellow solid, 23 mg, 79% yield. Melting point: > 220 °C.

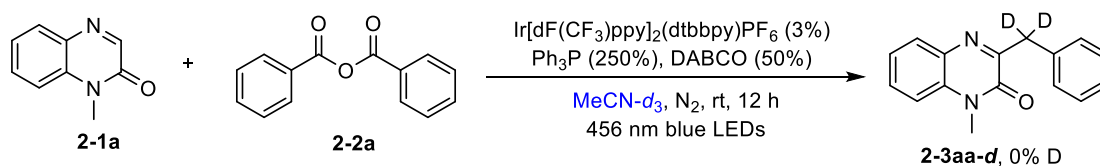
<sup>1</sup>H NMR (400 MHz, DMSO-*d*<sub>6</sub>) δ 7.79 (d, *J* = 8.0 Hz, 1H), 7.58 (t, *J* = 7.6 Hz, 1H), 7.47 (d, *J* = 8.4 Hz, 1H), 7.41 – 7.29 (m, 5H), 5.00 (s, 2H), 4.17 (s, 2H).

<sup>13</sup>C NMR (101 MHz, DMSO-*d*<sub>6</sub>) δ 169.2, 158.7, 154.2, 136.6, 133.0, 132.3, 131.6, 131.6, 130.8, 129.7, 128.7, 124.2, 115.1, 44.1, 39.3.

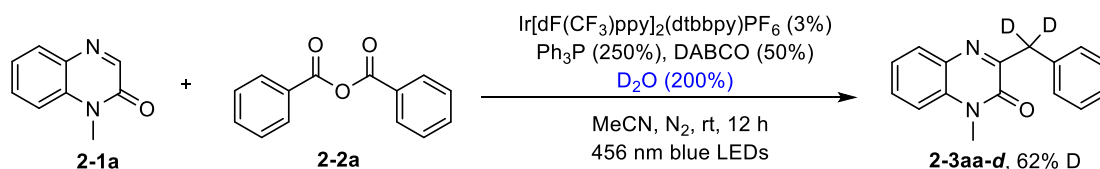
Data is in line with the literature.<sup>249</sup>

## Control experiments

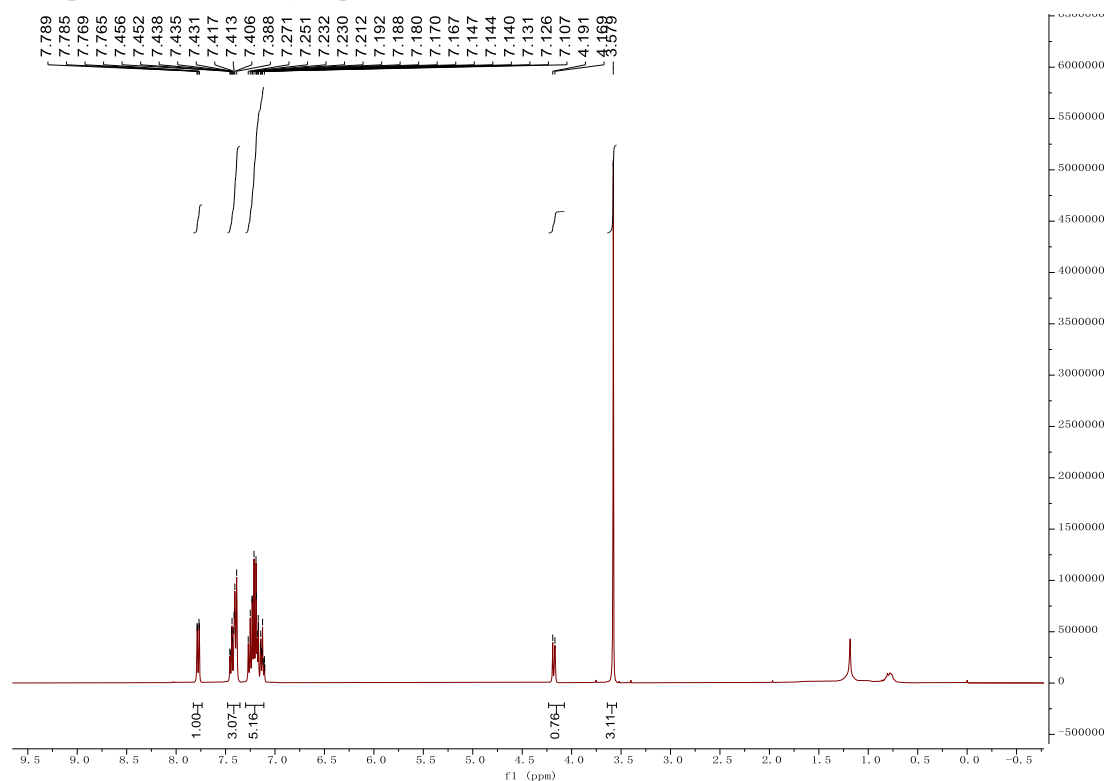
### (1) Deuterium labeling experiments



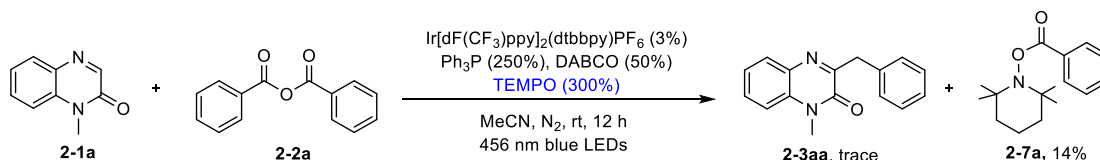
Prepared according to standard conditions using MeCN-*d*<sub>3</sub> replacing anhydrous MeCN, <sup>1</sup>H NMR analysis showed no deuterated product.



To a vial equipped with a stirring bar, quinoxalin-2(1*H*)-one **2-1a** (24 mg, 0.15 mmol), carboxylic acid anhydride **2-2a** (67.9 mg, 0.3 mmol), Ir[dF(CF<sub>3</sub>)ppy]<sub>2</sub>(dtbbpy)PF<sub>6</sub> (5.1 mg, 0.0045 mmol), Ph<sub>3</sub>P (98.4 mg, 0.375 mmol) and DABCO (8.4 mg, 0.075 mmol) were added. The vial was capped. After evacuation and backfilling with N<sub>2</sub> three times, anhydrous MeCN (1.5 mL) and D<sub>2</sub>O (5.4 μL, 0.3 mmol) were added via a syringe. The resulting solution was irradiated by 40W blue LEDs for 12 h at room temperature. Then saturated NaHCO<sub>3</sub> solution (15 mL) was added to the reaction system and stirred for 1 h. After extracting with EA (3 × 5 mL), the combined organic layer was dried by anhydrous Na<sub>2</sub>SO<sub>4</sub>, concentrated in vacuo, and purified by column chromatography (pentane/EA = 8:1) to afford 25 mg of the desired **2-3aa-d**. <sup>1</sup>H NMR analysis presented 62% deuterium incorporation at the benzylic position:



## (2) Radical trapping experiment



To a reaction vial equipped with a stirring bar were added quinoxalin-2(1*H*)-one **2-1a** (24 mg, 0.15 mmol), carboxylic acid anhydride **2-2a** (67.9 mg, 0.3 mmol), Ir[dF(CF<sub>3</sub>)ppy]<sub>2</sub>(dtbbpy)PF<sub>6</sub> (5.1 mg, 0.0045 mmol), Ph<sub>3</sub>P (98.4 mg, 0.375 mmol), DABCO (8.4 mg, 0.075 mmol) and TEMPO (70.3 mg, 0.45 mmol). The capped vial was evacuated and backfilled with N<sub>2</sub> three times before anhydrous MeCN (1.5 mL) was added, then the reaction mixture was exposed under 25 W blue LEDs

irradiation at room temperature. After 12 h, only a trace amount of **2-3aa** was detected by  $^1\text{H}$  NMR analysis of the crude reaction mixture. Trapped product **2-7a** was purified by silica gel column chromatography with pentane/EA (20:1). 11 mg product was obtained by 14% isolated yield as yellow solid.

$^1\text{H}$  NMR (600 MHz, Chloroform-*d*)  $\delta$  8.03 – 7.98 (m, 2H), 7.50 (tt,  $J$  = 7.4, 1.4 Hz, 1H), 7.39 ( $\approx$ t,  $J$  = 7.8 Hz, 2H), 1.75 – 1.67 (m, 2H), 1.67 – 1.60 (m, 1H), 1.55 – 1.49 (m, 2H), 1.40 – 1.36 (m, 1H), 1.21 (s, 6H), 1.05 (s, 6H).

$^{13}\text{C}$  NMR (151 MHz, Chloroform-*d*)  $\delta$  166.4, 132.8, 129.8, 129.6, 128.5, 60.4, 39.1, 32.0, 20.9, 17.0. Data is in line with the literature.<sup>299</sup>

### (3) Other control experiments

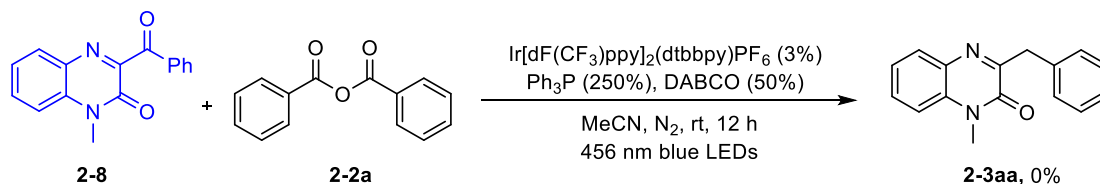
The compounds **2-8** and **2-9** were synthesized according to the literature.<sup>248, 300</sup>

**2-8**:  $^1\text{H}$  NMR (400 MHz, Chloroform-*d*)  $\delta$  7.95 ( $\approx$ d,  $J$  = 8.0 Hz, 2H), 7.88 ( $\approx$ d,  $J$  = 8.2 Hz, 1H), 7.64 ( $\approx$ t,  $J$  = 7.9 Hz, 1H), 7.59 ( $\approx$ t,  $J$  = 7.4 Hz, 1H), 7.44 (t,  $J$  = 7.5 Hz, 2H), 7.40 – 7.33 (m, 2H), 3.70 (s, 3H). Melting point: 150.8 – 152.2 °C.

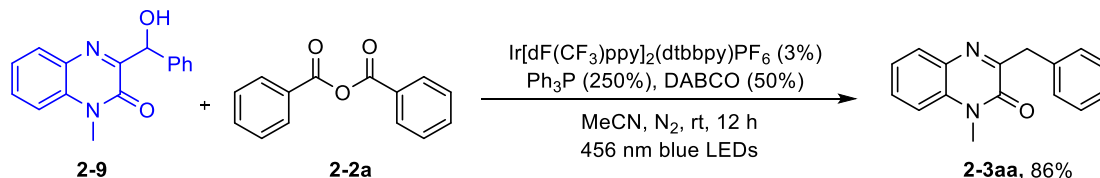
$^{13}\text{C}$  NMR (151 MHz, Chloroform-*d*)  $\delta$  191.8, 154.7, 153.3, 134.9, 134.3, 133.9, 132.2, 132.1, 130.9, 130.0, 128.7, 124.2, 114.1, 29.1.

**2-9**:  $^1\text{H}$  NMR (400 MHz, Chloroform-*d*)  $\delta$  7.87 (dd,  $J$  = 8.0, 1.6 Hz, 1H), 7.54 – 7.43 (m, 3H), 7.32 ( $\approx$ t,  $J$  = 7.7 Hz, 1H), 7.27 – 7.21 (m, 3H), 7.20 – 7.15 (m, 1H), 5.97 (s, 1H), 4.98 (broad s, 1H), 3.55 (s, 3H). Melting point: 91.7 – 92.8 °C.

$^{13}\text{C}$  NMR (101 MHz, Chloroform-*d*)  $\delta$  158.4, 153.6, 140.5, 133.4, 131.7, 130.7, 129.9, 128.4, 127.9, 127.3, 124.0, 113.8, 73.0, 29.0.



A mixture of **2-8** (39.7 mg, 0.15 mmol), carboxylic acid anhydride **2-2a** (67.9 mg, 0.3 mmol), Ir[dF(CF<sub>3</sub>)ppy]<sub>2</sub>(dtbbpy)PF<sub>6</sub> (5.1 mg, 0.0045 mmol), Ph<sub>3</sub>P (98.4 mg, 0.375 mmol), and DABCO (8.4 mg, 0.075 mmol) were added to a vial with a stirring bar. Then the vial with a screw cap and a silicone seal was evacuated and backfilled N<sub>2</sub> (three times). After anhydrous acetonitrile (MeCN, 1.5 mL) was added, the reaction mixture was exposed under blue LEDs irradiation (40 W, 456 nm) at room temperature. After 12 h, no desired product **2-3aa** was detected by TLC.



To a 10 mL vial equipped with a stirring bar, **2-9** (40 mg, 0.15 mmol), carboxylic acid anhydride **2-2a** (67.9 mg, 0.3 mmol), Ir[dF(CF<sub>3</sub>)ppy]<sub>2</sub>(dtbbpy)PF<sub>6</sub> (5.1 mg, 0.0045 mmol), Ph<sub>3</sub>P (98.4 mg, 0.375 mmol), and DABCO (8.4 mg, 0.075 mmol) were added. Then the capped vial was evacuated and backfilled N<sub>2</sub> (three times). After anhydrous acetonitrile (MeCN, 1.5 mL) was added, the reaction mixture was exposed under blue LEDs irradiation (40 W, 456 nm) at room temperature for 12 h. Then saturated aqueous NaHCO<sub>3</sub> solution (15 mL) was added to the reaction. The mixture was stirred for 1 h and then extracted with EA (3 × 5 mL). After being dried over anhydrous Na<sub>2</sub>SO<sub>4</sub> and



concentrated in vacuo, the crude product was purified by column chromatography using pentane/EA as eluent to give the 3-benzylquinoxalin-2(1*H*)-one **2-3aa** with 86% yield.

### Stern-Volmer fluorescence studies

The Agilent Cary Eclipse Fluorescence Spectrometer is used to conduct Stern-Volmer fluorescence quenching analysis. The following parameters were employed: excitation wavelength = 400 nm, emission wavelength = 410 nm, excitation slit width = 10 nm, emission slit width = 10 nm, scan rate = 600 nm/min, averaging time = 0.1s, data interval = 1 nm. The samples were measured at Hellma fluorescence QS quartz cuvette (chamber volume = 1.4 mL, light path = 10 × 4 mm) with a closed screw cap and silicone seal.

All the solutions were prepared with dry degassed MeCN. The concentration of photocatalyst  $[\text{Ir}(\text{dF}(\text{CF}_3)\text{ppy})_2(\text{dtbbpy})]\text{PF}_6$  is  $2 \times 10^{-5}$  M in MeCN, then by adding certain amount of a solution of quencher to  $[\text{Ir}(\text{dF}(\text{CF}_3)\text{ppy})_2(\text{dtbbpy})]\text{PF}_6$  solution, the samples with different concentrations were obtained, and their fluorescence spectra were collected immediately with forementioned parameters.  $I_0$  is the fluorescence intensity without quencher,  $I$  is the fluorescence intensity with quencher.

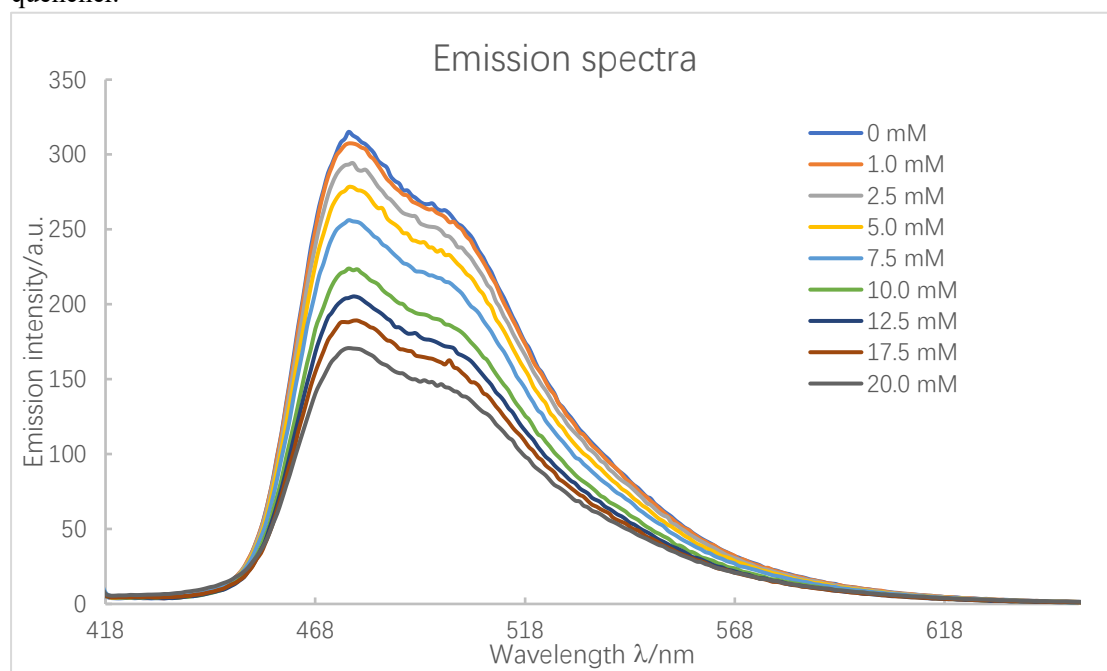


**Figure 2-S1** Emission spectra of  $[\text{Ir}(\text{dF}(\text{CF}_3)\text{ppy})_2(\text{dtbbpy})]\text{PF}_6$  with increasing concentrations of  $\text{Ph}_3\text{P}$  (The concentration of  $[\text{Ir}(\text{dF}(\text{CF}_3)\text{ppy})_2(\text{dtbbpy})]\text{PF}_6$  is  $1.8 \times 10^{-5}$  M in MeCN)

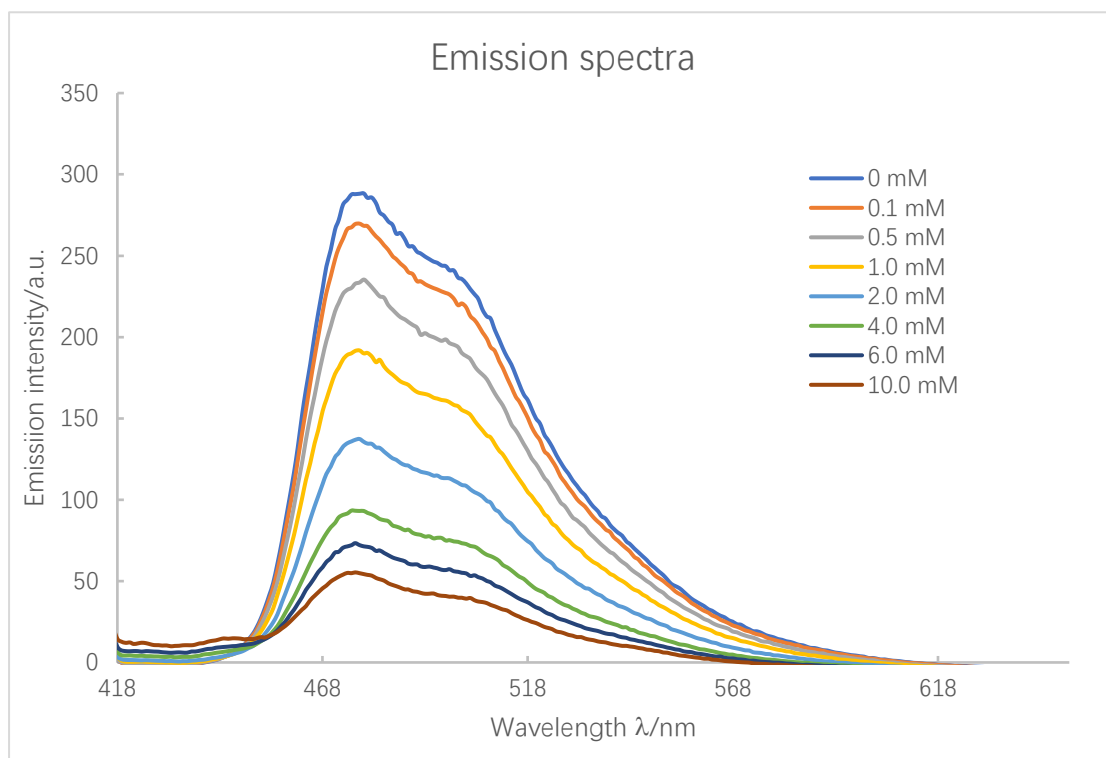


**Figure 2-S2** Emission spectra of  $[\text{Ir}(\text{dF}(\text{CF}_3)\text{ppy})_2(\text{dtbbpy})]\text{PF}_6$  with increasing concentrations of quinoxalinone **2-1a** (The concentration of  $[\text{Ir}(\text{dF}(\text{CF}_3)\text{ppy})_2(\text{dtbbpy})]\text{PF}_6$  is  $1.8 \times 10^{-5}$  M in MeCN)

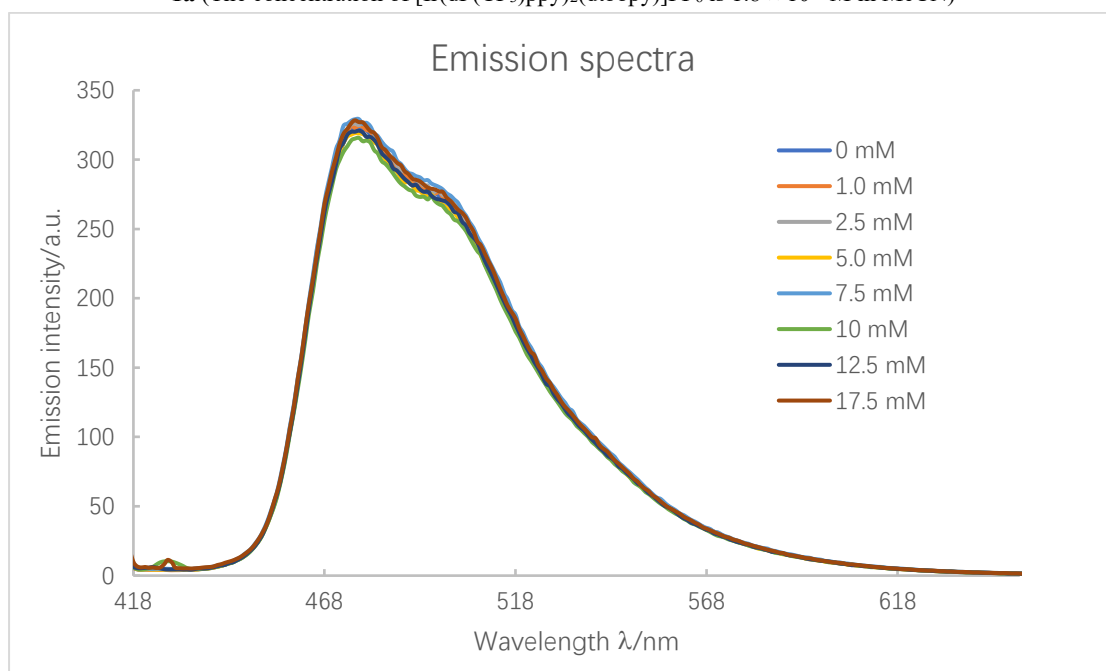


**Figure 2-S3** Emission spectra of  $[\text{Ir}(\text{dF}(\text{CF}_3)\text{ppy})_2(\text{dtbbpy})]\text{PF}_6$  with increasing concentrations of anhydride **2-2a** (The concentration of  $[\text{Ir}(\text{dF}(\text{CF}_3)\text{ppy})_2(\text{dtbbpy})]\text{PF}_6$  is  $1.8 \times 10^{-5}$  M in MeCN)

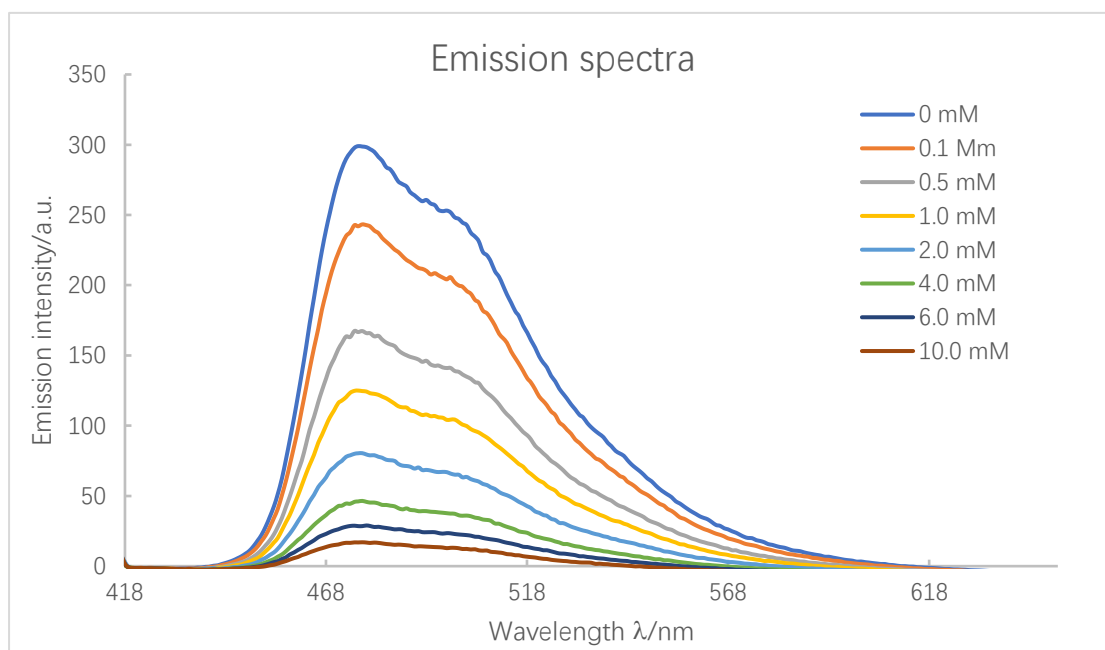


**Figure 2-S4** Emission spectra of  $[\text{Ir}(\text{dF}(\text{CF}_3)\text{ppy})_2(\text{dtbbpy})]\text{PF}_6$  with increasing concentrations of DABCO (The concentration of  $[\text{Ir}(\text{dF}(\text{CF}_3)\text{ppy})_2(\text{dtbbpy})]\text{PF}_6$  is  $1.8 \times 10^{-5}$  M in MeCN)

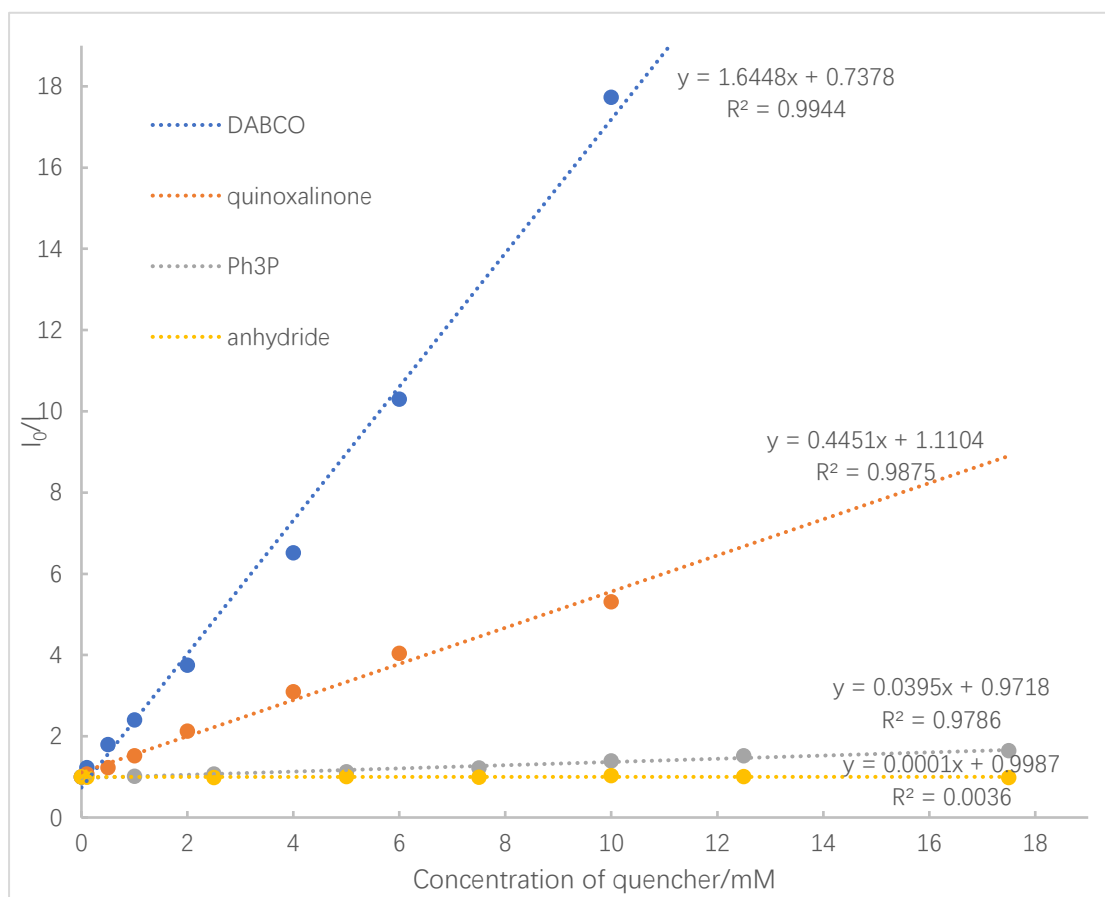
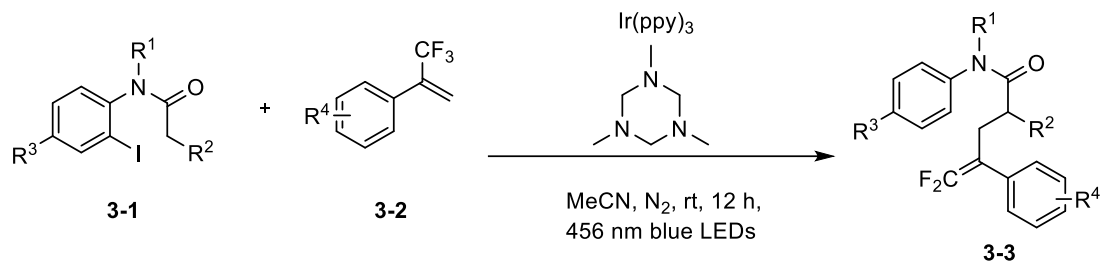


**Figure 2-S5** Stern-Volmer plot of  $[\text{Ir}(\text{dF}(\text{CF}_3)\text{ppy})_2(\text{dtbbpy})]\text{PF}_6$  with increasing concentrations of DABCO, quinoxalinone **2-1a**,  $\text{Ph}_3\text{P}$ , and anhydride **2-2a**

#### 4.2.3 Visible-light-mediated radical $\alpha$ -C(sp<sup>3</sup>)-H *gem*-difluoroallylation of amides with trifluoromethyl alkenes via halogen atom transfer and 1,5-hydrogen atom transfer

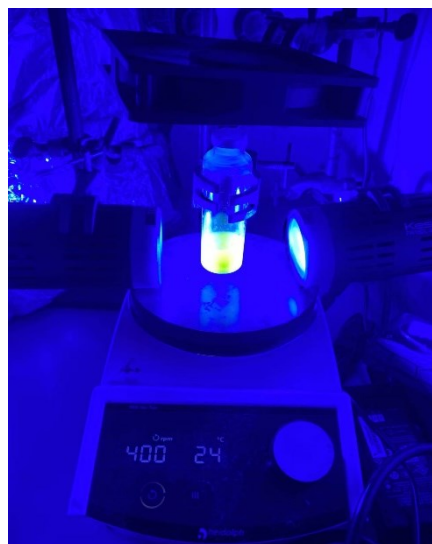
##### General procedure for $\alpha$ -C(sp<sup>3</sup>)-H *gem*-difluoroallylation of amides



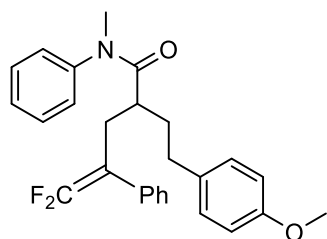
Procedure A: To a glass vial equipped with a stirring bar, amide **3-1** (0.15 mmol, 1 equiv.) and photocatalyst Ir(ppy)<sub>3</sub> (0.003 mmol, 2 mol%) were added, then the capped vial was evacuated and backfilled N<sub>2</sub> for three times. Next, trifluoromethyl arene **3-2** (0.3 mmol, 2 equiv.) was added, as well as triazinane (0.3 mmol, 2 equiv.) and anhydrous MeCN (1.5 mL). The reaction system was then irradiated by 456 nm blue LEDs (40W) at room temperature for 12 h. Thereafter, the crude product was purified by column chromatography using pentane/EA or pentane/EA/CH<sub>2</sub>Cl<sub>2</sub> as eluent to give target product **3-3**.

Procedure B: A glass vial with a stirring bar was charged with amide **3-1f** (0.15 mmol, 1 equiv.), trifluoromethyl arene **3-2** (0.45 mmol, 3 equiv.), Ir(ppy)<sub>3</sub> (0.003 mmol, 2 mol%) and 2.0 mL anhydrous MeCN. Then, the vial was sealed with an open-top screw cap fitted with a PTFE septum, and degassed by bubbling N<sub>2</sub> through the reaction solution for 3 min. After adding triazinane (0.3 mmol, 2 equiv.), the reaction system was exposed to 456 nm blue LEDs (40W) irradiation at room temperature for 12 h. The desired *gem*-difluoroalkene **3-3** could be obtained by column chromatography using pentane/EA as eluent.

Scale-up (1 mmol) procedure C: Amide **3-1** (1 mmol, 1 equiv.) and photocatalyst Ir(ppy)<sub>3</sub> (0.02 mmol, 2 mol%) were added to a glass vial equipped with a stirring bar, then the capped vial was evacuated and backfilled with N<sub>2</sub> for three times. Next, trifluoromethyl arene **3-2** (2 mmol, 2 equiv.) was added, as well as triazinane (2 mmol, 2 equiv.) and anhydrous MeCN (10 mL). The reaction system was then irradiated by 456 nm blue LEDs (40W) at room temperature for 24 h. Thereafter, the crude product was purified by column chromatography using pentane/EA as eluent to give target product **3-3**.



##### Product Characterization



### 5,5-Difluoro-2-(4-methoxyphenethyl)-*N*-methyl-*N*,4-diphenylpent-4-enamide (3-3aa)

Following procedure A, the crude mixture was purified by silica gel column chromatography with pentane/EA (6:1). 38 mg product was obtained, 58% isolated yield, as colorless liquid.

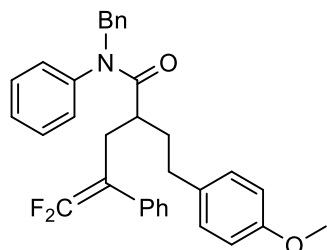
$^1\text{H}$  NMR (600 MHz, Chloroform-*d*)  $\delta$  7.20 – 7.09 (m, 6H), 6.89 (d,  $J$  = 7.2 Hz, 2H), 6.74 (d,  $J$  = 7.8 Hz, 2H), 6.68 (d,  $J$  = 7.8 Hz, 2H), 6.63 (d,  $J$  = 7.8 Hz, 2H), 3.70 (s, 3H), 3.13 (s, 3H), 2.61 – 2.56 (m, 1H), 2.49 – 2.45 (m, 1H), 2.44 – 2.33 (m, 2H), 2.27 – 2.23 (m, 1H), 1.85 – 1.80 (m, 1H), 1.58 – 1.47 (m, 1H).

$^{13}\text{C}$  NMR (151 MHz, Chloroform-*d*)  $\delta$  174.6, 157.8, 154.0 (dd,  $J$  = 291.3 Hz, 288.3 Hz), 143.4, 133.4, 132.8 (t,  $J$  = 4.1 Hz), 129.6, 129.1, 128.4, 128.1 (t,  $J$  = 3.2 Hz), 127.5, 127.3, 127.1, 113.7, 90.2 (dd,  $J$  = 21.4 Hz, 13.7 Hz), 55.3, 39.2 (t,  $J$  = 2.4 Hz), 37.5, 32.8, 32.1, 29.8.

$^{19}\text{F}$  NMR (565 MHz, Chloroform-*d*)  $\delta$  -89.12 (d,  $J$  = 39.2 Hz, 1F), -89.94 (d,  $J$  = 38.4 Hz, 1F).

HRMS (ESI-MS) Calcd. For  $\text{C}_{27}\text{H}_{27}\text{F}_2\text{NO}_2\text{Na}$   $[\text{M}+\text{Na}]^+$  458.1902, found: 458.1902.

IR (neat,  $\text{cm}^{-1}$ ):  $\tilde{\nu}$ : 3480, 2929, 2856, 2320, 2090, 1885, 1725, 1651, 1595, 1447, 1343, 1298, 1176, 1118, 1033, 951, 914, 827, 764, 699, 664.



### *N*-Benzyl-5,5-difluoro-2-(4-methoxyphenethyl)-*N*,4-diphenylpent-4-enamide (3-3ba)

Following procedure A, the crude mixture was purified by silica gel column chromatography with pentane/EA (15:1). 44 mg product was obtained by 57% isolated yield as colorless liquid.

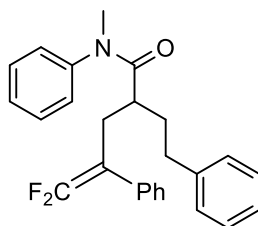
$^1\text{H}$  NMR (600 MHz, Chloroform-*d*)  $\delta$  7.18 – 7.14 (m, 3H), 7.13 – 7.03 (m, 6H), 6.99 (t,  $J$  = 7.8 Hz, 2H), 6.83 (d,  $J$  = 7.6 Hz, 2H), 6.69 (d,  $J$  = 8.4 Hz, 2H), 6.60 (d,  $J$  = 8.4 Hz, 2H), 6.40 (d,  $J$  = 7.8 Hz, 2H), 4.75 (d,  $J$  = 14.2 Hz, 1H), 4.72 (d,  $J$  = 14.1 Hz, 1H), 3.68 (s, 3H), 2.65 – 2.61 (m, 1H), 2.50 – 2.46 (m, 1H), 2.42 – 2.37 (m, 1H), 2.30 – 2.24 (m, 2H), 1.88 – 1.81 (m, 1H), 1.59 – 1.53 (m, 1H).

$^{13}\text{C}$  NMR (151 MHz, Chloroform-*d*)  $\delta$  174.3, 157.8, 154.0 (dd,  $J$  = 291.7, 288.7 Hz), 141.6, 137.6, 133.3, 132.6 (t,  $J$  = 3.9 Hz), 129.3, 129.1, 128.9, 128.5, 128.4, 128.3, 128.0 (t,  $J$  = 3.3 Hz), 127.6, 127.4, 127.1, 113.8, 90.2 (dd,  $J$  = 21.4, 13.6 Hz), 55.3, 53.1, 39.3, 32.7, 32.0, 29.6.

$^{19}\text{F}$  NMR (565 MHz, Chloroform-*d*)  $\delta$  -88.78 (d,  $J$  = 39.6 Hz, 1F), -89.88 (d,  $J$  = 40.1 Hz, 1F).

HRMS (ESI-MS) Calcd. For  $\text{C}_{33}\text{H}_{31}\text{F}_2\text{NO}_2\text{Na}$   $[\text{M}+\text{Na}]^+$  534.2215, found: 534.2210.

IR (neat,  $\text{cm}^{-1}$ ):  $\tilde{\nu}$ : 3060, 2928, 2325, 2081, 1886, 1725, 1651, 1595, 1446, 1298, 1240, 1177, 1074, 914, 823, 758, 698.



### 5,5-Difluoro-N-methyl-2-phenethyl-N,4-diphenylpent-4-enamide (3-3ca)

Following procedure A, the crude mixture was purified by silica gel column chromatography with pentane/EA (15:1). 33 mg product was obtained by 54% isolated yield as colorless liquid.

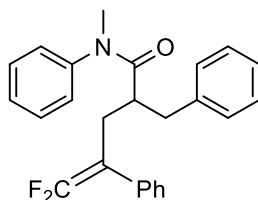
$^1\text{H}$  NMR (600 MHz, Chloroform-*d*)  $\delta$  7.17 – 7.04 (m, 9H), 6.88 (d,  $J$  = 7.8 Hz, 2H), 6.85 – 6.82 (m, 2H), 6.70 – 6.65 (m, 2H), 3.13 (s, 3H), 2.59 (ddt,  $J$  = 14.4, 6.6, 3.0 Hz, 1H), 2.52 – 2.44 (m, 2H), 2.41 – 2.27 (m, 2H), 1.91 – 1.83 (m, 1H), 1.60 – 1.53 (m, 1H).

$^{13}\text{C}$  NMR (151 MHz, Chloroform-*d*)  $\delta$  174.5, 154.0 (dd,  $J$  = 291.3, 288.3 Hz), 143.4, 141.3, 132.7 (t,  $J$  = 3.8 Hz), 129.6, 128.4, 128.3, 128.2, 128.1 (t,  $J$  = 3.3 Hz), 127.5, 127.3, 127.1, 125.8, 90.2 (dd,  $J$  = 21.4, 13.9 Hz), 39.2 (t,  $J$  = 2.4 Hz), 37.5, 33.0, 32.5, 29.9.

$^{19}\text{F}$  NMR (565 MHz, Chloroform-*d*)  $\delta$  -89.13 (d,  $J$  = 39.0 Hz, 1F), -89.92 (d,  $J$  = 39.0 Hz, 1F).

HRMS (ESI-MS) Calcd. For  $\text{C}_{26}\text{H}_{25}\text{F}_2\text{NONa}$   $[\text{M}+\text{Na}]^+$  428.1796, found: 428.1791.

IR (neat,  $\text{cm}^{-1}$ ):  $\tilde{\nu}$ : 3479, 3060, 2925, 2857, 2331, 2116, 1994, 1886, 1726, 1652, 1594, 1494, 1388, 1343, 1298, 1235, 1118, 1029, 950, 913, 842, 758, 698.



### 2-Benzyl-5,5-difluoro-N-methyl-N,4-diphenylpent-4-enamide (3-3da)

Following procedure A, the crude mixture was purified by silica gel column chromatography with pentane/EA (15:1). 36 mg product was obtained by 61% isolated yield as colorless liquid.

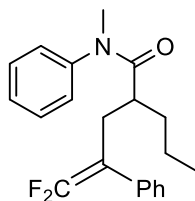
$^1\text{H}$  NMR (600 MHz, Chloroform-*d*)  $\delta$  7.18 – 7.07 (m, 7H), 7.02 – 6.95 (m, 4H), 6.74 – 6.69 (m, 2H), 6.24 (broad s, 2H), 3.01 (s, 3H), 2.87 – 2.77 (m, 1H), 2.68 – 2.61 (m, 1H), 2.56 – 2.44 (m, 3H).

$^{13}\text{C}$  NMR (151 MHz, Chloroform-*d*)  $\delta$  174.0, 154.1 (dd,  $J$  = 291.9, 288.7 Hz), 143.1, 139.5, 132.8 (t,  $J$  = 3.8 Hz), 129.3, 129.1, 128.4, 128.3, 128.0 (t,  $J$  = 3.5 Hz), 127.4, 127.2, 127.1, 126.3, 90.3 (dd,  $J$  = 21.3, 13.7 Hz), 42.7 (t,  $J$  = 2.6 Hz), 38.2, 37.2, 29.9.

$^{19}\text{F}$  NMR (565 MHz, Chloroform-*d*)  $\delta$  -88.82 (d,  $J$  = 37.9 Hz, 1F), -89.73 (d,  $J$  = 38.4 Hz, 1F).

HRMS (ESI-MS) Calcd. For  $\text{C}_{25}\text{H}_{23}\text{F}_2\text{NONa}$   $[\text{M}+\text{Na}]^+$  414.1640, found: 414.1636.

IR (neat,  $\text{cm}^{-1}$ ):  $\tilde{\nu}$ : 3475, 3060, 2924, 2857, 2329, 2109, 1949, 1807, 1726, 1652, 1594, 1494, 1447, 1389, 1340, 1297, 1236, 1118, 1022, 940, 915, 847, 760, 698.



### 5,5-Difluoro-N-methyl-N,4-diphenyl-2-propylpent-4-enamide (3-3ea)

Following procedure A, the crude mixture was purified by silica gel column chromatography with pentane/EA (20:1). 32 mg product was obtained by 62% isolated yield as colorless liquid.

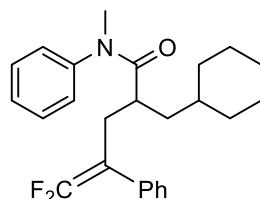
$^1\text{H}$  NMR (600 MHz, Chloroform-*d*)  $\delta$  7.19 – 7.11 (m, 6H), 7.01 (d,  $J$  = 7.8, 2H), 6.83 – 6.79 (m, 2H), 3.13 (s, 3H), 2.61 – 2.55 (m, 1H), 2.47 – 2.43 (m, 1H), 2.35 – 2.29 (m, 1H), 1.56 – 1.47 (m, 1H), 1.21 – 1.13 (m, 2H), 1.01 – 0.94 (m, 1H), 0.62 (t,  $J$  = 7.2 Hz, 3H).

$^{13}\text{C}$  NMR (151 MHz, Chloroform-*d*)  $\delta$  175.1, 154.0 (dd,  $J$  = 291.4, 288.4 Hz), 143.6, 133.1 (t,  $J$  = 4.1 Hz), 129.5, 128.4, 128.1 (t,  $J$  = 3.5 Hz), 127.5, 127.4, 127.1, 90.5 (dd,  $J$  = 21.3, 13.4 Hz), 39.8 (t,  $J$  = 2.6 Hz), 37.4, 34.2, 30.3, 20.4, 13.9.

$^{19}\text{F}$  NMR (565 MHz, Chloroform-*d*)  $\delta$  -89.20 (d,  $J$  = 38.4 Hz, 1F), -90.08 (d,  $J$  = 39.1 Hz, 1F).

HRMS (ESI-MS) Calcd. For  $\text{C}_{21}\text{H}_{23}\text{F}_2\text{NONa}$   $[\text{M}+\text{Na}]^+$  366.1640, found: 366.1635.

IR (neat,  $\text{cm}^{-1}$ ):  $\tilde{\nu}$ : 3484, 3060, 2958, 2869, 2332, 2108, 1885, 1726, 1653, 1594, 1495, 1388, 1340, 1301, 1234, 1118, 998, 765, 698.



### 2-(Cyclohexylmethyl)-5,5-difluoro-N-methyl-N,4-diphenylpent-4-enamide (3-3fa)

Following procedure A, the crude mixture was purified by silica gel column chromatography with pentane/EA (15:1). 40 mg product was obtained by 67% isolated yield as colorless liquid.

Following procedure C (1 mmol scale), the crude mixture was purified by silica gel column chromatography with pentane/EA (15:1). 214 mg product was obtained, 54% isolated yield.

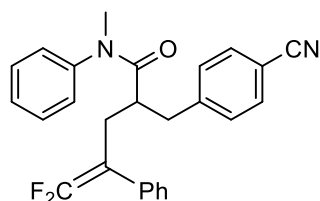
$^1\text{H}$  NMR (600 MHz, Chloroform-*d*)  $\delta$  7.18 – 7.11 (m, 6H), 7.00 (d,  $J$  = 7.8 Hz, 2H), 6.81 – 6.74 (m, 2H), 3.13 (s, 3H), 2.58 – 2.54 (m, 1H), 2.48 – 2.43 (m, 1H), 2.41 – 2.35 (m, 1H), 1.51 – 1.42 (m, 4H), 1.33 – 1.28 (m, 1H), 1.06 – 0.90 (m, 6H), 0.59 – 0.37 (m, 2H).

$^{13}\text{C}$  NMR (151 MHz, Chloroform-*d*)  $\delta$  175.4, 154.0 (dd,  $J$  = 290.8, 288.3 Hz), 143.5, 133.0 (t,  $J$  = 3.8 Hz), 129.4, 128.3, 128.2 (t,  $J$  = 3.3 Hz), 127.5, 127.3, 127.2, 90.6 (dd,  $J$  = 21.7, 14.0 Hz), 39.6, 37.5, 37.3 (t,  $J$  = 2.6 Hz), 35.3, 33.4, 33.1, 30.4, 26.4, 26.2, 26.1.

$^{19}\text{F}$  NMR (565 MHz, Chloroform-*d*)  $\delta$  -89.64 (d,  $J$  = 39.6 Hz, 1F), -90.40 (d,  $J$  = 40.1 Hz, 1F).

HRMS (ESI-MS) Calcd. For  $\text{C}_{25}\text{H}_{29}\text{F}_2\text{NONa}$   $[\text{M}+\text{Na}]^+$  420.2109, found: 420.2104.

IR (neat,  $\text{cm}^{-1}$ ):  $\tilde{\nu}$ : 3480, 3060, 2922, 2852, 2663, 2334, 2132, 1950, 1884, 1728, 1654, 1595, 1446, 1341, 1236, 1118, 1009, 941, 839, 764, 698, 665.



### 2-(4-Cyanobenzyl)-5,5-difluoro-N-methyl-N,4-diphenylpent-4-enamide (3-3ga)

Following procedure A, the crude mixture was purified by silica gel column chromatography with pentane/EA (4:1). 38 mg product was obtained by 60% isolated yield as white solid. Melting point: 89.2 – 90.5  $^{\circ}\text{C}$ .

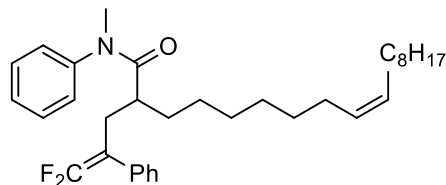
$^1\text{H}$  NMR (600 MHz, Chloroform-*d*)  $\delta$  7.40 (d,  $J$  = 8.2 Hz, 2H), 7.19 – 7.12 (m, 4H), 7.06 (t,  $J$  = 7.8 Hz, 2H), 6.97 – 6.92 (m, 2H), 6.81 (d,  $J$  = 7.8 Hz, 2H), 6.32 (broad s, 2H), 3.02 (s, 3H), 2.91 – 2.84 (m, 1H), 2.67 – 2.61 (m, 1H), 2.56 – 2.47 (m, 3H).

$^{13}\text{C}$  NMR (151 MHz, Chloroform-*d*)  $\delta$  173.2, 154.2 (dd,  $J$  = 292.3, 288.9 Hz), 145.4, 142.9, 132.4 (t,  $J$  = 3.6 Hz), 132.0, 129.8, 129.5, 128.5, 128.0 (t,  $J$  = 3.5 Hz), 127.8, 127.4, 127.0, 118.9, 110.2,

89.9 (dd,  $J = 21.1, 14.2$  Hz), 42.4 (t,  $J = 2.7$  Hz), 37.8, 37.3, 30.1.

$^{19}\text{F}$  NMR (565 MHz, Chloroform- $d$ )  $\delta$  -88.66 (d,  $J = 39.3$  Hz, 1F), -89.28 (d,  $J = 38.4$  Hz, 1F).  
HRMS (EI-MS) Calcd. For  $\text{C}_{26}\text{H}_{22}\text{F}_2\text{N}_2\text{O}$  416.1695, found: 416.1693.

IR (neat,  $\text{cm}^{-1}$ ):  $\tilde{\nu}$ : 3495, 3060, 2929, 2862, 2228, 1953, 1728, 1650, 1596, 1496, 1390, 1299, 1170, 1117, 1021, 941, 843, 699, 665.



### (Z)-2-(3,3-Difluoro-2-phenylallyl)-N-methyl-N-phenyloctadec-9-enamide (3-3ha)

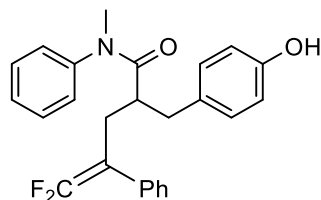
Following procedure A, the crude mixture was purified by silica gel column chromatography with pentane/EA (15:1). 54 mg product was obtained by 68% isolated yield as colorless liquid.

$^1\text{H}$  NMR (600 MHz, Chloroform- $d$ )  $\delta$  7.18 – 7.12 (m, 6H), 7.01 (d,  $J = 7.8$ , 2H), 6.83 – 6.77 (m, 2H), 5.31 – 5.22 (m, 2H), 3.13 (s, 3H), 2.62 – 2.54 (m, 1H), 2.48 – 2.42 (m, 1H), 2.34 – 2.27 (m, 1H), 1.95 – 1.87 (m, 4H), 1.54 – 1.48 (m, 1H), 1.26 – 1.09 (m, 18H), 1.01 – 0.93 (m, 3H), 0.81 (t,  $J = 6.6$  Hz, 3H).

$^{13}\text{C}$  NMR (151 MHz, Chloroform- $d$ )  $\delta$  175.0, 154.0 (dd,  $J = 291.6, 288.6$  Hz), 143.6, 133.1 (t,  $J = 4.1$  Hz), 130.0, 129.8, 129.5, 128.3, 128.1 (t,  $J = 3.5$  Hz), 127.5, 127.4, 127.1, 90.4 (dd,  $J = 21.6, 13.7$  Hz), 39.9 (t,  $J = 2.9$  Hz), 37.4, 31.9, 30.2, 29.8, 29.7, 29.5, 29.4, 29.34, 29.32, 29.1, 27.24, 27.19, 27.17, 22.7, 14.1.

$^{19}\text{F}$  NMR (565 MHz, Chloroform- $d$ )  $\delta$  -89.19 (d,  $J = 39.0$  Hz, 1F), -90.10 (d,  $J = 39.0$  Hz, 1F).  
HRMS (ESI-MS) Calcd. For  $\text{C}_{34}\text{H}_{47}\text{F}_2\text{NONa}$   $[\text{M}+\text{Na}]^+$  546.3518, found: 546.3510.

IR (neat,  $\text{cm}^{-1}$ ):  $\tilde{\nu}$ : 3458, 3004, 2924, 2854, 2322, 2092, 1991, 1657, 1595, 1451, 1387, 1300, 1236, 1119, 1023, 956, 844, 764, 698.



### 5,5-Difluoro-2-(4-hydroxybenzyl)-N-methyl-N,4-diphenylpent-4-enamide (3-3ia)

Following procedure A, the crude mixture was purified by silica gel column chromatography with pentane/EA (2:1). 25 mg product was obtained by 41% isolated yield as white solid. Single crystals were obtained via slow evaporation of  $\text{CH}_2\text{Cl}_2$ . Melting point: 165.9 – 167.2  $^\circ\text{C}$ .

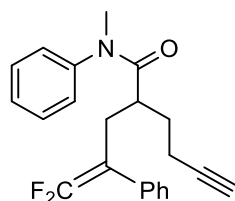
$^1\text{H}$  NMR (400 MHz, Chloroform- $d$ )  $\delta$  7.20 – 6.91 (m, 8H), 6.69 – 6.55 (m, AA'BB' 4 spin system, AA' and BB' parts, 4H), 6.31 (broad s, 2H), 3.02 (s, 3H), 2.76 (dd,  $J = 12.8, 8.0$  Hz, 1H), 2.67 – 2.60 (m, 1H), 2.57 – 2.38 (m, 3H).

$^{13}\text{C}$  NMR (101 MHz, Chloroform- $d$ )  $\delta$  174.5, 154.7, 154.1 (dd,  $J = 292.8, 292.7$  Hz), 143.0, 132.8 (t,  $J = 4.0$  Hz), 131.0, 130.1, 129.3, 128.4, 128.0 (t,  $J = 3.3$  Hz), 127.6, 127.2, 127.1, 115.2, 90.2 (dd,  $J = 21.4, 13.7$  Hz), 42.9 (t,  $J = 2.5$  Hz), 37.4, 37.3, 29.9.

$^{19}\text{F}$  NMR (565 MHz, Chloroform- $d$ )  $\delta$  -88.80 (d,  $J = 38.4$  Hz, 1F), -89.72 (d,  $J = 38.4$  Hz, 1F).  
HRMS (EI-MS) Calcd. For  $\text{C}_{25}\text{H}_{23}\text{F}_2\text{NO}_2$  407.1691, found: 407.1687.

IR (neat,  $\text{cm}^{-1}$ ):  $\tilde{\nu}$ : 3160, 2924, 2856, 2690, 2317, 2107, 1994, 1887, 1734, 1588, 1510, 1449, 1376, 1233, 1120, 1023, 940, 831, 758, 696.





### 2-(3,3-Difluoro-2-phenylallyl)-N-methyl-N-phenylhex-5-ynamide (3-3ja)

Following procedure A, the crude mixture was purified by silica gel column chromatography with pentane/EA (15:1). 34 mg product was obtained by 64% isolated yield as colorless liquid.

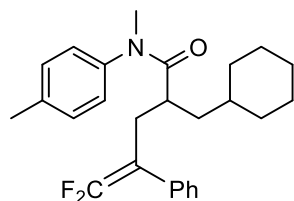
$^1\text{H}$  NMR (600 MHz, Chloroform-*d*)  $\delta$  7.19 – 7.10 (m, 6H), 6.99 – 6.85 (m, 4H), 3.13 (s, 3H), 2.60 – 2.50 (m, 2H), 2.48 – 2.44 (m, 1H), 2.09 – 2.04 (m, 1H), 1.99 – 1.89 (m, 1H), 1.86 – 1.77 (m, 1H), 1.63 – 1.60 (m, 1H), 1.46 – 1.41 (m, 1H).

$^{13}\text{C}$  NMR (151 MHz, Chloroform-*d*)  $\delta$  174.1, 154.1 (dd,  $J = 291.3, 288.3$  Hz), 143.2, 132.7 (t,  $J = 3.8$  Hz), 129.6, 128.3, 128.1 (t,  $J = 3.2$  Hz), 127.6, 127.4, 127.2, 90.1 (dd,  $J = 21.3, 14.3$  Hz), 83.4, 68.8, 38.9 (t,  $J = 2.4$  Hz), 37.6, 30.1, 30.0, 16.3.

$^{19}\text{F}$  NMR (565 MHz, Chloroform-*d*)  $\delta$  -89.24 (d,  $J = 39.0$  Hz, 1F), -89.74 (d,  $J = 39.6$  Hz, 1F).

HRMS (ESI-MS) Calcd. For  $\text{C}_{22}\text{H}_{21}\text{F}_2\text{NONa}$   $[\text{M}+\text{Na}]^+$  376.1483, found: 376.1479.

IR (neat,  $\text{cm}^{-1}$ ):  $\tilde{\nu}$ : 3478, 3301, 3060, 2930, 2859, 2324, 2114, 1991, 1895, 1726, 1650, 1495, 1444, 1390, 1343, 1235, 1119, 1030, 955, 766, 698.



### 2-(Cyclohexylmethyl)-5,5-difluoro-N-methyl-4-phenyl-N-(p-tolyl)pent-4-enamide (3-3ka)

Following procedure A, the crude mixture was purified by silica gel column chromatography with pentane/EA (15:1). 38 mg product was obtained by 61% isolated yield as colorless liquid.

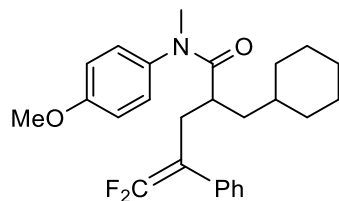
$^1\text{H}$  NMR (600 MHz, Chloroform-*d*)  $\delta$  7.18 – 7.12 (m, 3H), 7.00 – 6.95 (m, 2H), 6.93 (d,  $J = 7.8$  Hz, 2H), 6.67 (d,  $J = 7.4$  Hz, 2H), 3.10 (s, 3H), 2.56 – 2.35 (m, 3H), 2.25 (s, 3H), 1.54 – 1.41 (m, 4H), 1.34 (d,  $J = 13.2$  Hz, 1H), 1.09 – 0.92 (m, 6H), 0.62 – 0.56 (m, 1H), 0.45 – 0.39 (m, 1H).

$^{13}\text{C}$  NMR (151 MHz, Chloroform-*d*)  $\delta$  175.5, 154.0 (dd,  $J = 290.7, 288.3$  Hz), 140.9, 137.4, 133.0 (t,  $J = 3.6$  Hz), 130.0, 128.3 (t,  $J = 3.0$  Hz), 128.2, 127.1, 127.0, 90.6 (dd,  $J = 21.3, 14.0$  Hz), 39.4, 37.5, 37.3 (t,  $J = 2.6$  Hz), 35.4, 33.6, 33.1, 30.5, 26.5, 26.2, 26.1, 21.0.

$^{19}\text{F}$  NMR (565 MHz, Chloroform-*d*)  $\delta$  -89.83 (d,  $J = 39.0$  Hz, 1F), -90.45 (d,  $J = 40.1$  Hz, 1F).

HRMS (ESI-MS) Calcd. For  $\text{C}_{26}\text{H}_{31}\text{F}_2\text{NONa}$   $[\text{M}+\text{Na}]^+$  434.2266, found: 434.2261.

IR (neat,  $\text{cm}^{-1}$ ):  $\tilde{\nu}$ : 3480, 3031, 2922, 2851, 2664, 2324, 2075, 2007, 1902, 1728, 1654, 1512, 1445, 1386, 1235, 1117, 1012, 941, 825, 759, 697.



### 2-(Cyclohexylmethyl)-5,5-difluoro-N-(4-methoxyphenyl)-N-methyl-4-phenylpent-4-enamide (3-3la)

Following procedure A, the crude mixture was purified by silica gel column chromatography with

pentane/EA (10:1). 26 mg product was obtained by 40% isolated yield as colorless liquid.

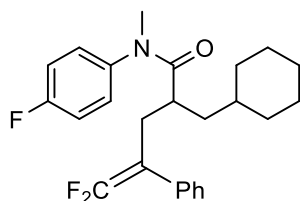
$^1\text{H}$  NMR (600 MHz, Chloroform-*d*)  $\delta$  7.21 – 7.13 (m, 3H), 6.99 (d,  $J$  = 7.8 Hz, 2H), 6.74 – 6.60 (m, 4H), 3.71 (s, 3H), 3.09 (s, 3H), 2.55 – 2.50 (m, 1H), 2.46 – 2.42 (m, 1H), 2.40 – 2.36 (m, 1H), 1.52 – 1.46 (m, 4H), 1.37 – 1.30 (m, 1H), 1.08 – 0.91 (m, 6H), 0.62 – 0.56 (m, 1H), 0.49 – 0.40 (m, 1H).

$^{13}\text{C}$  NMR (151 MHz, Chloroform-*d*)  $\delta$  175.7, 158.7, 154.0 (dd,  $J$  = 290.8, 288.6 Hz), 136.3, 133.1 (t,  $J$  = 3.8 Hz), 128.29, 128.25, 127.1, 114.5, 90.6 (dd,  $J$  = 21.4, 14.0 Hz), 55.5, 39.5, 37.6, 37.2 (t,  $J$  = 2.6 Hz), 35.4, 33.6, 33.1, 30.5, 26.5, 26.2, 26.1.

$^{19}\text{F}$  NMR (565 MHz, Chloroform-*d*)  $\delta$  -89.70 (d,  $J$  = 40.1 Hz, 1F), -90.39 (d,  $J$  = 40.1 Hz, 1F).

HRMS (ESI-MS) Calcd. For  $\text{C}_{26}\text{H}_{31}\text{F}_2\text{NO}_2\text{Na}$   $[\text{M}+\text{Na}]^+$  450.2215, found: 450.2202.

IR (neat,  $\text{cm}^{-1}$ ):  $\tilde{\nu}$ : 3465, 2922, 2850, 2324, 2083, 1886, 1728, 1651, 1509, 1387, 1343, 1296, 1241, 1169, 1116, 1034, 941, 837, 760, 698.



### 2-(Cyclohexylmethyl)-5,5-difluoro-*N*-(4-fluorophenyl)-*N*-methyl-4-phenylpent-4-enamide (3ma)

Following procedure A, the crude mixture was purified by silica gel column chromatography with pentane/EA (15:1). 24 mg product was obtained by 38% isolated yield as colorless liquid.

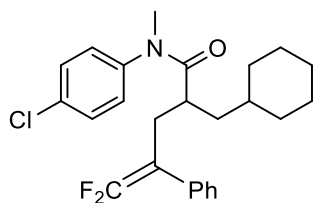
$^1\text{H}$  NMR (400 MHz, Chloroform-*d*)  $\delta$  7.25 – 7.16 (m, 3H), 7.06 – 6.98 (m, 2H), 6.79 (t,  $J$  = 8.4 Hz, 2H), 6.70 (t,  $J$  = 6.8 Hz, 2H), 3.09 (s, 3H), 2.57 – 2.50 (m, 1H), 2.48 – 2.42 (m, 1H), 2.38 – 2.28 (m, 1H), 1.55 – 1.43 (m, 4H), 1.33 – 1.26 (m, 1H), 1.12 – 0.94 (m, 6H), 0.63 – 0.41 (m, 2H).

$^{13}\text{C}$  NMR (101 MHz, Chloroform-*d*)  $\delta$  175.4, 161.5 (dd,  $J$  = 248.6 Hz), 154.0 (dd,  $J$  = 291.6, 289.2 Hz), 139.5 (d,  $J$  = 3.2 Hz), 133.0 (t,  $J$  = 3.7 Hz), 128.9 (d,  $J$  = 8.7 Hz), 128.4, 128.2 (t,  $J$  = 3.2 Hz), 127.3, 116.3 (d,  $J$  = 22.7 Hz), 90.5 (dd,  $J$  = 32.2, 14.2 Hz), 39.6, 37.6, 37.3 (t,  $J$  = 2.5 Hz), 35.3, 33.4, 33.2, 30.4 (d,  $J$  = 1.8 Hz), 26.4, 26.2, 26.1.

$^{19}\text{F}$  NMR (565 MHz, Chloroform-*d*)  $\delta$  -89.62 (d,  $J$  = 39.6 Hz, 1F), -90.21 (d,  $J$  = 39.0 Hz, 1F), -113.74 (tt,  $J$  = 8.8, 5.0 Hz, 1F).

HRMS (ESI-MS) Calcd. For  $\text{C}_{25}\text{H}_{28}\text{F}_3\text{NONa}$   $[\text{M}+\text{Na}]^+$  438.2015, found: 438.2012.

IR (neat,  $\text{cm}^{-1}$ ):  $\tilde{\nu}$ : 3483, 3059, 2923, 2851, 2329, 1893, 1729, 1655, 1506, 1446, 1387, 1302, 1231, 1118, 1011, 941, 843, 760, 689.



### *N*-(4-Chlorophenyl)-2-(cyclohexylmethyl)-5,5-difluoro-*N*-methyl-4-phenylpent-4-enamide (3na)

Following procedure A, the crude mixture was purified by silica gel column chromatography with pentane/EA (15:1). 26 mg product was obtained by 40% isolated yield as colorless liquid.

$^1\text{H}$  NMR (600 MHz, Chloroform-*d*)  $\delta$  7.23 – 7.17 (m, 3H), 7.08 (d,  $J$  = 8.4 Hz, 2H), 7.01 – 6.96 (m, 2H), 6.67 (d,  $J$  = 7.8 Hz, 2H), 3.09 (s, 3H), 2.53 – 2.49 (m, 1H), 2.47 – 2.43 (m, 1H), 2.35 – 2.31 (m, 1H), 1.54 – 1.44 (m, 4H), 1.35 – 1.29 (m, 1H), 1.11 – 0.94 (m, 6H), 0.58 (qd,  $J$  = 12.3, 2.9 Hz,

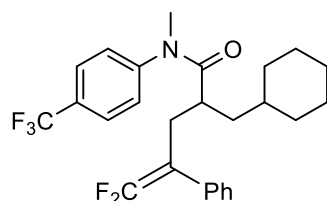
1H), 0.48 (qd,  $J = 12.2, 3.7$  Hz, 1H).

$^{13}\text{C}$  NMR (101 MHz, Chloroform- $d$ )  $\delta$  175.2, 154.0 (dd,  $J = 291.5, 289.5$  Hz), 142.0, 133.3, 132.9 (t,  $J = 4.0$  Hz), 129.6, 128.6, 128.4, 128.2 (t,  $J = 3.2$  Hz), 127.4, 90.4 (dd,  $J = 21.3, 14.3$  Hz), 39.5, 37.5, 37.4 (t,  $J = 2.5$  Hz), 35.4, 33.5, 33.2, 30.4 (d,  $J = 1.8$  Hz), 26.4, 26.2, 26.1.

$^{19}\text{F}$  NMR (565 MHz, Chloroform- $d$ )  $\delta$  -89.74 (d,  $J = 39.6$  Hz, 1F), -90.18 (d,  $J = 39.6$  Hz, 1F).

HRMS (ESI-MS) Calcd. For  $\text{C}_{25}\text{H}_{28}\text{F}_2\text{NOCINa}$   $[\text{M}+\text{Na}]^+$  454.1720, found: 454.1716.

IR (neat,  $\text{cm}^{-1}$ ):  $\tilde{\nu}$ : 3482, 3059, 2922, 2851, 2664, 2325, 2060, 1901, 1729, 1656, 1490, 1339, 1303, 1278, 1164, 1095, 1012, 942, 837, 759, 720, 698.



### 2-(Cyclohexylmethyl)-5,5-difluoro-N-methyl-4-phenyl-N-(4-(trifluoromethyl)phenyl)pent-4-enamide (3-30a)

Following procedure A, the crude mixture was purified by silica gel column chromatography with pentane/EA (15:1). 23 mg product was obtained by 32% isolated yield as colorless liquid.

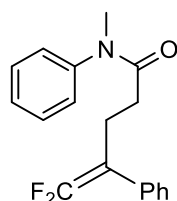
$^1\text{H}$  NMR (600 MHz, Chloroform- $d$ )  $\delta$  7.35 (d,  $J = 7.8$  Hz, 2H), 7.21 – 7.16 (m, 3H), 7.02 – 6.96 (m, 2H), 6.84 (d,  $J = 7.8$  Hz, 2H), 3.13 (s, 3H), 2.57 – 2.43 (m, 2H), 2.34 – 2.27 (m, 1H), 1.53 – 1.43 (m, 4H), 1.29 (d,  $J = 12.6$  Hz, 1H), 1.13 – 0.95 (m, 6H), 0.60 – 0.44 (m, 2H).

$^{13}\text{C}$  NMR (151 MHz, Chloroform- $d$ )  $\delta$  175.1, 154.0 (dd,  $J = 290.5, 288.7$  Hz), 146.6, 132.9 (dd,  $J = 3.2, 2.1$  Hz), 129.6 (q,  $J = 32.9$  Hz), 128.5, 128.2 (t,  $J = 3.3$  Hz), 127.6, 127.5, 126.6 (q,  $J = 3.9$  Hz), 123.6 (q,  $J = 272.4$  Hz), 90.3 (dd,  $J = 21.7, 15.1$  Hz), 39.7, 37.4 (t,  $J = 2.7$  Hz), 37.3, 35.4, 33.4, 33.2, 30.5, 26.4, 26.14, 26.10.

$^{19}\text{F}$  NMR (565 MHz, Chloroform- $d$ )  $\delta$  -62.63 (s, 3F), -89.82 (d,  $J = 40.1$  Hz, 1F), -90.11 (d,  $J = 39.6$  Hz, 1F).

HRMS (ESI-MS) Calcd. For  $\text{C}_{26}\text{H}_{28}\text{F}_5\text{NONa}$   $[\text{M}+\text{Na}]^+$  488.1983, found: 488.1972.

IR (neat,  $\text{cm}^{-1}$ ):  $\tilde{\nu}$ : 3061, 2924, 2852, 2658, 2323, 2094, 2011, 1949, 1731, 1661, 1612, 1447, 1389, 1324, 1239, 1123, 1068, 1013, 942, 850, 759, 728, 700.



### 5,5-Difluoro-N-methyl-N,4-diphenylpent-4-enamide (3-3pa)

Following procedure A, the crude mixture was purified by silica gel column chromatography with pentane/EA (15:1). 10 mg product was obtained by 22% isolated yield as colorless liquid.

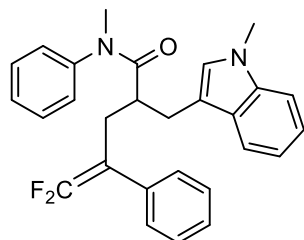
$^1\text{H}$  NMR (600 MHz, Chloroform- $d$ )  $\delta$  7.26 (t,  $J = 7.3$  Hz, 2H), 7.24 – 7.17 (m, 3H), 7.15 (t,  $J = 7.2$  Hz, 1H), 7.09 (d,  $J = 7.7$  Hz, 2H), 6.95 (d,  $J = 7.5$  Hz, 2H), 3.15 (s, 3H), 2.62 (t,  $J = 7.9$  Hz, 2H), 2.05 (t,  $J = 7.9$  Hz, 2H).

$^{13}\text{C}$  NMR (151 MHz, Chloroform- $d$ )  $\delta$  171.8, 153.5 (dd,  $J = 290.8, 287.8$  Hz), 143.8, 132.9 (t,  $J = 3.9$  Hz), 129.7, 128.4, 128.1 (t,  $J = 3.6$  Hz), 127.8, 127.3, 127.2, 91.4 (dd,  $J = 21.3, 13.9$  Hz), 37.3, 32.3 (t,  $J = 2.9$  Hz), 23.7.

$^{19}\text{F}$  NMR (376 MHz, Chloroform- $d$ )  $\delta$  -90.25 (d,  $J = 41.0$  Hz, 1F), -90.60 (d,  $J = 41.0$  Hz, 1F).

HRMS (ESI-MS) Calcd. For  $C_{18}H_{17}F_2NONa$   $[M+Na]^+$  324.1170, found: 324.1170.

IR (neat,  $cm^{-1}$ ):  $\tilde{\nu}$ : 3482, 3059, 2927, 2323, 1952, 1729, 1655, 1495, 1384, 1233, 1118, 1022, 917, 764, 698.



**5,5-Difluoro-N-methyl-2-((1-methyl-1H-indol-3-yl)methyl)-N,4-diphenylpent-4-enamide (3-3ra)**

Following procedure A, the crude mixture was purified by silica gel column chromatography with pentane/EA (4:1). 26 mg product was obtained by 39% isolated yield as white solid. Melting point: 127.3 -128.4 °C.

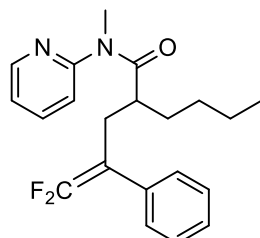
$^1H$  NMR (600 MHz, Chloroform-*d*)  $\delta$  7.15 – 7.02 (m, 6H), 6.90 (d,  $J$  = 8.0 Hz, 2H), 6.85 (t,  $J$  = 7.7 Hz, 2H), 6.71 (t,  $J$  = 7.4 Hz, 1H), 6.61 (s, 1H), 6.34 (d,  $J$  = 7.9 Hz, 1H), 6.18 (broad s, 2H), 3.60 (s, 3H), 3.00 (s, 3H), 2.92 (dd,  $J$  = 13.9, 8.7 Hz, 1H), 2.78 (quint,  $J$  = 7.2 Hz, 1H), 2.69 – 2.61 (m, 2H), 2.50 (broad dd,  $J$  = 14.7, 7.7 Hz, 1H).

$^{13}C$  NMR (151 MHz, Chloroform-*d*)  $\delta$  174.8, 154.0 (dd,  $J$  = 291.7, 288.3 Hz), 143.2, 137.0, 132.7 (t,  $J$  = 4.1 Hz), 129.2, 128.4, 128.1 (t,  $J$  = 3.5 Hz), 127.7, 127.4, 127.18, 127.16, 127.1, 121.4, 119.0, 118.5, 111.8, 108.9, 90.4 (dd,  $J$  = 21.0, 13.0 Hz), 41.0, 37.3, 32.5, 29.5, 27.7.

$^{19}F$  NMR (565 MHz, Chloroform-*d*)  $\delta$  -88.90 (d,  $J$  = 39.0 Hz, 1F), -89.95 (d,  $J$  = 39.0 Hz, 1F).

HRMS (ESI-MS) Calcd. For  $C_{28}H_{26}F_2N_2ONa$   $[M+Na]^+$  467.1905, found: 467.1903.

IR (neat,  $cm^{-1}$ ):  $\tilde{\nu}$ : 3379, 3059, 2923, 2853, 2320, 2115, 1983, 1890, 1726, 1652, 1473, 1444, 1377, 1325, 1231, 1119, 1012, 933, 868, 738, 699.



**2-(3,3-Difluoro-2-phenylallyl)-N-methyl-N-(pyridin-2-yl)hexanamide (3-3sa)**

Following procedure A, the crude mixture was purified by silica gel column chromatography with pentane/EA (3:1). 22 mg product was obtained by 41% isolated yield as yellow liquid.

$^1H$  NMR (600 MHz, Chloroform-*d*)  $\delta$  8.28 (dd,  $J$  = 5.4, 1.8 Hz, 1H), 7.45 (t,  $J$  = 7.9 Hz, 1H), 7.23 – 7.04 (m, 5H), 7.02 (dd,  $J$  = 7.5, 4.9 Hz, 1H), 6.71 (broad s, 1H), 3.17 (s, 3H), 2.70 (d,  $J$  = 11.1 Hz, 1H), 2.50 (dd,  $J$  = 13.4, 7.2 Hz, 1H), 2.39 (broad s, 1H), 1.65 – 1.56 (m, 1H), 1.28 (broad s, 1H), 1.15 – 0.92 (m, 4H), 0.72 (t,  $J$  = 7.2 Hz, 3H).

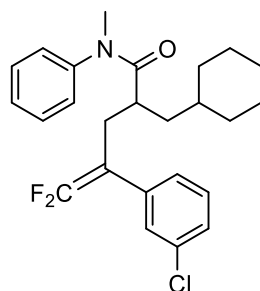
$^{13}C$  NMR (151 MHz, Chloroform-*d*)  $\delta$  175.5, 156.1, 154.0 (dd,  $J$  = 290.8, 288.3 Hz), 149.1, 138.0, 133.2 (t,  $J$  = 3.9 Hz), 128.3, 128.2 (t,  $J$  = 3.5 Hz), 127.2, 121.9, 120.9, 90.5 (dd,  $J$  = 21.7, 14.0 Hz), 40.8, 35.5, 31.7, 30.5, 29.3, 22.6, 13.8.

$^{19}F$  NMR (376 MHz, Chloroform-*d*)  $\delta$  -89.69 (d,  $J$  = 39.6 Hz, 1F), -90.33 (d,  $J$  = 39.9 Hz, 1F).

HRMS (EI-MS): Calcd. For  $C_{21}H_{23}F_2N_2O$   $[M-H]^+$  357.1773, found 357.1772.

IR (neat,  $cm^{-1}$ ):  $\tilde{\nu}$ : 3304, 3060, 2929, 2862, 2322, 2113, 1986, 1727, 1654, 1583, 1465, 1339, 1230,

1127, 1011, 937, 847, 792, 754.



**4-(3-Chlorophenyl)-2-(cyclohexylmethyl)-5,5-difluoro-N-methyl-N-phenylpent-4-enamide (3-3fb)**

Following procedure B, the crude mixture was purified by silica gel column chromatography with pentane/EA (15:1). 36 mg product was obtained by 55% isolated yield as white solid. Melting point: 60.7 – 61.8 °C.

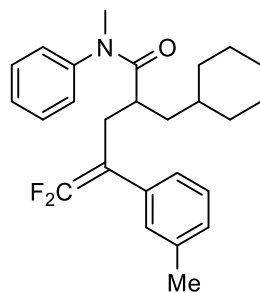
$^1\text{H}$  NMR (600 MHz, Chloroform-*d*)  $\delta$  7.19 – 7.12 (m, 4H), 7.10 (t,  $J$  = 7.7 Hz, 1H), 7.04 (s, 1H), 6.89 (d,  $J$  = 7.8 Hz, 1H), 6.80 (d,  $J$  = 6.6 Hz, 2H), 3.13 (s, 3H), 2.57 – 2.51 (m, 1H), 2.46 – 2.40 (m, 1H), 2.38 – 2.30 (m, 1H), 1.53 – 1.44 (m, 4H), 1.29 (d,  $J$  = 11.4 Hz, 1H), 1.10 – 0.93 (m, 6H), 0.56 (qd,  $J$  = 12.5, 3.1 Hz, 1H), 0.47 (qd,  $J$  = 12.0, 3.6 Hz, 1H).

$^{13}\text{C}$  NMR (151 MHz, Chloroform-*d*)  $\delta$  175.2, 154.1 (dd,  $J$  = 291.7, 289.3 Hz), 143.4, 135.0 (t,  $J$  = 3.8 Hz), 134.2, 129.6, 129.5, 128.3 (t,  $J$  = 3.2 Hz), 127.7, 127.4, 127.2, 126.4 (t,  $J$  = 3.2 Hz), 89.9 (dd,  $J$  = 22.5, 13.9 Hz), 39.7, 37.5, 37.3 (t,  $J$  = 2.9 Hz), 35.3, 33.4, 33.2, 30.3, 26.4, 26.2, 26.1.

$^{19}\text{F}$  NMR (565 MHz, Chloroform-*d*)  $\delta$  -88.38 (d,  $J$  = 36.2 Hz, 1F), -88.90 (d,  $J$  = 37.3 Hz, 1F).

HRMS (ESI-MS) Calcd. For  $\text{C}_{25}\text{H}_{28}\text{F}_2\text{NOCINa}$   $[\text{M}+\text{Na}]^+$  454.1720, found: 454.1726.

IR (neat,  $\text{cm}^{-1}$ ):  $\tilde{\nu}$ : 3062, 2922, 2853, 2314, 2102, 1966, 1733, 1640, 1594, 1448, 1342, 1239, 1122, 1025, 896, 775, 700.



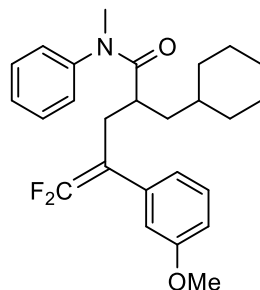
**2-(Cyclohexylmethyl)-5,5-difluoro-N-methyl-N-phenyl-4-(*m*-tolyl)pent-4-enamide (3-3fc)**

Following procedure B, the crude mixture was purified by silica gel column chromatography with pentane/EA (15:1). 37 mg product was obtained by 60% isolated yield as colorless liquid.

$^1\text{H}$  NMR (600 MHz, Chloroform-*d*)  $\delta$  7.15 – 7.09 (m, 3H), 7.07 (t,  $J$  = 7.8 Hz, 1H), 6.97 (d,  $J$  = 7.8 Hz, 1H), 6.84 (s, 1H), 6.81 (d,  $J$  = 7.8 Hz, 1H), 6.75 (d,  $J$  = 7.2 Hz, 2H), 3.12 (s, 3H), 2.59 – 2.53 (m, 1H), 2.46 – 2.35 (m, 2H), 2.22 (s, 3H), 1.53 – 1.41 (m, 4H), 1.27 (d,  $J$  = 13.0 Hz, 1H), 1.12 – 0.95 (m, 6H), 0.58 – 0.41 (m, 2H).

$^{13}\text{C}$  NMR (151 MHz, Chloroform-*d*)  $\delta$  175.5, 153.9 (dd,  $J$  = 289.8, 288.6 Hz), 143.5, 137.8, 133.1 (t,  $J$  = 3.6 Hz), 129.3, 128.9 (t,  $J$  = 3.2 Hz), 128.3, 128.0, 127.5, 127.2, 125.3 (t,  $J$  = 3.2 Hz), 90.6 (dd,  $J$  = 21.1, 14.3 Hz), 39.7, 37.5, 37.3 (t,  $J$  = 2.7 Hz), 35.3, 33.3, 33.2, 30.5, 26.5, 26.21, 26.16, 21.4.

$^{19}\text{F}$  NMR (565 MHz, Chloroform-*d*)  $\delta$  -89.95 (d,  $J$  = 40.7 Hz, 1F), -90.37 (d,  $J$  = 40.1 Hz, 1F). HRMS (ESI-MS) Calcd. For  $\text{C}_{26}\text{H}_{31}\text{F}_2\text{NONa}$   $[\text{M}+\text{Na}]^+$  434.2266, found: 434.2262. IR (neat,  $\text{cm}^{-1}$ ):  $\tilde{\nu}$ : 3481, 2922, 2851, 2322, 2114, 1883, 1728, 1654, 1595, 1494, 1388, 1242, 1118, 1027, 959, 838, 782, 700.



**2-(Cyclohexylmethyl)-5,5-difluoro-4-(3-methoxyphenyl)-N-methyl-N-phenylpent-4-enamide (3-3fd)**

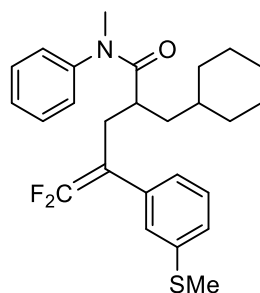
Following procedure B, the crude mixture was purified by silica gel column chromatography with pentane/EA (15:1). 41 mg product was obtained by 64% isolated yield as colorless liquid.

$^1\text{H}$  NMR (600 MHz, Chloroform-*d*)  $\delta$  7.16 – 7.05 (m, 4H), 6.80 – 6.70 (m, 3H), 6.63 – 6.57 (m, 2H), 3.70 (s, 3H), 3.13 (s, 3H), 2.59 – 2.52 (m, 1H), 2.47 – 2.36 (m, 2H), 1.53 – 1.43 (m, 4H), 1.30 (d,  $J$  = 13.2 Hz, 1H), 1.11 – 0.95 (m, 6H), 0.59 – 0.42 (m, 2H).

$^{13}\text{C}$  NMR (151 MHz, Chloroform-*d*)  $\delta$  175.5, 159.5, 154.0 (dd,  $J$  = 291.3, 288.7 Hz), 143.5, 134.5 (t,  $J$  = 3.5 Hz), 129.4, 129.3, 127.5, 127.2, 120.7 (t,  $J$  = 3.0 Hz), 114.0 (t,  $J$  = 3.3 Hz), 112.9, 90.6 (dd,  $J$  = 21.3, 14.0 Hz), 55.2, 39.8, 37.5, 37.4 (t,  $J$  = 2.4 Hz), 35.3, 33.4, 33.2, 30.6, 26.4, 26.2, 26.1.

$^{19}\text{F}$  NMR (565 MHz, Chloroform-*d*)  $\delta$  -89.44 (d,  $J$  = 39.6 Hz, 1F), -89.63 (d,  $J$  = 39.6 Hz, 1F). HRMS (ESI-MS) Calcd. For  $\text{C}_{26}\text{H}_{31}\text{F}_2\text{NO}_2\text{Na}$   $[\text{M}+\text{Na}]^+$  450.2215, found: 450.2219.

IR (neat,  $\text{cm}^{-1}$ ):  $\tilde{\nu}$ : 3062, 2922, 2850, 2323, 2082, 1950, 1729, 1654, 1594, 1493, 1388, 1284, 1117, 1019, 960, 836, 774, 699.



**2-(Cyclohexylmethyl)-5,5-difluoro-N-methyl-4-(3-(methylthio)phenyl)-N-phenylpent-4-enamide (3-3fe)**

Following procedure B, the crude mixture was purified by silica gel column chromatography with pentane/EA (15:1). 35 mg product was obtained by 52% isolated yield as colorless liquid.

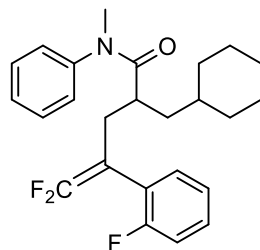
$^1\text{H}$  NMR (600 MHz, Chloroform-*d*)  $\delta$  7.17 – 7.05 (m, 5H), 6.95 (s, 1H), 6.80 – 6.72 (m, 3H), 3.13 (s, 3H), 2.59 – 2.52 (m, 1H), 2.46 – 2.34 (m, 2H), 2.38 (s, 3H), 1.53 – 1.44 (m, 4H), 1.28 (d,  $J$  = 13.3 Hz, 1H), 1.11 – 0.95 (m, 6H), 0.59 – 0.43 (m, 2H).

$^{13}\text{C}$  NMR (151 MHz, Chloroform-*d*)  $\delta$  175.4, 154.0 (dd,  $J$  = 290.7, 289.0 Hz), 143.4, 138.7, 133.9 (t,  $J$  = 3.9 Hz), 129.4, 128.7, 127.6, 127.2, 126.4 (t,  $J$  = 3.3 Hz), 125.6, 125.0 (t,  $J$  = 3.2 Hz), 90.4 (dd,  $J$  = 21.7, 13.9 Hz), 39.9, 37.5, 37.3 (t,  $J$  = 3.0 Hz), 35.3, 33.32, 33.29, 30.5, 26.4, 26.2, 26.1,

15.8.

$^{19}\text{F}$  NMR (565 MHz, Chloroform-*d*)  $\delta$  -89.14 (d,  $J$  = 38.4 Hz, 1F), -89.50 (d,  $J$  = 39.0 Hz, 1F).  
HRMS (ESI-MS) Calcd. For  $\text{C}_{26}\text{H}_{31}\text{F}_2\text{NOSNa}$   $[\text{M}+\text{Na}]^+$  466.1987, found: 466.1991.

IR (neat,  $\text{cm}^{-1}$ ):  $\tilde{\nu}$ : 3061, 2922, 2850, 2325, 2085, 1952, 1728, 1653, 1593, 1494, 1444, 1340, 1236, 1119, 1020, 955, 886, 775, 699.



**2-(Cyclohexylmethyl)-5,5-difluoro-4-(2-fluorophenyl)-N-methyl-N-phenylpent-4-enamide (3-3ff)**

Following procedure B, the crude mixture was purified by silica gel column chromatography with pentane/EA (20:1). 19 mg product was obtained by 30% isolated yield as colorless liquid.

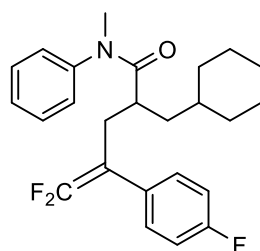
$^1\text{H}$  NMR (600 MHz, Chloroform-*d*)  $\delta$  7.19 – 7.14 (m, 1H), 7.14 – 7.09 (m, 3H), 6.98 – 6.89 (m, 3H), 6.86 – 6.81 (m, 2H), 3.13 (s, 3H), 2.49 (dt,  $J$  = 6.6, 2.4 Hz, 2H), 2.30 – 2.24 (m, 1H), 1.52 – 1.43 (m, 4H), 1.33 (d,  $J$  = 13.0 Hz, 1H), 1.09 – 0.93 (m, 6H), 0.59 (qd,  $J$  = 12.5, 3.0 Hz, 1H), 0.43 ( $\approx$ qd,  $J$  = 12.9, 4.1 Hz, 1H).

$^{13}\text{C}$  NMR (151 MHz, Chloroform-*d*)  $\delta$  175.3, 160.0 (d,  $J$  = 248.4 Hz), 153.8 (t,  $J$  = 289.5 Hz), 143.5, 130.8 ( $\approx$ q,  $J$  = 2.4 Hz), 129.42, 129.36, 127.5, 127.1, 124.0 (d,  $J$  = 3.6 Hz), 120.7 (ddd,  $J$  = 15.3, 4.8, 2.1 Hz), 115.8 (d,  $J$  = 22.3 Hz), 85.2 (dd,  $J$  = 25.0, 16.8 Hz), 39.3, 37.41, 37.39 (t,  $J$  = 2.6 Hz), 35.4, 33.6, 32.8, 30.7, 26.4, 26.3, 26.2.

$^{19}\text{F}$  NMR (565 MHz, Chloroform-*d*)  $\delta$  -87.01 (dd,  $J$  = 35.8, 13.1 Hz, 1F), -89.94 (d,  $J$  = 35.6 Hz, 1F), -113.30 to -113.39 (m, 1F).

HRMS (ESI-MS) Calcd. For  $\text{C}_{25}\text{H}_{28}\text{F}_3\text{NONa}$   $[\text{M}+\text{Na}]^+$  438.2015, found: 438.1999.

IR (neat,  $\text{cm}^{-1}$ ):  $\tilde{\nu}$ : 3484, 3063, 2922, 2851, 2326, 2102, 1737, 1654, 1594, 1493, 1388, 1248, 1118, 1010, 944, 760, 699.



**2-(Cyclohexylmethyl)-5,5-difluoro-4-(4-fluorophenyl)-N-methyl-N-phenylpent-4-enamide (3-3fg)**

Following procedure B, the crude mixture was purified by silica gel column chromatography with pentane/EA (15:1). 40 mg product was obtained by 64% isolated yield as colorless liquid.

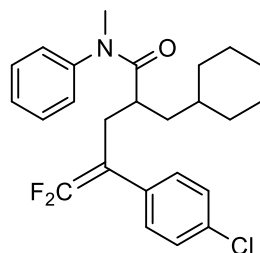
$^1\text{H}$  NMR (600 MHz, Chloroform-*d*)  $\delta$  7.19 – 7.16 (m, 3H), 6.98 – 6.92 (m, 2H), 6.88 – 6.79 (m, 4H), 3.13 (s, 3H), 2.53 – 2.47 (m, 1H), 2.46 – 2.41 (m, 1H), 2.37 – 2.32 (m, 1H), 1.54 – 1.45 (m, 4H), 1.32 (d,  $J$  = 13.2 Hz, 1H), 1.07 – 0.94 (m, 6H), 0.58 (qd,  $J$  = 12.6, 3.0 Hz, 1H), 0.43 (qd,  $J$  = 12.5, 3.5 Hz, 1H).

$^{13}\text{C}$  NMR (151 MHz, Chloroform-*d*)  $\delta$  175.3, 161.8 (d,  $J$  = 246.6 Hz), 154.0 (t,  $J$  = 289.5 Hz), 143.5, 129.9 (dt,  $J$  = 8.3, 3.2 Hz), 129.5, 128.9 ( $\approx$ q,  $J$  = 3.6 Hz), 127.7, 127.3, 115.3 (d,  $J$  = 21.7 Hz), 89.7 (dd,  $J$  = 22.3, 14.0 Hz), 39.4, 37.5, 37.3 (t,  $J$  = 2.4 Hz), 35.3, 33.5, 33.1, 30.6, 26.4, 26.2, 26.1.

$^{19}\text{F}$  NMR (565 MHz, Chloroform-*d*)  $\delta$  -89.64 (d,  $J$  = 40.1 Hz, 1F), -90.34 (dd,  $J$  = 40.1, 3.4 Hz, 1F), -114.69 to -114.76 (m, 1F).

HRMS (ESI-MS) Calcd. For  $\text{C}_{25}\text{H}_{29}\text{F}_3\text{NO}$   $[\text{M}+\text{H}]^+$  416.2196, found: 416.2198.

IR (neat,  $\text{cm}^{-1}$ ):  $\tilde{\nu}$ : 3483, 3061, 2922, 2851, 2327, 1997, 1892, 1728, 1653, 1509, 1389, 1236, 1118, 1010, 890, 837, 771, 700, 656.



#### 4-(4-Chlorophenyl)-2-(cyclohexylmethyl)-5,5-difluoro-N-methyl-N-phenylpent-4-enamide (3-fh)

Following procedure B, the crude mixture was purified by silica gel column chromatography with pentane/EA (15:1). 32 mg product was obtained by 49% isolated yield as colorless liquid.

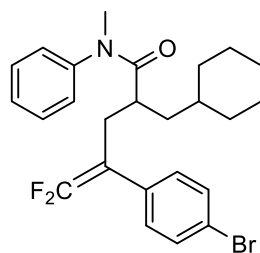
$^1\text{H}$  NMR (600 MHz, Chloroform-*d*)  $\delta$  7.22 – 7.16 (m, 3H), 7.14 (d,  $J$  = 8.2 Hz, 2H), 6.92 (d,  $J$  = 8.4 Hz, 2H), 6.80 (d,  $J$  = 7.2 Hz, 2H), 3.13 (s, 3H), 2.53 – 2.47 (m, 1H), 2.45 – 2.40 (m, 1H), 2.38 – 2.32 (m, 1H), 1.53 – 1.46 (m, 4H), 1.32 (d,  $J$  = 13.2 Hz, 1H), 1.08 – 0.95 (m, 6H), 0.58 (qd,  $J$  = 12.5, 3.1 Hz, 1H), 0.45 (qd,  $J$  = 12.0, 3.7 Hz, 1H).

$^{13}\text{C}$  NMR (151 MHz, Chloroform-*d*)  $\delta$  175.2, 154.0 (dd,  $J$  = 291.3, 289.0 Hz), 143.5, 133.0, 131.6 (t,  $J$  = 3.6 Hz), 129.50, 129.49 (t,  $J$  = 3.3 Hz), 128.5, 127.7, 127.2, 89.8 (dd,  $J$  = 22.0, 13.6 Hz), 39.6, 37.5, 37.3 (t,  $J$  = 2.7 Hz), 35.3, 33.5, 33.2, 30.4, 26.4, 26.2, 26.1.

$^{19}\text{F}$  NMR (565 MHz, Chloroform-*d*)  $\delta$  -88.72 (d,  $J$  = 37.9 Hz, 1F), -89.40 (dd,  $J$  = 38.4, 2.8 Hz, 1F).

HRMS (ESI-MS) Calcd. For  $\text{C}_{25}\text{H}_{28}\text{F}_2\text{NOCINa}$   $[\text{M}+\text{Na}]^+$  454.1720, found: 454.1697.

IR (neat,  $\text{cm}^{-1}$ ):  $\tilde{\nu}$ : 3062, 2922, 2851, 2323, 2107, 1900, 1726, 1654, 1594, 1494, 1341, 1240, 1094, 941, 829, 771, 700.



#### 4-(4-Bromophenyl)-2-(cyclohexylmethyl)-5,5-difluoro-N-methyl-N-phenylpent-4-enamide (3-fi)

Following procedure B, the crude mixture was purified by silica gel column chromatography with pentane/EA (15:1). 40 mg product was obtained by 55% isolated yield as colorless liquid.

$^1\text{H}$  NMR (600 MHz, Chloroform-*d*)  $\delta$  7.29 (d,  $J$  = 9.0 Hz, 2H), 7.22 – 7.13 (m, 3H), 6.86 (d,  $J$  = 8.4 Hz, 2H), 6.79 (d,  $J$  = 7.2 Hz, 2H), 3.12 (s, 3H), 2.52 – 2.47 (m, 1H), 2.44 – 2.40 (m, 1H), 2.38 – 2.31 (m, 1H), 1.53 – 1.46 (m, 4H), 1.31 (d,  $J$  = 12.7 Hz, 1H), 1.09 – 0.95 (m, 6H), 0.57 (qd,  $J$  =



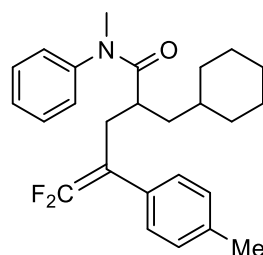
12.6, 3.0 Hz, 1H), 0.45 (qd,  $J = 11.9, 3.5$  Hz, 1H).

$^{13}\text{C}$  NMR (151 MHz, Chloroform- $d$ )  $\delta$  175.1, 153.9 (dd,  $J = 291.6, 289.2$  Hz), 143.4, 132.1 (t,  $J = 3.6$  Hz), 131.5, 129.8 (t,  $J = 3.5$  Hz), 129.5, 127.7, 127.2, 121.1, 89.8 (dd,  $J = 22.3, 13.9$  Hz), 39.6, 37.5, 37.3 (t,  $J = 2.6$  Hz), 35.3, 33.5, 33.2, 30.3, 26.4, 26.2, 26.1.

$^{19}\text{F}$  NMR (565 MHz, Chloroform- $d$ )  $\delta$  -88.60 (d,  $J = 38.4$  Hz, 1F), -89.28 (dd,  $J = 38.4$  Hz, 1F).

HRMS (ESI-MS) Calcd. For  $\text{C}_{25}\text{H}_{28}\text{F}_2\text{NOBrNa}$   $[\text{M}+\text{Na}]^+$  498.1215, found: 498.1207.

IR (neat,  $\text{cm}^{-1}$ ):  $\tilde{\nu}$ : 3484, 3062, 2922, 2851, 2329, 1983, 1725, 1653, 1492, 1389, 1239, 1118, 1006, 940, 827, 700, 659.



### 2-(Cyclohexylmethyl)-5,5-difluoro-*N*-methyl-*N*-phenyl-4-(*p*-tolyl)pent-4-enamide (3-3fj)

Following procedure B, the crude mixture was purified by silica gel column chromatography with pentane/EA (15:1). 44 mg product was obtained by 71% isolated yield as colorless liquid.

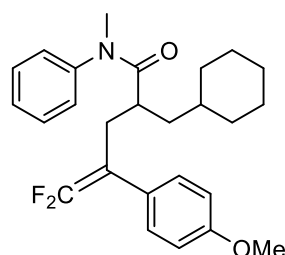
$^1\text{H}$  NMR (600 MHz, Chloroform- $d$ )  $\delta$  7.18 – 7.09 (m, 3H), 6.98 (d,  $J = 7.8$  Hz, 2H), 6.89 (d,  $J = 7.8$  Hz, 2H), 6.77 (d,  $J = 7.2$  Hz, 2H), 3.12 (s, 3H), 2.56 – 2.51 (m, 1H), 2.45 – 2.35 (m, 2H), 2.27 (s, 3H), 1.54 – 1.42 (m, 4H), 1.30 (d,  $J = 13.2$  Hz, 1H), 1.10 – 0.93 (m, 6H), 0.55 (qd,  $J = 12.2, 3.4$  Hz, 1H), 0.44 (qd,  $J = 12.1, 3.7$  Hz, 1H).

$^{13}\text{C}$  NMR (151 MHz, Chloroform- $d$ )  $\delta$  175.5, 153.9 (dd,  $J = 290.4, 287.8$  Hz), 143.5, 136.8, 130.1 (t,  $J = 3.9$  Hz), 129.4, 129.0, 128.0 (t,  $J = 3.0$  Hz), 127.4, 127.3, 90.4 (dd,  $J = 21.1, 14.0$  Hz), 39.7, 37.5, 37.4 (t,  $J = 2.4$  Hz), 35.3, 33.4, 33.1, 30.5, 26.5, 26.2, 26.1, 21.1.

$^{19}\text{F}$  NMR (565 MHz, Chloroform- $d$ )  $\delta$  -90.08 (d,  $J = 40.7$  Hz, 1F), -90.71 (d,  $J = 39.6$  Hz, 1F).

HRMS (ESI-MS) Calcd. For  $\text{C}_{26}\text{H}_{31}\text{F}_2\text{NONa}$   $[\text{M}+\text{Na}]^+$  434.2266, found: 434.2260.

IR (neat,  $\text{cm}^{-1}$ ):  $\tilde{\nu}$ : 3480, 3032, 2922, 2851, 2326, 2114, 1902, 1726, 1654, 1446, 1340, 1235, 1113, 1008, 941, 819, 770, 700.



### 2-(Cyclohexylmethyl)-5,5-difluoro-4-(4-methoxyphenyl)-*N*-methyl-*N*-phenylpent-4-enamide (3-3fk)

Following procedure B, the crude mixture was purified by silica gel column chromatography with pentane/EA (10:1). 33 mg product was obtained by 51% isolated yield as colorless liquid.

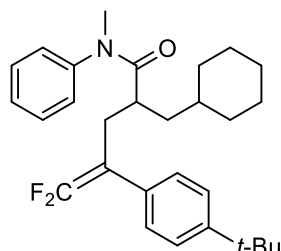
$^1\text{H}$  NMR (600 MHz, Chloroform- $d$ )  $\delta$  7.18 – 7.13 (m, 3H), 6.91 (d,  $J = 9.0$  Hz, 2H), 6.83 – 6.78 (m, 2H), 6.71 (d,  $J = 8.7$  Hz, 2H), 3.74 (s, 3H), 3.13 (s, 3H), 2.54 – 2.48 (m, 1H), 2.45 – 2.36 (m, 2H), 1.54 – 1.44 (m, 4H), 1.31 (d,  $J = 12.8$  Hz, 1H), 1.09 – 0.95 (m, 6H), 0.56 (qd,  $J = 12.5, 3.1$  Hz, 1H), 0.44 (qd,  $J = 11.9, 3.7$  Hz, 1H).

$^{13}\text{C}$  NMR (151 MHz, Chloroform-*d*)  $\delta$  175.5, 158.6, 153.9 (dd,  $J = 289.5, 287.2$ , Hz), 143.6, 129.4, 129.3 (t,  $J = 3.0$  Hz), 127.5, 127.3, 125.2 (t,  $J = 3.6$  Hz), 113.8, 90.0 (dd,  $J = 21.3, 13.9$  Hz), 55.3, 39.6, 37.5, 37.4 (t,  $J = 2.7$  Hz), 35.3, 33.5, 33.1, 30.6, 26.4, 26.2, 26.1.

$^{19}\text{F}$  NMR (565 MHz, Chloroform-*d*)  $\delta$  -90.58 (d,  $J = 42.4$  Hz, 1F), -91.23 (d,  $J = 42.4$  Hz, 1F).

HRMS (ESI-MS) Calcd. For  $\text{C}_{26}\text{H}_{31}\text{F}_2\text{NO}_2\text{Na}$   $[\text{M}+\text{Na}]^+$  450.2215, found: 450.2205.

IR (neat,  $\text{cm}^{-1}$ ):  $\tilde{\nu}$ : 3479, 3039, 2922, 2850, 2240, 1885, 1727, 1653, 1598, 1448, 1389, 1240, 1113, 1029, 941, 832, 700.



#### 4-(4-(*tert*-Butyl)phenyl)-2-(cyclohexylmethyl)-5,5-difluoro-*N*-methyl-*N*-phenylpent-4-enamide (3-3fl)

Following procedure B, the crude mixture was purified by silica gel column chromatography with pentane/EA (15:1). 47 mg product was obtained by 69% isolated yield as colorless liquid.

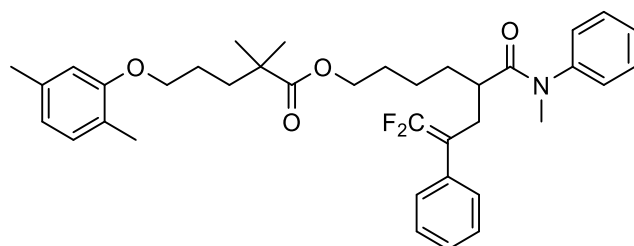
$^1\text{H}$  NMR (600 MHz, Chloroform-*d*)  $\delta$  7.19 (d,  $J = 8.4$  Hz, 2H), 7.14 – 7.09 (m, 3H), 6.93 (d,  $J = 8.4$  Hz, 2H), 6.79 – 6.71 (m, 2H), 3.12 (s, 3H), 2.58 – 2.53 (m, 1H), 2.46 – 2.41 (m, 1H), 2.40 – 2.33 (m, 1H), 1.52 – 1.39 (m, 4H), 1.25 (s, 9H), 1.21 – 1.17 (m, 1H), 1.10 – 0.93 (m, 6H), 0.53 (qd,  $J = 11.6, 3.2$  Hz, 1H), 0.41 (qd,  $J = 13.3, 3.7$  Hz, 1H).

$^{13}\text{C}$  NMR (151 MHz, Chloroform-*d*)  $\delta$  175.5, 154.0 (dd,  $J = 290.2, 288.0$  Hz), 150.1, 143.6, 129.9 (t,  $J = 3.9$  Hz), 129.4, 127.9 (t,  $J = 3.0$  Hz), 127.4, 127.3, 125.2, 90.3 (dd,  $J = 21.3, 14.3$  Hz), 39.6, 37.5, 37.3 (t,  $J = 2.6$  Hz), 35.3, 34.5, 33.4, 33.1, 31.3, 30.3, 26.5, 26.2, 26.1.

$^{19}\text{F}$  NMR (565 MHz, Chloroform-*d*)  $\delta$  -90.00 (d,  $J = 40.7$  Hz, 1F), -90.72 (d,  $J = 39.6$  Hz, 1F).

HRMS (ESI-MS) Calcd. For  $\text{C}_{29}\text{H}_{37}\text{F}_2\text{NONa}$   $[\text{M}+\text{Na}]^+$  476.2735, found: 476.2729.

IR (neat,  $\text{cm}^{-1}$ ):  $\tilde{\nu}$ : 3482, 3037, 2923, 2853, 2664, 2066, 1988, 1728, 1656, 1595, 1448, 1340, 1236, 1107, 942, 834, 771, 700.



#### 8,8-Difluoro-5-(methyl(phenyl)carbamoyl)-7-phenyloct-7-en-1-yl 5-(2,5-dimethylphenoxy)-2,2-dimethylpentanoate (3-3ta)

Following procedure A, the crude mixture was purified by silica gel column chromatography with pentane/EA (15:1). 55 mg product was obtained by 60% isolated yield as colorless liquid.

$^1\text{H}$  NMR (600 MHz, Chloroform-*d*)  $\delta$  7.18 – 7.11 (m, 6H), 6.99 (d,  $J = 7.8$  Hz, 2H), 6.92 (d,  $J = 7.8$  Hz, 1H), 6.83 – 6.77 (m, 2H), 6.58 (d,  $J = 7.2$  Hz, 1H), 6.53 (s, 1H), 3.87 (t,  $J = 6.6$  Hz, 2H), 3.83 (t,  $J = 5.4$  Hz, 2H), 3.12 (s, 3H), 2.61 – 2.55 (m, 1H), 2.45 (ddd,  $J = 14.5, 8.0, 2.4$  Hz, 1H), 2.34 – 2.28 (m, 1H), 2.23 (s, 3H), 2.09 (s, 3H), 1.63 – 1.51 (m, 4H), 1.34 – 1.16 (m, 5H), 1.12 (s, 6H), 1.04

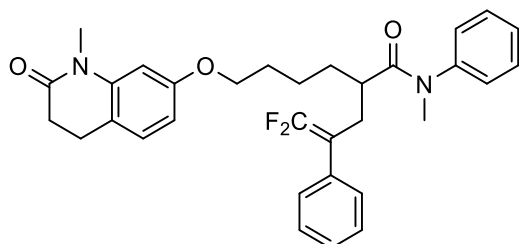
– 0.99 (m, 1H).

$^{13}\text{C}$  NMR (151 MHz, Chloroform-*d*)  $\delta$  177.8, 174.7, 157.0, 154.0 (dd,  $J = 291.6, 288.3$  Hz), 143.5, 136.5, 132.9 (t,  $J = 4.1$  Hz), 130.3, 129.6, 128.4, 128.0 (t,  $J = 3.5$  Hz), 127.6, 127.3, 127.2, 123.6, 120.7, 112.0, 90.4 (dd,  $J = 21.4, 13.7$  Hz), 67.9, 64.1, 42.1, 39.9 (t,  $J = 2.4$  Hz), 37.5, 37.1, 31.5, 30.2, 28.6, 25.2, 23.6, 21.4, 15.8.

$^{19}\text{F}$  NMR (565 MHz, Chloroform-*d*)  $\delta$  -89.04 (d,  $J = 39.0$  Hz, 1F), -89.86 (d,  $J = 38.7$  Hz, 1F).

HRMS (ESI-MS) Calcd. For  $\text{C}_{37}\text{H}_{45}\text{F}_2\text{NO}_4\text{Na}$   $[\text{M}+\text{Na}]^+$  628.3209, found: 628.3196.

IR (neat,  $\text{cm}^{-1}$ ):  $\tilde{\nu}$ : 3500, 2929, 2866, 2174, 1950, 1884, 1724, 1655, 1593, 1498, 1451, 1388, 1238, 1129, 1042, 805, 765, 699.



**2-(3,3-Difluoro-2-phenylallyl)-*N*-methyl-6-((1-methyl-2-oxo-1,2,3,4-tetrahydroquinolin-7-yl)oxy)-*N*-phenylhexanamide (3-3ua)**

Following procedure A, the crude mixture was purified by silica gel column chromatography with pentane/EA/ $\text{CH}_2\text{Cl}_2$  (1:1:0.1). 36 mg product was obtained by 45% isolated yield as colorless liquid.

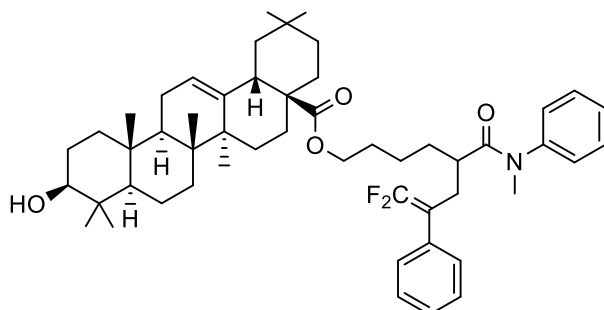
$^1\text{H}$  NMR (400 MHz, Chloroform-*d*)  $\delta$  7.19 – 7.10 (m, 6H), 7.02 – 6.94 (m, 3H), 6.87 – 6.80 (m, 2H), 6.45 (d,  $J = 2.3$  Hz, 1H), 6.42 (dd,  $J = 8.1, 2.4$  Hz, 1H), 3.84 – 3.72 (m, 2H), 3.25 (s, 3H), 3.13 (s, 3H), 2.75 (t,  $J = 6.6$  Hz, 2H), 2.63 – 2.42 (m, 4H), 2.40 – 2.30 (m, 1H), 1.64 – 1.42 (m, 3H), 1.32 – 1.16 (m, 3H).

$^{13}\text{C}$  NMR (101 MHz, Chloroform-*d*)  $\delta$  174.7, 170.6, 158.6, 154.1 (dd,  $J = 292.7, 289.4$  Hz), 143.5, 141.6, 132.9 (t,  $J = 3.8$  Hz), 129.6, 128.4, 128.1, 128.0 (t,  $J = 3.3$  Hz), 127.6, 127.4, 127.2, 118.3, 107.1, 103.0, 90.3 (dd,  $J = 21.2, 13.5$  Hz), 67.8, 40.0 (t,  $J = 2.4$  Hz), 37.5, 32.1, 31.5, 30.3, 29.6, 29.2, 24.6, 23.8.

$^{19}\text{F}$  NMR (565 MHz, Chloroform-*d*)  $\delta$  -88.97 (d,  $J = 39.0$  Hz, 1F), -89.83 (d,  $J = 38.4$  Hz, 1F).

HRMS (ESI-MS) Calcd. For  $\text{C}_{32}\text{H}_{34}\text{F}_2\text{N}_2\text{O}_3\text{Na}$   $[\text{M}+\text{Na}]^+$  555.2430, found: 555.2413.

IR (neat,  $\text{cm}^{-1}$ ):  $\tilde{\nu}$ : 3482, 3032, 2937, 2865, 2244, 1911, 1727, 1654, 1613, 1446, 1355, 1230, 1125, 1066, 1000, 914, 844, 765, 729, 700.



**(3-3va)**

Following procedure A, the crude mixture was purified by silica gel column chromatography with pentane/EA/ $\text{CH}_2\text{Cl}_2$  (2:1:0.1). 71 mg mixture of diastereomers (dr = 1.1:1, determined by  $^{19}\text{F}$  NMR analysis of the mixture) was obtained by 58% isolated yield as colorless liquid.

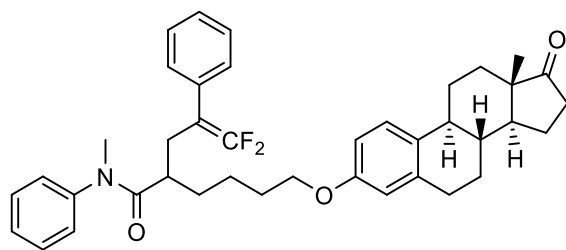
$^1\text{H}$  NMR (600 MHz, Chloroform-*d*)  $\delta$  7.19 – 7.11 (m, 6H), 7.00 (d,  $J$  = 6.4 Hz, 2H), 6.84 – 6.77 (m, 2H), 5.20 (dt,  $J$  = 10.8, 3.6 Hz, 1H), 3.86 – 3.78 (m, 2H), 3.18 – 3.13 (m, 1H), 3.12 (s, 3H), 2.77 (dd,  $J$  = 14.4, 4.8 Hz, 1H), 2.61 – 2.54 (m, 1H), 2.45 (ddd,  $J$  = 14.6, 8.0, 2.4 Hz, 1H), 2.35 – 2.28 (m, 1H), 1.88 (td,  $J$  = 14.6, 4.1 Hz, 1H), 1.84 – 1.75 (m, 2H), 1.61 – 1.20 (m, 22H), 1.13 – 0.95 (m, 4H), 1.06 (s, 3H), 0.91 (s, 3H), 0.85 (s, 3H), 0.83 (s, 6H), 0.71 (s, 3H), 0.64 (s, 3H).

$^{13}\text{C}$  NMR (151 MHz, Chloroform-*d*)  $\delta$  177.6, 174.7, 154.0 (dd,  $J$  = 291.6, 288.4 Hz), 143.8, 143.7, 143.5, 132.9 (t,  $J$  = 4.1 Hz), 129.6, 128.4, 128.0 (t,  $J$  = 3.3 Hz), 127.6, 127.3, 127.2, 122.40, 122.35, 90.3 (dd,  $J$  = 21.4, 13.7 Hz), 79.0, 63.90, 63.86, 55.2, 47.6, 46.6, 45.9, 41.7, 41.3, 39.9 – 39.8 (m), 39.3, 38.8, 38.5, 37.5, 37.0, 33.9, 33.1, 32.8, 32.5, 31.53, 31.51, 30.7, 30.3, 28.6, 28.5, 28.1, 27.68, 27.66, 27.2, 25.88, 25.87, 23.71, 23.68, 23.6, 23.4, 23.0, 18.3, 17.0, 15.6, 15.3.

$^{19}\text{F}$  NMR (565 MHz, Chloroform-*d*) diastereomer 1 (minor)  $\delta$  -88.99 (d,  $J$  = 39.0 Hz, 1F), -89.83 (d,  $J$  = 39.0 Hz, 1F), diastereomer 2 (major) -89.01 (d,  $J$  = 39.0 Hz, 1.1F), -89.86 (d,  $J$  = 39.0 Hz, 1.1F).

HRMS (ESI-MS) Calcd. For  $\text{C}_{52}\text{H}_{71}\text{F}_2\text{NO}_4\text{Na}$   $[\text{M}+\text{Na}]^+$  834.5243, found: 834.5238.

IR (neat,  $\text{cm}^{-1}$ ):  $\tilde{\nu}$ : 3465, 2940, 2867, 2246, 2092, 1946, 1728, 1649, 1595, 1455, 1382, 1298, 1238, 1167, 1042, 1000, 914, 764, 731, 700.



### (3-3wa)

Following procedure A, the crude mixture was purified by silica gel column chromatography with pentane/EA (4:1). 42 mg product was obtained by 44% isolated yield as white solid. Melting point: 116.8 – 118.1 °C.

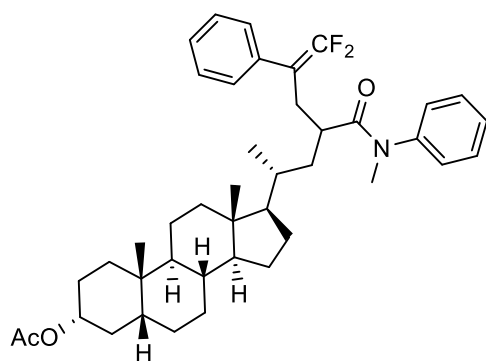
$^1\text{H}$  NMR (600 MHz, Chloroform-*d*)  $\delta$  7.18 – 7.09 (m, 7H), 6.99 ( $\approx$ d,  $J$  = 7.9 Hz, 2H), 6.85 – 6.79 (m, 2H), 6.60 (dd,  $J$  = 8.4, 2.8 Hz, 1H), 6.53 (d,  $J$  = 2.4 Hz, 1H), 3.80 – 3.68 (m, 2H), 3.13 (s, 3H), 2.86 – 2.78 (m, 2H), 2.62 – 2.55 (m, 1H), 2.50 – 2.39 (m, 2H), 2.36 – 2.29 (m, 2H), 2.18 (td,  $J$  = 10.8, 4.8 Hz, 1H), 2.06 (dt,  $J$  = 18.6, 9.0 Hz, 1H), 2.02 – 1.86 (m, 3H), 1.62 – 1.21 (m, 12H), 0.83 (s, 3H).

$^{13}\text{C}$  NMR (151 MHz, Chloroform-*d*)  $\delta$  220.9, 174.8, 157.1, 154.1 (dd,  $J$  = 291.7, 288.3 Hz), 143.5, 137.7, 132.9 (t,  $J$  = 4.1 Hz), 131.9, 129.6, 128.4, 128.0 (t,  $J$  = 3.2 Hz), 127.6, 127.4, 127.2, 126.3, 114.5, 112.2, 90.4 (dd,  $J$  = 21.3, 13.4 Hz), 67.5, 50.4, 48.0, 44.0, 40.0 (t,  $J$  = 2.6 Hz), 38.4, 37.5, 35.9, 31.63, 31.61, 30.3, 29.7, 29.2, 26.6, 26.0, 23.9, 21.6, 13.9.

$^{19}\text{F}$  NMR (565 MHz, Chloroform-*d*)  $\delta$  -89.00 (d,  $J$  = 39.0 Hz, 1F), -89.88 (d,  $J$  = 38.4 Hz, 1F).

HRMS (ESI-MS) Calcd. For  $\text{C}_{40}\text{H}_{46}\text{F}_2\text{NO}_3$   $[\text{M}+\text{H}]^+$  626.3440, found: 626.3443.

IR (neat,  $\text{cm}^{-1}$ ):  $\tilde{\nu}$ : 3455, 3034, 2927, 2865, 2244, 2068, 1734, 1651, 1597, 1495, 1449, 1278, 1238, 1117, 1056, 913, 764, 730, 698.



**(3xa)**

Following procedure A, the crude mixture was purified by silica gel column chromatography with pentane/EA/CH<sub>2</sub>Cl<sub>2</sub> (10:1:0.1). 33 mg diastereomers **1** was obtained by 33% isolated yield as white solid. Melting point: 135.7 – 136.4 °C. 18 mg diastereomers **2** was obtained by 18% isolated yield as colorless liquid.

Diastereomer 1 <sup>1</sup>H NMR (400 MHz, Chloroform-*d*) δ 7.19 – 7.08 (m, 6H), 6.97 – 6.82 (m, 4H), 4.64 (tt, *J* = 11.6, 4.8 Hz, 1H), 3.15 (s, 3H), 2.51 – 2.45 (m, 2H), 2.43 – 2.33 (m, 1H), 1.95 (s, 3H), 1.87 – 1.57 (m, 8H), 1.50 – 1.23 (m, 9H), 1.01 – 0.69 (m, 9H), 0.85 (s, 3H), 0.54 (s, 3H), 0.25 (d, *J* = 6.4 Hz, 3H).

<sup>13</sup>C NMR (101 MHz, Chloroform-*d*) δ 175.3, 170.6, 154.1 (dd, *J* = 291.5, 289.4 Hz), 143.5, 132.8 (t, *J* = 3.3 Hz), 129.5, 128.3, 128.2 (t, *J* = 3.1 Hz), 127.5, 127.4, 127.1, 90.4 (dd, *J* = 21.4, 14.3 Hz), 74.4, 56.8, 56.5, 42.7, 41.9, 40.4, 40.1, 37.9, 37.6, 37.4 (t, *J* = 2.4 Hz), 35.8, 35.1, 34.6, 34.2, 32.3, 31.1, 28.4, 27.0, 26.7, 26.3, 24.2, 23.3, 21.5, 20.8, 18.7, 12.1.

<sup>19</sup>F NMR (565 MHz, Chloroform-*d*) δ -89.93 (d, *J* = 40.7 Hz, 1H), -90.39 (d, *J* = 41.8 Hz, 1H). HRMS (ESI-MS) Calcd. For C<sub>42</sub>H<sub>55</sub>F<sub>2</sub>NO<sub>3</sub>Na [M+Na]<sup>+</sup> 682.4042, found: 682.4019.

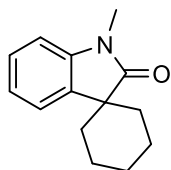
IR (neat, cm<sup>-1</sup>): ν̃: 2931, 2865, 2246, 2119, 1989, 1730, 1652, 1595, 1448, 1383, 1240, 1118, 1025, 912, 761, 730, 699.

Diastereomer 2 <sup>1</sup>H NMR (600 MHz, Chloroform-*d*) δ 7.26 – 7.22 (m, 2H), 7.21 – 7.19 (m, 1H), 7.14 – 7.07 (m, 5H), 6.62 (broad s, 2H), 4.64 (tt, *J* = 11.4, 4.8 Hz, 1H), 3.08 (s, 3H), 2.75 – 2.68 (m, 1H), 2.43 – 2.34 (m, 2H), 1.95 (s, 3H), 1.82 – 1.58 (m, 8H), 1.49 – 1.26 (m, 9H), 1.05 – 0.80 (m, 9H), 0.84 (s, 3H), 0.51 (s, 3H), 0.24 (d, *J* = 6.6 Hz, 3H).

<sup>13</sup>C NMR (151 MHz, Chloroform-*d*) δ 175.3, 170.6, 153.8 (dd, *J* = 291.3, 288.4 Hz), 143.5, 133.3 (t, *J* = 3.8 Hz), 129.3, 128.4, 128.2 (t, *J* = 3.5 Hz), 127.4, 127.3, 127.2, 90.9 (dd, *J* = 21.3, 13.1 Hz), 74.4, 57.0, 56.5, 42.8, 41.9, 40.4, 40.1, 39.2, 37.8, 37.4, 35.8, 35.0, 34.6, 33.8, 32.3, 28.8, 28.4, 27.0, 26.6, 26.3, 24.2, 23.3, 21.5, 20.8, 17.8, 12.0.

<sup>19</sup>F NMR (565 MHz, Chloroform-*d*) δ -89.00 (d, *J* = 39.0 Hz, 1F), -90.53 (d, *J* = 39.6 Hz, 1F). HRMS (ESI-MS) Calcd. For C<sub>42</sub>H<sub>55</sub>F<sub>2</sub>NO<sub>3</sub>Na [M+Na]<sup>+</sup> 682.4042, found: 682.4039.

IR (neat, cm<sup>-1</sup>): ν̃: 2932, 2863, 2206, 2160, 1983, 1730, 1657, 1595, 1495, 1447, 1381, 1237, 1026, 927, 768, 699.



**1'-Methylspiro[cyclohexane-1,3'-indolin]-2'-one (3-4y)**

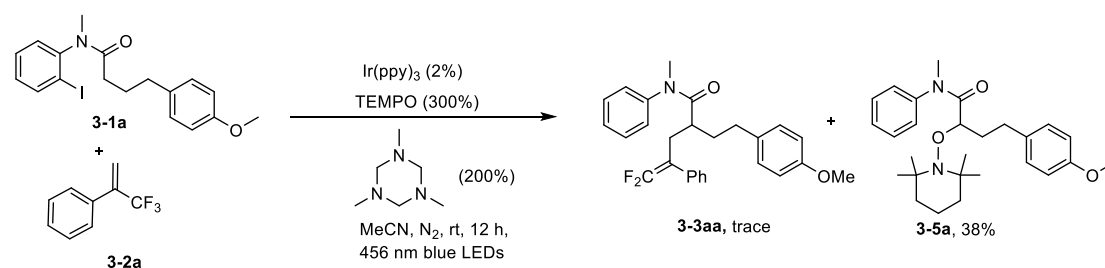
Following procedure A, the crude mixture was purified by silica gel column chromatography with pentane/EA (20:1). 27 mg product was obtained by 83% isolated yield as colorless liquid.

$^1\text{H}$  NMR (600 MHz, Chloroform-*d*)  $\delta$  7.38 (d,  $J$  = 7.4 Hz, 1H), 7.20 (t,  $J$  = 7.6 Hz, 1H), 6.97 (t,  $J$  = 7.6 Hz, 1H), 6.77 (d,  $J$  = 7.7 Hz, 1H), 3.13 (s, 3H), 1.90 – 1.83 (m, 2H), 1.80 – 1.73 (m, 2H), 1.72 – 1.61 (m, 3H), 1.60 – 1.52 (m, 1H), 1.52 – 1.45 (m, 2H).

$^{13}\text{C}$  NMR (151 MHz, Chloroform-*d*)  $\delta$  180.7, 142.8, 135.4, 127.4, 123.9, 121.9, 107.9, 47.5, 33.0, 26.1, 25.2, 21.2.

The data is consistent with the literature.<sup>301</sup>

### Radical trapping experiment



To a reaction vial equipped with a magnetic stirring bar were added amide **3-1a** (0.15 mmol, 61.4 mg),  $\text{Ir(ppy)}_3$  (0.003 mmol, 2 mg) and TEMPO (0.45 mmol, 70.3 mg). The capped vial was evacuated and backfilled with  $\text{N}_2$  three times before anhydrous MeCN (1.5 mL), trifluoromethyl arene **3-2a** (0.3 mmol, 45  $\mu\text{L}$ ) and triazinane (0.3 mmol, 43  $\mu\text{L}$ ) was added. Then the reaction was stirred at room temperature under blue LEDs irradiation (40 W). After 12 h, only a trace amount of **3-3aa** was detected by  $^{19}\text{F}$  NMR of the crude reaction mixture. The crude mixture was further purified by silica gel column chromatography with pentane/EA (4:1). 25 mg TEMPO adduct **3-5a** was obtained by 38% isolated yield as colorless liquid.

$^1\text{H}$  NMR (600 MHz, Chloroform-*d*)  $\delta$  7.35 – 7.22 (m, 5H), 6.96 (d,  $J$  = 8.4 Hz, 2H), 6.71 (d,  $J$  = 8.4 Hz, 2H), 4.33 (dd,  $J$  = 9.0, 4.8 Hz, 1H), 3.70 (s, 3H), 3.23 (s, 3H), 2.44 (td,  $J$  = 13.2, 4.8 Hz, 1H), 2.29 (td,  $J$  = 13.2, 4.8 Hz, 1H), 2.08 – 1.99 (m, 1H), 1.86 – 1.78 (m, 1H), 1.52 – 1.35 (m, 3H), 1.29 – 1.23 (m, 3H), 1.09 (s, 3H), 1.01 (s, 3H), 0.97 (s, 3H), 0.58 (s, 3H).

$^{13}\text{C}$  NMR (151 MHz, Chloroform-*d*)  $\delta$  172.2, 157.8, 143.7, 133.9, 129.2, 129.1, 128.4, 127.5, 113.7, 78.4, 60.6, 59.3, 55.3, 40.8, 40.2, 37.8, 33.7, 32.8, 32.4, 30.4, 20.3, 20.1, 17.2.

HRMS (ESI-MS) Calcd. For  $\text{C}_{27}\text{H}_{39}\text{N}_2\text{O}_3[\text{M}+\text{H}]^+$  439.2955, found: 439.2961.

IR (neat,  $\text{cm}^{-1}$ ):  $\tilde{\nu}$ : 3479, 2928, 2324, 2080, 1883, 1739, 1662, 1509, 1458, 1383, 1245, 1126, 1035, 989, 825, 771, 699.

### Stern-Volmer fluorescence studies

The Agilent Cary Eclipse Fluorescence Spectrometer is used to conduct Stern-Volmer fluorescence quenching analysis. The following parameters were employed: excitation wavelength = 377 nm, emission wavelength = 400 nm, excitation slit width = 5 nm, emission slit width = 10 nm, scan rate = 600 nm/min, averaging time = 0.1 s, data interval = 1 nm. The samples were measured at Hellma fluorescence QS quartz cuvette (chamber volume = 1.4 mL, light path = 10  $\times$  4 mm) with a closed screw cap and silicone seal. All the solutions were prepared with dry degassed MeCN. The concentration of photocatalyst  $\text{Ir(ppy)}_3$  is  $2 \times 10^{-6}$  M in MeCN, then by adding certain amount of a solution of quencher to  $\text{Ir(ppy)}_3$  solution, the samples with different concentrations were obtained,

and their fluorescence spectra were collected immediately with forementioned parameters.  $I_0$  is the fluorescence intensity without quencher,  $I$  is the fluorescence intensity with quencher.

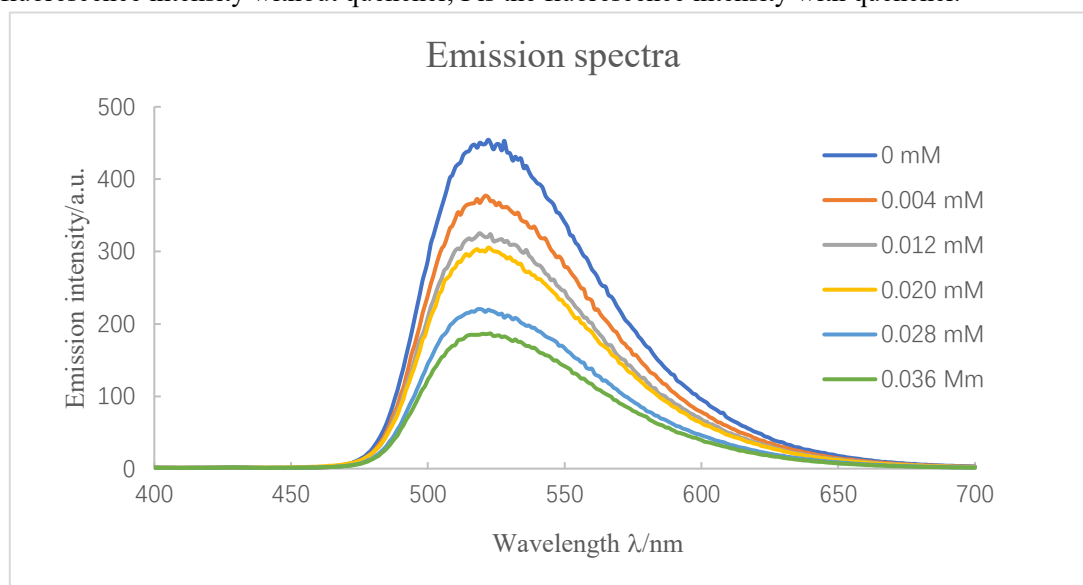


**Figure 3-S1:** Emission spectra of Ir(ppy)<sub>3</sub> with increasing concentrations of triazinane (The concentration of Ir(ppy)<sub>3</sub> is  $2 \times 10^{-6}$  M in MeCN)

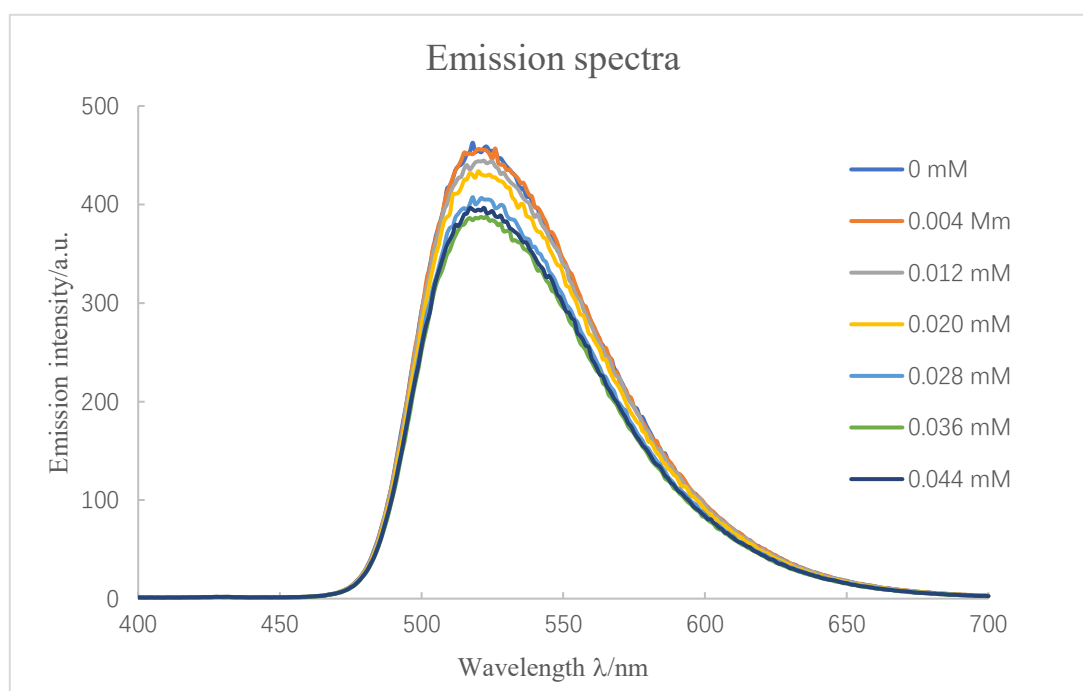


**Figure 3-S2:** Emission spectra of Ir(ppy)<sub>3</sub> with increasing concentrations of amide **3-1f** (The concentration of Ir(ppy)<sub>3</sub> is  $2 \times 10^{-6}$  M in MeCN)

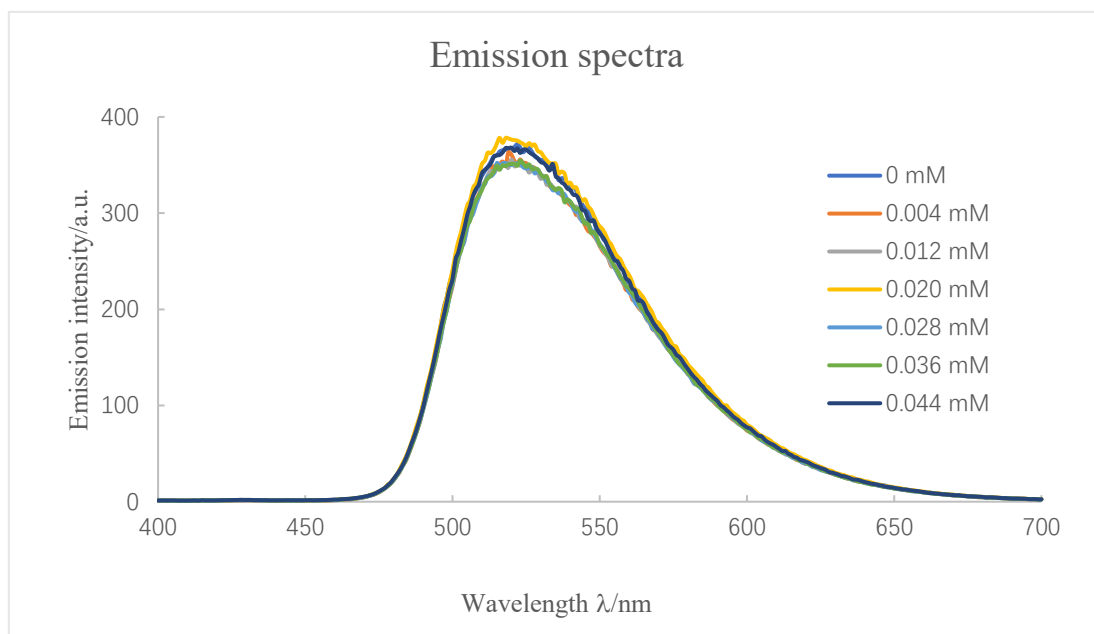


**Figure 3-S3:** Emission spectra of Ir(ppy)<sub>3</sub> with increasing concentrations of trifluoromethyl alkene **3-2a** (The concentration of Ir(ppy)<sub>3</sub> is  $2 \times 10^{-6}$  M in MeCN)

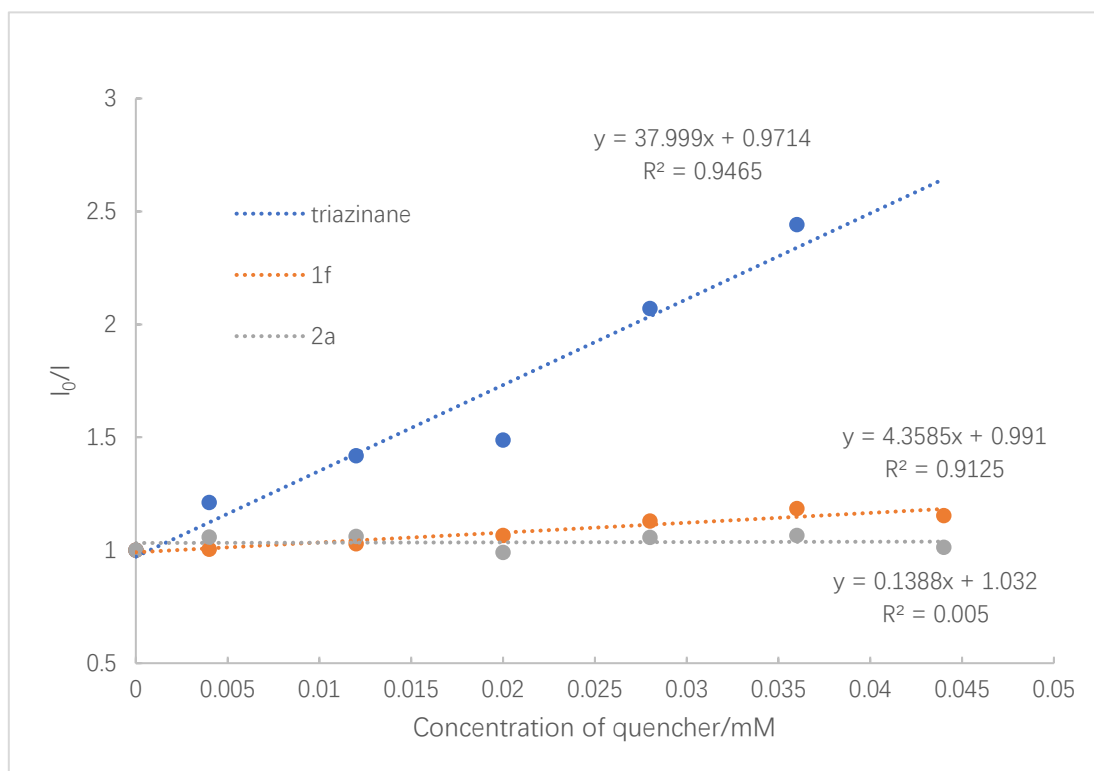


**Figure 3-S4:** Stern-Volmer plot of Ir(ppy)<sub>3</sub> with increasing concentrations of triazinane, amide **3-1f**, and trifluoromethyl arene **3-2a**.



## 5 List of abbreviation

Ac	acetyl
aq	aqueous
Ar	aryl
Binap	1,1'-binaphthyl-2,2'-diphemyl phosphine
Boc	<i>tert</i> -butyloxycarbonyl
BDE	bond dissociation energy
Bpin	pinacol boronic ester
br	broad
Bu	butyl
Bn	benzyl
BNAH	1-benzyl-1,4-dihydronicotinamide
Bz	benzoyl
bpy	2,2'-bipyridine
°C	centigrade
Calcd	calculated
Cbz	benzyloxycarbonyl
CFL	compact fluorescent lamp
Cy	cyclohexyl
Co(dmgH)(dmgH <sub>2</sub> )Cl <sub>2</sub>	dichlorobis(dimethylglyoximato)cobalt(III)
DCE	1,2-dichloroethane
DCA	9,10-dicyanoanthracene
DIPEA	<i>N,N</i> -diisopropylethylamine
diglyme	bis(2-methoxyethyl) ether
DMF	<i>N,N</i> -dimethylformamide
DME	1,2-dimethoxyethane
DMA	<i>N,N</i> -dimethylacetamide
DMSO	dimethyl sulfoxide
dr	diastereomeric excess
dtbbpy	4,4'-di- <i>tert</i> -butyl-2,2'-dipyridyl
EA	ethyl acetate
EI	electron ionization
equiv.	equivalent
ESI	electrospray ionization
ET	energy transfer
Et	ethyl
Fmoc	fluorenylmethyloxycarbonyl
h	hour
HE	Hantzsch ester
HRMS	high resolution mass spectroscopy
Hz	Hertz

IR	infrared spectroscopy
<i>i</i> -Pr	isopropyl
Incl.	include
<i>J</i>	coupling constant (in NMR spectroscopy)
Me	methyl
mol	mole
MS	mass spectroscopy
N.D.	not detected
NHC	<i>N</i> -heterocyclic carbene
Ni(cod) <sub>2</sub>	bis(cyclooctadiene)nickel(0)
Ni(COD)(DQ)	bis(1,5-cyclooctadiene)(duroquinone) nickel(0)
NMR	nuclear magnetic resonance
ox	oxidized
PCET	proton-coupled electron transfer
Ph	phenyl
phen	phenanthroline
Py	pyridyl
ppy	2-phenylpyridine
Piv	pivaloyl
rt	room temperature
Ref.	reference
SET	single electron transfer
<i>t</i> -Bu	<i>tert</i> -butyl
TBAI	tetrabutylammonium iodide
THF	tetrahydrofuran
TMS	trimethylsilyl
TFA	trifluoroacetic acid
TfOH	trifluoromethanesulfonic acid
TFE	trifluoroethanol
Tol	toluene
Ts	<i>p</i> -toluenesulfonyl
δ	chemical shift

## 6 References

- [1] Renaud, P.; Sibi, M. P. Eds. *Radicals in Organic Synthesis*; Wiley-VCH: Weinheim, Germany, **2001**.
- [2] Lalevée, J.; Fouassier, J. P. *Overview of Radical Initiation. Encyclopedia of Radicals in Chemistry, Biology and Materials*; John Wiley & Sons, Inc.: Hoboken, NJ, USA, **2012**; DOI: 10.1002/9781119953678.
- [3] Zard, S. Z. *Radical reactions in organic synthesis*; Oxford University Press, **2003**.
- [4] Yan, M.; Lo, J. C.; Edwards, J. T.; Baran, P. S. *J. Am. Chem. Soc.* **2016**, *138*, 12692.
- [5] Studer, A.; Curran, D. P. *Angew. Chem. Int. Ed.* **2016**, *55*, 58.
- [6] Kuivila, H. G.; Menapace, L. W. *J. Org. Chem.* **1963**, *28*, 2165.
- [7] Boger, D. L.; Mathvink, R. J. *J. Org. Chem.* **1992**, *57*, 1429.
- [8] Boger, D. L.; Mathvink, R. J. *J. Org. Chem.* **1989**, *54*, 1777.
- [9] Galli, C.; Pau, T. *Tetrahedron* **1998**, *54*, 2893–2904.
- [10] Luo, Y.-R. *Comprehensive Handbook of Chemical Bond Energies*; CRC Press: Boca Raton, **2007**.
- [11] Giese, B. *Angew. Chem., Int. Ed.* **1983**, *22*, 753.
- [12] Curran, D. P. *Synthesis* **1988**, 1988, 417.
- [13] Jasperse, C. P.; Curran, D. P.; Fevig, T. L. *Chem. Rev.* **1991**, *91*, 1237.
- [14] Ryu, I.; Sonoda, N.; Curran, D. P. *Chem. Rev.* **1996**, *96*, 177.
- [15] Davies, A. G. *Organotin Chemistry, Second*; Wiley-VCH: Weinheim, Germany, **2004**.
- [16] Lewis, R. J. *Sax's Dangerous Properties of Industrial Materials*; John Wiley & Sons, Inc.: Hoboken, NJ, USA, **2004**.
- [17] Chatgililoglu, C.; Ferreri, C.; Landais, Y.; Timokhin, V. I. T. *Chem. Rev.* **2018**, *118*, 651.
- [18] Gagosz, F.; Moutrille, C.; Zard, S. Z. *Org. Lett.* **2002**, *4*, 2707.
- [19] Tsai, L.-C.; You, M.-L.; Ding, M.-F.; Shu, C.-M. *Molecules* **2012**, *17*, 8056.
- [20] Wang, H.; Guo, L.-N.; Duan, X.-H. *Adv. Synth. Catal.* **2013**, *355*, 2222.
- [21] Chaubey, N. R.; Singh, K. N. *Tetrahedron Lett.* **2017**, *58*, 2347.
- [22] Meng, M.; Wang, G.; Yang, L.; Cheng, K.; Qi, C. *Adv. Synth. Catal.* **2018**, *360*, 1218.
- [23] Quiclet-Sire, B.; Zard, S. Z. *Chem. - Eur. J.* **2006**, *12*, 6002.
- [24] Darmency, V.; Renaud, P. *Tin-Free Radical Reaction Mediated by Organoboron Compounds. In Radicals in Synthesis I*; Springer-Verlag: Berlin, **2006**.
- [25] Studer, A.; Amrein, S. *Synthesis* **2002**, 2002, 835.
- [26] Snider, B. B. *Chem. Rev.* **1996**, *96*, 339.
- [27] Streuff, J. *Chem. Rec.* **2014**, *14*, 1100.
- [28] Molander, G. A.; Harris, C. R. *Chem. Rev.* **1996**, *96*, 307.
- [29] Wu, X.-F. *Chem. Eur. J.* **2015**, *21*, 12252.
- [30] Staveness, D.; Bosque, I.; Stephenson, C. R. J. *Acc. Chem. Res.* **2016**, *49*, 2295.
- [31] Douglas, J. J.; Sevrin, M. J.; Stephenson, C. R. J. *Org. Process Res. Dev.* **2016**, *20*, 1134.
- [32] Gentry, E. C.; Knowles, R. R. *Acc. Chem. Res.* **2016**, *49*, 1546.
- [33] Xie, J.; Jin, H.; Hashmi, A. S. K. *Chem. Soc. Rev.* **2017**, *46*, 5193.
- [34] Savateev, A.; Antonietti, M. *ACS Catal.* **2018**, *8*, 9790.
- [35] Lee, K. N.; Ngai, M.-Y. *Chem. Commun.* **2017**, *53*, 13093.
- [36] Skubi, K. L.; Blum, T. R.; Yoon, T. P. *Chem. Rev.* **2016**, *116*, 10035.

- [37] Twilton, J.; Le, C.; Zhang, P.; Shaw, M. H.; Evans, R. W.; MacMillan, D. W. C. *Nat. Rev. Chem.* **2017**, *1*, 0052.
- [38] Shaw, M. H.; Twilton, J.; MacMillan, D. W. C. *J. Org. Chem.* **2016**, *81*, 6898.
- [39] Romero, N. A.; Nicewicz, D. A. *Chem. Rev.* **2016**, *116*, 10075.
- [40] Narayanam, J. M. R.; Stephenson, C. R. J. *Chem. Soc. Rev.* **2011**, *40*, 102.
- [41] Strieth-Kalthoff, F.; James, M. J.; Teders, M.; Pitzer, L.; Glorius, F. *Chem. Soc. Rev.* **2018**, *47*, 7190.
- [42] Strieth-Kalthoff, F.; Glorius, F. *Chem.* **2020**, *6*, 1888.
- [43] Zhou, Q.-Q.; Zou, Y.-Q.; Lu, L.-Q.; Xiao W.-J. *Angew. Chem. Int. Ed.* **2019**, *58*, 1586.
- [44] Großkopf, J.; Kratz, T.; Rigotti, T.; Bach, T. *Chem. Rev.* **2022**, *122*, 1626.
- [45] Protti, S.; Manzini, S.; Fagnoni, M.; Albini, A. Chapter 2. *The Contribution of Photochemistry to Green Chemistry. In Eco-Friendly Synthesis of Fine Chemicals*; Roberto, Ballini., Ed.; The Royal Society of Chemistry, **2009**; pp 80–111.
- [46] Albini, A.; Fagnoni, M. *The Greenest Reagent in Organic Synthesis: Light. In Green Chemical Reactions*; Tundo, P., Esposito, V., Eds.; Springer Netherlands: Dordrecht, **2008**; pp 173–189.
- [47] Crespi, S.; Fagnoni, M. *Chem. Rev.* **2020**, *120*, 9790.
- [48] Banerjee, A.; Lei, Z.; Ngai, M.-Y. *Synthesis* **2019**, *51*, 303.
- [49] Cahiez, G.; Moyeux, A. *Chem. Rev.* **2010**, *110*, 1435.
- [50] Huang, L.; Arndt, M.; Gooßen, L. J. *Chem. Rev.* **2015**, *115*, 2596.
- [51] Ruiz-Castillo, P.; Buchwald, S. *Chem. Rev.* **2016**, *116*, 12564.
- [52] West, M. J.; Fyfe, J. W. B.; Vantourout, J. C. A.; Watson, J. B. *Chem. Rev.* **2019**, *119*, 12491.
- [53] McMurray, L.; MuGuire, T. M.; Howells, R. *Synthesis* **2020**, *52*, 1719.
- [54] Zhang, T.; Wang, N.-X.; Xing, Y. *J. Org. Chem.* **2018**, *83*, 7559.
- [55] Karmakar, S.; Silamkoti, A.; Meanwell, N. A.; Mathur, A.; Gupta, A. K. *Adv. Synth. Catal.* **2021**, *363*, 3693.
- [56] Murarka, S. *Adv. Synth. Catal.* **2018**, *360*, 1735.
- [57] Rahman, M.; Mukherjee, A.; Kovalev, I. S.; Kopchuk, D. S.; Zyryanov, G. V.; Tsurkan, M. V.; Majee, A.; Ranu, B.; Charushin, V. N.; Chupakhin, O. N.; Santra, S. *Adv. Synth. Catal.* **2019**, *361*, 2161.
- [58] G. G. dos P.; Wimmer, A.; Smith, J. M.; König, B.; Alabugin, I. V. *J. Org. Chem.* **2019**, *84*, 6232.
- [59] Agterberg, F. P. W.; Driessen, W. L.; Reedijk, J.; Oeveringb, H.; Buijs, W.; Surf, Stud. *Sci. Catal.* **1994**, *82*, 639.
- [60] Shi, J.; Huang, X.-Y.; Wang, J.-P.; Li, R. *Phys. Chem.* **2010**, *114*, 6263.
- [61] Guntreddi, T.; Vanjari, R.; Singh, K. N. *Org. Lett.* **2014**, *16*, 3624.
- [62] Xu, K.; Wang, Z.; Zhang, J.; Yu, L.; Tan, J. *Org. Lett.* **2015**, *17*, 4476.
- [63] Moon, P. J.; Wei, Z.; Lundgren, R. J. *J. Am. Chem. Soc.* **2018**, *140*, 17418.
- [64] Kong, D.; Moon, P. J.; Bsharat, O.; Lundgren, R. J. *Angew. Chem. Int. Ed.* **2020**, *59*, 1313.
- [65] Yoshimi, Y.; Itou, T.; Hatanaka, M. *Chem. Commun.* **2007**, 5244.
- [66] Itou, T.; Yoshimi, Y.; Morita, T.; Tokunaga, Y.; Hatanaka, M. *Tetrahedron* **2009**, *65*, 263.
- [67] Zuo, Z.; MacMillan, D. W. C. *J. Am. Chem. Soc.* **2014**, *136*, 5257.
- [68] McNally, A.; Prier, C. K.; MacMillan, D. W. C. *Science* **2011**, *334*, 1114.
- [69] Lipp, B.; Nauth, A. M.; Opatz, T. *J. Org. Chem.* **2016**, *81*, 6875.
- [70] Chen, Y.; Lu, P.; Wang, Y. *Org. Lett.* **2019**, *21*, 2130.

- [71] Noble, A.; MacMillan, D. W. C. *J. Am. Chem. Soc.* **2014**, *136*, 11602.
- [72] Roessler, F.; Ganzinger, D.; Johne, S.; Schöpp, E.; Hesse, M. *Helv. Chim. Acta* **1978**, *61*, 1200.
- [73] Marie, L.; Lipp, B.; Opatz, T. *J. Org. Chem.* **2019**, *84*, 2379.
- [74] Li, J.; Lefebvre, Q.; Yang, H.; Zhao, Y.; Fu, H. *Chem. Commun.* **2017**, *53*, 10299.
- [75] Chu, L.; Ohta, C.; Zuo, Z.; MacMillan, D. W. C. *J. Am. Chem. Soc.* **2014**, *136*, 10886.
- [76] Yoshimi, Y.; Masuda, M.; Mizunashi, T.; Nishikawa, K.; Maeda, K.; Koshida, N.; Itou, T.; Morita, T.; Hatanaka, M. *Org. Lett.* **2009**, *11*, 4652.
- [77] Lovett, G. H.; Sparling, B. A. *Org. Lett.* **2016**, *18*, 3494.
- [78] Inuki, S.; Sato, K.; Fukuyama, T.; Ryu, I.; Fujimoto, Y. *J. Org. Chem.* **2017**, *82*, 1248.
- [79] Noble, A.; Mega, R. S.; Pflästerer, D.; Myers, E. L.; Aggarwal, V. K. *Angew. Chem. Int. Ed.* **2018**, *57*, 2155.
- [80] Shah, A. A.; Perkins III, M. J. K. *J. Org. Lett.* **2020**, *22*, 2196.
- [81] Zhou, Q.-Q.; Guo, W.; Ding, W.; Wu, X.; Chen, X.; Lu, L.-Q.; Xiao, W.-J. *Angew. Chem. Int. Ed.* **2015**, *54*, 11196.
- [82] Liu, X.; Wang, Z.; Cheng, X.; Li, C. *J. Am. Chem. Soc.* **2012**, *134*, 14330.
- [83] Yang, C.; Yang, J.-D.; Li, Y.-H.; Li, X.; Cheng, J.-P. *J. Org. Chem.* **2016**, *81*, 12357.
- [84] Zuo, Z.; Ahneman, D. T.; Chu, L.; Terrett, J. A.; Doyle, A. G.; MacMillan, D. W. C. *Science* **2014**, *345*, 437.
- [85] Ma, Y.; Liu, S.; Xi, Y.; Li, H.; Yang, K.; Cheng, Z.; Wang, W.; Zhang, Y. *Chem. Commun.* **2019**, *55*, 14657.
- [86] Zuo, Z.; Cong, H.; Li, W.; Choi, J. G.; Fu, C.; MacMillan, D. W. C. *J. Am. Chem. Soc.* **2016**, *138*, 1832.
- [87] Luo, J.; Zhang, J. *ACS Catal.* **2016**, *6*, 873.
- [88] Pezzetta, C.; Bonifazi, D.; Davidson, R. W. M. *Org. Lett.* **2019**, *21*, 8957.
- [89] Fan, L.; Jia, J.; Hou, H.; Lefebvre, Q.; Rueping, M. *Chem. Eur. J.* **2016**, *22*, 16437.
- [90] Kölmel, D.; Meng, J.; Tsai, M.-H.; Que, J.; Loach, R. P.; Knauber, T.; Wan, J.; Flanagan, M. E. *ACS Comb. Sci.* **2019**, *21*, 588.
- [91] Noble, A.; McCarver, S. J.; MacMillan, D. W. C. *J. Am. Chem. Soc.* **2015**, *137*, 624.
- [92] Till, N. A.; Smith, R. T. D.; MacMillan, D. W. C. *J. Am. Chem. Soc.* **2018**, *140*, 5701.
- [93] Johnston, C. P.; Smith, R. T.; Allmendinger, S.; MacMillan, D. W. C. *Nature* **2016**, *536*, 322.
- [94] Zheng, C.; Cheng, W.-M.; Li, H.-L.; Na, R.-S.; Shang, R. *Org. Lett.* **2018**, *20*, 2559.
- [95] Garza, R.; Tlahuext, S. A.; Tavakoli, A. G.; Glorius, F. *ACS Catal.* **2017**, *7*, 4057.
- [96] Zhang, X.-Y.; Weng, W.-Z.; Liang, H.; Yang, H.; Zhang, B. *Org. Lett.* **2018**, *20*, 4686.
- [97] Okada, K.; Okamoto, K.; Oda, M. *J. Am. Chem. Soc.* **1988**, *110*, 8736.
- [98] Barton, D. H. R.; Crich, D.; Kretzschmar, G. *Tetrahedron Lett.* **1984**, *25*, 1055.
- [99] Barton, D. H. R.; Togo, H.; Zard, S. Z. *Tetrahedron* **1985**, *41*, 5507.
- [100] Barton, D. H. R.; Crich, D.; Kretzschmar, G. *J. Chem. Soc., Perkin Trans. 1*, **1986**, 39.
- [101] Barton, D. H. R.; Silva, E. d.; Zard, S. Z. *J. Chem. Soc. Chem. Commun.* **1988**, 285.
- [102] Parida, S. K.; Mandal, T.; Das, S.; Hota, S. K.; Sarkar, S. D.; Murarka, S. *ACS Catal.* **2021**, *11*, 1640.
- [103] Dai, G.-L.; Lai, S.-Z.; Luo, Z.; Tang, Z.-Y. *Org. Lett.* **2019**, *21*, 2269.
- [104] Yang, J.; Zhang, J.; Qi, L.; Hu, C.; Chen, Y. *Chem. Commun.* **2015**, *51*, 5275.
- [105] Okada, K.; Okamoto, K.; Morita, N.; Okubo, K.; Oda, M. *J. Am. Chem. Soc.* **1991**, *113*, 9401.
- [106] Tripathi, K. N.; Belal, M.; Singh, R. P. *J. Org. Chem.* **2020**, *85*, 1193.

- [107] Garrido-Castro, A. F.; Choubane, H.; Daaou, M.; Maestro, M. C.; Alemán, J. *Chem. Commun.* **2017**, 53, 7764.
- [108] Zhang, H.; Zhang, P.; Jiang, M.; Yang, H.; Fu, H. *Org. Lett.* **2017**, 19, 1016.
- [109] Wang, G.-Z.; Shang, R.; Fu, Y. *Org. Lett.* **2018**, 20, 888.
- [110] Sherwood, T. C.; Li, N.; Yazdani, A. N.; Dhar, T. G. M. *J. Org. Chem.* **2018**, 83, 3000.
- [111] Fu, M.-C.; Shang, R.; Zhao, B.; Wang, B.; Fu, Y. *Science* **2019**, 363, 1429.
- [112] Xia, Z.-H.; Zhang, C.-L.; Gao, Z.-H.; Ye, S. *Org. Lett.* **2018**, 20, 3496.
- [113] Guo, J.-Y.; Zhang, Z.-Y.; Guan, T.; Mao, L.-W.; Ban, Q.; Zhao, K.; Loh, T.-P. *Chem. Sci.* **2019**, 10, 8792.
- [114] Sha, W.; Ni, S.; Han, J.; Pan, Y. *Org. Lett.* **2017**, 19, 5900.
- [115] Zhao, Y.; Chen, J.-R.; Xiao, W.-J. *Org. Lett.* **2018**, 20, 224.
- [116] Li, X.; Zhang, Q.; Zhang, W.; Wang, Y.; Pan, Y. *J. Org. Chem.* **2019**, 84, 14360.
- [117] Mitsunobu, O.; Yamada, M. *Bull. Chem. Soc. Jpn.* **1967**, 40, 2380.
- [118] Schenk, S.; Weston, J.; Anders, E. *J. Am. Chem. Soc.* **2005**, 127, 12566.
- [119] Hirose, D.; Gazvoda, M.; Košmrlj, J.; Taniguchi, T. *Chem. Sci.* **2016**, 7, 5148.
- [120] Trost, B. M. *Science*, **1991**, 254, 1471.
- [121] Shao, X.; Zheng, Y.; Ramadoss, V.; Tian, L.; Wang, Y. *Org. Biomol. Chem.* **2020**, 18, 5994.
- [122] Zhang, M.; Xie, J.; Zhu, C. *Nat. Commun.* **2018**, 9, 3517.
- [123] Zhang, L.; Chen, S.; He, H.; Li, W.; Zhu, C.; Xie, J. *Chem. Commun.* **2021**, 57, 9064.
- [124] Nagaraju, A.; Saiaede, T.; Eghbarieh, N.; Masarwa, A. *Chem. Eur. J.* **2023**, 29, e202202646.
- [125] Guo, Y.-Q.; Wang, R.; Song, H.; Liu, Y.; Wang, Q. *Org. Lett.* **2020**, 22, 709.
- [126] Merkens, K.; Troyano, F. J. A.; Anwar, K.; Gomez-Suarez, A. *J. Org. Chem.* **2021**, 86, 8448.
- [127] Meng, L.; Yang, C.; Dong, J.; Wen, W.; Chen, J.; Fan, B. *Org. Chem. Front.* **2024**, 11, 21.
- [128] Li, G.-N.; Li, H.-C.; Wang, M.-R.; Lu, Z.; Yu, B. *Adv. Synth. Catal.* **2022**, 364, 3927.
- [129] Li, S.; Shu, H.; Wang, S.; Yang, W.; Tang, F.; Li, X.-X.; Fan, S.; Feng, Y.-S. *Org. Lett.* **2022**, 24, 5710.
- [130] Zhou, Y.; Zhao, L.; Hu, M.; Duan, X.-H.; Liu, L. *Org. Lett.* **2023**, 25, 5268.
- [131] Shimazumi, R.; Tanimoto, R.; Tobisu, M. *Org. Lett.* **2023**, 25, 6440.
- [132] Ruzi, R.; Ma, J.; Yuan, X.-A.; Wang, W.; Wang, S.; Zhang, M.; Dai, J.; Xie, J.; Zhu, C. *Chem. Eur. J.* **2019**, 25, 12724.
- [133] Li, Y.; Xu, W.; Zhu, C.; Xie, J. *Synlett* **2021**, 32, 387.
- [134] Jiang, H.; Mao, G.; Wu, H.; An, Q.; Zuo, M.; Guo, W.; Xu, C.; Sun, Z.; Chu, W. *Green Chem.* **2019**, 21, 5368.
- [135] Ruzi, R.; Liu, K.; Zhu, C.; Xie, J. *Nat. Commun.* **2020**, 11, 3312.
- [136] Li, Y.; Shao, Q.; He, H.; Zhu, C.; Xue, X.-S.; Xie, J. *Nat. Commun.* **2022**, 13, 10.
- [137] Zhang, M.; Yuan, X.-A.; Zhu, C.; Xie, J. *Angew. Chem. Int. Ed.* **2019**, 58, 312.
- [138] Marz, M.; Kohout, M.; Nevesely, T.; Chudoba, J.; Prukala, D.; Nizinski, S.; Sikorki, M.; Burdzinski, G.; Cibulka, R. *Org. Biomol. Chem.* **2018**, 16, 6809.
- [139] Su, J.; Mo, J.-N.; Chen, X.; Umanzor, A.; Zhang, Z.; Houk, K. N.; Zhao, J. *Angew. Chem. Int. Ed.* **2022**, 61, e202112668.
- [140] Wang, H.; Liu, Z.; Das, A.; Bellotti, P.; Megow, S.; Temps, F.; Qi, X.; Glorius, F. *Nat. Synth.* **2023**, 2, 1116.
- [141] Bergman, R. G. *Nature* **2007**, 446, 391.
- [142] Newhouse, T.; Baran, P. S. *Angew. Chem. Int. Ed.* **2011**, 50, 3362.

- [143] Yamaguchi, J.; Yamaguchi, A. D.; Itami, K. *Angew. Chem. Int. Ed.* **2012**, *51*, 8960.
- [144] Xue, X.-S.; Ji, P.; Zhou, B.; Cheng, J.-P. *Chem. Rev.* **2017**, *117*, 8622.
- [145] He, J.; Wasa, M.; Chan, K. S. L.; Shao, Q.; Yu, J.-Q. *Chem. Rev.* **2017**, *117*, 8754.
- [146] Ali, W.; Oliver, G. A.; Werz, D. B.; Maiti, D. *Chem. Soc. Rev.* **2024**, *53*, 9904.
- [147] Stateman, L. M.; Nakafuku, K. M.; Nagib, D. A. *Synthesis* **2018**, *50*, 1569.
- [148] Kumar, G.; Pradhan, S.; Chatterjee, I. *Chem. - Asian J.* **2020**, *15*, 651.
- [149] Xi, J.-M.; Liao, W.-W. *Org. Chem. Front.* **2022**, *9*, 4490.
- [150] Löffler, K.; Freytag, C. *Chem. Ber.* **1909**, *42*, 3427.
- [151] Barton, D. H. R.; Beaton, J. M. *J. Am. Chem. Soc.* **1960**, *82*, 2641.
- [152] Barton, D. H. R.; Beaton, J. M.; Geller, L. E.; Pechet, M. M. *J. Am. Chem. Soc.* **1961**, *83*, 4076.
- [153] Guo, W.; Wang, Q.; Zhu, J. *Chem. Soc. Rev.* **2021**, *50*, 7359.
- [154] Zhang, J.; Rueping, M. *Chem. Soc. Rev.* **2023**, *52*, 4099.
- [155] Chen, J.-Q.; Wei, Y.-L.; Xu, G.-Q.; Liang, Y.-M.; Xu, P.-F. *Chem. Commun.* **2016**, *52*, 6455.
- [156] Huang, H.; Lin, X.; Yang, F.; Ren, Y.; Gao, Y.; Su, W. *Org. Lett.* **2024**, *26*, 11195.
- [157] Zeng, L.; Xu, C.-H.; Zou, X.-Y.; Sun, Q.; Hu, M.; Ouyang, X.-H.; He, D.-L.; Li, J.-H. *Chem. Sci.* **2024**, *15*, 6522.
- [158] Wang, J.; Xie, Q.; Gao, G.; Li, H.; Lu, W.; Cai, X.; Chen, X.; Huang, B. *Org. Chem. Front.* **2023**, *10*, 4394.
- [159] Wang, J.; Xie, Q.; Gao, G.; Wei, G.; Wei, X.; Chen, X.; Zhang, D.; Li, H.; Huang, B. *Org. Chem. Front.* **2024**, *11*, 4522.
- [160] Lei, Z.; Zhang, W.; Wu, J. *ACS Catal.* **2023**, *13*, 16105.
- [161] Ratushnyy, M.; Kvasovs, N.; Sarkar, S.; Gevorgyan, V. *Angew. Chem. Int. Ed.* **2020**, *59*, 10316.
- [162] Yang, S.; Fan, H.; Xie, L.; Dong, G.; Chen, M. *Org. Lett.* **2022**, *24*, 6460.
- [163] Du, Y.-J.; Sheng, X.-X.; Li, J.-H.; Chen, J.-M.; Yang, S.; Chen, M. *Chem. Sci.* **2023**, *14*, 3580.
- [164] Li, P.; Teng, Q.-Q.; Chen, M. *Chem. Commun.* **2023**, *59*, 10620.
- [165] Lu, W.-D.; Zheng, Y.; Zhang, Z.-P.; Chen, H.-B.; Chen, K.; Xiang, H.-Y.; Yang, H. *Org. Lett.* **2023**, *25*, 6077.
- [166] Du, Y.-J.; Sheng, X.-X.; Tang, L.-N.; Chen, J.-M.; Liu, G.-Y.; Hu, H.; Yang, S.; Zhu, L.; Chen, M. *Org. Lett.* **2024**, *26*, 2662.
- [167] Sarkar, S.; Wagulde, S.; Jia, X.; Gevorgyan, V. *Chem.* **2022**, *8*, 3096.
- [168] Yang, Z.-S.; Tang, W.-X.; Zhang, B.-B.; Sun, D.-Q.; Chen, K.-Q.; Chen, X.-Y. *Org. Chem. Front.* **2023**, *10*, 1219.
- [169] Lu, J.; Yuan, K.; Zheng, J.; Zhang, H.; Chen, S.; Ma, J.; Liu, X.; Tu, B.; Zhang, G.; Guo, R. *Angew. Chem., Int. Ed.* **2024**, *63*, e202409310.
- [170] Wu, S.; Wu, X.; Wang, D.; Zhu, C. *Angew. Chem. Int. Ed.* **2019**, *58*, 1499.
- [171] Yang, S.; Wu, X.; Wu, S.; Zhu, C. *Org. Lett.* **2019**, *21*, 4837.
- [172] Wan, Y.; Shang, T.; Lu, Z.; Zhu, G. *Org. Lett.* **2019**, *21*, 4187.
- [173] Xie, S.; Li, Y.; Liu, P.; Sun, P. *Org. Lett.* **2020**, *22*, 8774.
- [174] Li, H.; Guo, L.; Feng, X.; Huo, L.; Zhu, S.; Chu, L. *Chem. Sci.* **2020**, *11*, 4904.
- [175] Ratushnyy, M.; Parasram, M.; Wang, Y.; Gevorgyan, V. *Angew. Chem. Int. Ed.* **2018**, *57*, 2712.
- [176] Wang, H.; Zhang, J.; Shi, J.; Li, F.; Zhang, S.; Xu, K. *Org. Lett.* **2019**, *21*, 5116.
- [177] Song, L.; Fu, D.-M.; Chen, L.; Jiang, Y.-X.; Ye, J.-H.; Zhu, L.; Lan, Y.; Fu, Q.; Yu, D.-G. *Angew. Chem., Int. Ed.* **2020**, *59*, 21121.

- [178] Wille, U. *Chem. Rev.* **2013**, *113*, 813.
- [179] Ding, K.; Lu, Y.; Nikolovska-Coleska, Z.; Wang, G.; Qiu, S.; Shangary, S.; Gao, W.; Qin, D.; Stuckey, J.; Krajewski, K.; Roller, P. P.; Wang, S. *J. Med. Chem.* **2006**, *49*, 3432.
- [180] Yu, B.; Yu, D. Q.; Liu, H. M. *Eur. J. Med. Chem.* **2015**, *97*, 763.
- [181] Kaur, M.; Singh, M.; Chadha, N.; Silakari, O. *Eur. J. Med. Chem.* **2016**, *123*, 858.
- [182] Dalpozzo, R.; Bartoli, G.; Bencivenni, G. *Chem. Soc. Rev.* **2012**, *41*, 7247.
- [183] Cao, Z.-Y.; Zhou, F.; Zhou, J. *Acc. Chem. Res.* **2018**, *51*, 1443.
- [184] Marchese, A. D.; Larin, E. M.; Mirabi, B.; Lautens, M. *Acc. Chem. Res.* **2020**, *53*, 1605.
- [185] Boddy, A. J.; Bull, J. A. *Org. Chem. Front.* **2021**, *8*, 1026.
- [186] Xu, Z.; Yan, C.; Liu, Z.-Q. *Org. Lett.* **2014**, *16*, 5670.
- [187] Dai, Q.; Yu, J.; Jiang, Y.; Guo, S.; Yang, H.; Cheng, J. *Chem. Commun.* **2014**, *50*, 3865.
- [188] Zhou, D.; Li, Z.-H.; Li, J.; Li, S.-H.; Wang, M.-W.; Luo, X.-L.; Ding, G.-L.; Sheng, R.-L.; Fu, M.-J.; Tang, S. *Eur. J. Org. Chem.* **2015**, 1606.
- [189] He, Z.-Y.; Guo, J.-Y.; Tian, S.-K. *Adv. Synth. Catal.* **2018**, *360*, 1544.
- [190] Shi, Y.; Xiao, H.; Xu, X.-H.; Huang, Y. *Org. Biomol. Chem.* **2018**, *16*, 8472.
- [191] Wang, X.-Y.; Zhong, Y.-F.; Mo, Z.-Y.; Wu, S.-H.; Xu, Y.-L.; Tang, H.-T.; Pan, Y.-M. *Adv. Synth. Catal.* **2021**, *363*, 208.
- [192] Wu, H.; Zhou, M.; Li, W.; Zhang, P. *Catal. Commun.* **2020**, *133*, 105832.
- [193] Fan, X.; Liu, H.; Ma, S.; Wang, F.; Yang, J.; Li, D. *Tetrahedron* **2022**, *117-118*, 132849.
- [194] Fan, J.-H.; Wei, W.-T.; Zhou, M.-B.; Song, R.-J.; Li, J.-H. *Angew. Chem. Int. Ed.* **2014**, *53*, 6650.
- [195] Biswas, P.; Paul, S.; Guin, J. *Angew. Chem. Int. Ed.* **2016**, *55*, 7756.
- [196] Tang, S.; Zhou, D.; Li, Z.-H.; Fu, M.-J.; Jie, L.; Sheng, R.-L.; Li, S.-H. *Synthesis* **2015**, *47*, 1567.
- [197] Wang, H.; Guo, L.; Duan, X.-H. *J. Org. Chem.* **2016**, *81*, 860.
- [198] Yang, Z.; Cheng, Y.; Long, J.; Feng, X.; Tang, R.; Wei, J. *New J. Chem.* **2019**, *43*, 18760.
- [199] Che, F.; Zhong, J.; Yu, L.; Ma, C.; Yu, C.; Wang, M.; Hou, Z.; Zhang, Y. *Adv. Synth. Catal.* **2020**, *362*, 5020.
- [200] Zhang, L.; Zhou, H.; Bai, S.; Li, S. *Dalton Trans.* **2021**, *50*, 3201.
- [201] Zhang, L.; Wang, Y.; Yang, Y.; Zhang, P.; Wang, C. *Org. Chem. Front.* **2020**, *7*, 3234.
- [202] Wang, C.; Liu, L. *Org. Chem. Front.* **2021**, *8*, 1454.
- [203] Su, L.; Sun, H.; Liu, J.; Wang, C. *Org. Lett.* **2021**, *23*, 4662.
- [204] Festa, A. A.; Voskressensky, L. G.; Van der Eycken, E. V. *Chem. Soc. Rev.* **2019**, *48*, 4401.
- [205] Singh, J.; Sharma, A. *Adv. Synth. Catal.* **2021**, *363*, 4284.
- [206] Ghosh, S.; Qu, Z.-W.; Pradhan, S.; Ghosh, A.; Grimme, S.; Chatterjee, I. *Angew. Chem. Int. Ed.* **2022**, *61*, 10.1002/anie.202115272.
- [207] An, Y.; Li, Y.; Wu, J. *Org. Chem. Front.* **2016**, *3*, 570.
- [208] Muralirajan, K.; Kancherla, R.; Gimnkhani, A.; Rueping, M. *Org. Lett.* **2021**, *23*, 6905.
- [209] Du, J.; Wang, X.; Wang, H.; Wei, J.; Huang, X.; Song, J.; Zhang, J. *Org. Lett.* **2021**, *23*, 5631.
- [210] Xie, J.; Xu, P.; Li, H.; Xue, Q.; Jin, H.; Cheng, Y.; Zhu, C. *Chem. Commun.* **2013**, *49*, 5672.
- [211] Tang, Q.; Liu, X.; Liu, S.; Xie, H.; Liu, W.; Zeng, J.; Cheng, P. *RSC Adv.* **2015**, *5*, 89009.
- [212] Jin, Y.; Jiang, M.; Wang, H.; Fu, H. *Sci. Rep.* **2016**, *6*, 20068.
- [213] Li, Z.; Zhang, Y.; Zhang, L.; Liu, Z.-Q. *Org. Lett.* **2014**, *16*, 382.
- [214] Li, X.; Han, M.-Y.; Wang, B.; Wang, L.; Wang, M. *Org. Biomol. Chem.* **2019**, *17*, 6612.



- [215] Zhao, Y.; Li, Z.; Sharma, U. K.; Sharma, N.; Song, G.; Van der Eycken, E. V. *Chem. Commun.* **2016**, 52, 6395.
- [216] Xu, P.; Xie, J.; Xue, Q.; Pan, C.; Cheng, Y.; Zhu, C. *Chem. – Eur. J.* **2013**, 19, 14039.
- [217] Chen, J.-Q.; Wei, Y.-L.; Xu, G.-Q.; Liang, Y.-M.; Xu, P.-F. *Chem. Commun.* **2016**, 52, 6455.
- [218] Wang, Y.-Z.; Lin, W.-J.; Zou, J.-Y.; Yu, W.; Liu, X.-Y. *Adv. Synth. Catal.* **2020**, 362, 3116.
- [219] Liu, T.; Zhou, Y.; Tang, J.; Wang, C. *Beilstein J. Org. Chem.* **2023**, 19, 1785.
- [220] Yu, Q.-S.; Pei, X.-F.; Holloway, H. W.; Greig, N. H.; Brossi, A. *J. Med. Chem.* **1997**, 40, 2895.
- [221] Suzuki, T.; Choi, J.-H.; Kawaguchi, T.; Yamashita, K.; Morita, A.; Hirai, H.; Nagai, K.; Hirose, T.; Ōmura, S.; Sunazuka, T.; Kawagishi, H. *Bioorg. Med. Chem. Lett.* **2012**, 22, 4246.
- [222] Sun, Z.; Huang, H.; Wang, Q.; Huang, C.; Mao, G.; Deng, G.-J. *Org. Chem. Front.* **2022**, 9, 3506.
- [223] Carta, A.; Piras, S.; Loriga, G.; Paglietti, G. *Mini-Rev. Med. Chem.* **2006**, 6, 1179.
- [224] Liu, R.; Huang, Z.-H.; Murray, M. G.; Guo, X.-Y.; Liu, G. *J. Med. Chem.* **2011**, 54, 5747.
- [225] Galal, S. A.; Khairat, S. H.M.; Ragab, F. A.F.; Abdelsamie, A. S.; Ali, M. M.; Soliman, S. M.; Mortier, J.; Wolber, G.; El Diwani, H. I. *Eur. J. Med. Chem.* **2014**, 86, 122.
- [226] Lawrence, D. S.; Copper, J. E.; Smith, C. D. *J. Med. Chem.* **2001**, 44, 594.
- [227] Kobayashi, Y.; Suzuki, Y.; Ogata, T.; Kimachi, T.; Takemoto, Y. *Tetrahedron Lett.* **2014**, 55, 3299.
- [228] Qin, X.; Hao, X.; Han, H.; Zhu, S.; Yang, Y.; Wu, B.; Hussain, S.; Parveen, S.; Jing, C.; Ma, B.; Zhu, C. *J. Med. Chem.* **2015**, 58, 1254.
- [229] Khattab, S. N.; Abdel Moneim, S. A. H.; Bekhit, A. A.; El Massry, A. M.; Hassan, S. Y.; El-Faham, A.; Ali Ahmed, H. E.; Amer, A. *Eur. J. Med. Chem.* **2015**, 93, 308.
- [230] Gao, Y.; Wu, Z.; Yu, L.; Wang, Y.; Pan, Y. *Angew. Chem. Int. Ed.* **2020**, 59, 10859.
- [231] Hu, L.; Yuan, J.; Fu, J.; Zhang, T.; Gao, L.; Xiao, Y.; Mao, P.; Qu, L. *Eur. J. Org. Chem.* **2018**, 4113.
- [232] Shi, Y.; Hou, J.; Wang, K.; Ding, Y.; Wei, T.; Yu, Z.; Su, W.; Xie, Y. *ChemistrySelect* **2022**, 7, No. e202203468.
- [233] Xie, D.; Tian, R.-G.; Zhang, X.-T.; Tian, S.-K. *Org. Biomol. Chem.* **2022**, 20, 4518.
- [234] He, X.-K.; Lu, J.; Zhang, A.-J.; Zhang, Q.-Q.; Xu, G.-Y.; Xuan, J. *Org. Lett.* **2020**, 22, 5984.
- [235] Zhu, X.; Jiang, M.; Li, X.; Zhu, E.; Deng, Q.; Song, X.; Lv, J.; Yang, D. *Org. Chem. Front.* **2022**, 9, 347.
- [236] Kishor, G.; Ramesh, V.; Rao, V. R.; Pabbaraja, S.; Adiyala, P. R. *RSC Adv.* **2022**, 12, 12235.
- [237] Yan, Q.; Cui, W.; Li, J.; Xu, G.; Song, X.; Lv, J.; Yang, D. *Org. Chem. Front.* **2022**, 9, 2653.
- [238] Xiang, P.; Sun, K.; Wang, S.; Chen, X.; Qu, L.; Yu, B. *Chin. Chem. Lett.* **2022**, 33, 5074.
- [239] Zeng, X.; Liu, C.; Wang, X.; Zhang, J.; Wang, X.; Hu, Y. *Org. Biomol. Chem.* **2017**, 15, 8929.
- [240] Xie, L.-Y.; Peng, S.; Fan, T.-G.; Liu, Y.-F.; Sun, M.; Jiang, L.-L.; Wang, X.-X.; Cao, Z.; He, W.-M. *Sci. China: Chem.* **2019**, 62, 460.
- [241] Lu, J.; He, X.-K.; Cheng, X.; Zhang, A.-J.; Xu, G.-Y.; Xuan, J. *Adv. Synth. Catal.* **2020**, 362, 2178.
- [242] Xie, L.-Y.; Bai, Y.-S.; Xu, X.-Q.; Peng, X.; Tang, H.-S.; Huang, Y.; Lin, Y.-W.; Cao, Z.; He, W.-M. *Green Chem.* **2020**, 22, 1720.
- [243] Bao, P.; Liu, F.; Lv, Y.; Yue, H.; Li, J.-S.; Wei, W. *Org. Chem. Front.* **2020**, 7, 492.
- [244] Ni, H.; Li, Y.; Shi, X.; Pang, Y.; Jin, C.; Zhao, F. *Tetrahedron Lett.* **2021**, 68, 152915.
- [245] Zhu, H.-L.; Zeng, F.-L.; Chen, X.-L.; Sun, K.; Li, H.-C.; Yuan, X.-Y.; Qu, L.-B.; Yu, B. *Org.*

- Lett.* **2021**, *23*, 2976.
- [246] Zeng, F.-L.; Xie, K.-C.; Liu, Y.-T.; Wang, H.; Yin, P.-C.; Qu, L.-B.; Chen, X.-L.; Yu, B. *Green Chem.* **2022**, *24*, 1732.
- [247] He, Y.; Wang, G.; Hu, W.; Wei, D.; Jia, J.; Li, H.; Yuan, B. *ACS Sustainable Chem. Eng.* **2023**, *11*, 910.
- [248] Aganda, K. C. C.; Hong, B.; Lee, A. *Adv. Synth. Catal.* **2021**, *363*, 1443.
- [249] Wu, B.; Yang, Y.; Qin, X.; Zhang, S.; Jing, C.; Zhu, C.; Ma, B. *ChemMedChem* **2013**, *8*, 1913.
- [250] Xue, W.; Su, Y.; Wang, K.-H.; Zhang, R.; Feng, Y.; Cao, L.; Huang, D.; Hu, Y. *Org. Biomol. Chem.* **2019**, *17*, 6654.
- [251] Stache, E. E.; Ertel, A. B.; Rovis, T.; Doyle, A. G. *ACS Catal.* **2018**, *8*, 11134.
- [252] Clarke, A. K.; Parkin, A.; Taylor, R. J. K.; Unsworth, W. P.; Rossi-Ashton, J. A. *ACS Catal.* **2020**, *10*, 5814.
- [253] Altenburger, J.-M.; Lassalle, G. Y.; Matrougui, M.; Galtier, D.; Jetha, J.-C.; Bocskei, Z.; Berry, C. N.; Lunven, C.; Lorrain, J.; Herault, J.-P.; Schaeffer, P.; O'Connor, S. E.; Herbert, J.-M. *Bioorg. Med. Chem.* **2004**, *12*, 1713.
- [254] Messaoudi, S.; Treguier, B.; Hamze, A.; Provot, O.; Peyrat, J.-F.; De Losada, J. R.; Liu, J.-M.; Bignon, J.; Wdzieczak-Bakala, J.; Thoret, S.; Dubois, J.; Brion J.-D.; Alami, M. *J. Med. Chem.* **2009**, *52*, 4538.
- [255] Chelucci, G. *Chem. Rev.* **2012**, *112*, 1344.
- [256] Zhang, X.; Cao, S. *Tetrahedron Lett.* **2017**, *58*, 375.
- [257] Pan, Y.; Qiu, J.; Silverman, R. B. *J. Med. Chem.* **2003**, *46*, 5292.
- [258] Magueur, G.; Crousse, B.; Ourévitich, M.; Bonnet-Delpon, D.; Bégué, J.-P. *J. Fluorine Chem.* **2006**, *127*, 637.
- [259] Fuchibe, K.; Takahashi, M.; Ichikawa, J. *Angew. Chem. Int. Ed.* **2012**, *51*, 12059.
- [260] Hu, M.; Ni, C.; Li, L.; Han, Y.; Hu, J. *J. Am. Chem. Soc.* **2015**, *137*, 14496.
- [261] Fuchibe, K.; Hatta, H.; Oh, K.; Oki, R.; Ichikawa, J. *Angew. Chem. Int. Ed.* **2017**, *56*, 5890.
- [262] Wang, M.; Pu, X.; Zhao, Y.; Wang, P.; Li, Z.; Zhu, C.; Shi, Z. *J. Am. Chem. Soc.* **2018**, *140*, 9061.
- [263] Yao, C.; Wang, S.; Norton, J.; Hammond, M. *J. Am. Chem. Soc.* **2020**, *142*, 4793.
- [264] Zhang, C.; Lin, Z.; Zhu, Y.; Wang, C. *J. Am. Chem. Soc.* **2021**, *143*, 11602.
- [265] Liu, Y.; Zhou, Y.; Zhao, Y.; Qu, J. *Org. Lett.* **2017**, *19*, 946.
- [266] Gao, P.; Yuan, C.; Zhao, Y.; Shi, Z. *Chem* **2018**, *4*, 2201.
- [267] Kojima, R.; Akiyama, S.; Ito, H. *Angew. Chem. Int. Ed.* **2018**, *57*, 7196.
- [268] Paioti, P. H. S.; del Pozo, J.; Mikus, M. S.; Lee, J.; Koh, M. J.; Romiti, F.; Torker, S.; Hoveyda, A. H. *J. Am. Chem. Soc.* **2019**, *141*, 19917.
- [269] Dong, H.; Lin, Z.; Wang, C. *J. Org. Chem.* **2022**, *87*, 892.
- [270] Qiu, J.; Wang, C.; Zhou, L.; Lou, Y.; Yang, K.; Song, Q. *Org. Lett.* **2022**, *24*, 2446.
- [271] He, Y.; Anand, D.; Sun, Z.; Zhou, L. *Org. Lett.* **2019**, *21*, 3769.
- [272] Zeng, W.; Li, L.; Wang, C.; Wang, D.; Zhou, L. *Adv. Synth. Catal.* **2022**, *364*, 3310.
- [273] Wang, B.; Wang, C.-T.; Li, X.-S.; Liu, X.-Y.; Liang, Y.-M. *Org. Lett.* **2022**, *24*, 6566.
- [274] Cai, Z.; Gu, R.; Si, W.; Xiang, Y.; Sun, J.; Jiao, Y.; Zhang, X. *Green Chem.* **2022**, *24*, 6830.
- [275] Li, F.; Pei, C.; Koenigs, R. M. *Angew. Chem. Int. Ed.* **2022**, *61*, e202111892.
- [276] Zhao, Y.; Empel, C.; Liang, W.; Koenigs, R. M.; Patureau, *Org. Lett.* **2022**, *24*, 8753.
- [277] Savchenko, A. G.; Zubkov, M. O.; Kokorekin, V. A.; Hu, J.; Dilmann, A. D. *ChemCatChem*

- 2023**, *15*, e202300505.
- [278] Chen, B.; Chen, Q.; Liu, Y.; Chen, J.; Zhou, X.; Wang, H.; Yan, Q.; Wang, W.; Cai, Z.; Chen, F.-E. *Org. Lett.* **2023**, *25*, 9124.
- [279] Zhang, Y.; Mao, J.; Wang, Z.; Tang, L.; Fan, Z. *Green Chem.* **2024**, *26*, 9371.
- [280] Yan, X.; Wang, S.; Liu, Z.; Luo, Y.; Wang, P.; Shi, W.; Qi, X.; Huang, Z.; Lei, A. *Sci. China: Chem.* **2022**, *65*, 762.
- [281] Claraz, A.; Allain, C.; Masson, G. *Chem. Eur. J.* **2022**, *28*, e202103337.
- [282] Zhang, H.; Liang, M.; Zhang, X.; He, M.-K.; Yang, C.; Guo, L.; Xia, W. *Org. Chem. Front.* **2022**, *9*, 95.
- [283] Golden, D. L.; Suh, S.-E.; Stahl, S. S. *Nat. Rev. Chem.* **2022**, *6*, 405.
- [284] Holmberg-Douglas, N.; Nicewicz, D. A. *Chem. Rev.* **2022**, *122*, 1925.
- [285] Bellotti, P.; Huang, H.-M.; Faber, T.; Glorius, F. *Chem. Rev.* **2023**, *123*, 4237.
- [286] Xu, G.-Q.; Wang, W. D.; Xu, P.-F. *J. Am. Chem. Soc.* **2024**, *146*, 1209.
- [287] Anand, D.; Sun, Z.; Zhou, L. *Org. Lett.* **2020**, *22*, 2371.
- [288] Hu, Q.-P.; Cheng, J.; Wang, Y.; Shi, J.; Wang, B.-Q.; Hu, P.; Zhao, K.-Q.; Pan, F. *Org. Lett.* **2021**, *23*, 4457.
- [289] Yue, W.-J.; Day, C. S.; Martin, R. *J. Am. Chem. Soc.* **2021**, *143*, 6395.
- [290] Guo, Y.-Q.; Wu, Y.; Wang, R.; Song, H.; Liu, Y.; Wang, Q. *Org. Lett.* **2021**, *23*, 2353.
- [291] Zhu, C.-M.; Liang, R.-B.; Xiao, Y.; Zhou, W.; Tong, Q.-X.; Zhong, J.-J. *Green Chem.* **2023**, *25*, 960.
- [292] Yuan, Z.-H.; Xin, H.; Zhang, L.; Gao, P.; Yang, X.; Duan, X.-H.; Guo, L.-N. *Green Chem.* **2023**, *25*, 6733.
- [293] Pizzio, M. G.; Mata, E. G.; Dauban, P.; Saget, T. *Eur. J. Org. Chem.* **2023**, *26*, e202300616.
- [294] Sheng, X.-x.; Qiu, C.-y.; Wang, L.-n.; Du, Y.-j.; Tang, L.-n.; Chen, J.-m.; Liu, G.-y.; Yang, S.; Zheng, P.-f.; Chen, M. *Chem. Eur. J.* **2024**, *30*, e202402402.
- [295] Kostromitin, V. S.; Sorokin, A. O.; Levin, V. V.; Dilmann, A. D. *Chem. Sci.* **2023**, *14*, 3229.
- [296] Constantin, T.; Zanini, M.; Regni, A.; Sheikh, N. S.; Juliá, F.; Leonori, D. *Science* **2020**, *367*, 1021.
- [297] Li, Z.-S.; Wang, W.-X.; Yang, J.-D.; Wu, Y.-W.; Zhang, W. *Org. Lett.* **2013**, *15*, 3820.
- [298] Ghosh, P.; Byun, Y.; Kwon, N. Y.; Kang, J. Y.; Mishra, N. K.; Park, J. S.; Kim, I. S. *Cell Rep. Phys. Sci.* **2022**, *3*, 100819.
- [299] Prince; Monika; Kumar, P.; Singh; B. K. *ACS Omega* **2024**, *9*, 651.
- [300] Hong, Y.-Y.; Peng, Z.; Ma, H.; Zhu, Q.; Xu, X.-Q.; Yang, L.-H.; Xie, L.-Y. *Tetrahedron Lett.* **2022**, *89*, 153595.
- [301] Ma, C.; Guo, Q.; Meng, H.; Yan, S.; Ding, Q.; Jiang, Y.; Yu, B. *Org. Lett.* **2024**, *26*, 8503.

## 7 Acknowledgements

Firstly, I would like to express my deepest gratitude to my supervisor, Prof. Dr. Frederic W. Patureau. His unwavering support, insightful guidance, and profound expertise have been invaluable throughout my doctoral journey. From the very beginning, he has not only provided me with the academic freedom to explore my research interests but also continuously challenged and inspired me to think critically and push the boundaries of my work. His patience, encouragement, and belief in my abilities have played a crucial role in shaping both my scientific development and personal growth. I am truly grateful for the opportunity to be his student.

I would also like to extend my thanks to my colleagues who have supported me in countless ways during my PhD. I sincerely appreciate the generous help and collaboration from Jiaxiang Xiang, Yue Zhao, Raolin Huang, Xinben Wang, Yun Yang, Fang Xiao, Long Huang, Vinzenz Thönnißen, Alina Paffen, Alija Spahic, Shiny Nandi, Pooja Vemuri, Alexander Schacht, Leander Bruck and Melissa Hohenadel. Their insightful discussions, technical assistance, and, most importantly, their friendship have made this journey not only more manageable but also much more enjoyable. The time spent working together, discussing science, and sharing laughter in the lab is something I will always cherish.

I am also deeply grateful to the China Scholarship Council (CSC) for providing me with the predoctoral stipend that made it possible for me to pursue my research at RWTH Aachen University. Their financial support has been instrumental in allowing me to focus entirely on my studies and research.

Finally, I would like to thank my family and friends for their endless love, patience, and encouragement. Their unwavering belief in me has been a source of strength through all the challenges and triumphs of this journey. Without their support, this achievement would not have been possible.

## 8 Curriculum vitae

Name: Dan Liu

Date of Birth: 10.09.1995

Nationality: China

Education:

10/2021-present Doctoral study

RWTH Aachen University (Aachen, Germany)

Institute of Organic Chemistry

Supervisor: Prof. Dr. Frederic W. Patureau

09/2018 - 03/2021 Chemistry, Master

Shanghai Jiaotong University, Shanghai, China

Supervisors: Prof. Dr. Wanbin Zhang and Prof. Dr. Deyue Yan

09/2014 - 07/2018 Macromolecular Materials and Engineering, Bachelor

Anhui University, Hefei, China

Journal publications:

1. Dan Liu, F. Xiao, B. Ebel, I. M. Oppel and F. W. Patureau, Visible-light-mediated radical  $\alpha$ -C(sp<sup>3</sup>)-H *gem*-difluoroallylation of amides with trifluoromethyl alkenes via halogen atom transfer and 1,5-hydrogen atom transfer. *Org. Lett.* **2025**, 27, 2377.
2. Dan Liu, and F. W. Patureau, Visible-light-induced photocatalytic deoxygenative benzylation of quinoxalin-2-(1*H*)-ones with carboxylic acid anhydrides. *Org. Lett.* **2024**, 26, 6841.
3. Dan Liu, Y. Zhao and F. W. Patureau, NaI/PPh<sub>3</sub>-catalyzed visible-light-mediated decarboxylative radical cascade cyclization of *N*-arylacrylamides for the efficient synthesis of quaternary oxindoles. *Beilstein J. Org. Chem.* **2023**, 19, 57.
4. B. Li, J. Chen, Dan Liu, I. D. Gridnev and W. Zhang, Nickel-catalyzed asymmetric hydrogenation of oximes. *Nat. Chem.* **2022**, 14, 920.
5. B. Li, Dan Liu, Y. Hu, J. Chen, Z. Zhang and W. Zhang. Nickel-catalyzed asymmetric hydrogenation of hydrazones. *Eur. J. Org. Chem.* **2021**, 23, 3421.
6. Dan Liu, B. Li, J. Chen, I. D. Gridnev, D. Yan and W. Zhang, Ni-catalyzed asymmetric hydrogenation of *N*-aryl imino esters for the efficient synthesis of chiral  $\alpha$ -aryl glycines. *Nat Commun.* **2020**, 11, 5935.